[redacted]

NASA Contractor Report 187096

P-188

In Flight Measurement of Steady and Unsteady Blade Surface Pressure of a Single Rotation Large Scale Advanced Prop-Fan Installed on the PTA Aircraft

D. Parzych, L. Boyd,
W. Meissner, and A. Wyrostek
United Technologies Corporation
Windsor Locks, Connecticut

September 1991

ORIGINAL CONTAINS
COLOR ILLUSTRATIONS

Prepared for
Lewis Research Center
Under Contract NAS3-23051

Date for general release October 1993.

NASA
National Aeronautics and
Space Administration

[redacted]

(NASA-CR-187096) IN FLIGHT MEASUREMENT OF STEADY AND UNSTEADY BLADE SURFACE PRESSURE OF A SINGLE ROTATION LARGE SCALE ADVANCED PROP-FAN INSTALLED ON THE PTA AIRCRAFT Final Report (United Technologies Corp.) 188 p

N94-32859

Unclas

G3/07 0011973

IN FLIGHT MEASUREMENT OF STEADY AND UNSTEADY BLADE SURFACE PRESSURE OF A SINGLE ROTATION LARGE SCALE ADVANCED PROP-FAN INSTALLED ON THE PTA AIRCRAFT

by

D. Parzych, L. Boyd,
W. Meissner, and A. Wyrostek

UNITED TECHNOLOGIES CORPORATION
Hamilton Standard Division

Prepared for
National Aeronautics and Space Administration
NASA Lewis Research Center
Contract NAS3-23051

TABLE OF CONTENTS

SUMMARY

An experiment was performed by Hamilton Standard, Division of United Technologies Corporation, under contract by the NASA-Lewis Research Center, to measure the blade surface pressure of a large scale, 8 blade, model Prop-Fan in flight. The test bed was the Gulfstream II Prop-Fan Test Assessment (PTA) aircraft.

The objective of the test was to measure the steady and periodic blade surface pressure resulting from three different Prop-Fan air inflow angles at various takeoff and cruise conditions. The inflow angles were obtained by varying the nacelle tilt angles, which ranged from -3 to +2 degrees. A range of power loadings, tip speeds and altitudes were tested at each nacelle tilt angle over the flight Mach number range of 0.30 to 0.80.

This report presents unsteady blade pressure data tabulated as Fourier coefficients for the first 35 harmonics of shaft rotational frequency and the steady (non-varying) pressure component.

INTRODUCTION

Since the mid 1970's, NASA has sponsored numerous research programs aimed at developing fuel efficient high flight speed turboprops (Prop-Fans). The research has progressed from wind tunnel testing of small .61 meter (2.0 Ft.) scale models to the current large scale Prop-Fan flight tests aboard the Prop-Fan Test Assessment (PTA) aircraft. While the early model testing focused on obtaining the basic aerodynamic performance and acoustic data needed to verify the Prop-Fan concept, the current focus is on obtaining more detailed aerodynamic flow characteristics.

The flow on the Prop-Fan blades has been found to be complicated, containing features such as three dimensional boundary layer effects, shock waves and leading edge/tip vortices. These effects are difficult to accurately predict with current design methods. The need for detailed blade aerodynamic measurement exists to provide an understanding of the specific nature of the airflow over the Prop-Fan. This understanding is vital to the process of refining design methodologies, which in turn can improve the performance and lower the noise of future Prop-Fan designs.

In 1987, NASA and Hamilton Standard obtained both steady and unsteady blade surface pressure data (References 1 and 2, respectively) of the large scale SR-7L Prop-Fan model in the ONERA S1-MA wind tunnel located in Modane, France. To further broaden this data base, a flight test of the PTA SR-7L model has been made with pressure transducer instrumented blades.

Initially, the test was to be conducted in two parts: a steady surface pressure portion, with pressure taps covering 14 radial positions with several chordwise stations for each radial position, and an unsteady portion with pressure transducers at three radial positions and several chordwise positions. Because of limited funding, the steady portion of the test was not conducted. However, some steady surface pressure data was obtained during the unsteady pressure test by retaining the DC component of the pressure signal.

A summary of the experiment, along with tabulations of the measured unsteady and steady pressure data, is presented and discussed in this report.

NOMENCLATURE

a_k, b_k	-	Real and imaginary Fourier coefficients (single sided)
CP	-	Power coefficient = (power absorbed/$\rho(2\pi\Omega)^3 D^5$)
C_p	-	Pressure coefficient at transducer
C_k	-	Complex Fourier coefficients
i	-	$(-1)^{\frac{1}{2}}$
D	-	Prop-Fan diameter
J	-	Advance ratio
L, ℓ	-	Total number of revolutions that waveform is averaged over revolution number.
k	-	Harmonic of blade rotational frequency
Mx	-	Inflow Mach number
N,n	-	Total number of samples of waveform, sample number
P	-	Static pressure
P_o	-	Reference pressure (101325 Pascals)
P_c	-	Corrected pressure at transducer
$P(\theta)$	-	Varying pressure waveform
q	-	Dynamic pressure
RIB	-	Rotating interface board
RTD	-	Resistance temperature detector
r	-	Radial distance from Prop-Fan center line to transducer
r_t	-	Tip radius = D/2
t	-	time
Vx	-	Inflow velocity
VCO	-	Voltage controlled oscillator
VDC	-	Voltage (direct current)
X/C	-	Non-dimensional chord location
Ω	-	rotor speed (radians/second)
θ	-	azimuthal position of blade at time (t)
ρ	-	Air density
ρ_o	-	Air density at sea level standard (0.12492 KG*sec^2/M^4)

PROP-FAN/TEST BED DESCRIPTION

Prop-Fan

The SR-7L Large Scale Advanced Prop-Fan, illustrated in Figure 1, is a 2.74 meter (9 foot) diameter, eight blade tractor configuration which was designed for 0.8 Mach number cruise speed at an altitude of 10,667 meters (35,000 feet), ISA. The SR-7L Prop-Fan was designed for high efficiency and low noise while maintaining the necessary restrictions on blade stress, stability and frequency characteristics. Additional parameters at the design point are:

Disc loading (Power/diameter^2)	259.6 kW/m^2	(32 shp/ft^2)
Tip speed	243.8 m/s	(800 ft/s)
Advance ratio	3.06	
Power coefficient	1.448	
Activity factor per blade	227.3	
Integrated design lift coeff.	0.191	

Rotation of the Prop-Fan is counterclockwise as viewed from the rear looking forward. The hub to tip ratio is 0.24, and the blades incorporate NACA Series 65/CA airfoils from the root to the 36% radius and NACA Series 16 airfoils from the 52% radius to the tip, with "transition" airfoils in the remaining "middle" portion of the blade. The blade's mid-chord line sweeps back to a maximum of 36° at the tip station. Additional information on the SR-7L Prop-Fan design can be found in Reference 3.

Test Bed

Shown in Figure 2 is the PTA aircraft. The aircraft is a Gulfstream Aerospace Corporation GII that has been modified to accept a Prop-Fan propulsion system. The basic aircraft and modifications, discussed in Reference 4, is a low-wing jet aircraft powered by two aft mounted Rolls Royce 511-8 Spey Turbine engines. The aircraft has a ramp weight of 30,000 kg (66,000 lbs) with full fuel and payload and can cruise at 0.85 Mach number. The propulsion system, mounted on the left wing of the aircraft was powered by a 6000 SHP Allison model 570 engine through a modified T56-A-14 gearbox. The nacelle was designed to allow the Prop-Fan tilt angle to be varied. This allowed various inflow angles to be evaluated at the Prop-Fan.

The fuselage cabin interior trim and furnishings were removed aft of the cockpit and replaced by data systems used for monitoring flight conditions and Prop-Fan data. A picture of the modified cabin can be seen in Figure 3.

INSTRUMENTATION

LAP Instrumentation System

A general schematic of the LAP instrumentation system can be seen in Figure 4. The LAP dynamic pressure blade was instrumented with thirty pressure transducers and six resistance temperature detectors (RTD's). Signal conditioning and bridge completion were provided by a printed circuit board located in the cuff of the blade. Programmable connector sockets were used as an interface between the signal conditioning boards and the rotating interface board (RIB).

As shown, the RIB provided signal and power interconnection between components of the rotating system. All signals from the programmable connector were routed through the RIB to the Voltage Controlled Oscillators (VCO) cases. The output of each VCO case was a 16 channel FM (frequency multiplexed) signal which was transmitted to the non-rotating instrumentation via a pair of slip rings. This system, therefore, could handle up to 32 active channels.

A signal conditioning board was mounted in the cuff of the dynamic pressure blade. It provided three functions:

1) Pressure transducer to instrumentation interface
2) Resistance temperature devices (RTD) bridge completion
3) Voltage substitution calibration via semiconductor switching

The unsteady pressure instrumentation utilized two identical VCO cases each containing 16 VCO's and one mixing amplifier/line driver. Each VCO consisted of both a preamplifier and VCO module which were matched in pairs. The preamplifiers had a nominal fixed gain of 250 to accommodate conditioned pressure and RTD signals. The VCO subcarrier frequencies were all standard IRIG A constant bandwidth channels (1A-16A) with a frequency response of 1000 Hz. All 16 VCO outputs in each case were mixed into a single 16 channel frequency multiplexed signal.

A rotating power supply provided ± 5 VDC excitation for the pressure transducers and RTDs and supplied the 25.5 VDC power required for the rotating electronics. It derived its power through slip rings from the primary power supply located on the non-rotating side. The primary power supply output voltage could be set by the user at one of three levels. This level was sensed by the rotating power supply and forced into one of three possible modes - the USE, FULL SCALE STANDARDIZE or the ZERO mode.

In the USE mode the system was connected to an excited transducer. In ZERO the system was connected via semiconductor switching to an unexcited transducer. In FULL SCALE, again through semiconductor switching, a voltage was substituted in place of the transducer voltage. These features were to be used to standardize the data acquisition system prior to data taking. However, the test crew experienced problems in trying to get the FULL SCALE mode to operate properly. Because of the short test window it was decided to not troubleshoot this problem. In place of the standardize scheme, a two point system calibration was substituted in which two known pressures were applied to each transducer on the blade prior to each flight, thus providing a system end-to-end calibration.

The LAP instrumentation slip ring was an eight-ring platter-type assembly which provided the electrical interface for the propeller measurements between the rotating propeller assembly and the non-rotating propeller control. Five of the eight rings were used for the dynamic pressure instrumentation.

Each of the two detranslators accepted a 16 channel VCO case output. The detranslator, utilizing a filtering and heterodyning process, converted the multiplex signal into four groups with four subcarriers each. These subcarriers were IRIG channels 1A, 2A, 3A and 4A in all cases. A total of eight multiplex groups originated at the detranslators and were recorded directly on tape.

Instrumented Blade

The unsteady blade surface pressure data was obtained with a total of 30 Endevco model 8515b-15 pressure transducers. The location of the transducers and the nomenclature used to describe each transducer can be found in Figures 5 and 6 for the blade camber (suction) and face (pressure) surfaces, respectively. The camber surface had a total of 20 transducers distributed over 3 radial locations. The face surface had a total of 10 transducers distributed over 2 radial locations.

The nomenclature used to define the location of the pressure transducers follow a format as:

sr-c

(s) is the SIDE - the letter defines the side of the blade the pressure transducer is located on, Face (F) or Camber (C).

(r) is the ROW - the next number defines the radial location on the blade. ROW 4 is at a radial location at 68% of the tip radius, ROW 7 is at 87% and ROW 10 is at 94.6%

(c) is % CHORD - the last number defines the distance from the leading edge as a percentage of the chord.

The blade was fabricated such that the pressure transducers were mounted flush with the blade surface while not disrupting the blade's integral structure. This was accomplished as shown in Figure 7 by applying a thin 0.67mm (0.027inch) layer of sprayed Hysol EC934 epoxy with a 0.076mm (0.003 inch) layer of white erosion coat. The coating provided room for flush mounting of the pressure transducers while maintaining a smooth blade surface.

List of Inoperable Transducers

The following list defines the inoperable or erratic transducers observed for each run.

TRANSDUCER	RUNS WITH ERRATIC BEHAVIOR
F4-15	ALL RUNS DURING -3 DEGREE NACELLE TILT
F10-58	39, 40, 41, 43, 44
C4-10	ALL RUNS, ALL NACELLE TILTS
C4-15	41
C4-40	117
C4-60	117
C4-80	117
C10-75	ALL RUNS, ALL NACELLE TILTS

Thermography

The high degree of temperature sensitivity of the blade surface pressure transducers required that the blade surface temperature distribution be accurately known. In-flight blade temperatures were determined experimentally using the United Technologies Research Center's optical thermography infrared video system[5]. The video system was mounted in the PTA aircraft where the SR-7L blades were viewed through a modified aircraft window. The video system was used to record the infrared images of both the suction and pressure sides of a SR-7L blade after the steady-state flight conditions were achieved. The thermography data was then used to evaluate the effects of blade frictional heating due to the leading edge vortex, blade section relative speeds and air density. This data base provided the information needed to accurately correct the pressure data for transducer temperature offset.

Additional information on the thermography testing and a complete set of infrared photos are included in Appendix A.

Pressure Measurement Uncertainty

A pressure measurement uncertainty analysis was preformed for the data collected during the PTA/SR-7L unsteady pressure flight tests. The analysis resulted from significant calibration efforts, modeling of systematic sensitivities and several

piecewise uncertainty analyses. The methods applied in the analysis followed a consistent plan to reduce the limits of uncertainty to the extent practical. The methods used to derive the equations and to determine the uncertainties are discussed further in Appendix B.

Initially, data reduction equations were modeled from component calibration data acquired prior to assembly, under controlled laboratory conditions. However, these equations proved to be invalid due to significant shifts in the transducer characteristics when the transducers were installed in the blade. The planned quasi-ratio data reduction technique, which uses the ratio of remotely switched zero standardize and output voltages to compensate gain and off-set for ambient effects, also proved to be invalid due to higher-than-expected input bias currents in the rotating preamplifiers.

The pressure measurement uncertainty approach used was based on systematic, end-to-end calibrations recorded on the aircraft prior to the first flight and temperature corrections determined from post-test calibrations conducted at Hamilton Standard.

The various calibrations performed included:

- 3 preinstallation transducer calibrations, -65° to 80° F, of 30 transducers and associated signal conditioning circuitry.
- 3 pretest data path calibrations, -65° to 80° F, for 6 channels with DC inputs.
- 3 pretest data path calibrations, -65° to 80° F, for 30 channels with AC inputs.
- 3 preflight end-to-end system calibrations for 30 channels at two pressure levels: 4 psia and barometric pressure.
- 3 posttest instrumented blade calibrations from -25° to 90° F, for 30 transducers, 6 resistance temperature detectors (RTD) and associated circuitry.
- 8 posttest low-pass filter calibrations.

The system modeling included:

- offset and gain equations for end-to-end calibration of 30 pressure and 6 temperature channels.

- quadratic expressions to correct pressure offset for temperature on 30 channels.

- quadratic expressions to correct pressure gain for temperature on 30 channels.

- fifth-order polynomials used to correct the high P-order unsteady pressures for low-pass filter attenuation.

The uncertainty analysis included:

- post-test transducer calibrations and data reduction equations for 30 pressure and 6 RTD channels

- temperature at transducer locations for in-flight test conditions obtained with strobed infrared video thermography.

- data path calibrations from signal source to digitized data.

- recommended method for combining reported uncertainties at test conditions.

Since the end-to-end calibration consisted of only two pressures, the correction of pressure transducer non-linearity was not considered justified. As a result, a small uncorrected bias remains in the reduced data for the steady pressure measurements. All remaining uncertainties were considered to have collectively occurred essentially at random and thus, were reported equivalent to two standard deviations.

The resultant uncertainties are tabulated in Table 1 for both the unsteady and steady pressures at each transducer location. The worst case uncertainty for unsteady pressure, ± 0.02 PSI @ 1 PSI peak pressure, was well within the ± 0.034 PSI estimated for the preliminary design review. The uncertainties for the steady pressure measurements were reported as the "best effort" results, as agreed upon with NASA Lewis following cancellation of Scanivalve/steady pressure flight test program.

TEST DESCRIPTION AND OPERATING CONDITIONS

The test conditions for each of the three nacelle tilt angles can be divided into three major sections:

A) Low altitude (580 meters) low flight speed (0.3 Mn)
B) High altitude (10,500 meters), high flight speed (0.8 Mn)
C) A compressibility series where the flight Mach number was varied while the Prop-Fan advance ratio and power coefficient (blade angle) were held constant.

The nominal flight conditions for the low altitude series (A) and high altitude series (B) included varying tip speed and power loading. The compressibility series (C), matched one blade angle and advance ratio for three Mach numbers, 0.6, 0.7 and 0.8. For this series, the altitude was varied at each Mach number to maintain a constant aircraft attitude and inflow angle at the Prop-Fan.

The aircraft was stabilized prior to each test point to ensure the correct flight conditions and Prop-Fan operating conditions. The Spey engine power was varied to maintain straight and level flight. Two minutes of data was recorded for each point.

The format of the experiment follows that found in Tables 2, 3, and 4 for the -1 degree, +2 degree and -3 degree nacelle tilts, respectively. The run number at the left of the table is unique for each condition and nacelle tilt. This number can be used to identify specific cases in the tabulated pressure data found in the Appendix C. The "ID" column can be used to identify similar conditions of each of the three nacelle tilts. For example, an ID of "10A" has the same nominal operating condition for all three nacelle tilts. The letter portion of the ID (A, B, or C) defines the low altitude, high altitude and compressibility series. The other parameters in the table, flight Mach number, advance ratio, power coefficient, etc., are the measured flight test conditions.

PRESENTATION OF DATA

Processing Used

The measured waveforms were processed to express the periodic pressure signals in Fourier coefficient form. This allows the data to be presented in a compact form of tabulated harmonics of the rotational frequency of the rotor while also allowing the original waveform to be reconstructed.

The Fourier coefficients were obtained by using the once-per-revolution pip signal to divide the continuous pressure signals into a series of 1024 waveforms, each with the period corresponding to one revolution of the rotor. The position of the instrumented blade was 250 degrees before Top-Dead-Center when the pip signal fired. A digital Fourier transform analyzer was then used to obtain the first 35 Fourier coefficients of each waveform. Average values of the coefficients were then determined from the 1024 waveforms sampled. Using the pip signal to synchronize the waveform sampling provides a means of rejecting signals not related to the periodicity of the rotor. This allows better resolution of the higher order harmonics that are normally masked by broadband noise.

The first 35 harmonics were assessed to be adequate in defining the waveform. Also, the 35th load harmonic approximately corresponds to a frequency of 1000 Hz, which is the upper limit the data acquisition system linearity.

Shown in Figure 8 is a comparison of an un-averaged waveform over four (4) revolutions with a waveform re-created with the 35 averaged Fourier coefficients. It can be seen that the re-created waveform provides a good representation of the measured waveform.

Definition of Coefficients

The single-sided complex Fourier coefficients are defined as:

$$C_k = 1/\pi \int_{-\pi}^{+\pi} P(\theta) e^{-ik} \, d\theta \qquad (1)$$

where $P(\theta)$ is the pressure waveform and k is the harmonic of blade rotational frequency.

This can be written in terms of a summation for "N" samples of the waveform and averaged over "L" revolutions as:

$$C_k = a_k - ib_k \tag{2}$$

where: $$a_k = 2/L \sum_{\ell=1}^{L} 1/N \sum_{n=1}^{N} P(n,\ell) \cos(2\pi kn/N) \tag{3}$$

and $$b_k = 2/L \sum_{\ell=1}^{L} 1/N \sum_{n=1}^{N} P(n,\ell) \sin(2\pi kn/N) \tag{4}$$

The waveform shape can be re-constructed using the inverse transform:

$$P(n) = \sum_{k=1}^{k=\infty} C_k e^{+i(2\pi kn/N)} \tag{5}$$

Accounting for 35 harmonics and ignoring the offset caused by the steady pressure:

$$P(n) = \sum_{k=1}^{k=35} C_k e^{+i(2\pi kn/N)} \tag{6}$$

Substituting for C_k and expanding equation (6) yields the following:

$$P(n) = \sum_{k=1}^{k=35} (a_k\cos(2\pi kn/N) + b_k\sin(2\pi kn/N)) \tag{7}$$

It should be noted that the complex coefficients given in Appendix C are of the form:

$$C_k = a_k - ib_k$$

In re-constructing the waveform (using equation 7), the imaginary portion of the coefficient, given in Appendix C, must be multiplied by (-1) as the sign, or "-i" is included in the coefficient. Neglecting this will cause the re-constructed waveform to appear as progressing backward in time.

The definition of the pressure coefficient (C_p) is:

$$C_p = (P_c - P) / q \qquad (8)$$

where P_c is the "corrected" pressure at each transducer, P is the static pressure, and q is the dynamic pressure defined as:

$$1/2\ \rho(Vx^2 + (D/2 * \Omega * r/r_t)^2) \qquad (9)$$

The r/r_t used for the calculation of the dynamic pressure are: 0.680 for the F4 and C4 transducers, 0.860 for the C7 transducers, and 0.946 for the F10 and C10 transducers.

<u>Form of Unsteady Data</u>

The unsteady data are presented in a tabulated form along with information defining the test condition and transducer. An example of the tabulated data can be found in Figure 9. The unsteady blade surface pressure is given in both pressure and coefficient form. In pressure form, the phase is retained so waveforms can be recreated. In coefficient form, only the amplitude is given.

The data can be found tabulated in this report and in Appendix C (C1, C2 and C3) for the -1 degree, +2 degree and -3 degree nacelle tilt angles, respectively.

<u>Form of Steady Data</u>

The steady pressure data is presented in pressure coefficient form. The coefficients were plotted as a function of blade chord for the face and camber blade surfaces at each radial location. An example of the steady pressure coefficient plots can be seen in Figure 10. A complete set of plots can be found in Appendix D, (D1, D2 and D3) for the -1 degree, +2 degree and -3 degree nacelle tilts, respectively. Also, the steady pressure coefficients can be found tabulated in Appendix C.

<u>Typical Waveform and Spectrum Plots</u>

Plotted in Figures 11 through 14 are typical chordwise waveform distributions for a take-off and cruise condition at the blade tip. Figures 11 and 12 present the face and camber blade sides, respectively, for the take-off condition while Figures 13 and 14 present both blade sides for the cruise condition. It can be seen that the maximum unsteady pressure occurs on the blades camber side slightly behind of the blade's leading edge.

Shown in Figures 15 through 18 are typical spectra observed at the transducer closest to the blade's leading edge for the two previous cases shown. The spectra shown are averaged narrow-band spectra. No special processing to suppress the broadband signal, as was performed to obtain the tabulated coefficients in Appendix C, was used in this case. The spectra are included here to show the relative levels between broadband and tone signals. It can be seen that broadband levels are typically 30 dB or more below the fundamental frequency component. Also, it should be noted that the higher frequency harmonics (above 10 per-revolution), would be masked by broadband noise if the signal processing were not synchronized to the once-per-rev pipper.

CONCLUSIONS

- o Steady and unsteady blade surface pressure were successfully collected over a range of take-off and cruise conditions for the SR7-L Prop-Fan installed on the PTA aircraft.

- o Presenting the data as Fourier coefficients for the first 35 harmonics of rotational frequency provides a good representation of the data in a compact tabular form.

- o The data presented in this report are considered suitable for correlation with prediction methods of steady and unsteady blade surface pressure. In such correlation studies the accuracy of the data as discussed in this report should be considered.

REFERENCES

1. Bushnell, P. "Measurement of the Steady Surface Pressure Distribution on a Single Rotation Large Scale Advanced Prop-Fan Blade at Mach Numbers from 0.03 to 0.78, NASA Lewis Contract NAS3-23051, NASA CR-182124, July, 1988.

2. Bushnell, P., Gruber, M., Parzych, D., "Measurement of Unsteady Blade Surface Pressure on a Single Rotation Large Scale Advanced Prop-Fan with Angular and Wake Inflow at Mach Numbers from 0.02 to 0.07", NASA Lewis Contract NAS3-23051.

3. Sullivan, W., Turnberg, J. Violette, J. "Large Scale Advanced Prop-Fan (LAP) Blade Design", NASA Lewis Contract NAS3-23051, NASA CR-174790, October 3, 1985.

4. Little, B.H., Poland, D.T., Bartel, H.W., Withers, C.C., Brown, P.C., "Prop-Fan Test Assessment (PTA) Final Project Report", NASA Lewis Contract NAS3-24339, NASA CR-185138, July 1989.

5. Skebe, Stanley A., "Synchronous Thermography", UTRC90-10, presented at the third Japan-China Joint Conference on Fluid Machinery, Osaka, Japan, April 23-25, 1990.

Table 1. Pressure Measurement Uncertainty

transducer	steady pressure systematic PSI	steady pressure random PSI*	steady pressure random % point*	unsteady** random % point
C4-5	+0.0107	±0.0560	±0.93	±0.96
C4-10	+0.0285	±0.0322	±0.95	±1.64
C4-15	+0.0185	±0.0438	±0.74	±1.04
C4-25	+0.0223	±0.0296	±0.60	±1.16
C4-40	+0.0328	±0.0370	±0.55	±1.66
C4-60	+0.0225	±0.0340	±0.67	±1.21
C4-80	+0.0224	±0.0532	±0.87	±1.33
C7-7	+0.0133	±0.0528	±0.80	±0.92
C7-15	+0.0144	±0.0549	±0.74	±0.91
C7-25	+0.0131	±0.0317	±0.66	±0.78
C7-37	+0.0198	±0.0435	±0.69	±1.10
C7-50	+0.0238	±0.0284	±0.53	±1.20
C7-70	+0.0179	±0.0269	±0.59	±0.96
C7-90	+0.0156	±0.0273	±0.55	±0.82
C10-8	+0.0126	±0.0940	±1.31	±1.36
C10-25	+0.0115	±0.1432	±1.03	±1.07
C10-42	+0.0248	±0.0620	±0.81	±1.65
C10-58	+0.0093	±0.0372	±1.02	±1.01
C10-75	+0.0142	±0.1425	±1.35	±1.27
C10-92	+0.0164	±0.0985	±1.57	±1.41
F4-15	+0.0127	±0.0238	±0.56	±0.69
F4-40	+0.0241	±0.0284	±0.50	±1.20
F4-60	+0.0289	±0.0333	±0.52	±1.45
F4-80	+0.0125	±0.0269	±0.61	±0.72
F10-8	+0.0145	±0.0522	±0.70	±0.87
F10-25	+0.0135	±0.0281	±0.60	±0.76
F10-42	+0.0159	±0.0262	±0.55	±0.82
F10-58	+0.0131	±0.0401	±0.57	±0.70
F10-75	+0.0253	±0.0412	±0.63	±1.66
F10-92	+0.0293	±0.0494	±0.73	±1.56

* Random uncertainty for steady pressure to be combined in consistent units with root-sum-squared method.

** Uncertainty due to frequency to be combined with unsteady random uncertainty with root-sum-squared method.

Data frequency	Uncertainty
10 to 140 Hz	±0.5 % point
@ 420 Hz	±1.0 % point
@ 600 Hz	±1.4 % point
@ 1050 Hz	±3.5 % point

Table 2. TEST CONDITIONS FOR THE -1 DEGREE NACELLE TILT ANGLE

RUN	ID	MX	J	CP	ALT. METERS	TEMP. DEG C	P/PO	ρ/ρ_0	INFLOW/SLIP ANGLE * DEGREES
36	10A	0.308	1.773	0.953	602.	28.	0.931	0.892	4.5 / 1.2
37	1A	0.307	1.767	1.484	605.	28.	0.930	0.892	4.7 / 0.4
38	11A	0.307	1.765	1.890	574.	28.	0.934	0.895	4.4 / 0.0
39	2A	0.309	1.757	2.103	622.	28.	0.929	0.890	4.1 /-1.0
40	3A	0.307	1.562	1.006	607.	27.	0.930	0.892	4.2 / 0.3
41	5A	0.312	1.591	1.639	703.	27.	0.920	0.883	4.0 /-1.2
43	7A	0.316	1.419	0.691	622.	28.	0.929	0.890	4.2 / 0.8
44	9A	0.308	1.400	1.122	664.	27.	0.924	0.887	4.4 /-1.9
47	1B	0.807	4.115	0.723	10788.	-37.	0.231	0.282	1.1 /-0.2
48	2B	0.808	4.120	1.682	10794.	-37.	0.231	0.282	1.1 / 0.0
49	3B	0.807	4.110	2.775	10796.	-37.	0.231	0.282	1.1 /-0.2
50	4B	0.809	4.128	3.134	10790.	-36.	0.231	0.281	1.1 /-0.2
51	11B	0.816	3.733	0.589	10793.	-36.	0.231	0.281	0.9 / 0.1
52	12B	0.806	3.677	1.326	10789.	-36.	0.231	0.281	1.0 / 0.0
53	13B	0.806	3.657	2.057	10785.	-37.	0.231	0.281	1.1 /-0.2
54	14B	0.810	3.661	2.395	10790.	-38.	0.231	0.283	1.0 /-0.2
56	22B	0.814	3.236	0.935	10801.	-38.	0.231	0.282	0.9 /-0.3
57	23B	0.810	3.220	1.496	10792.	-37.	0.231	0.282	1.0 /-0.5
58	24B	0.812	3.216	1.734	10796.	-38.	0.231	0.283	1.0 /-0.4
59	3C	0.811	3.205	1.600	11726.	-40.	0.199	0.247	1.4 /-0.3
60	2C	0.696	3.155	1.521	9558.	-29.	0.279	0.329	1.5 /-0.1
61	1C	0.603	3.152	1.520	7113.	-17.	0.399	0.448	0.8 /-0.4

NOTE: PO $= 101325.\ N / M^2$
ρ_0 $= 0.12492\ KG \cdot SEC^2 / M^4$
TEMPERATURE, PRESSURE AND DENSITY ARE STATIC CONDITION

* INFLOW ANGLE IS AIRPLANE ANGLE-OF-ATTACK + NACELLE TILT
SLIP ANGLE IS AIRPLANE SIDESLIP

Table 3. TEST CONDITIONS FOR THE +2 DEGREE NACELLE TILT ANGLE

RUN	ID	MX	J	CP	ALT. METERS	TEMP. DEG C	P/PO	ρ/ρ_0	INFLOW/SLIP ANGLE * DEGREES
107	10A	0.310	1.805	0.975	610.	34.	0.930	0.871	12.3 / 4.7
109	1A	0.310	1.803	1.536	607.	34.	0.930	0.872	13.6 / 4.6
110	11A	0.310	1.800	1.950	618.	34.	0.929	0.872	13.5 / 4.4
111	2A	0.311	1.813	2.116	626.	35.	0.928	0.872	13.8 / 3.5
113	3A	0.313	1.611	1.034	613.	34.	0.929	0.873	7.1 / 0.1
114	5A	0.315	1.620	1.508	626.	34.	0.928	0.871	7.3 /-1.3
115	7A	0.315	1.427	0.705	604.	34.	0.930	0.873	7.4 / 0.2
117	6A	0.315	1.433	1.059	643.	34.	0.926	0.869	7.3 /-1.4
120	10B	0.816	4.122	0.739	10677.	-40.	0.235	0.290	3.9 /-0.1
121	11B	0.823	4.147	1.690	10829.	-41.	0.230	0.286	3.9 /-0.2
122	12B	0.820	4.132	2.726	10823.	-41.	0.230	0.286	4.0 /-0.2
123	1B	0.822	4.135	3.372	10821.	-41.	0.230	0.286	3.9 / 0.1
132	3B	0.816	3.670	1.221	10807.	-40.	0.230	0.285	3.6 / 0.3
133	4B	0.819	3.688	2.007	10794.	-40.	0.231	0.285	3.6 / 0.1
134	5B	0.816	3.665	2.517	10804.	-40.	0.230	0.285	3.7 / 0.0
136	7B	0.820	3.244	0.886	10807.	-40.	0.230	0.285	3.5 /-0.1
137	8B	0.815	3.232	1.486	10794.	-40.	0.231	0.285	3.6 / 0.0
138	9B	0.816	3.236	1.836	10795.	-40.	0.231	0.285	3.6 /-0.1
140	3C	0.803	3.130	1.493	11581.	-47.	0.204	0.260	3.9 /-0.1
142	2C	0.701	3.177	1.533	9616.	-30.	0.276	0.328	3.8 /-0.2
144	1C	0.603	3.196	1.475	6998.	-8.	0.405	0.441	3.6 / 0.4

NOTE: PO = 101325. N / M^2
ρ_0 = 0.12492 $KG \cdot SEC^2 / M^4$
TEMPERATURE, PRESSURE & DENSITY ARE STATIC CONDITION

* INFLOW ANGLE IS AIRPLANE ANGLE-OF-ATTACK + NACELLE TILT
SLIP ANGLE IS AIRPLANE SIDESLIP

Table 4. TEST CONDITIONS FOR THE -3 DEGREE NACELLE TILT ANGLE

RUN	ID	MX	J	CP	ALT. METERS	TEMP. DEG C	P/PO	ρ/ρ_0	INFLOW/SLIP ANGLE * DEGREES
182	10A	0.310	1.792	0.957	610.	30.	0.930	0.884	1.8 / 0.8
183	1A	0.315	1.820	1.498	654.	30.	0.925	0.880	2.1 / 0.5
184	11A	0.312	1.803	1.935	620.	30.	0.929	0.883	2.2 / 0.3
185	2A	0.311	1.803	2.206	602.	31.	0.930	0.883	2.4 /-1.3
187	3A	0.310	1.589	1.016	601.	30.	0.931	0.886	2.6 / 0.0
188	5A	0.312	1.598	1.662	696.	30.	0.920	0.875	2.3 /-2.2
189	7A	0.316	1.427	0.693	599.	30.	0.931	0.885	2.3 / 0.1
190	6A	0.319	1.443	1.111	754.	29.	0.914	0.871	2.3 /-1.9
193	11B	0.821	4.062	1.640	10818.	-40.	0.230	0.284	-1.2 / 0.0
194	12B	0.820	4.070	2.603	10805.	-40.	0.230	0.285	-1.2 / 0.0
195	1B	0.815	4.137	3.389	10804.	-40.	0.231	0.285	-1.2 / 0.4
196	3B	0.803	3.647	1.266	10803.	-40.	0.231	0.284	-1.3 / 0.1
197	4B	0.809	3.680	2.082	10799.	-40.	0.231	0.285	-1.2 / 0.2
198	5B	0.816	3.701	2.567	10800.	-40.	0.231	0.285	-1.2 / 0.3
199	7B	0.814	3.212	0.915	10805.	-40.	0.230	0.285	-1.4 / 0.1
201	8B	0.815	3.228	1.488	10802.	-40.	0.231	0.285	-1.4 / 0.2
202	9B	0.817	3.232	1.824	10804.	-40.	0.231	0.285	-1.4 / 0.1
205	3C	0.795	3.122	1.484	11414.	-44.	0.209	0.263	-0.9 / 0.3
206	2C	0.697	3.142	1.517	9591.	-31.	0.278	0.330	-1.1 /-0.9
207	1C	0.605	3.176	1.529	7028.	-13.	0.404	0.447	-1.3 / 0.5

NOTE: PO = 101325. N / M^2
ρ_0 = 0.12492 KG-SEC^2/ M^4
TEMPERATURE, PRESSURE & DENSITY ARE STATIC CONDITION

* INFLOW ANGLE IS AIRPLANE ANGLE-OF-ATTACK + NACELLE TILT
SLIP ANGLE IS AIRPLANE SIDESLIP

FIGURES

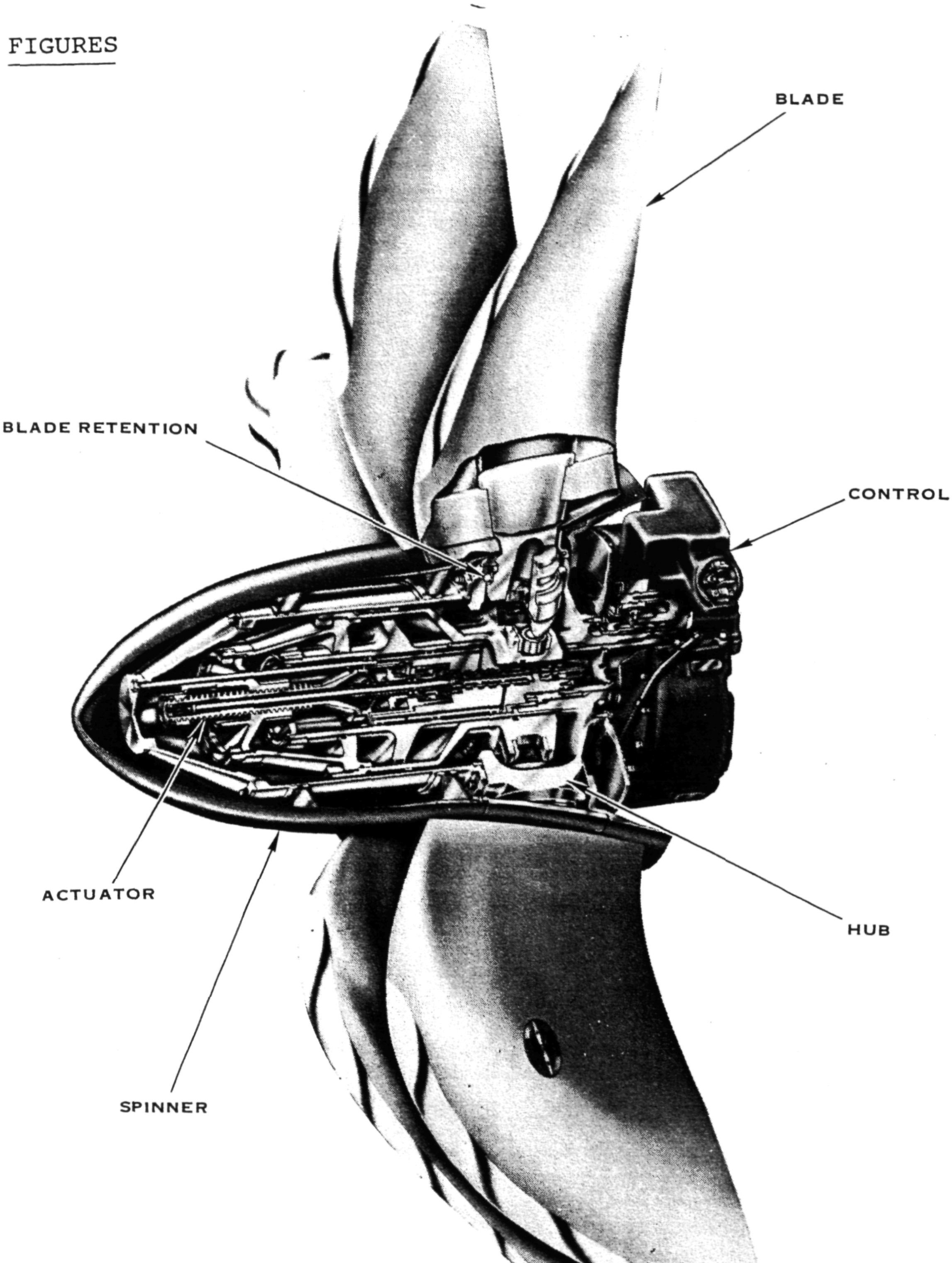

FIGURE 1. LARGE SCALE ADVANCED PROP-FAN (LAP)

FIGURE 2. SR-7L LAP PROP-FAN INSTALLED ON PTA AIRCRAFT

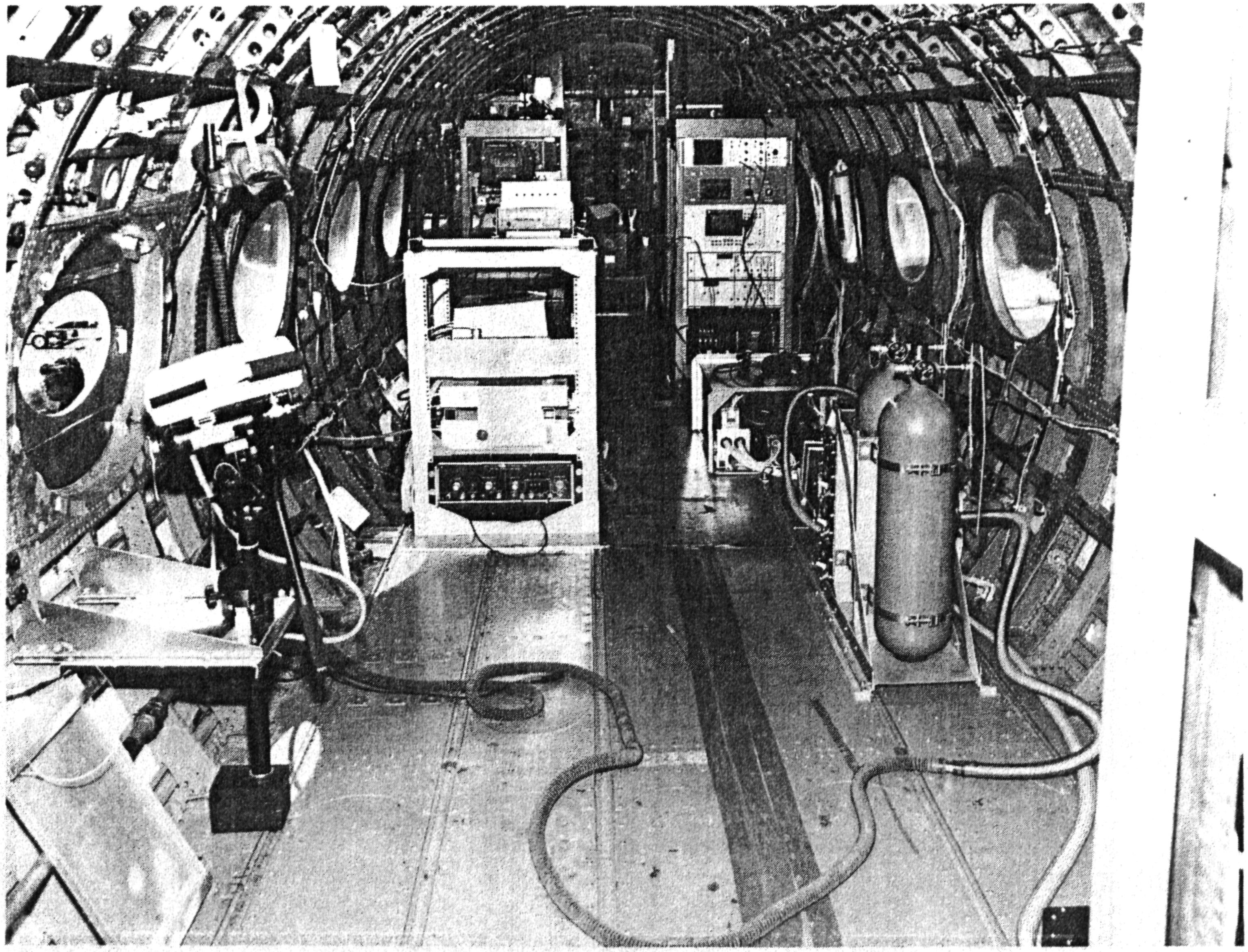

FIGURE 3. PTA AIRCRAFT INTERIOR

ORIGINAL PAGE
BLACK AND WHITE PHOTOGRAPH

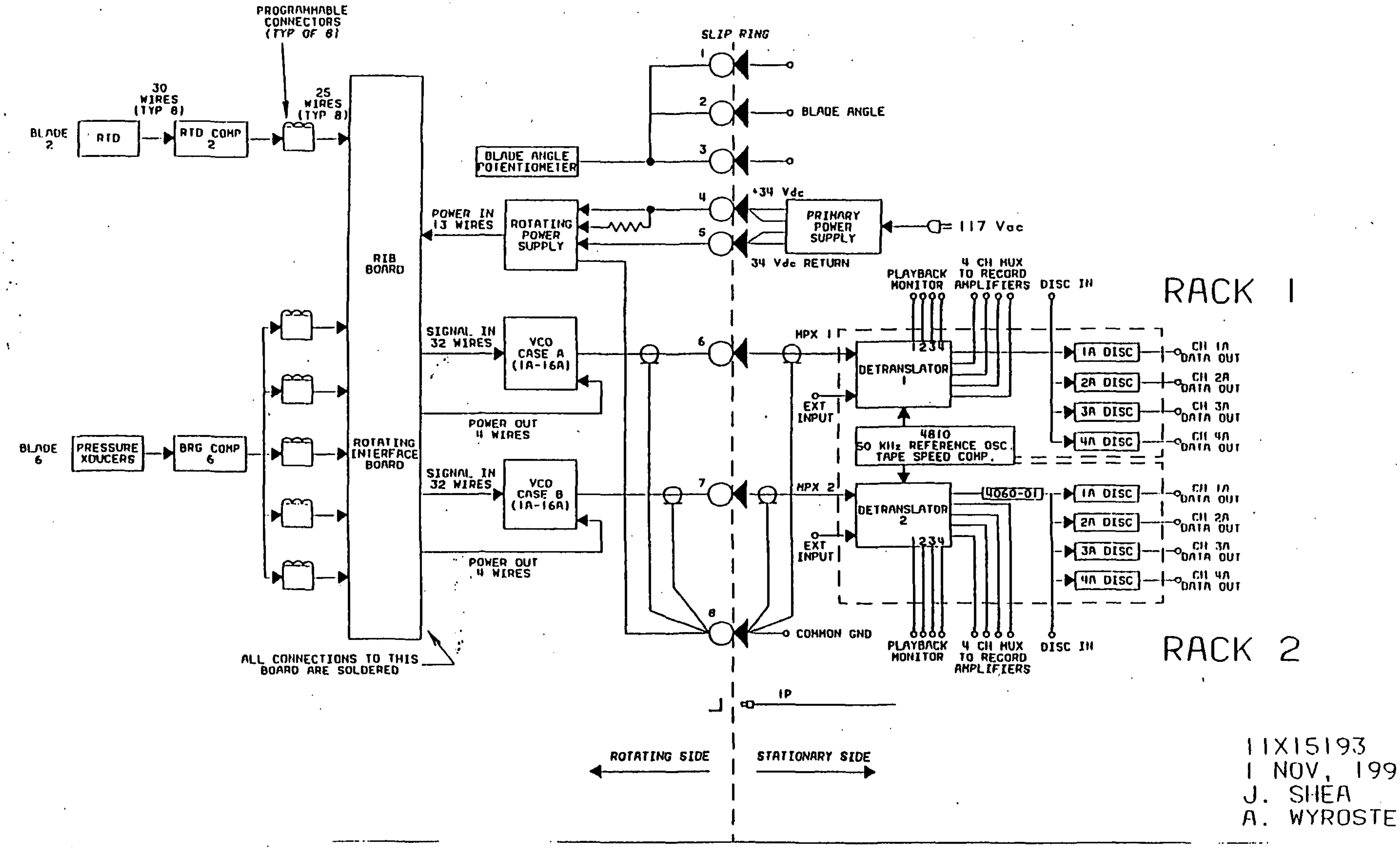

FIGURE 4. LAP FOLLOW-ON INSTRUMENTATION BLOCK DIAGRAM

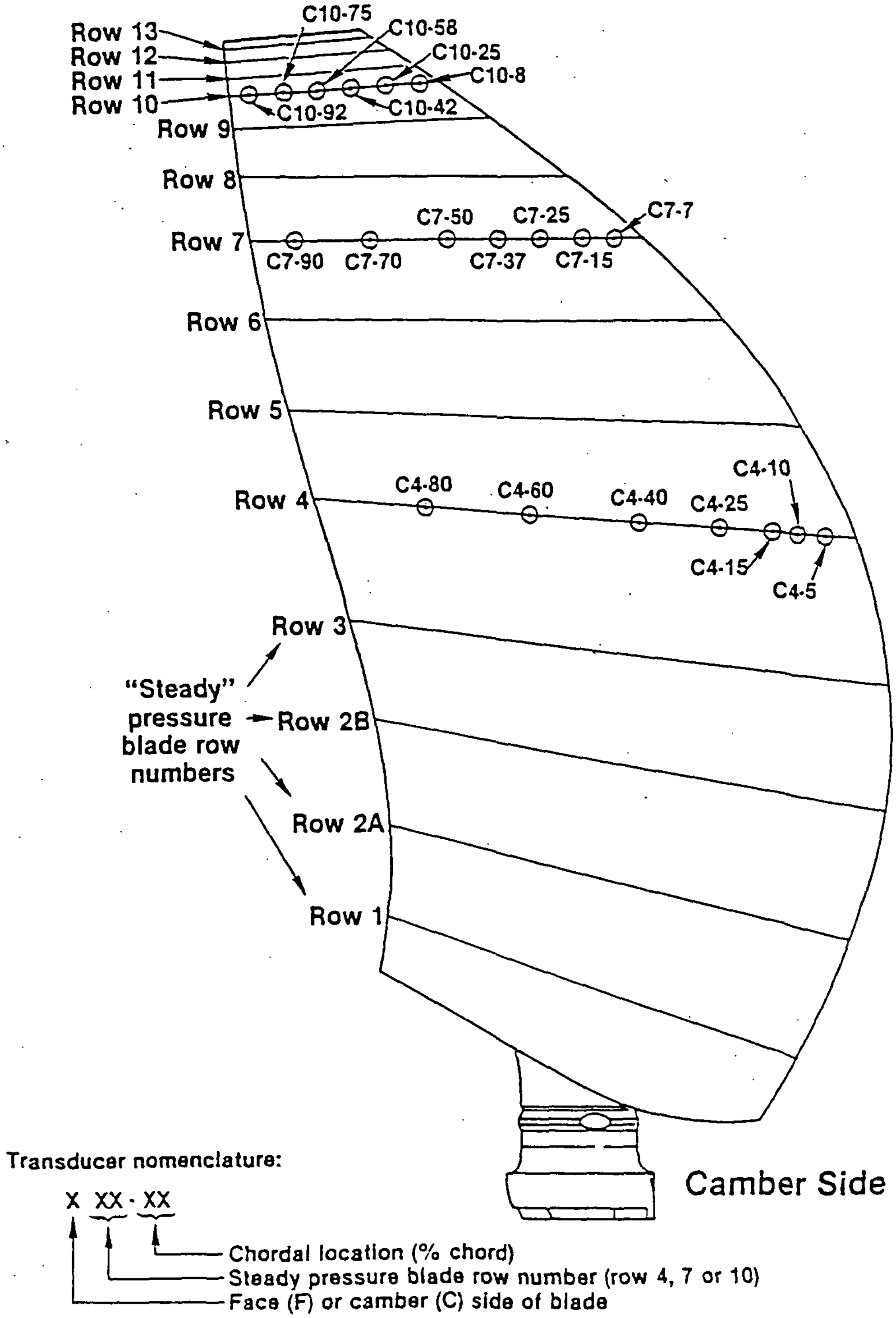

FIGURE 5. UNSTEADY PRESSURE BLADE TRANSDUCER LOCATIONS

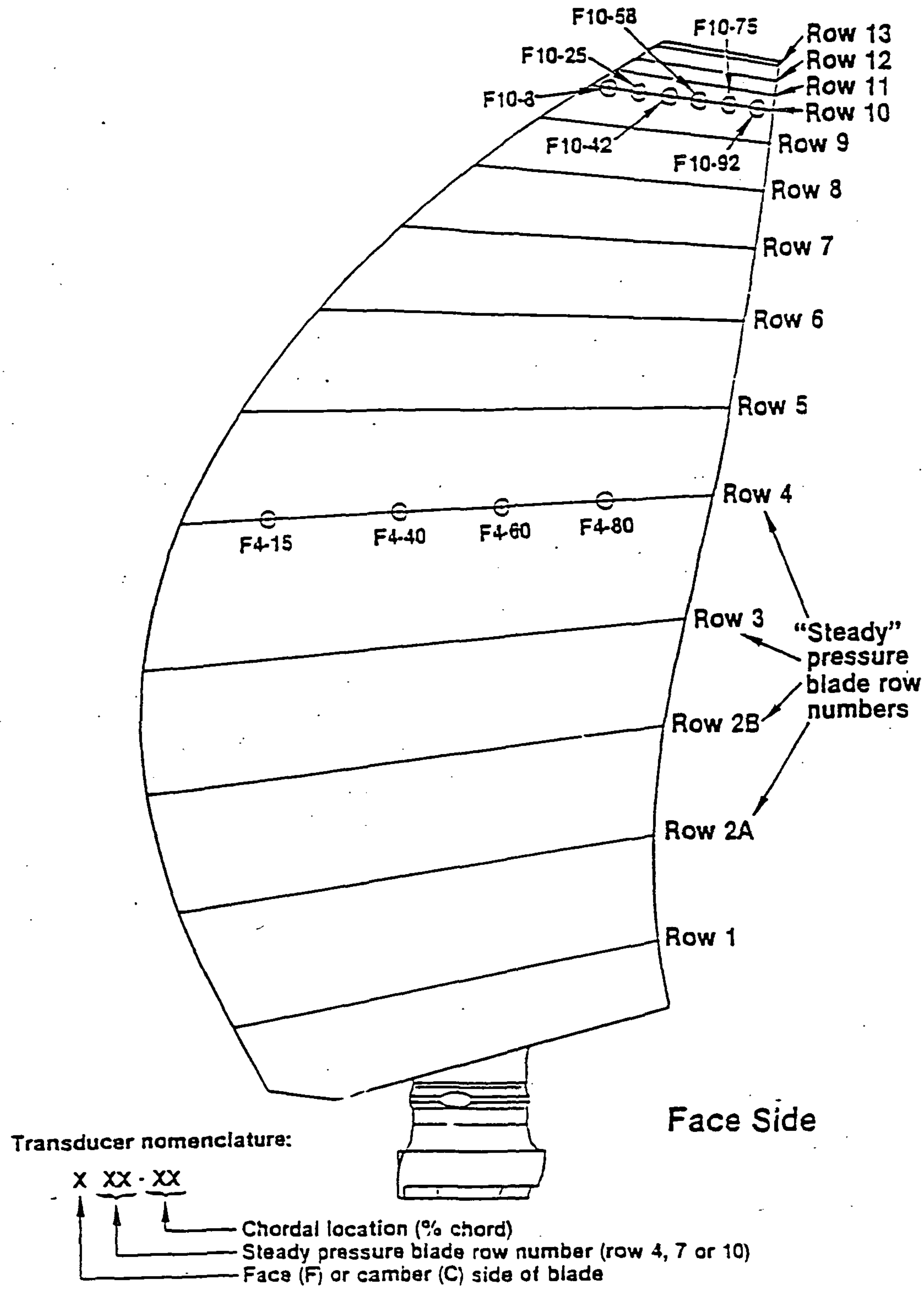

FIGURE 6. UNSTEADY PRESSURE BLADE TRANSDUCER LOCATIONS

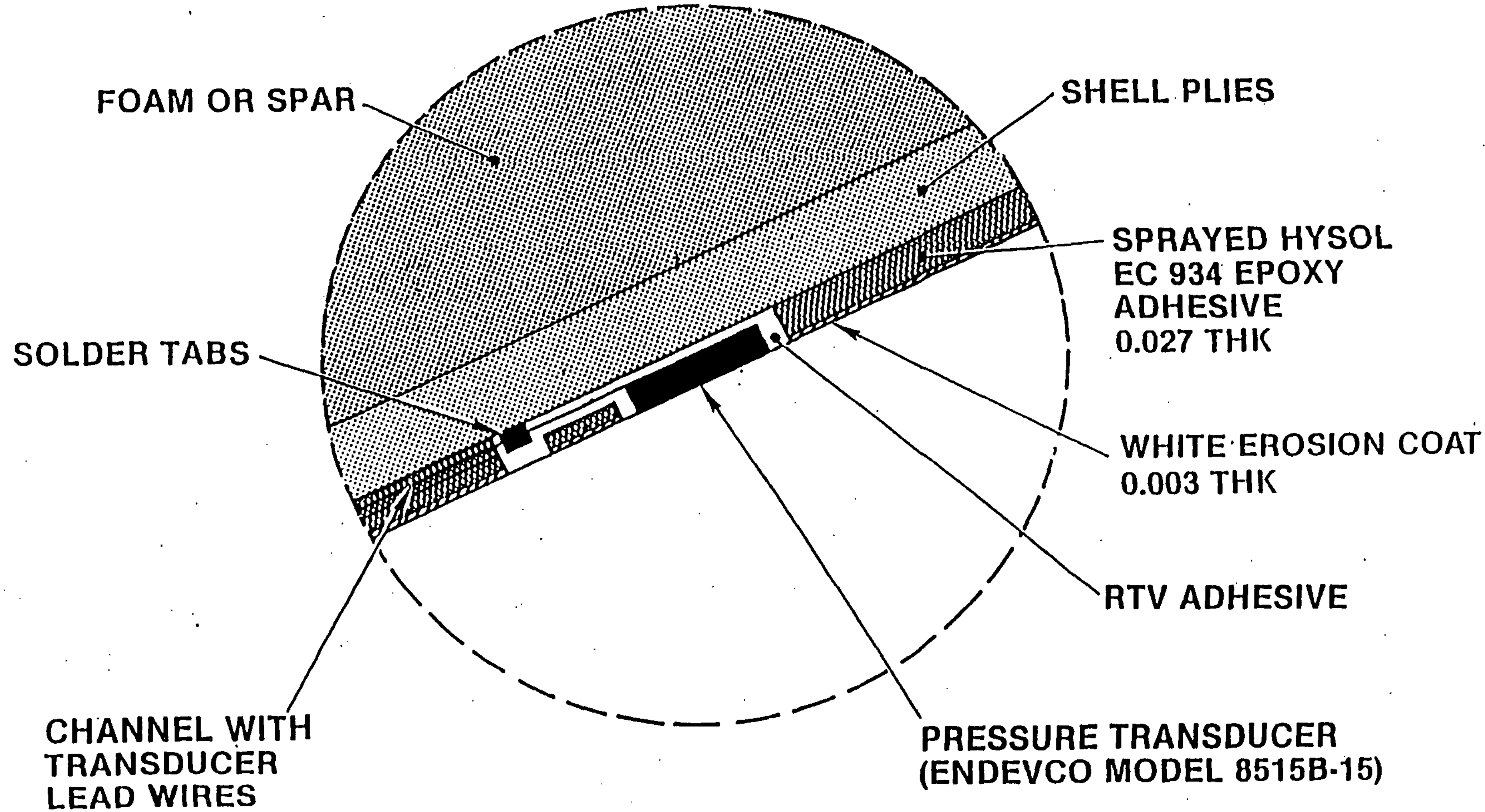

FIGURE 7. LAP UNSTEADY PRESSURE BLADE TRANSDUCER MOUNTING

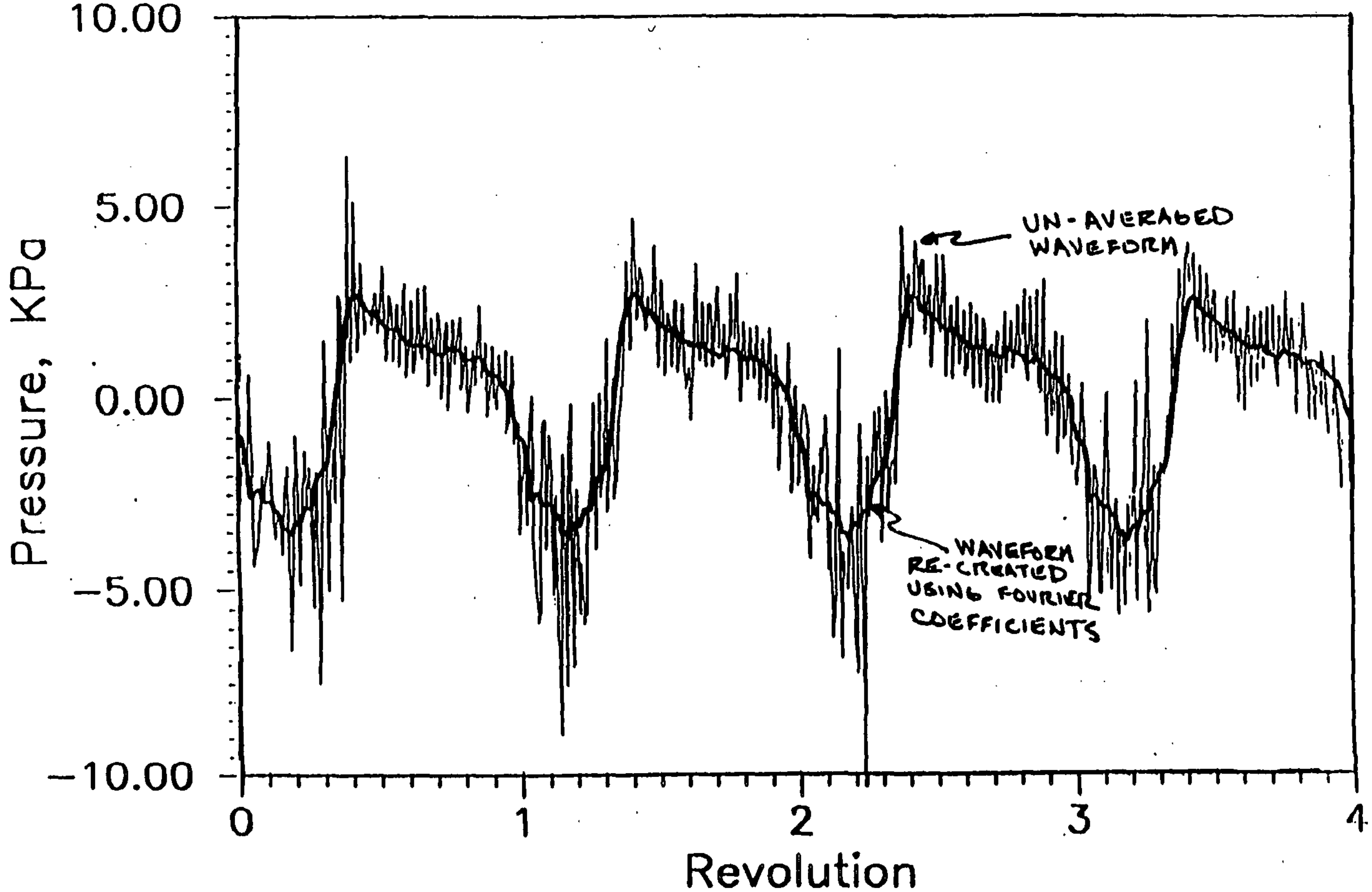

FIGURE 8. COMPARISON OF UN-AVERAGED WAVEFORM AND WAVEFORM CREATED WITH FOURIER COEFFICIENTS

RUN NUMBER: 182 TEST ID: 10A TRANSDUCER: C4-5

NACELLE TILT: -3 DEGREES
ALTITUDE: 610. METERS
STATIC PRESSURE RATIO: 0.930
BLADE ANGLE: 38.7 DEGREES
MACH NUMBER: 0.310

RADIUS RATIO: 0.680
TEMP: 32. DEGREES C
DENSITY RATIO: 0.884
POWER COEFFICIENT: 0.957
ADVANCE RATIO: 1.792

BLADE SURFACE STEADY PRESSURE COEFFICIENT: -0.146

K	PRESSURE IN PASCALS REAL	IMAGINARY	AMPLITUDE	PRESSURE COEFFICIENT
1	-.1937E+04	0.1345E+04	0.2358E+04	0.1527E+00
2	0.4319E+03	0.6398E+02	0.4366E+03	0.2827E-01
3	-.6393E+02	-.1598E+02	0.6590E+02	0.4268E-02
4	0.4793E+02	0.1598E+02	0.5052E+02	0.3272E-02
5	-.1597E+02	-.1597E+02	0.2259E+02	0.1463E-02
6	-.1597E+02	0.1597E+02	0.2258E+02	0.1463E-02
7	0.1597E+02	-.3194E+02	0.3571E+02	0.2312E-02
8	-.1597E+02	0.3194E+02	0.3571E+02	0.2313E-02
9	-.1597E+02	-.1597E+02	0.2258E+02	0.1463E-02
10	0.3195E+02	0.0000E+00	0.3195E+02	0.2069E-02
11	-.1598E+02	0.0000E+00	0.1598E+02	0.1035E-02
12	0.0000E+00	0.1598E+02	0.1598E+02	0.1035E-02
13	0.0000E+00	-.1598E+02	0.1598E+02	0.1035E-02
14	-.1598E+02	0.1598E+02	0.2260E+02	0.1464E-02
15	-.1598E+02	-.1598E+02	0.2260E+02	0.1464E-02
16	0.0000E+00	0.1598E+02	0.1598E+02	0.1035E-02
17	0.1599E+02	-.1599E+02	0.2261E+02	0.1464E-02
18	-.1599E+02	0.1599E+02	0.2261E+02	0.1464E-02
19	0.1599E+02	0.0000E+00	0.1599E+02	0.1035E-02
20	-.1598E+02	0.0000E+00	0.1598E+02	0.1035E-02
21	0.0000E+00	-.1598E+02	0.1598E+02	0.1035E-02
22	0.1598E+02	0.1598E+02	0.2261E+02	0.1464E-02
23	-.1598E+02	0.0000E+00	0.1598E+02	0.1035E-02
24	0.0000E+00	0.0000E+00	0.0000E+00	0.0000E+00
25	0.0000E+00	0.0000E+00	0.0000E+00	0.0000E+00
26	0.0000E+00	0.1599E+02	0.1599E+02	0.1035E-02
27	0.0000E+00	-.1599E+02	0.1599E+02	0.1036E-02
28	0.0000E+00	0.0000E+00	0.0000E+00	0.0000E+00
29	0.0000E+00	-.1600E+02	0.1600E+02	0.1036E-02
30	0.0000E+00	0.0000E+00	0.0000E+00	0.0000E+00
31	0.1602E+02	0.0000E+00	0.1602E+02	0.1038E-02
32	0.0000E+00	0.0000E+00	0.0000E+00	0.0000E+00
33	-.1606E+02	0.0000E+00	0.1606E+02	0.1040E-02
34	0.0000E+00	0.0000E+00	0.0000E+00	0.0000E+00
35	0.0000E+00	-.1611E+02	0.1611E+02	0.1043E-02

FIGURE 9. EXAMPLE OF DATA PRESENTATION FORM

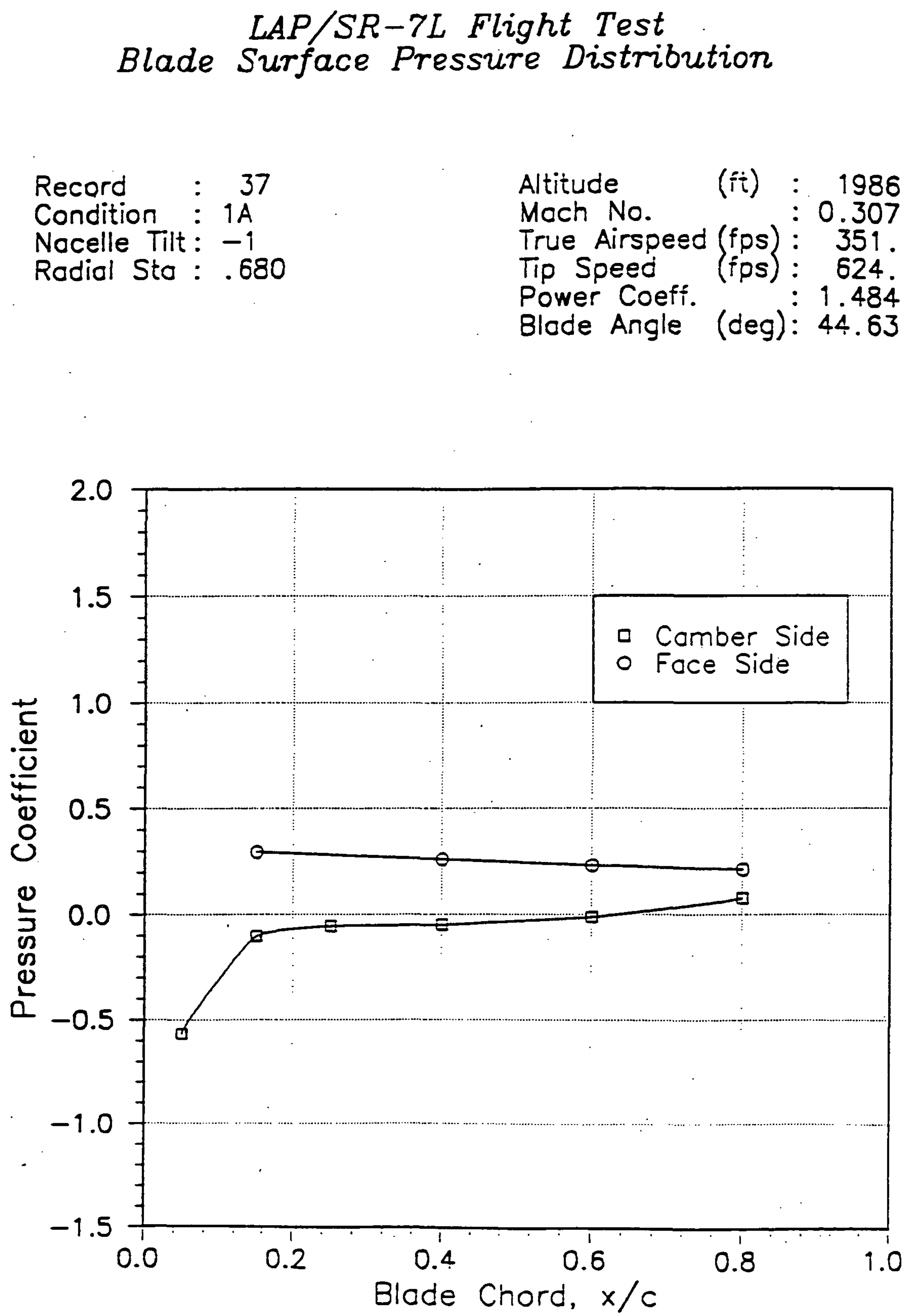

FIGURE 10. TYPICAL STEADY PRESSURE COEFFICIENT PLOT

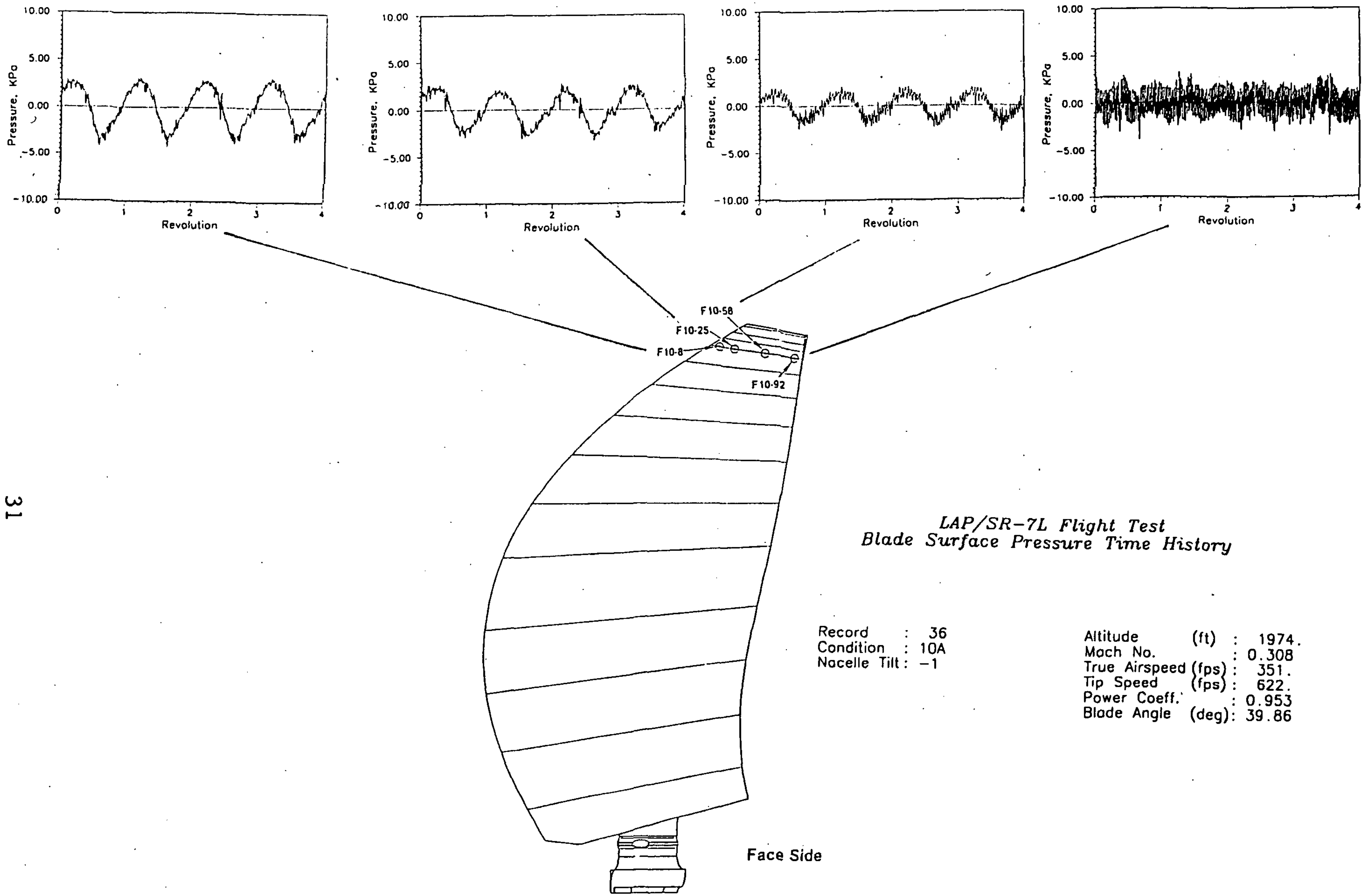

FIGURE 11. TYPICAL UNSTEADY BLADE SURFACE PRESSURE TIME HISTORIES AS A FUNCTION OF BLADE CHORD FOR A TYPICAL TAKE-OFF MACH NUMBER OF 0.30

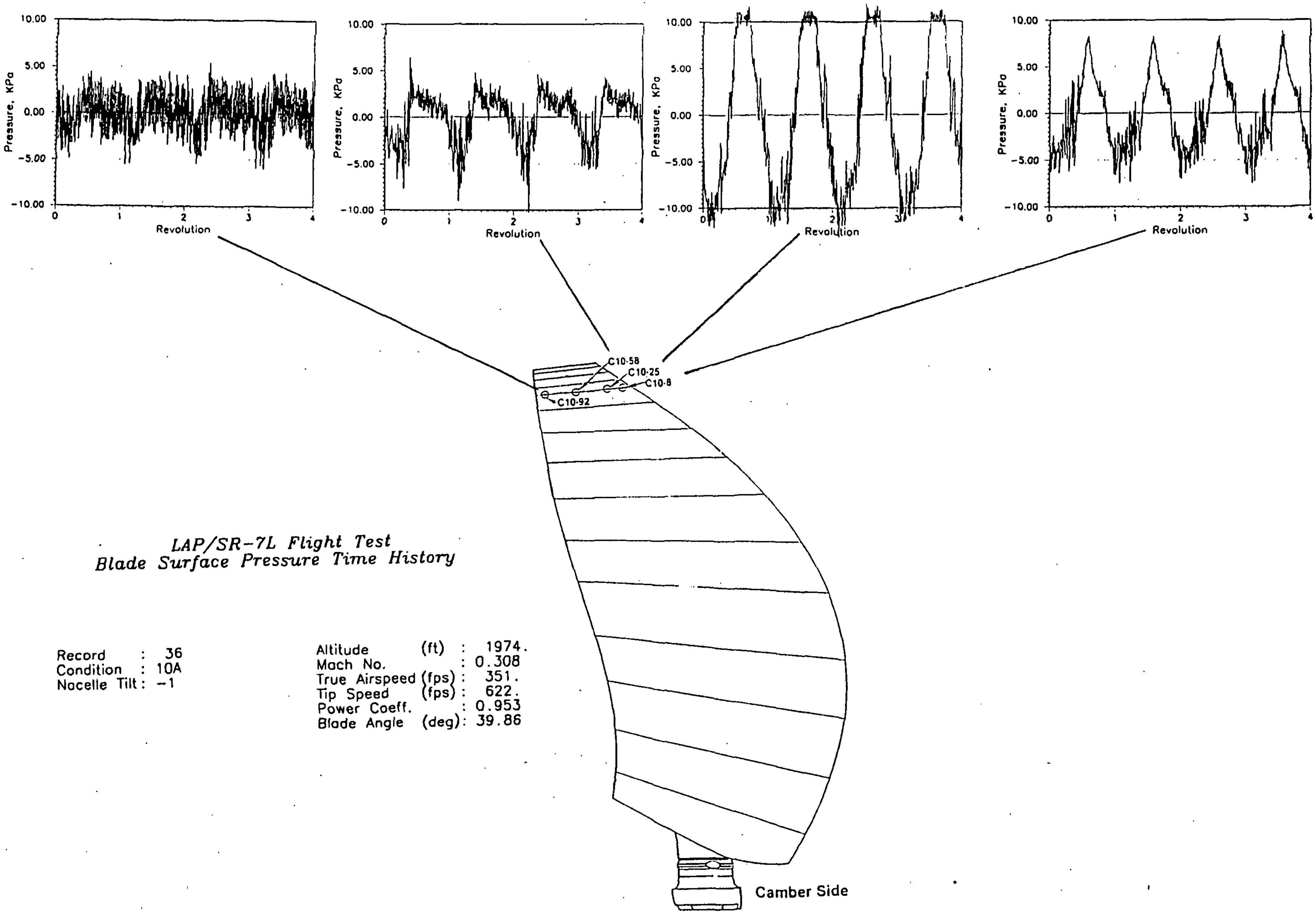

FIGURE 12. TYPICAL UNSTEADY BLADE SURFACE PRESSURE TIME HISTORIES AS A FUNCTION OF BLADE CHORD FOR A TAKE-OFF MACH NUMBER OF 0.30.

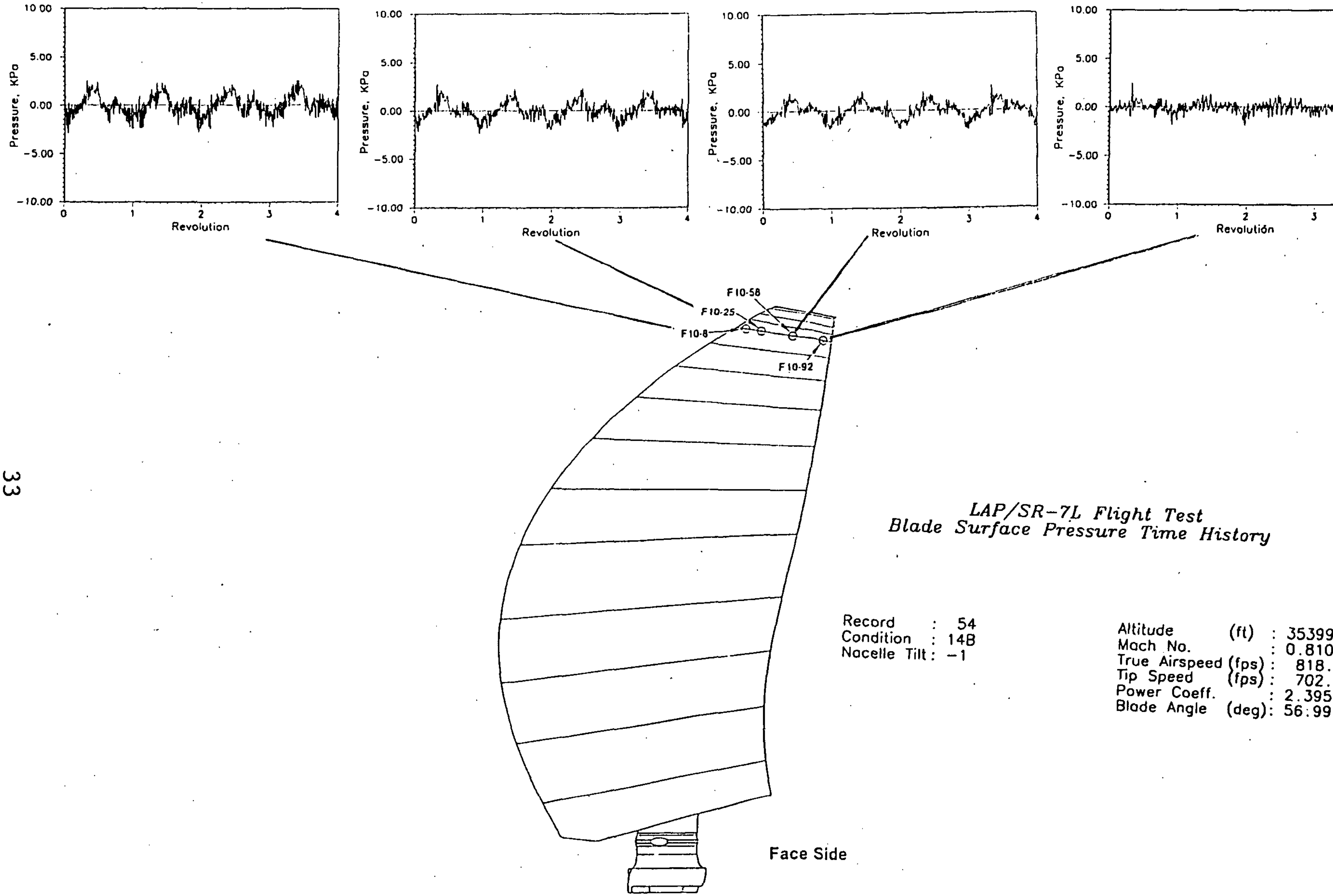

FIGURE 13. TYPICAL UNSTEADY BLADE SURFACE PRESSURE TIME HISTORIES AS A FUNCTION OF BLADE CHORD FOR A CRUISE MACH NUMBER OF 0.810

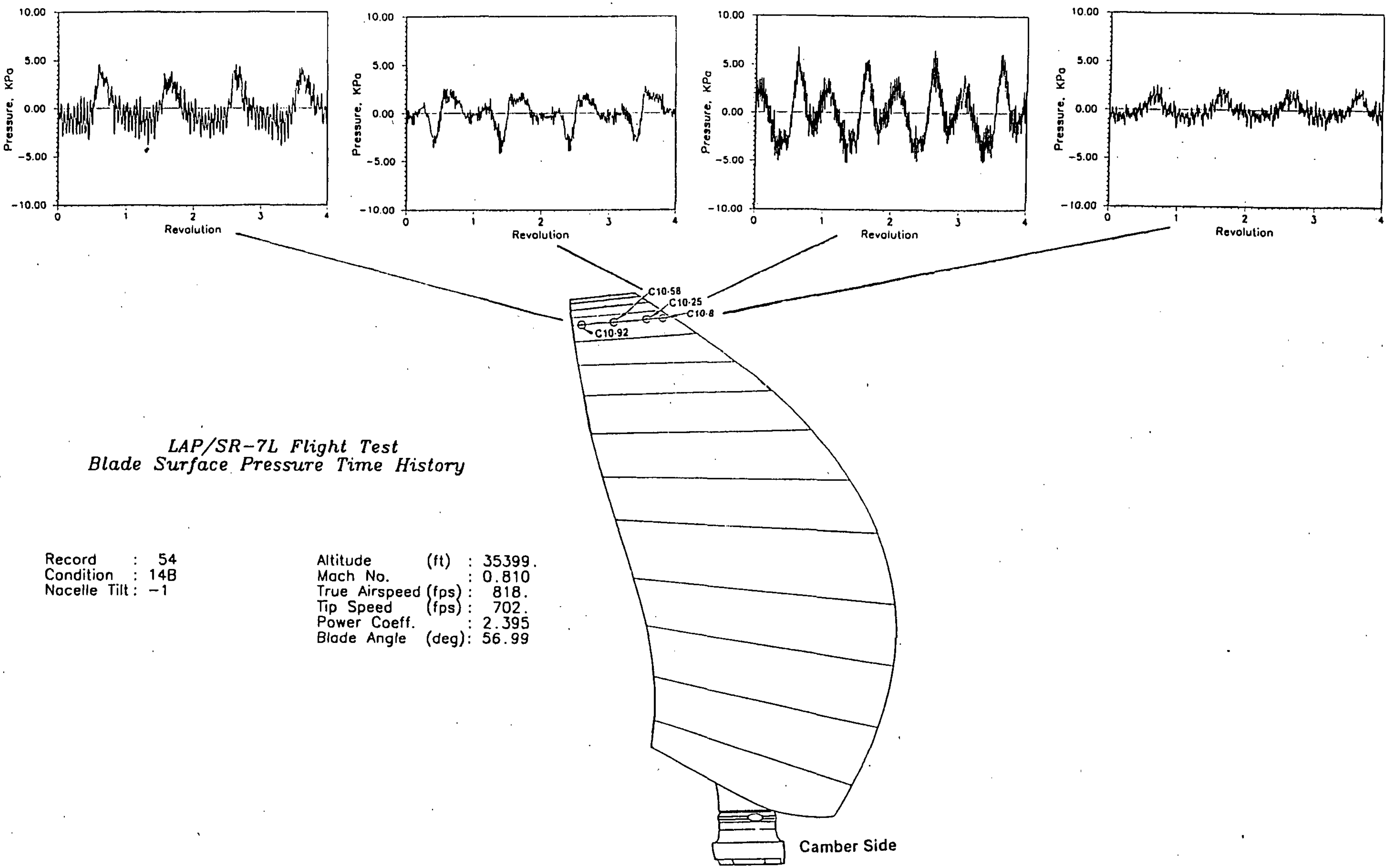

FIGURE 14. TYPICAL UNSTEADY BLADE SURFACE PRESSURE TIME HISTORIES AS A FUNCTION OF BLADE CHORD FOR A CRUISE MACH NUMBER OF 0.810

Record	: 36	Altitude	(ft)	:	1974.
Condition	: 10A	Mach No.		:	0.308
Nacelle Tilt	: −1	True Airspeed	(fps)	:	351.
Transducer	: F10−8	Tip Speed	(fps)	:	622.
		Power Coeff.		:	0.953
		Blade Angle	(deg)	:	39.86

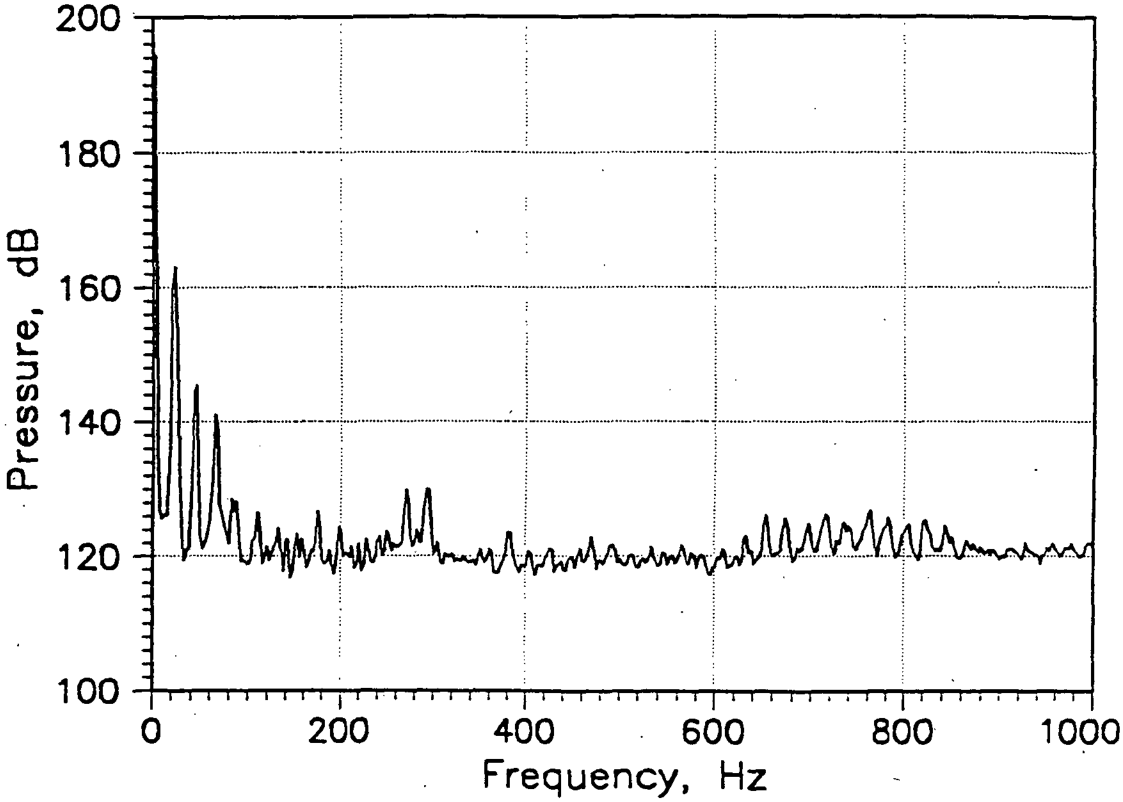

FIGURE 15. BLADE SURFACE PRESSURE SPECTRUM

Record	36	Altitude (ft)	1974.
Condition	10A	Mach No.	0.308
Nacelle Tilt	−1	True Airspeed (fps)	351.
Transducer	C10−8	Tip Speed (fps)	622.
		Power Coeff.	0.953
		Blade Angle (deg)	39.86

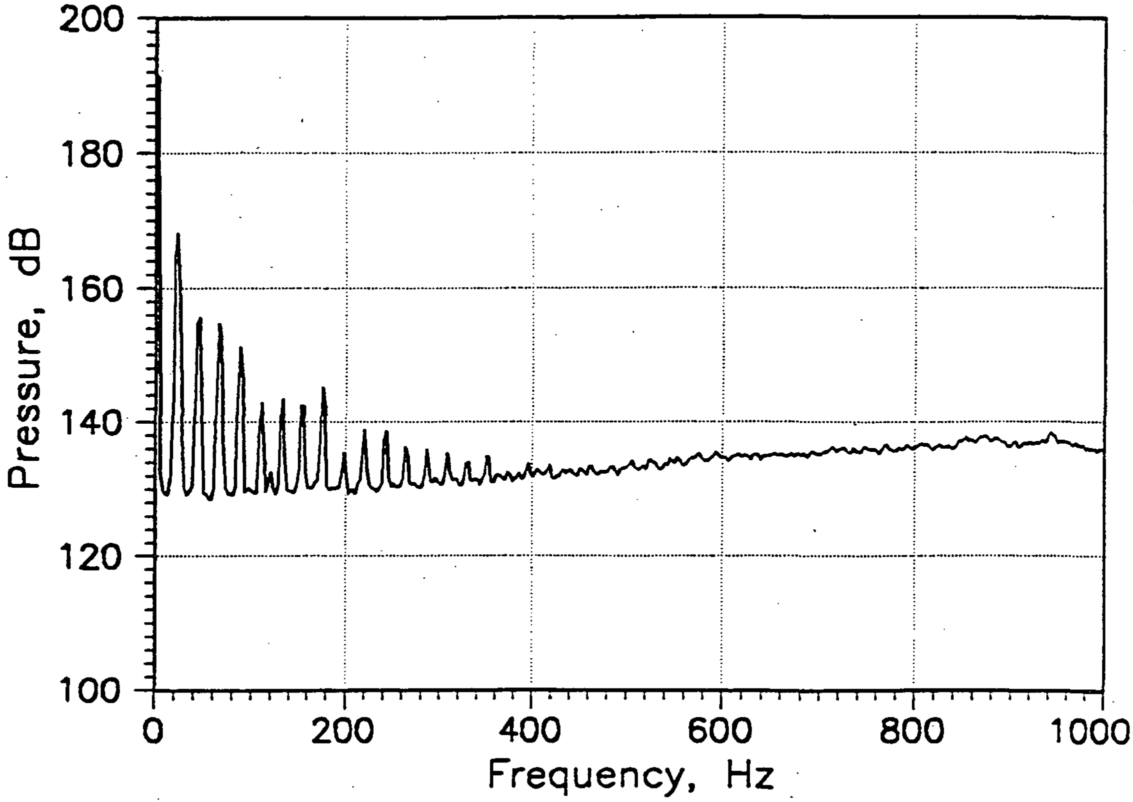

FIGURE 16. BLADE SURFACE PRESSURE SPECTRUM

Record : 54
Condition : 14B
Nacelle Tilt : −1
Transducer : F10−8

Altitude (ft) : 35399.
Mach No. : 0.810
True Airspeed (fps) : 818.
Tip Speed (fps) : 702.
Power Coeff. : 2.395
Blade Angle (deg) : 56.99

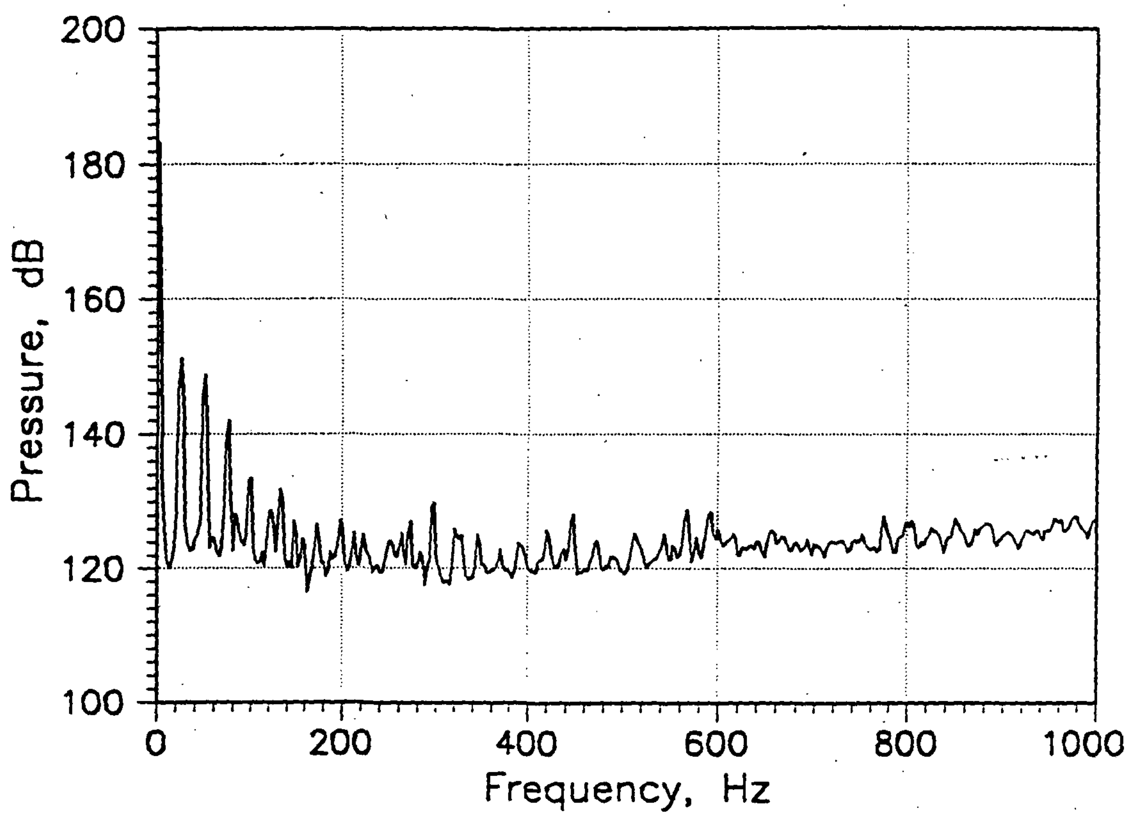

FIGURE 17. BLADE SURFACE PRESSURE SPECTRUM

Record	:	54	Altitude (ft)	:	35399.
Condition	:	14B	Mach No.	:	0.810
Nacelle Tilt	:	−1	True Airspeed (fps)	:	818.
Transducer	:	C10−8	Tip Speed (fps)	:	702.
			Power Coeff.	:	2.395
			Blade Angle (deg)	:	56.99

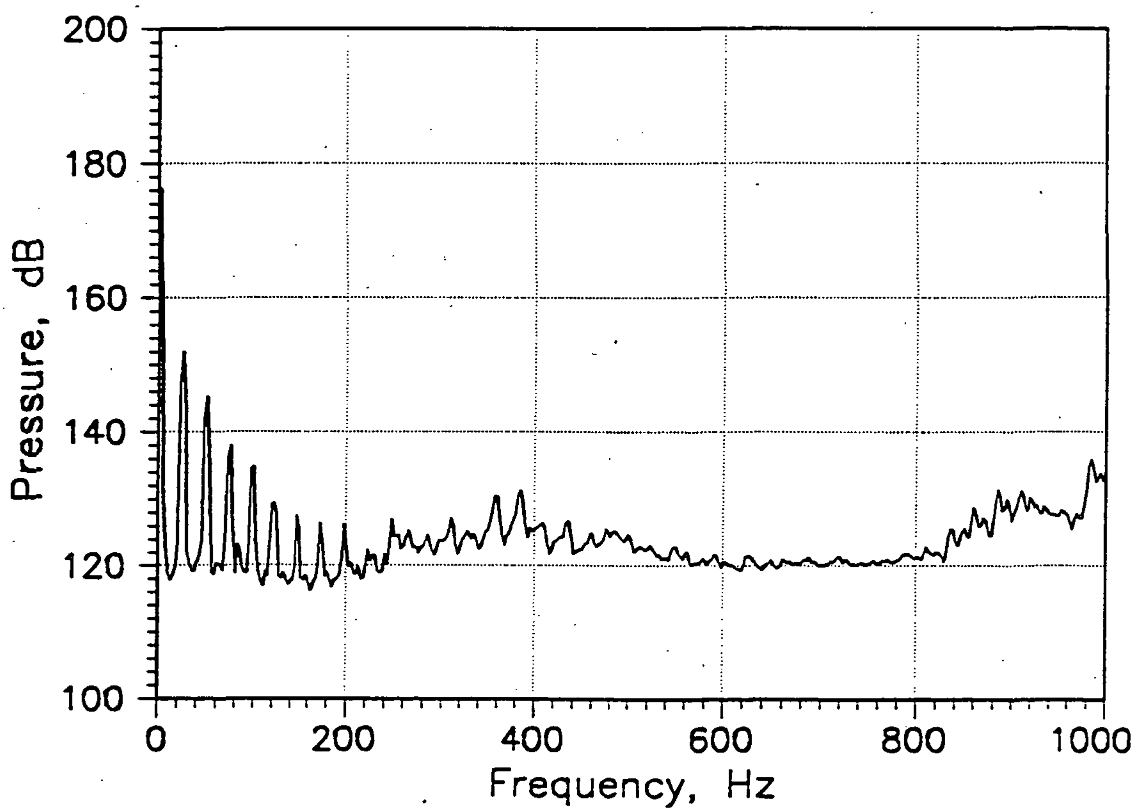

FIGURE 18. BLADE SURFACE PRESSURE SPECTRUM

APPENDIX A

THERMOGRAPHY DATA
(BLADE TEMPERATURE DISTRIBUTION)

Background

Concern that heating of the blades due to air friction could cause an unacceptable error in the pressure transducer data created the need to accurately define the blade surface temperatures. The heating is typically evaluated by classical adiabatic, flat plate theory at each radial location. The local blade surface temperatures are then used to correct the measured unsteady pressure transducer data. However, previous infrared photography of counter-rotating Prop-Fan models revealed that the blade leading edge is cooler, i.e., has less frictional heating, than the middle of the chord or the trailing edge of the blade. Thus, a thermographic evaluation of blade surface temperatures was made during the LAP/PTA Follow-on Flight Test Program to evaluate the chordwise temperature variation at the transducer locations.

Infrared Video Testing System

Hughes Thermographic equipment was used to display images of the blade surface temperatures. The thermography technique uses a detector material that is sensitive to incoming radiation and generates an electro-magnetic response that is translated into surface temperatures of an object. The Hughes thermographic equipment was chosen over other thermographic equipment for several reasons. The primary reason was because of its ability to permit 'strobe-like' imaging and therefore provide meaningful results for a rotating object.

The infrared video system was mounted in the PTA GII test aircraft where the SR-7L blades could be viewed through a modified aircraft window. In order to get views of both sides of the blades, separate flights were required for data taken on the face and camber sides of the blades.

Data Evaluation

The flight conditions chosen for evaluation are summarized in Table A1. The actual flight test data had some variation in the conditions, thus the parameters in Table A1 represent the target values. The thermography data was recorded on about 10 hours of video tape, copies of which were sent to NASA. The objective of this appendix is to summarize how that data was used.

The video data was used to obtain a set of still photographs which could be used to determine the blade surface temperatures at the locations of the pressure transducers. One blade was instrumented with Resistance Temperature Detectors (RTDs), which provided a means of verifying and correlating the thermography results. The pressure transducer and RTD locations and associated notation are shown in Figures A1 and A2 for the camber and face side of the blade, respectively.

Figure A3 shows an example thermographic picture. This illustrates how the vortex affects the temperature distribution along the leading edge on the camber (suction) side of the blade. It should be noted that the blades suction side can be identified by an "S" following the case number on each thermographic picture. At the tip of the blade, the temperature varies approximately 20^{o}F between the leading and trailing edge (green to red) for this case. The thermography for the face (pressure) side of the blade showed radial temperature variations and essentially no temperature variations chordwise, corresponding to no leading edge vortex and classical theory. For each test condition, approximately three pictures of both face and camber sides were evaluated to determine the temperature distribution at the pressure transducer and RTD locations. A set of the thermographic pictures is included in this appendix.

The average temperature corrections for each pressure transducer location are summarized in Table A2. They are expressed as an increase or decrease in temperature relative to the temperatures measured with the RTDs, which were located at the chord center line.

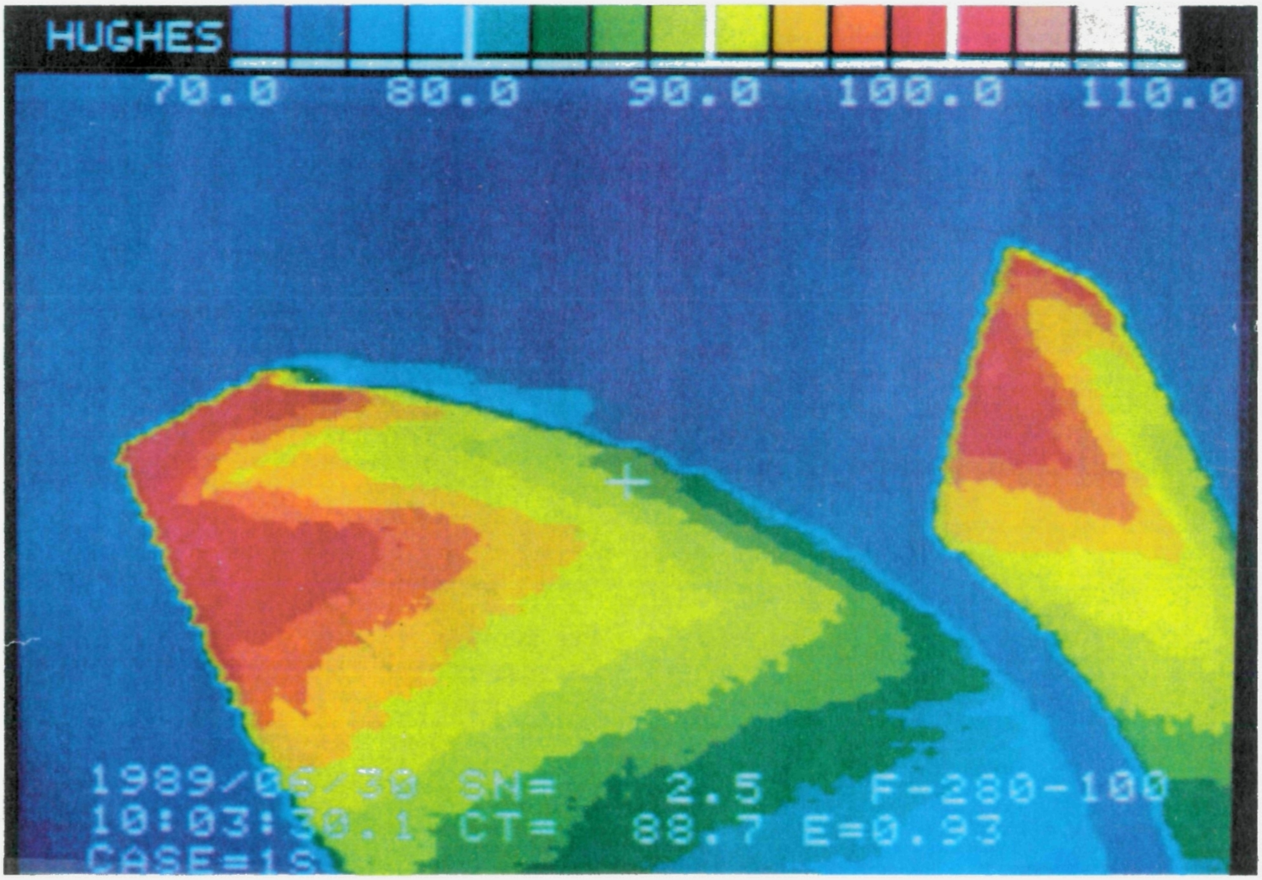

FIGURE A3. TYPICAL THERMOGRAPHY PHOTO

ORIGINAL PAGE
COLOR PHOTOGRAPH

TABLE A1.
PROP-FAN BLADE THERMOGRAPHY TEST CONDITIONS

Test Case	Altitude H_{PI} (Ft)	Airspeed (KIAS)	N_{pt} (%)	Torque (Ft-Lb)	Side of Blade
1	2,900	190	100	2703	Both
2				2163	
3				1622	
4	2,800	277	100	2740	
5				2316	
6				1737	
7	9,800	244	100	2466	
8				1973	
9				1480	
10			77	2857	
11				2285	
12				1714	
13	9,800	299	100	2599	
14				2079	
15				1559	
16	19,800	247	100	1999	Face
17				1600	
18				1200	
19	19,700	269	77	1204	
20	19,600	317	100	2199	
21				1759	
22				1319	

TABLE A2

Pressure Transducer Temperature Corrections

	Transducer Location	RTD Location	Correction to RTD Temperature (ºF)
F	F4-15	F3	0.
A	F4-40		0.
C	F4-60		0.
E	F4-80		0.
	F10-8	F1	0.
S	F10-25		0.
I	F10-42		0.
D	F10-58		0.
E	F10-75		0.
	F10-92		0.
C	C10-8	C1	-4.5
A	C10-25		-2.9
M	C10-42		0.
B	C10-58		+1.7
E	C10-75		+2.7
R	C10-92		+4.4
	C7-7	C2	-3.7
S	C7-15		-2.0
I	C7-25		-0.8
D	C7-37		-0.3
E	C7-50		0.0
	C7-70		0.5
	C7-90		0.7
	C4-5	C3	-1.8
	C4-10		-0.6
	C4-15		-0.3
	C4-25		-0.3
	C4-40		0.0
	C4-60		0.5
	C4-80		1.2

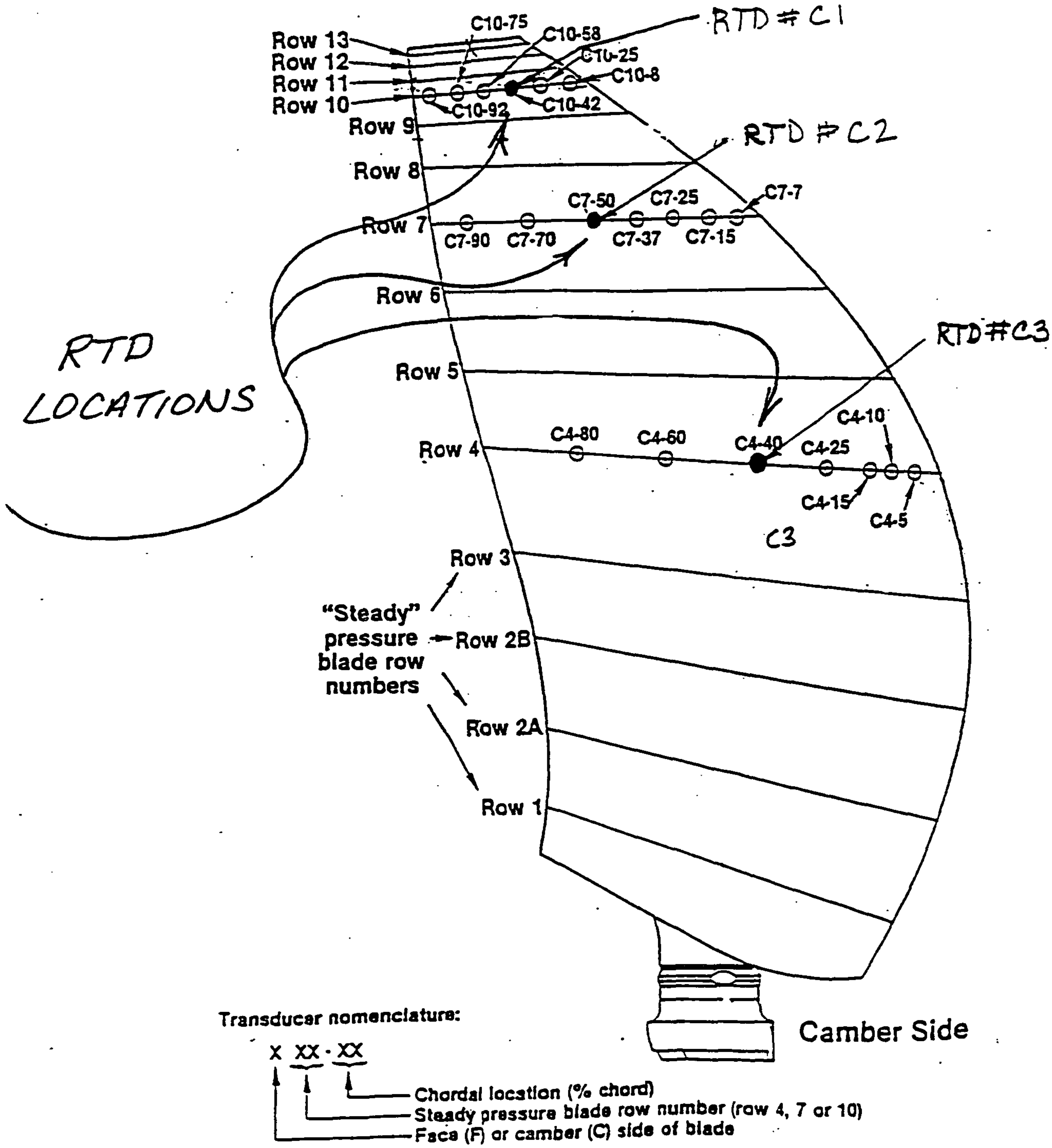

FIGURE A1. UNSTEADY PRESSURE BLADE TRANSDUCER LOCATIONS

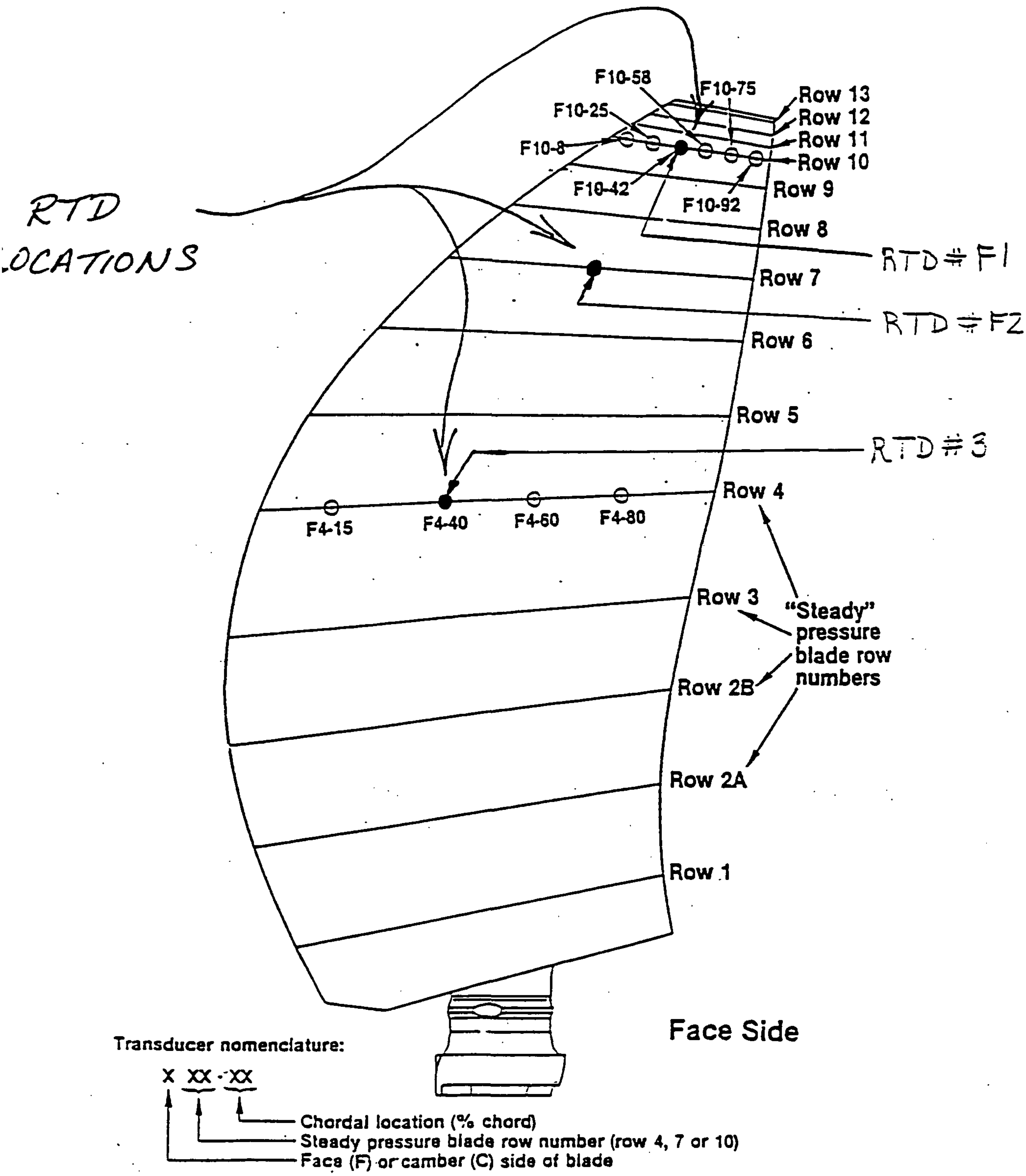

FIGURE A2. UNSTEADY PRESSURE BLADE TRANSDUCER LOCATIONS

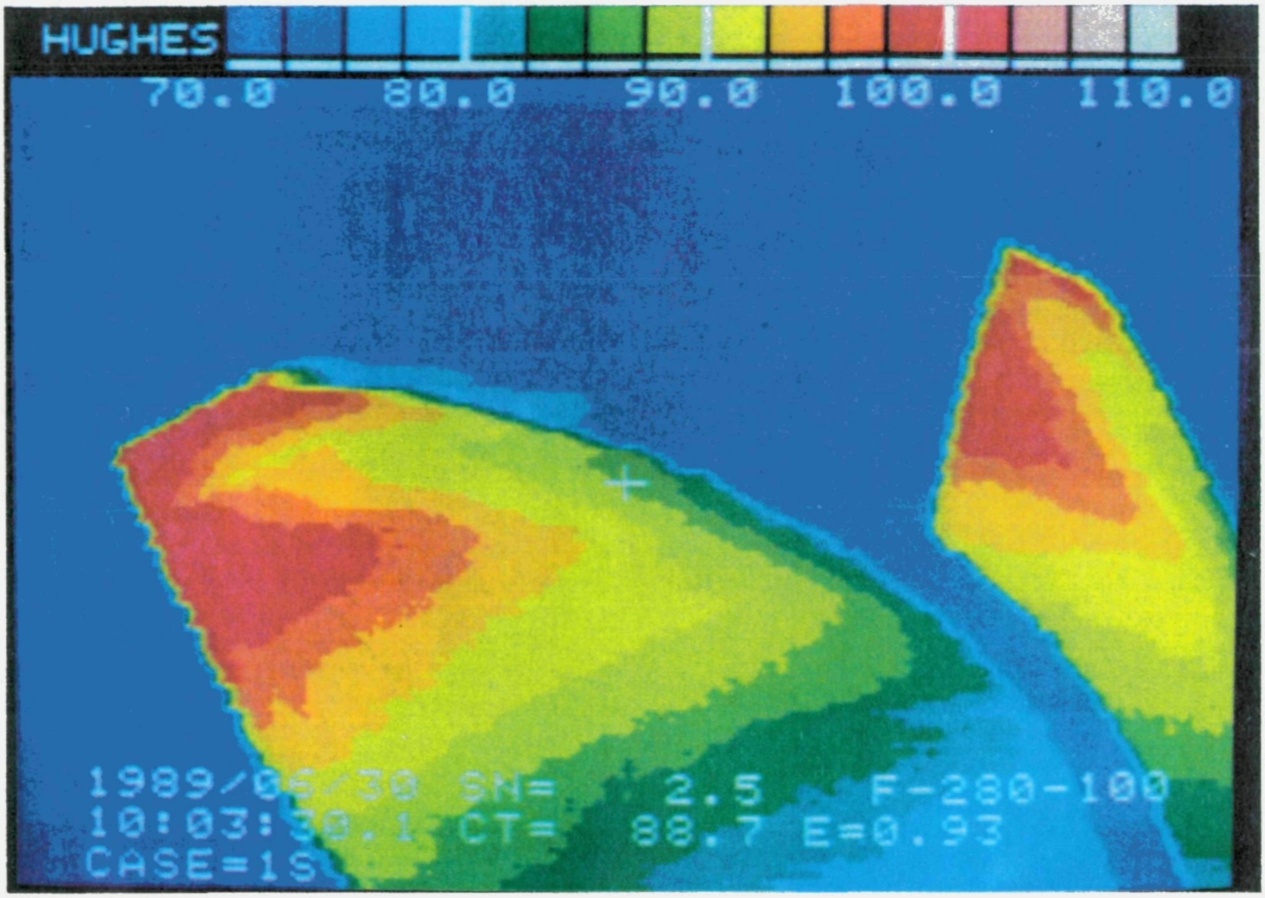

ORIGINAL PAGE
COLOR PHOTOGRAPH

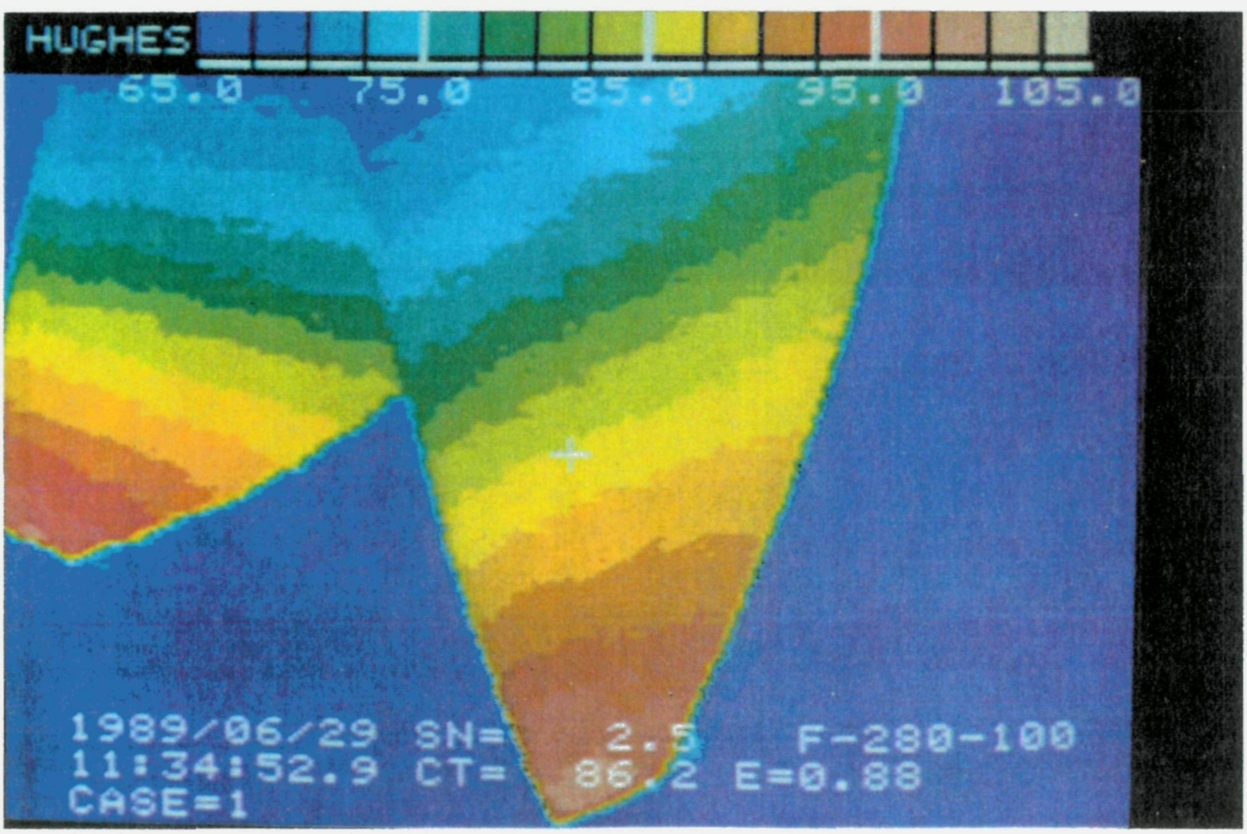

PAGE 46 INTENTIONALLY BLANK

PRECEDING PAGE BLANK NOT FILMED

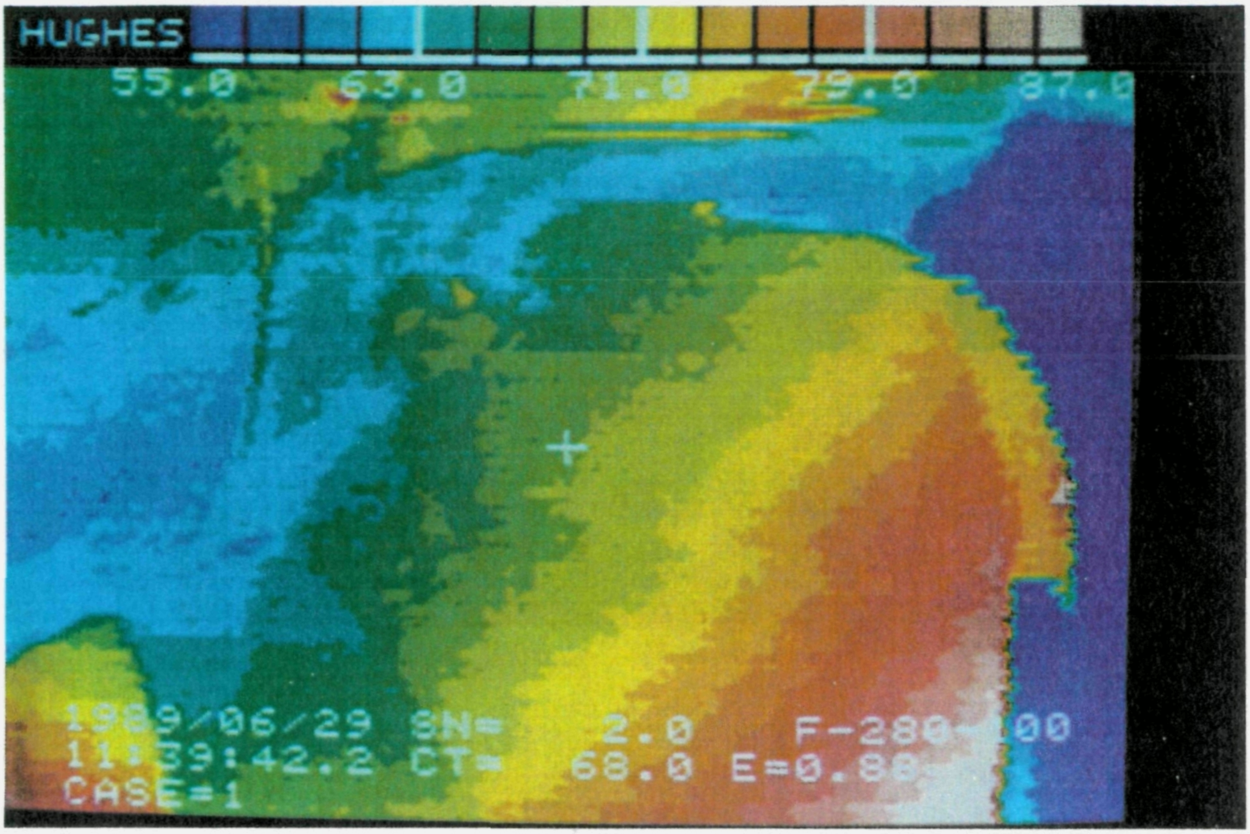

ORIGINAL PAGE
COLOR PHOTOGRAPH

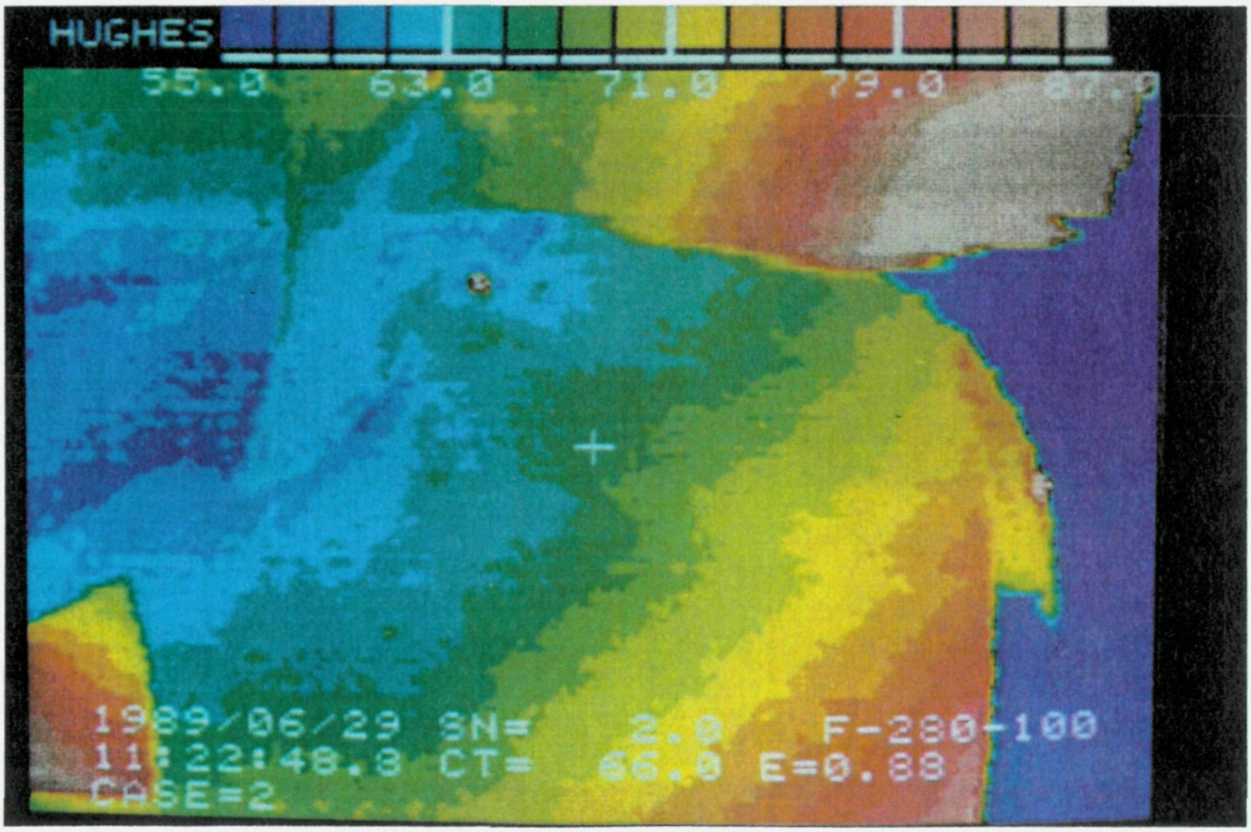

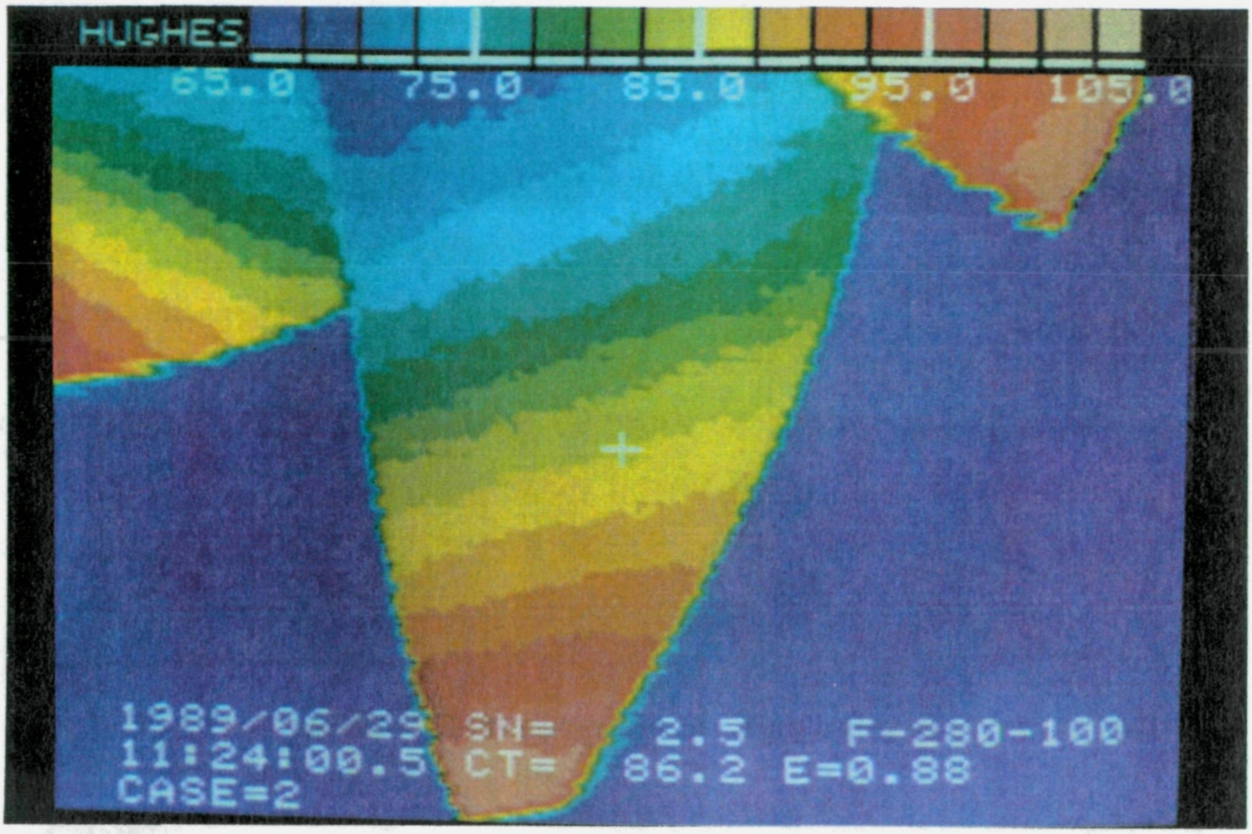

ORIGINAL PAGE
COLOR PHOTOGRAPH

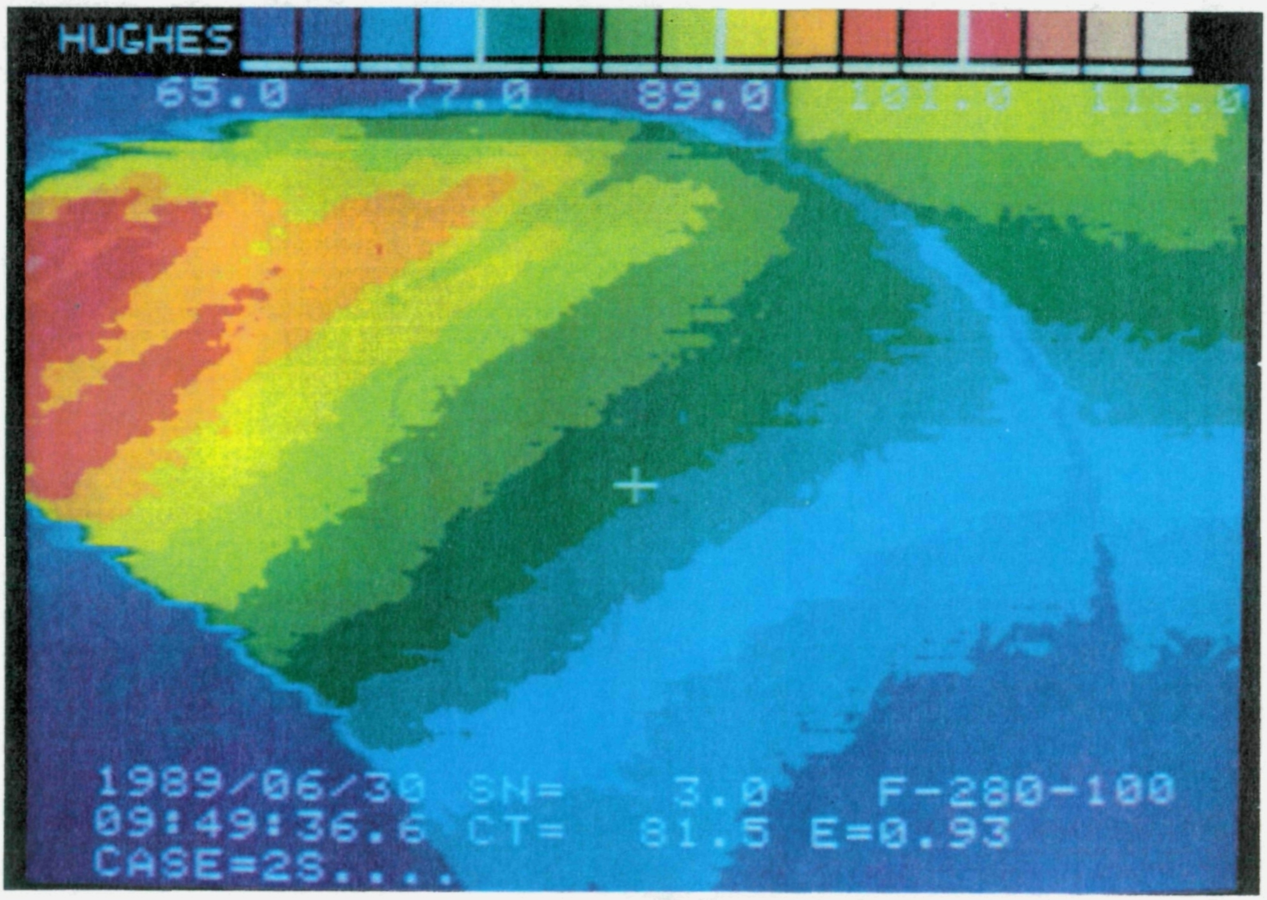

PAGE 50 INTENTIONALLY BLANK

PRECEDING PAGE BLANK NOT FILMED

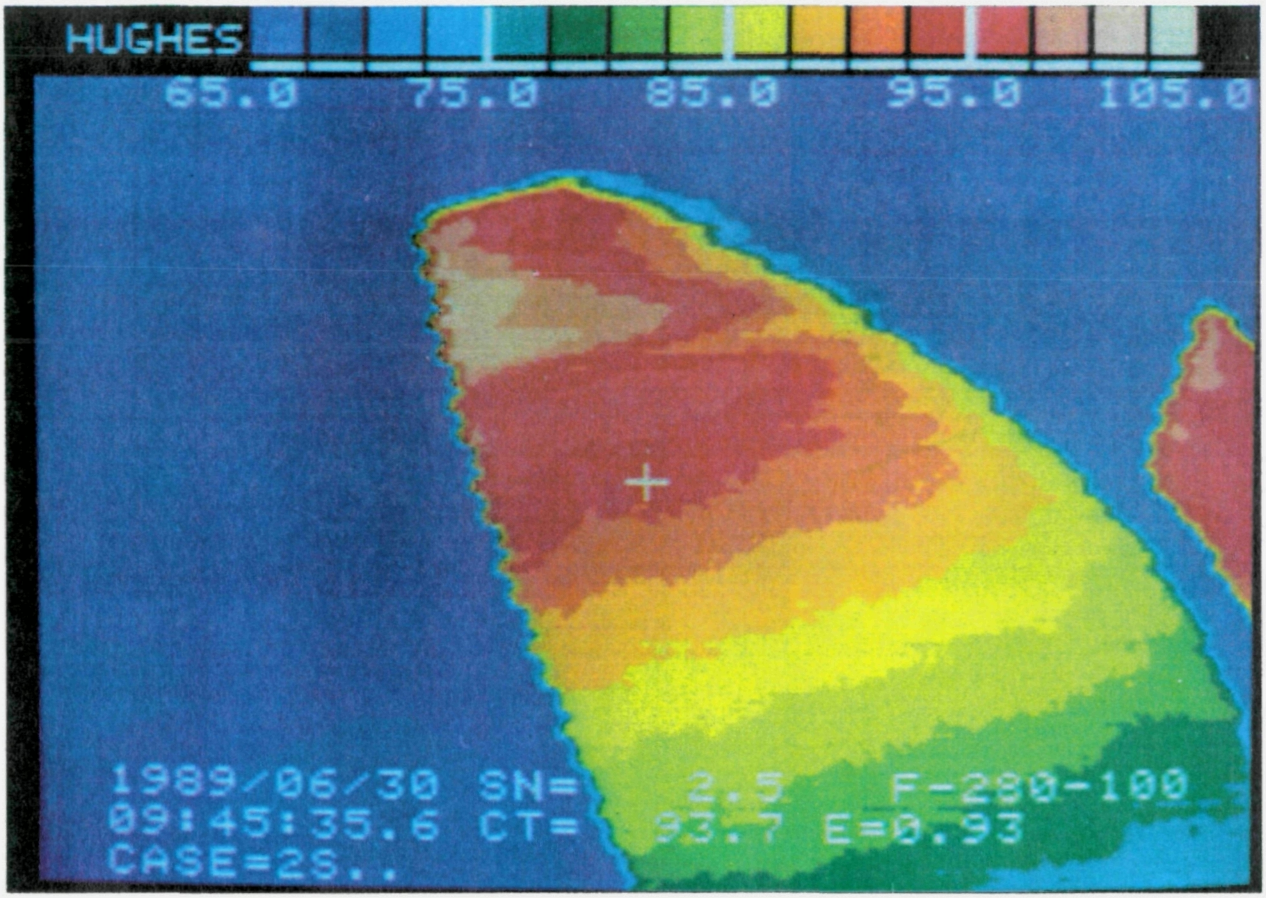
HUGHES
65.0 75.0 85.0 95.0 105.0
1989/06/30 SN= 2.5 F-280-100
09:45:35.6 CT= 93.7 E=0.93
CASE=2S..

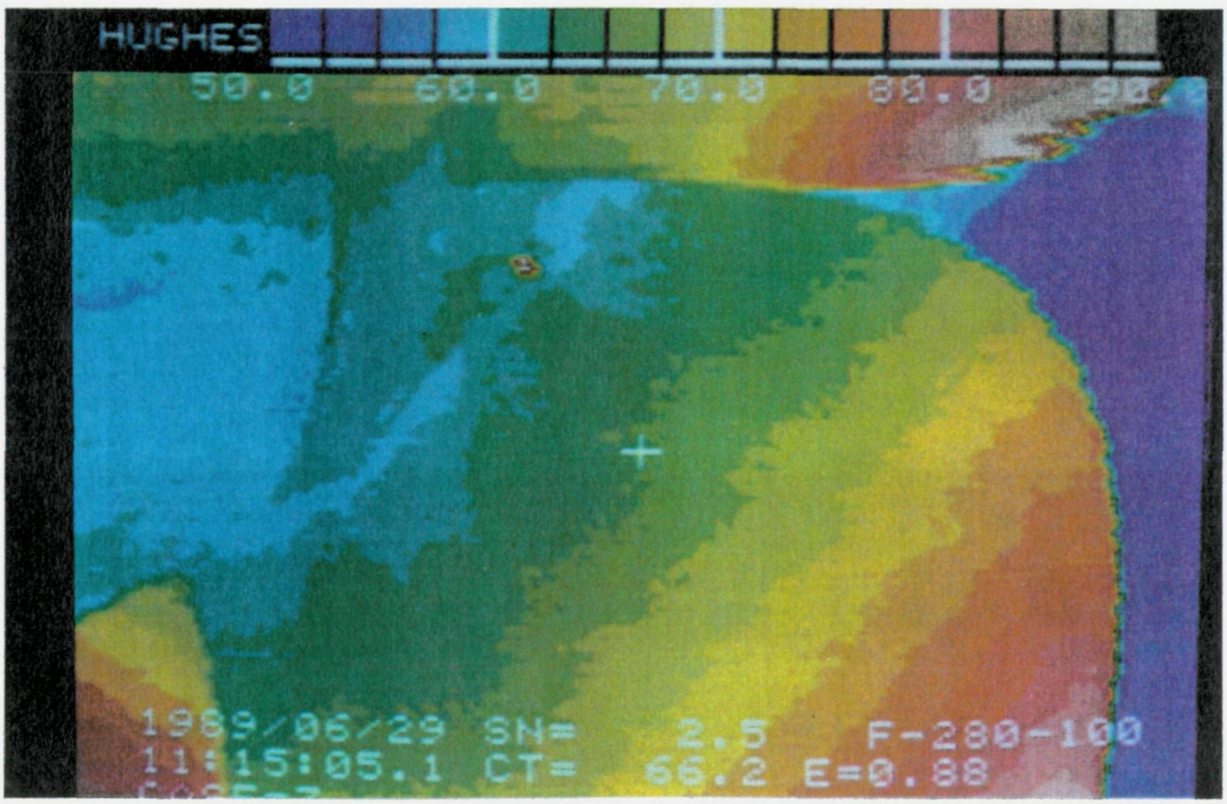
HUGHES
50.0 60.0 70.0 80.0
1989/06/29 SN= 2.5 F-280-100
11:15:05.1 CT= 66.2 E=0.88

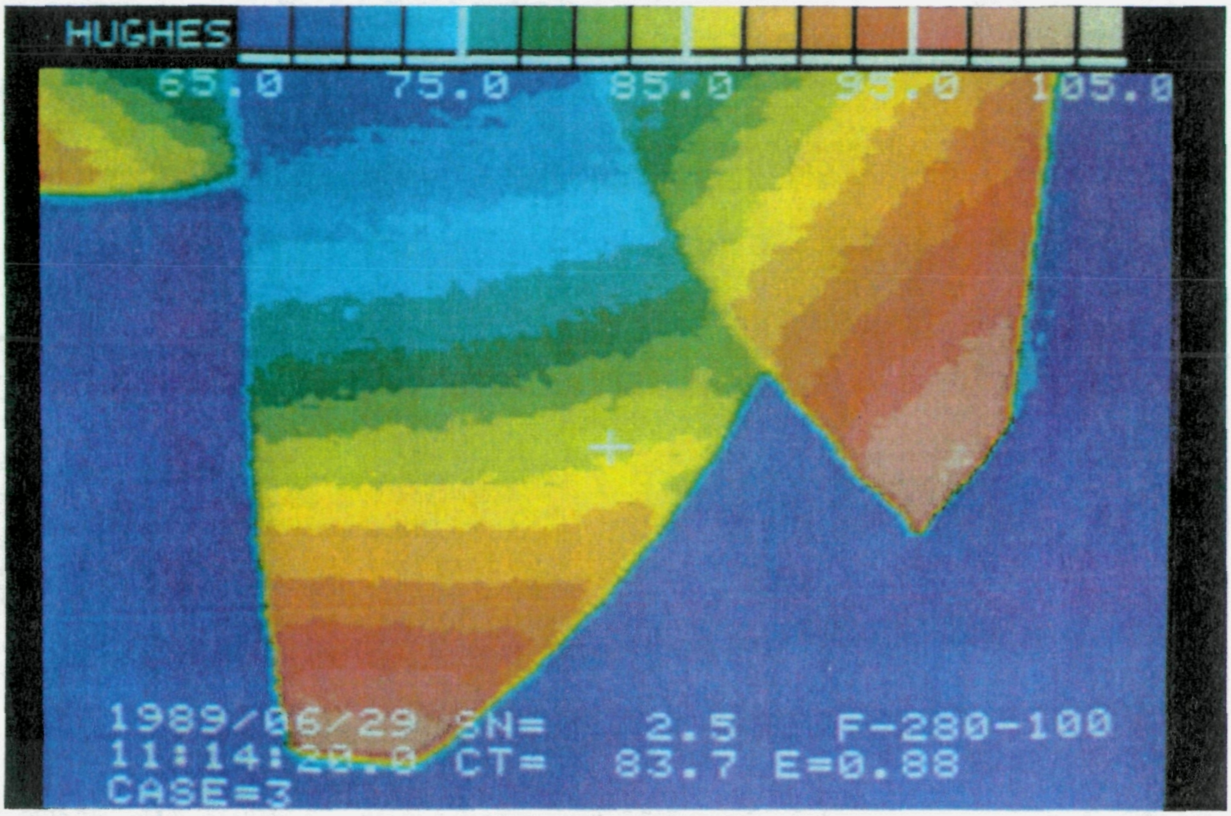

ORIGINAL PAGE
COLOR PHOTOGRAPH

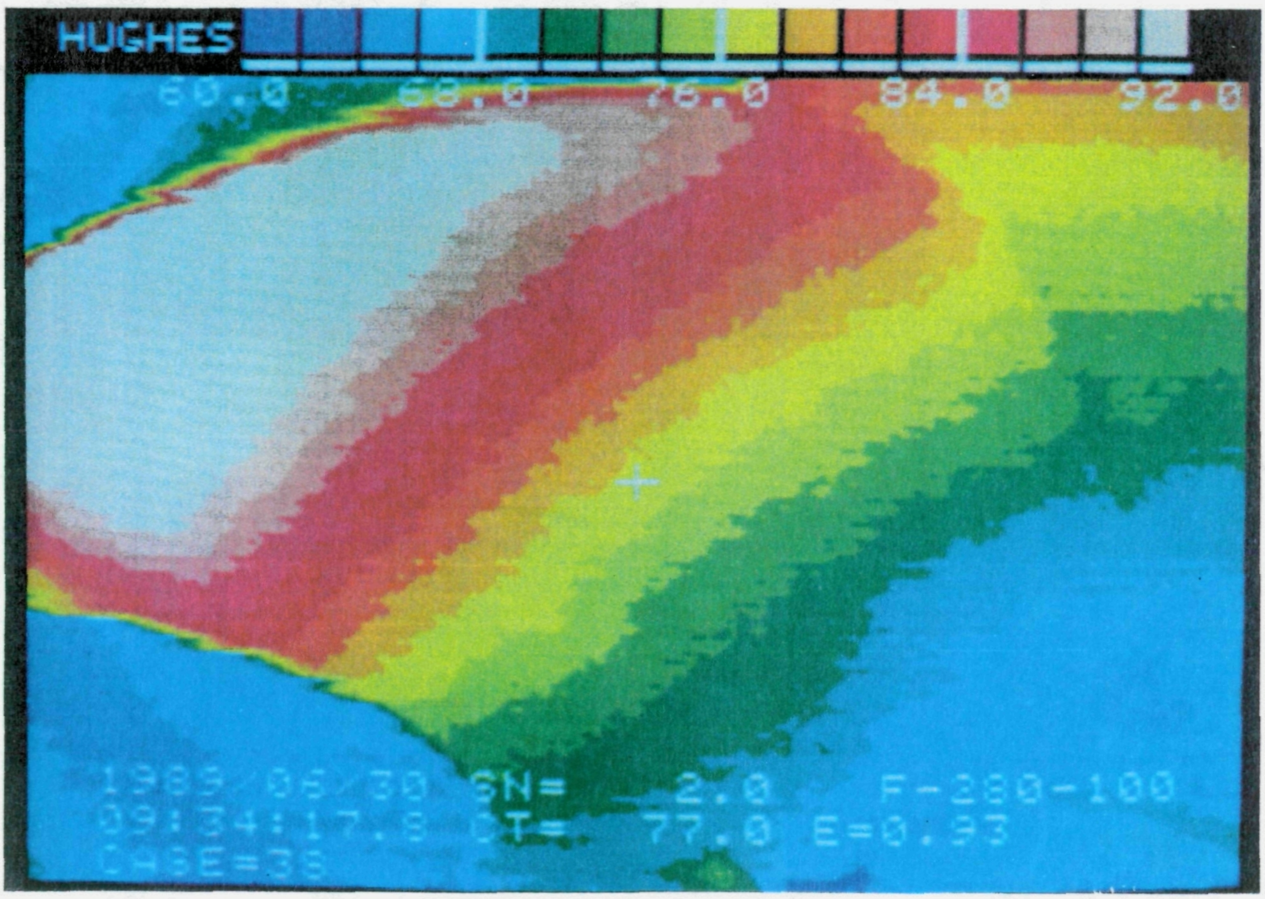

PRECEDING PAGE BLANK NOT FILMED

PAGE 54 INTENTIONALLY BLANK

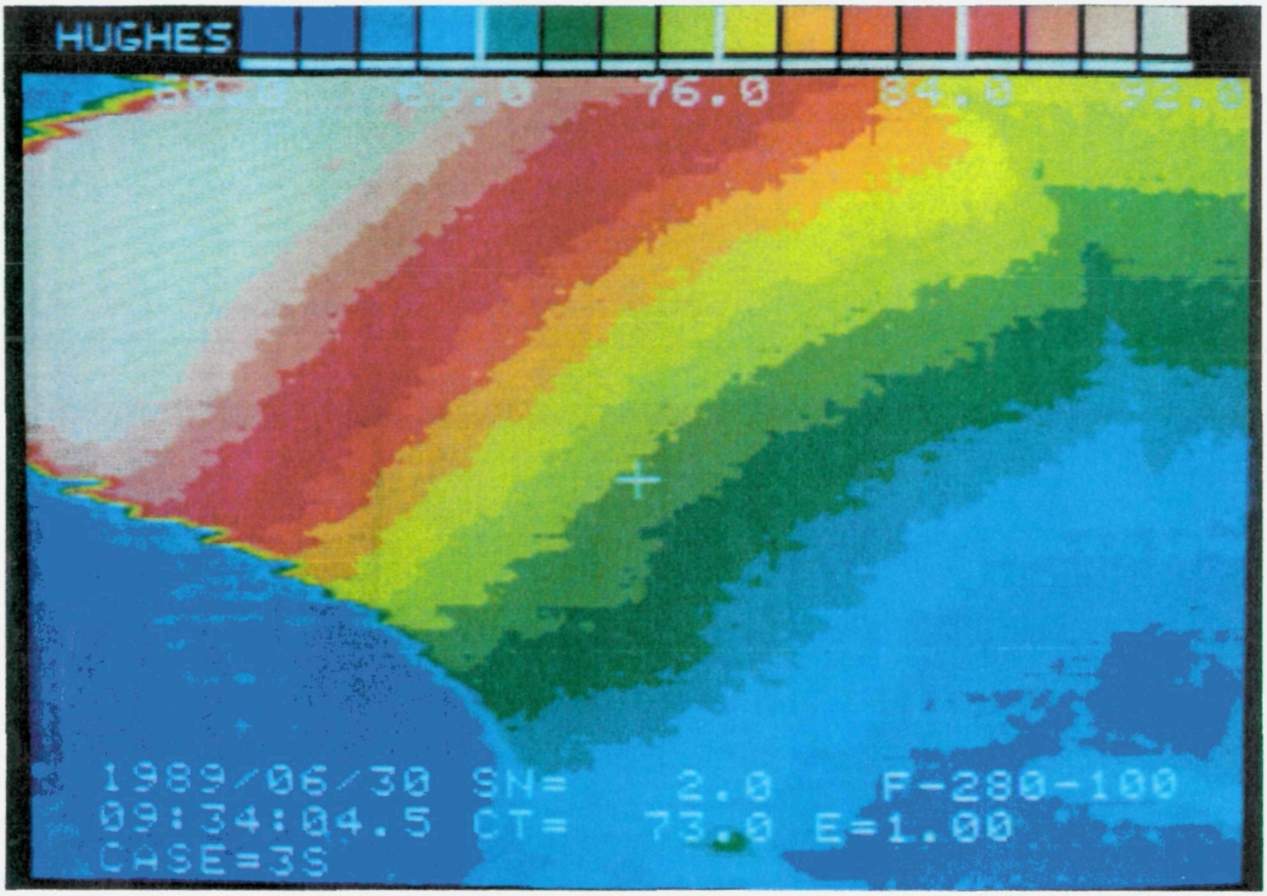
HUGHES
76.0
84.0
92.0
1989/06/30 SN= 2.0 F-280-100
09:34:04.5 CT= 73.0 E=1.00
CASE=3S

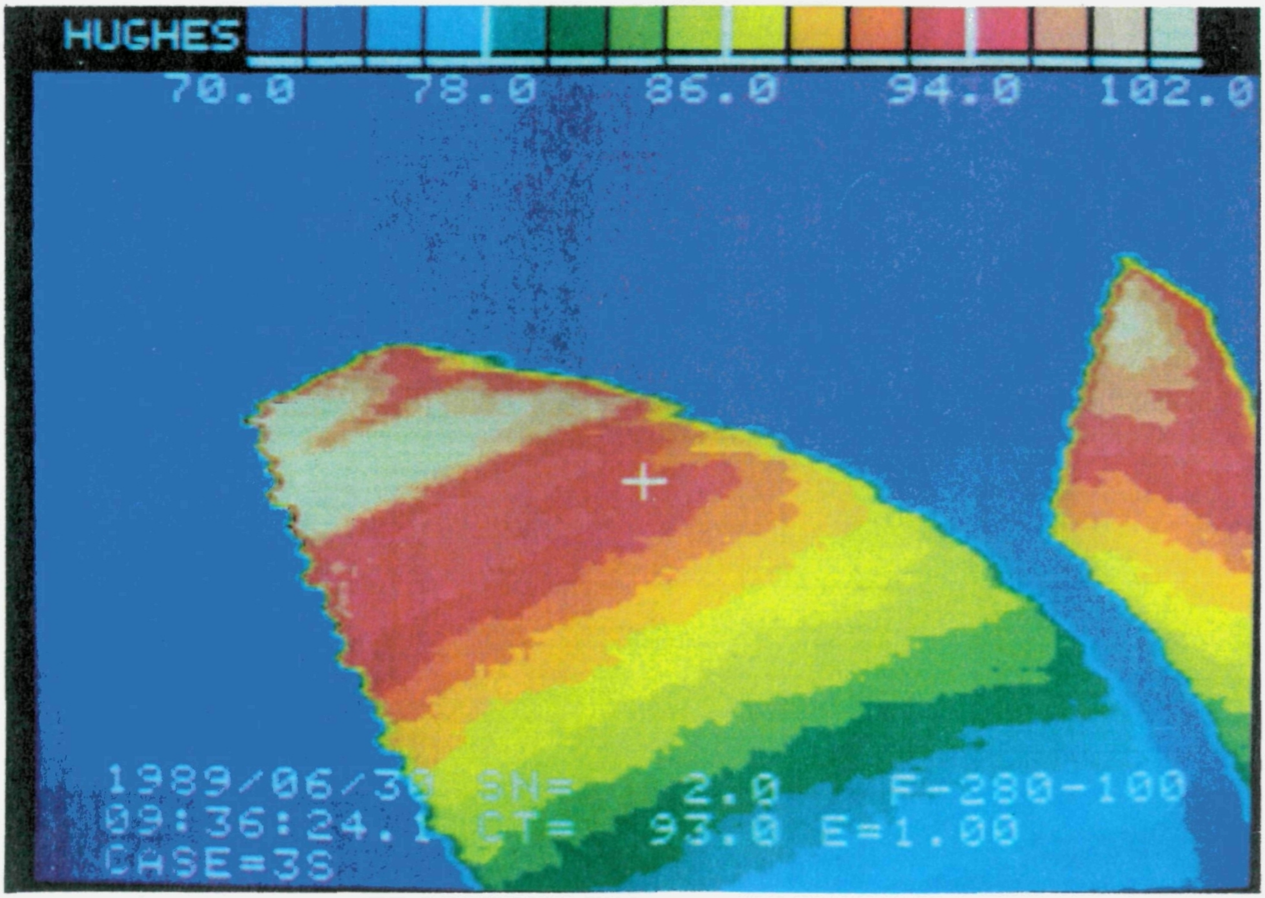
HUGHES
70.0 78.0 86.0 94.0 102.0
1989/06/30 SN= 2.0 F-280-100
09:36:24.1 CT= 93.0 E=1.00
CASE=3S

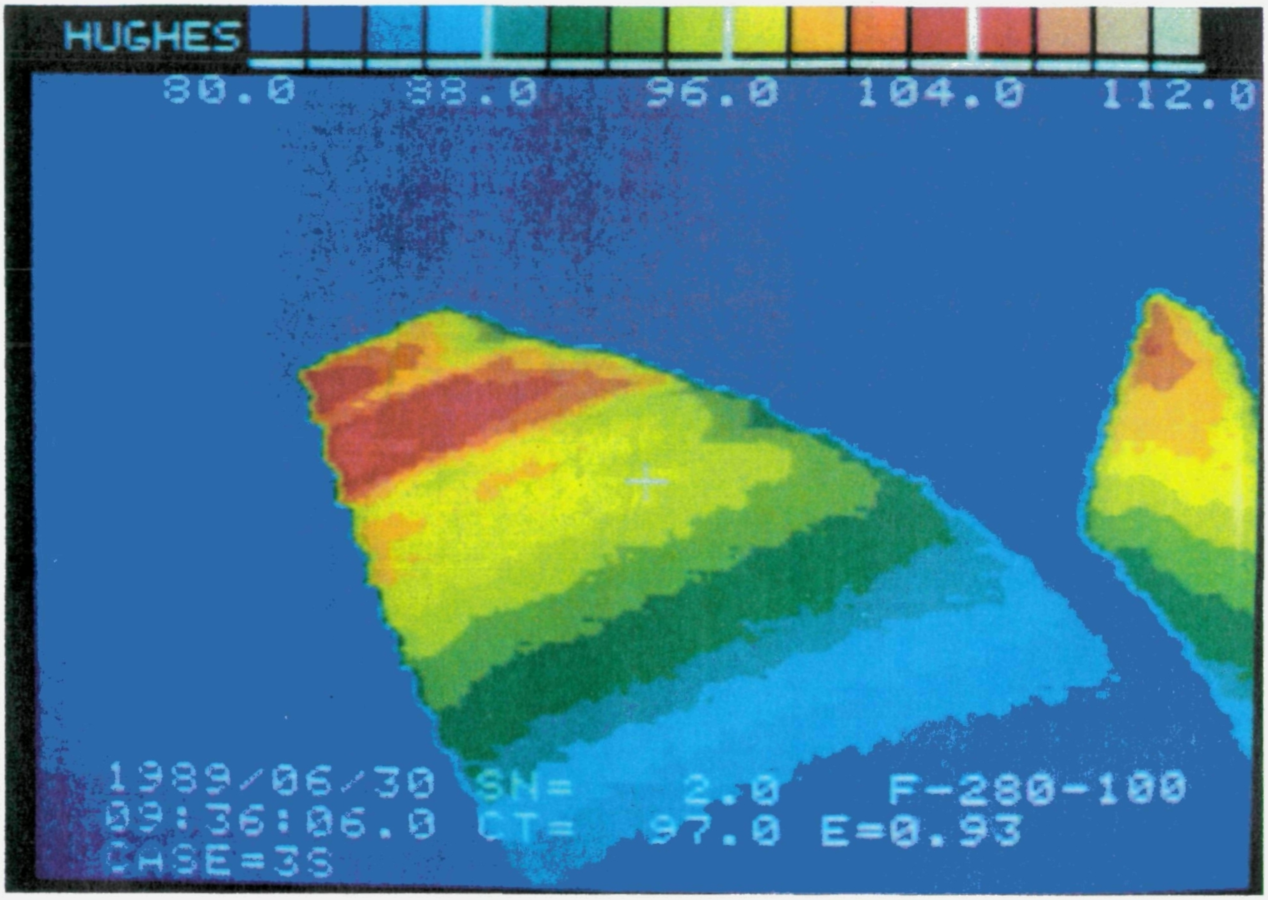

ORIGINAL PAGE
COLOR PHOTOGRAPH

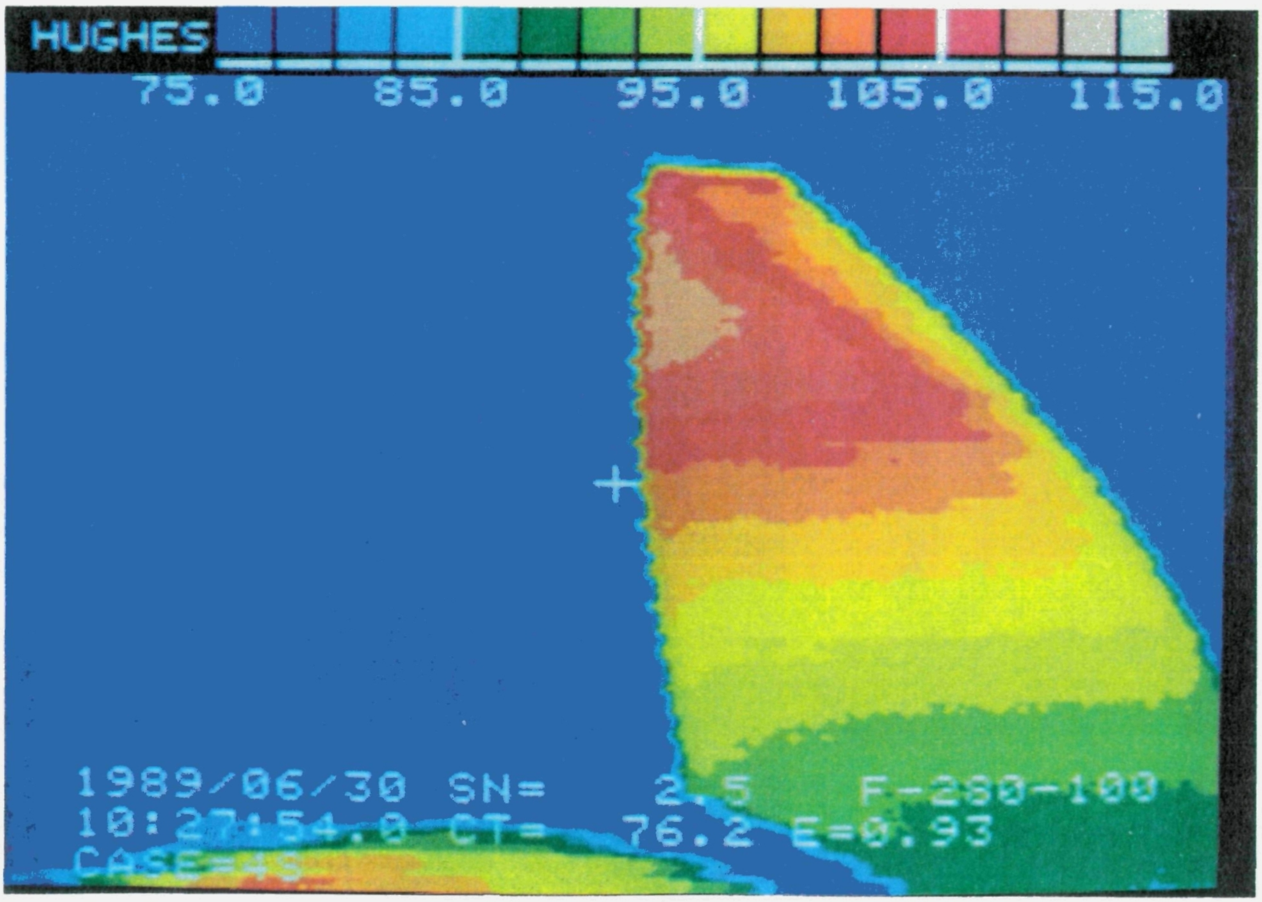

PAGE 58 INTENTIONALLY BLANK

PRECEDING PAGE BLANK NOT FILMED

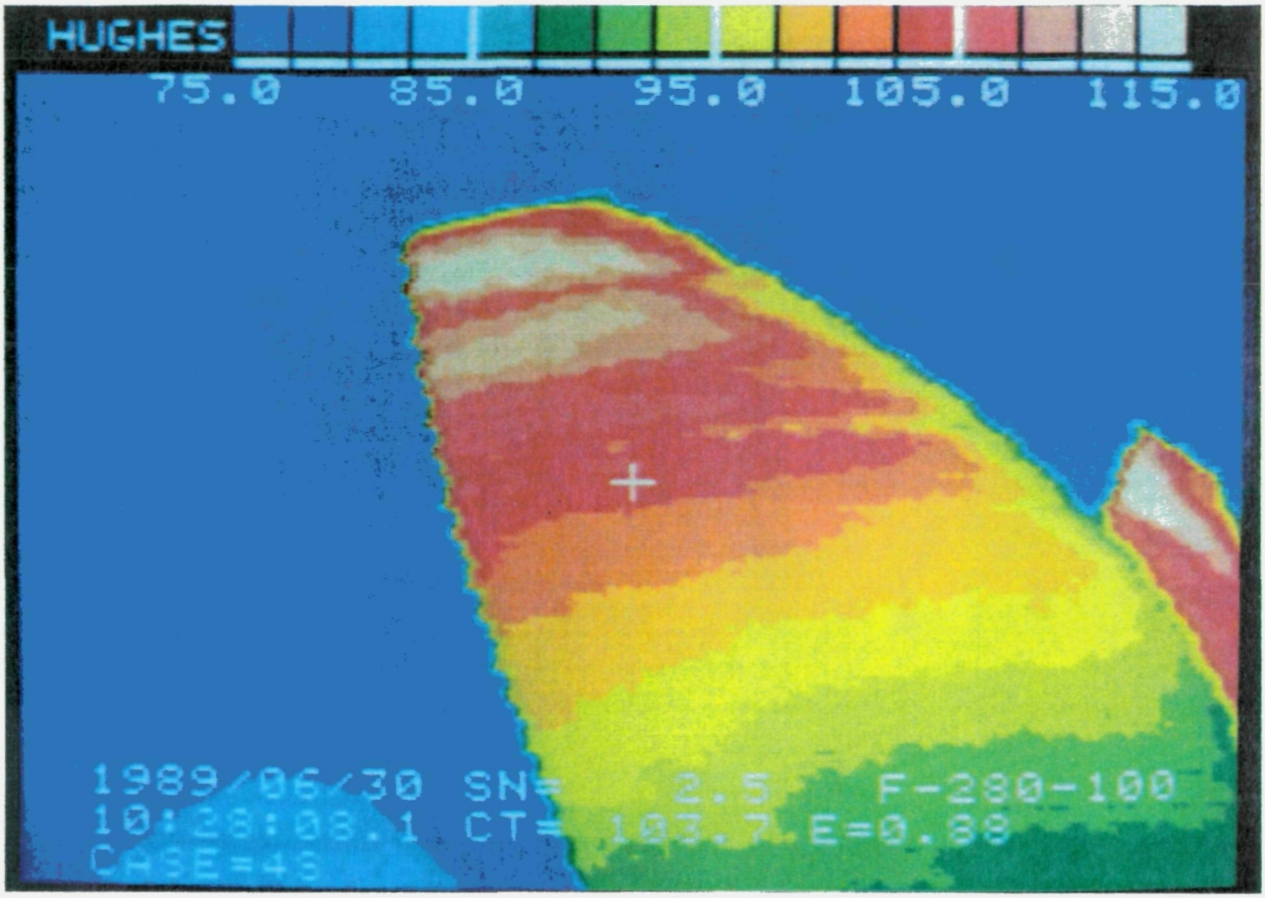
HUGHES
75.0 85.0 95.0 105.0 115.0
1989/06/30 SN= 2.5 F-280-100
10:28:08.1 CT= 103.7 E=0.88
CASE=46

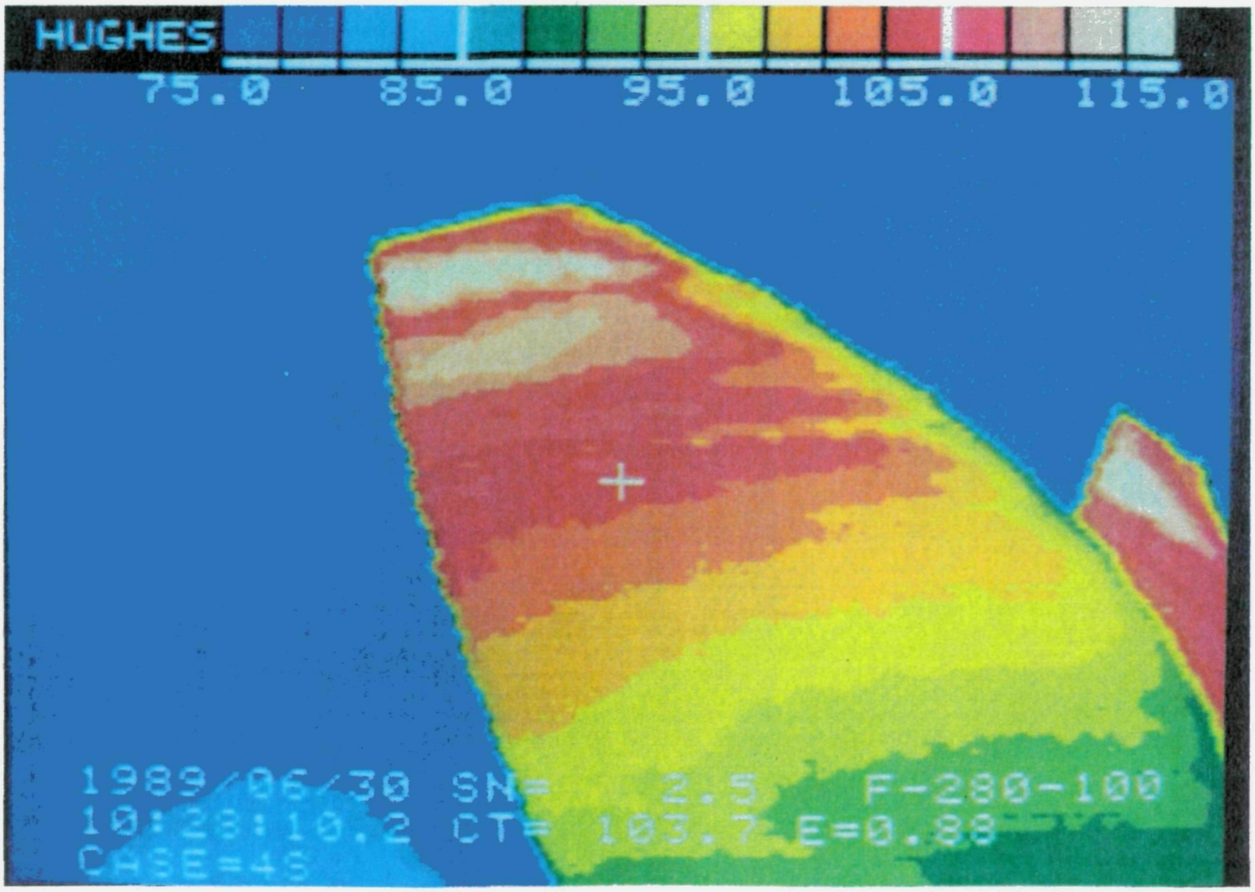
HUGHES
75.0 85.0 95.0 105.0 115.0
1989/06/30 SN= 2.5 F-280-100
10:28:10.2 CT= 103.7 E=0.88
CASE=46

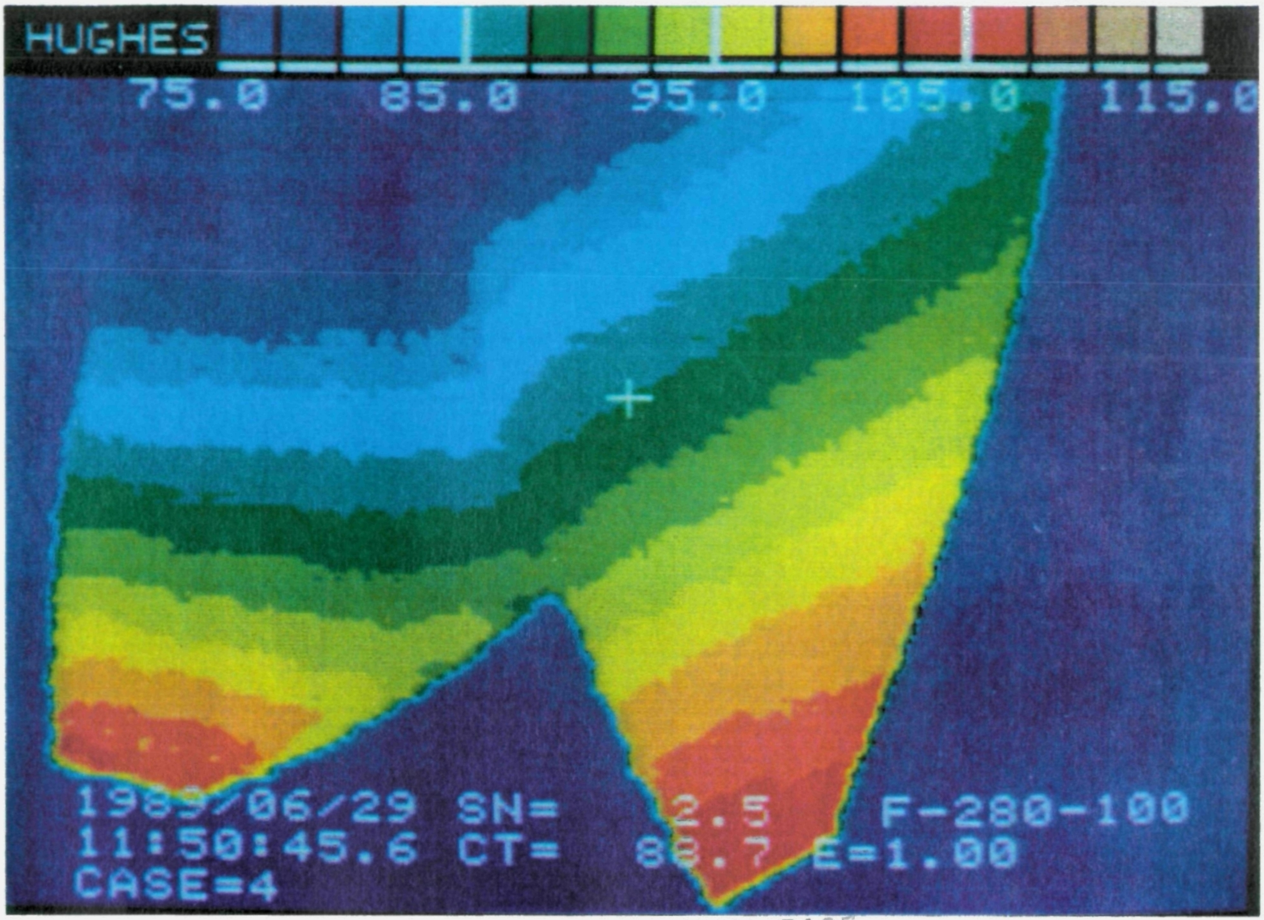

ORIGINAL PAGE
COLOR PHOTOGRAPH

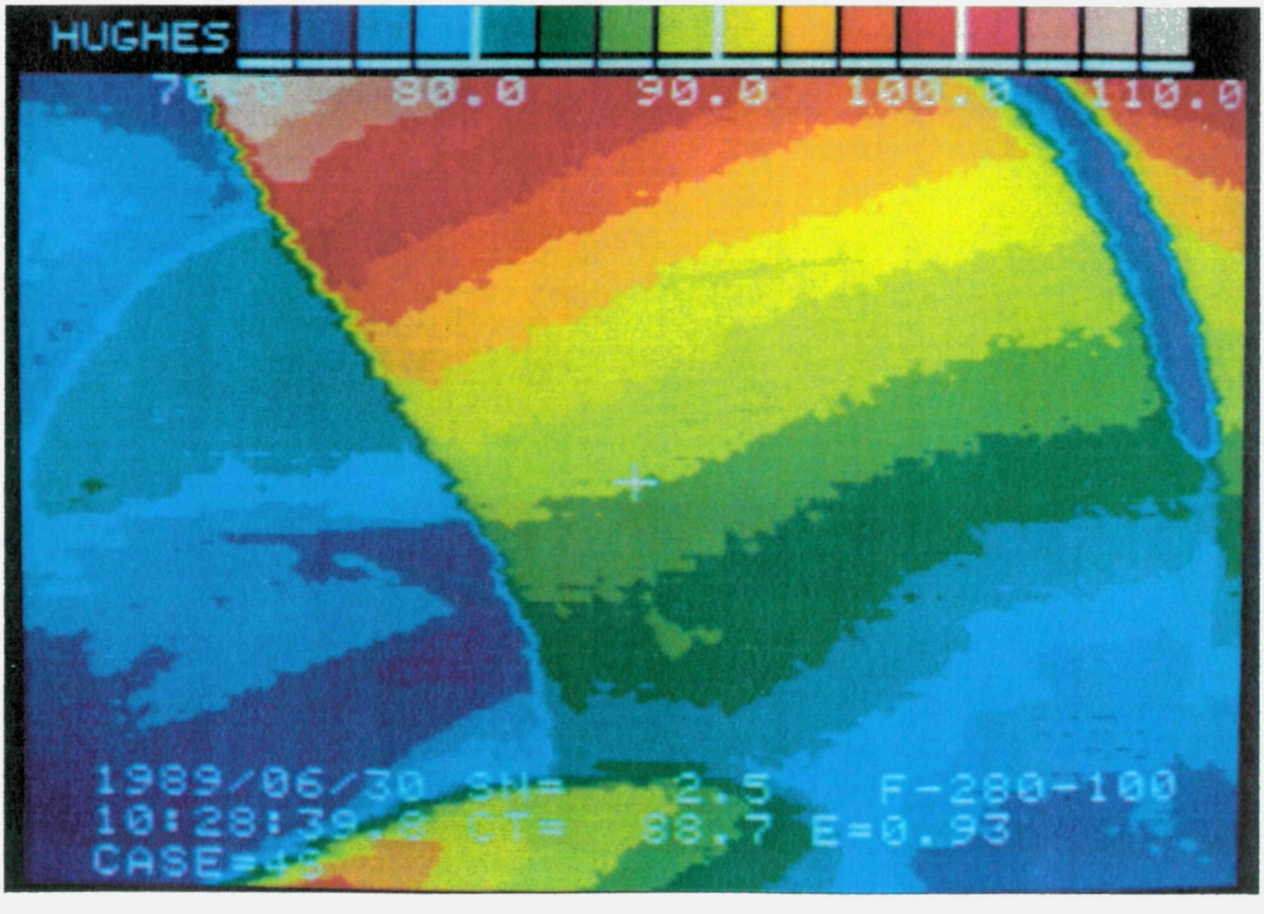

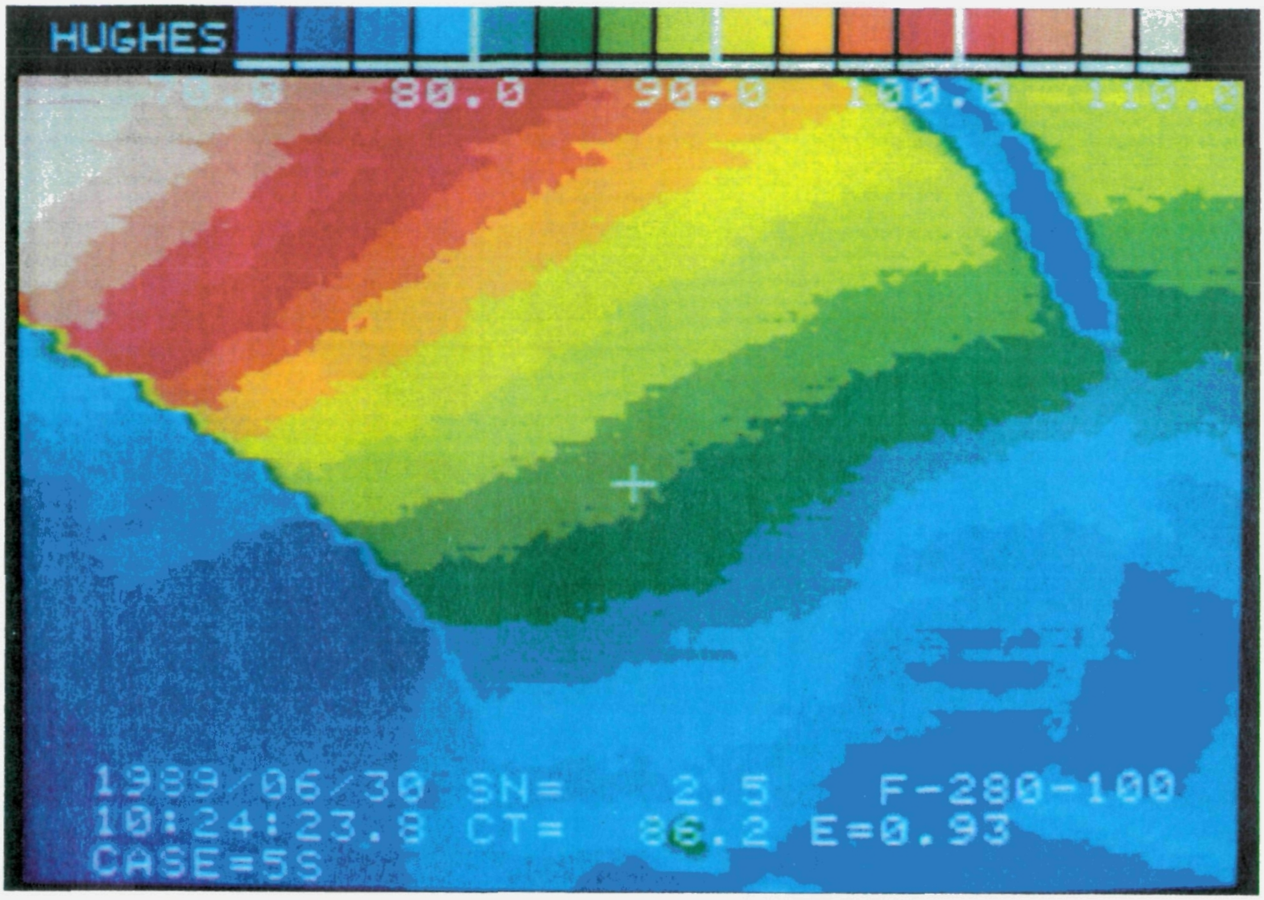
HUGHES
80.0 90.0 100.0 110.0
1989/06/30 SN= 2.5 F-280-100
10:24:23.8 CT= 86.2 E=0.93
CASE=5S

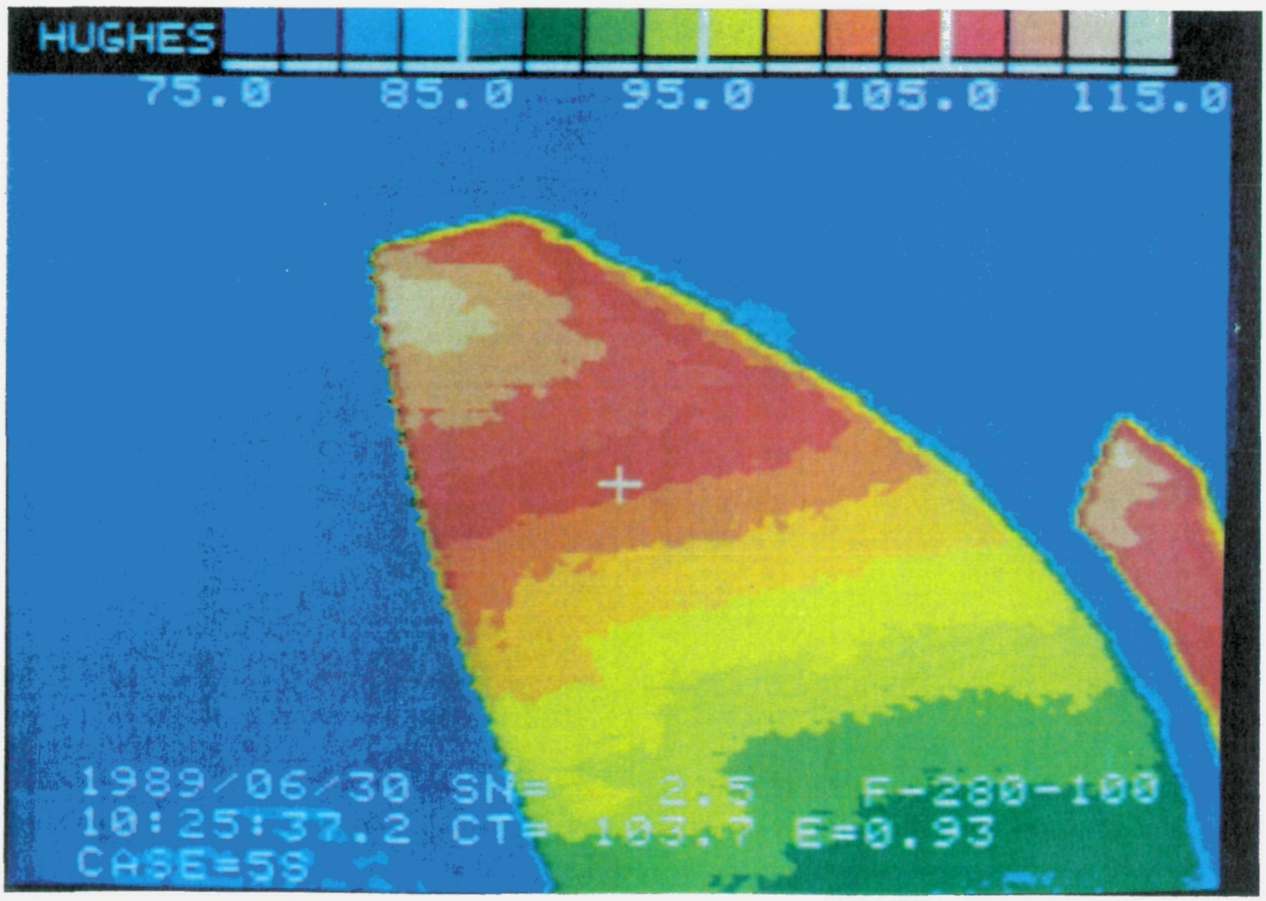
HUGHES
75.0 85.0 95.0 105.0 115.0
1989/06/30 SN= 2.5 F-280-100
10:25:37.2 CT= 103.7 E=0.93
CASE=5S

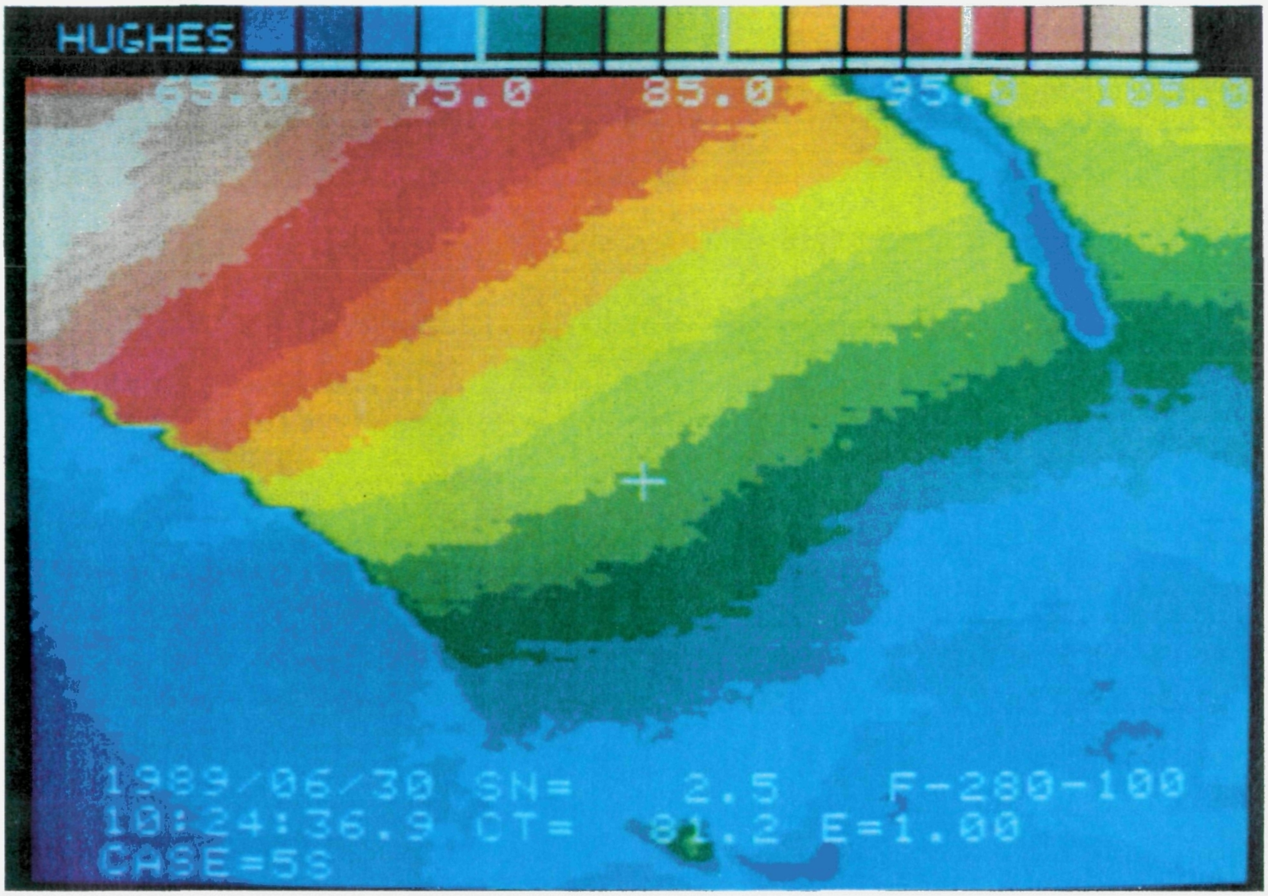

ORIGINAL PAGE
COLOR PHOTOGRAPH

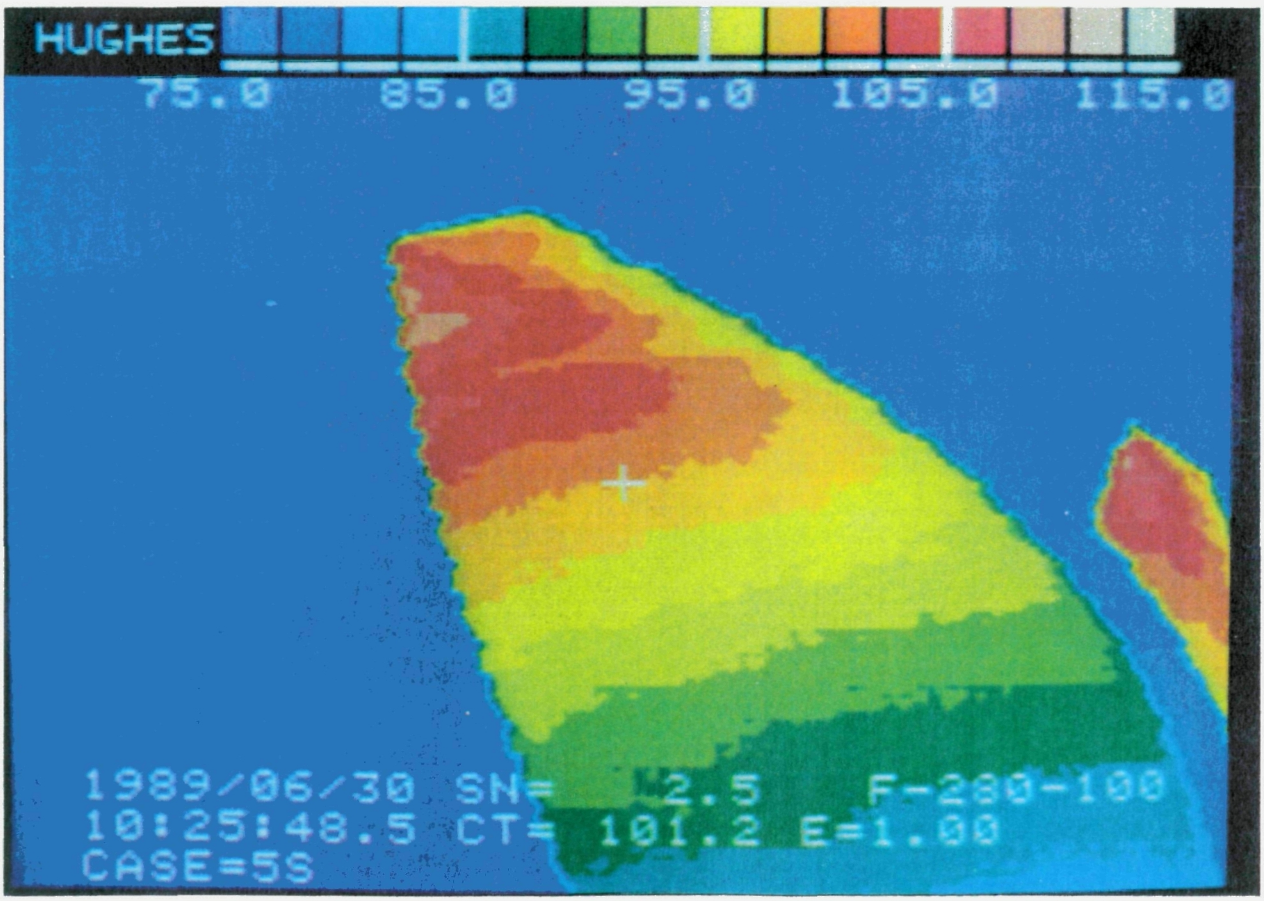

PAGE 66 INTENTIONALLY BLANK

PRECEDING PAGE BLANK NOT FILMED

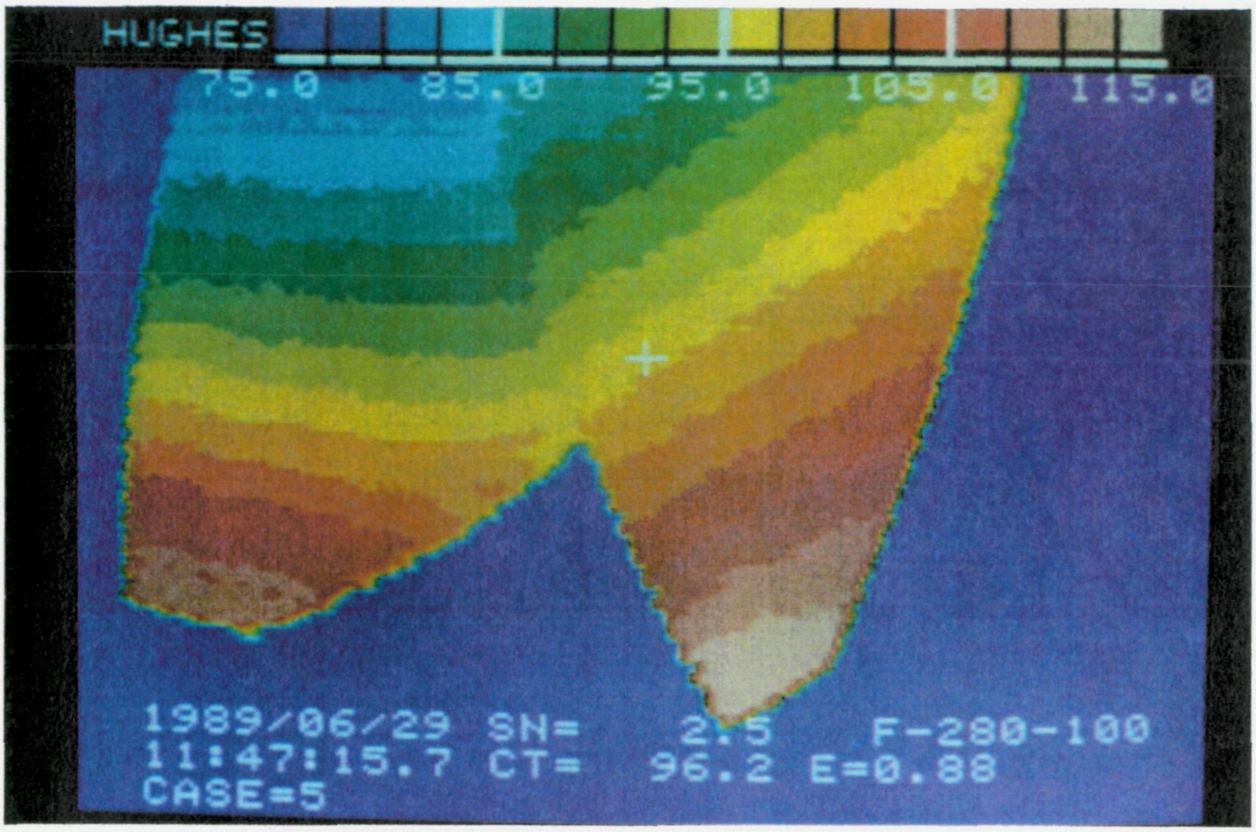

ORIGINAL PAGE
COLOR PHOTOGRAPH

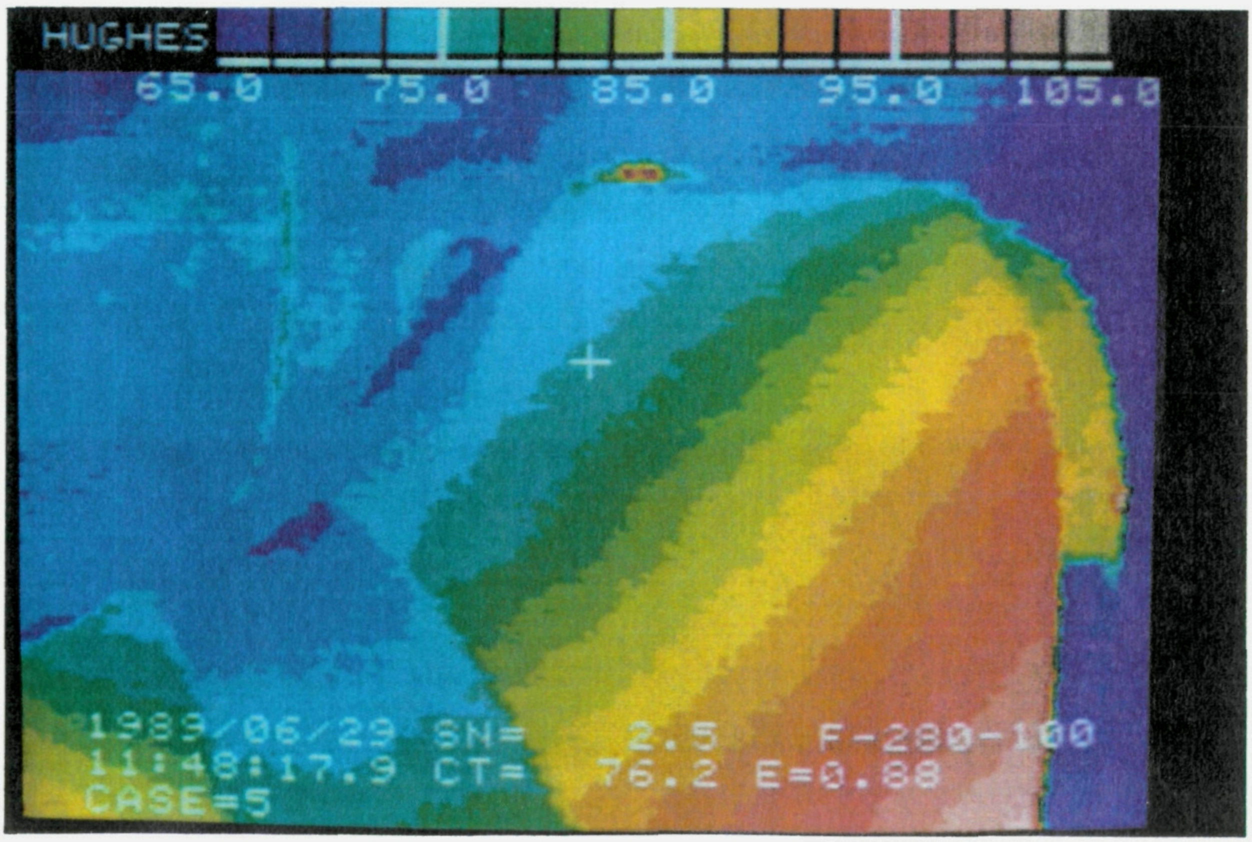

PAGE 68 INTENTIONALLY BLANK

PRECEDING PAGE BLANK NOT FILMED

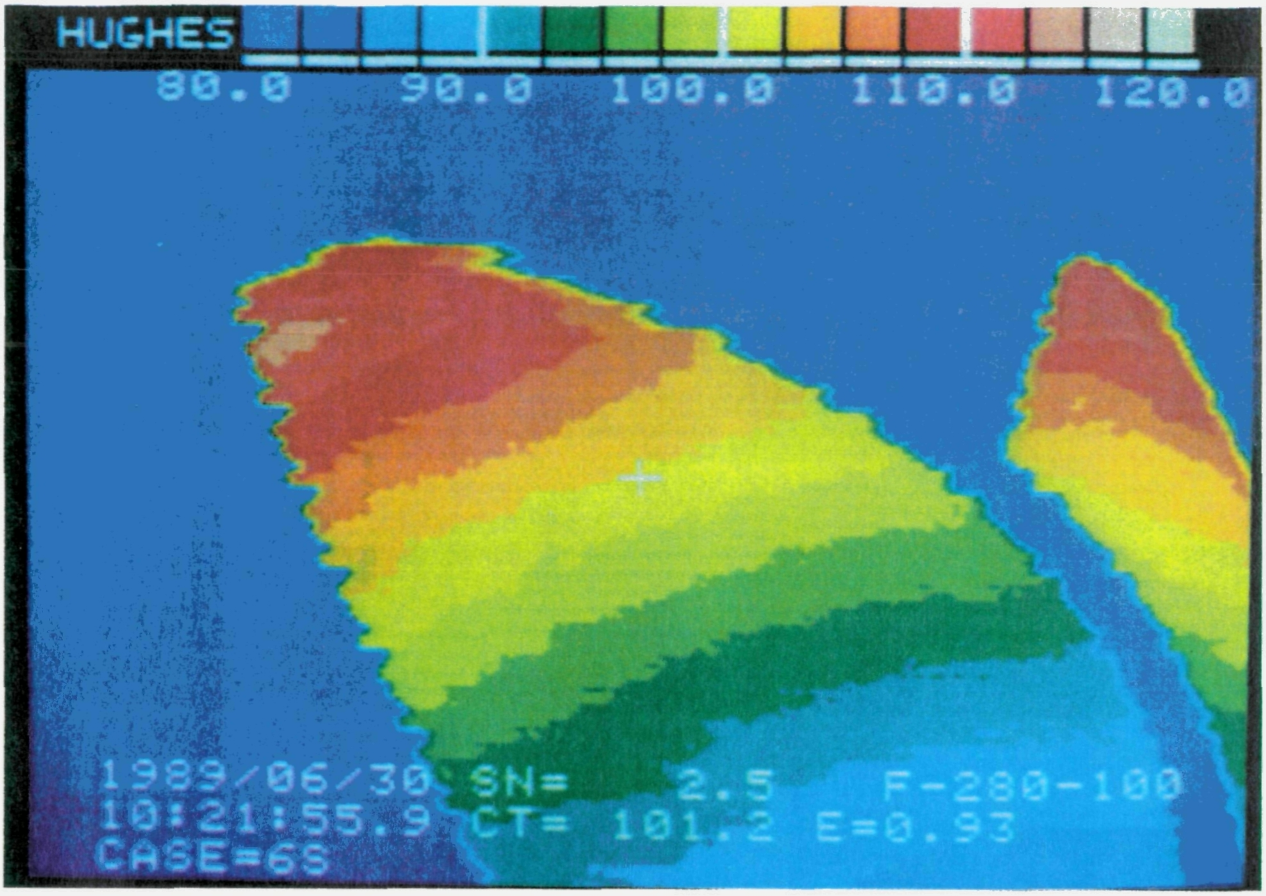

ORIGINAL PAGE
COLOR PHOTOGRAPH

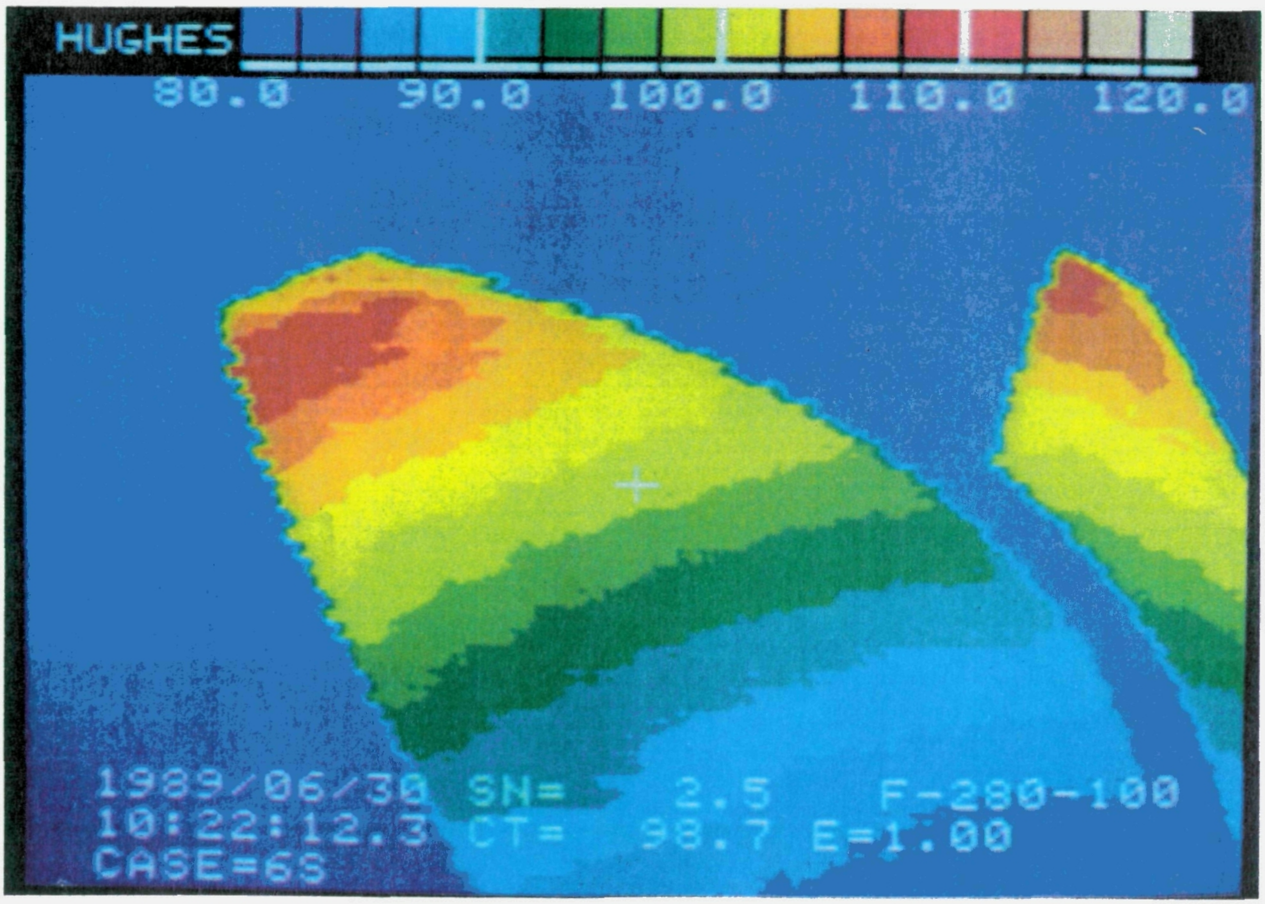

PAGE 70 INTENTIONALLY BLANK

PRECEDING PAGE BLANK NOT FILMED

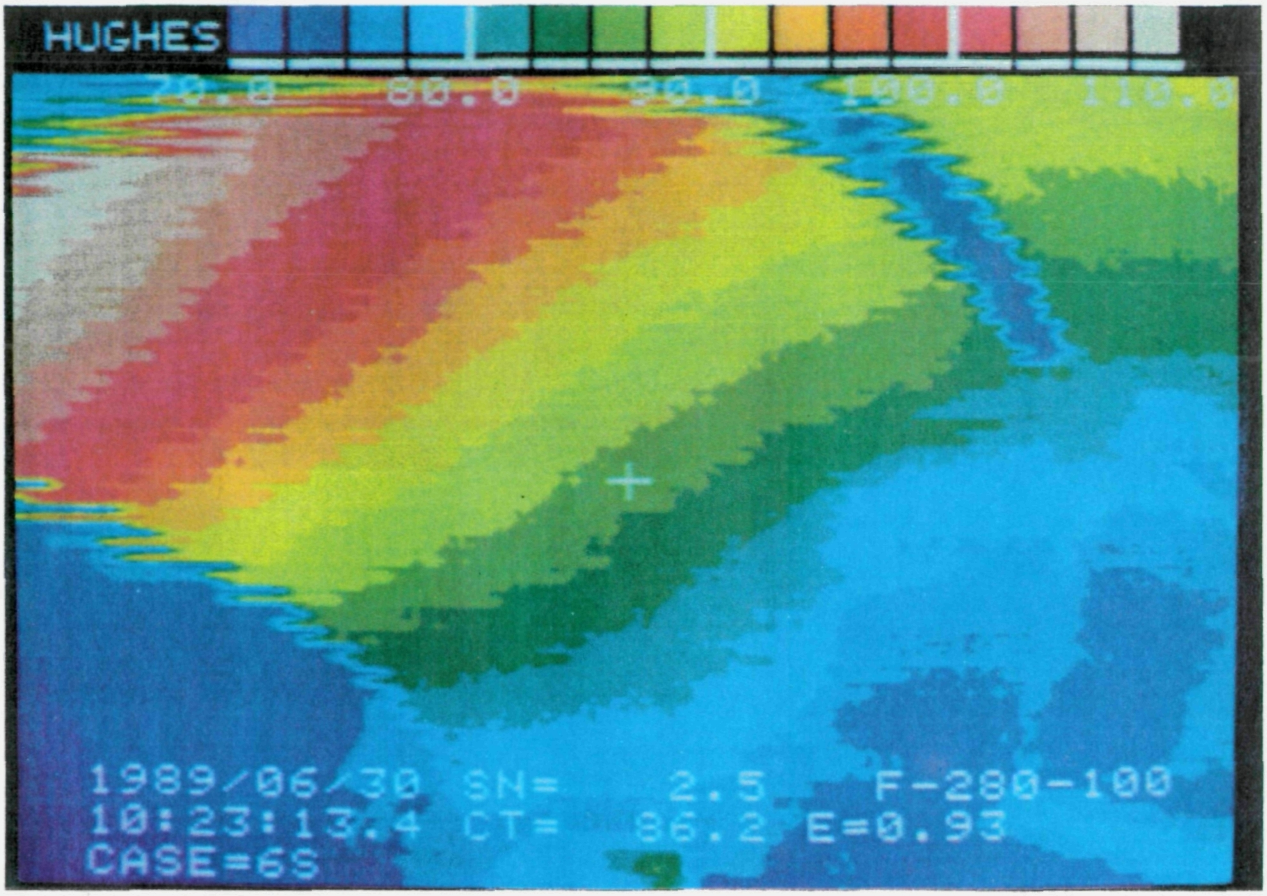

ORIGINAL PAGE
COLOR PHOTOGRAPH

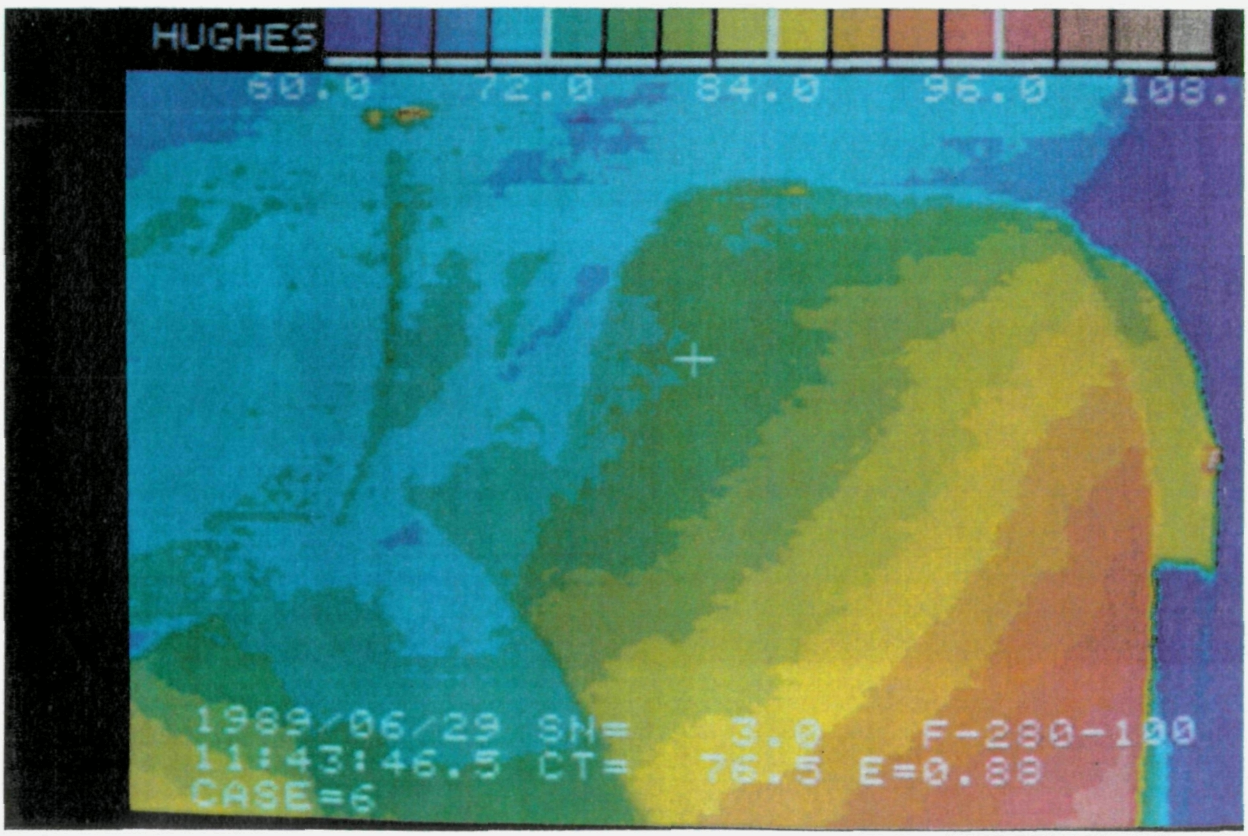

PRECEDING PAGE BLANK NOT FILMED

PAGE 72 INTENTIONALLY BLANK

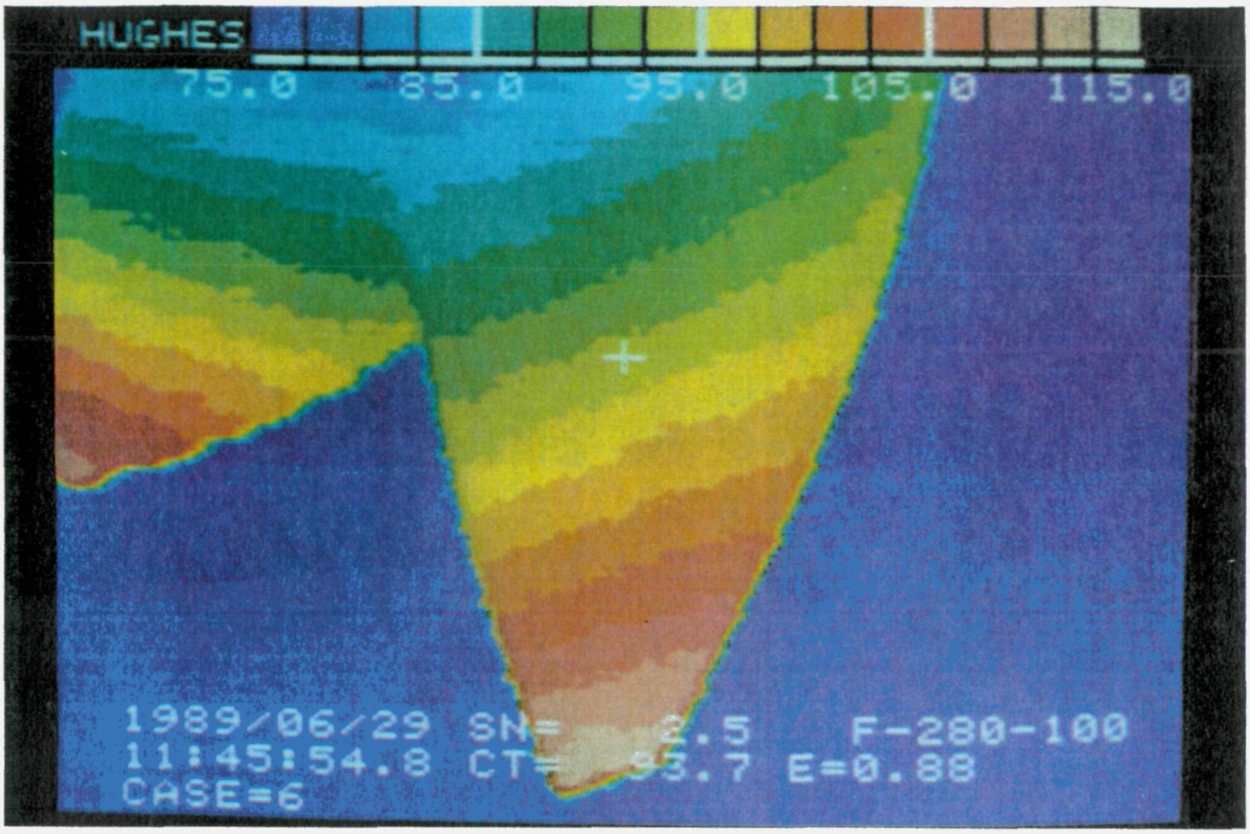

ORIGINAL PAGE
COLOR PHOTOGRAPH

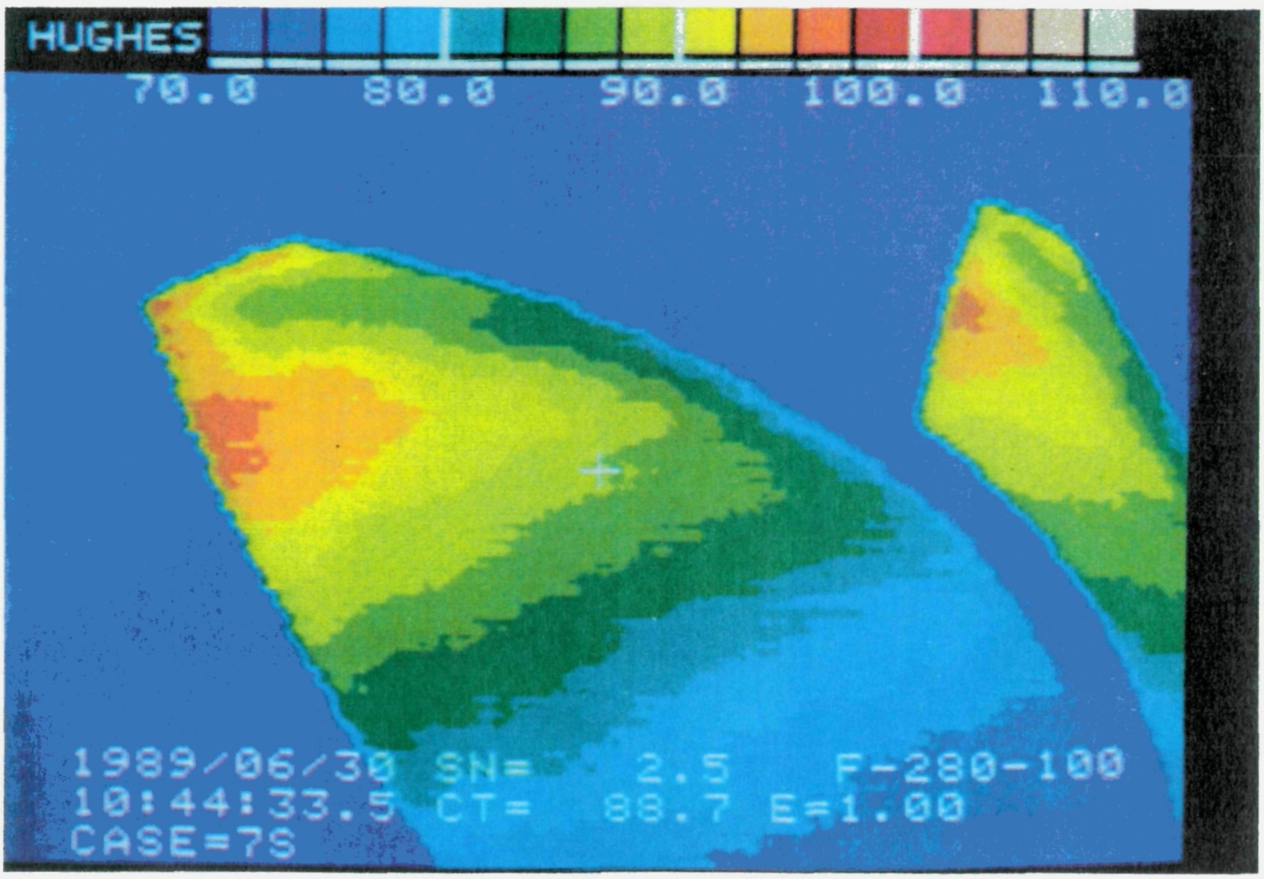

PRECEDING PAGE BLANK NOT FILMED

PAGE 74 INTENTIONALLY BLANK

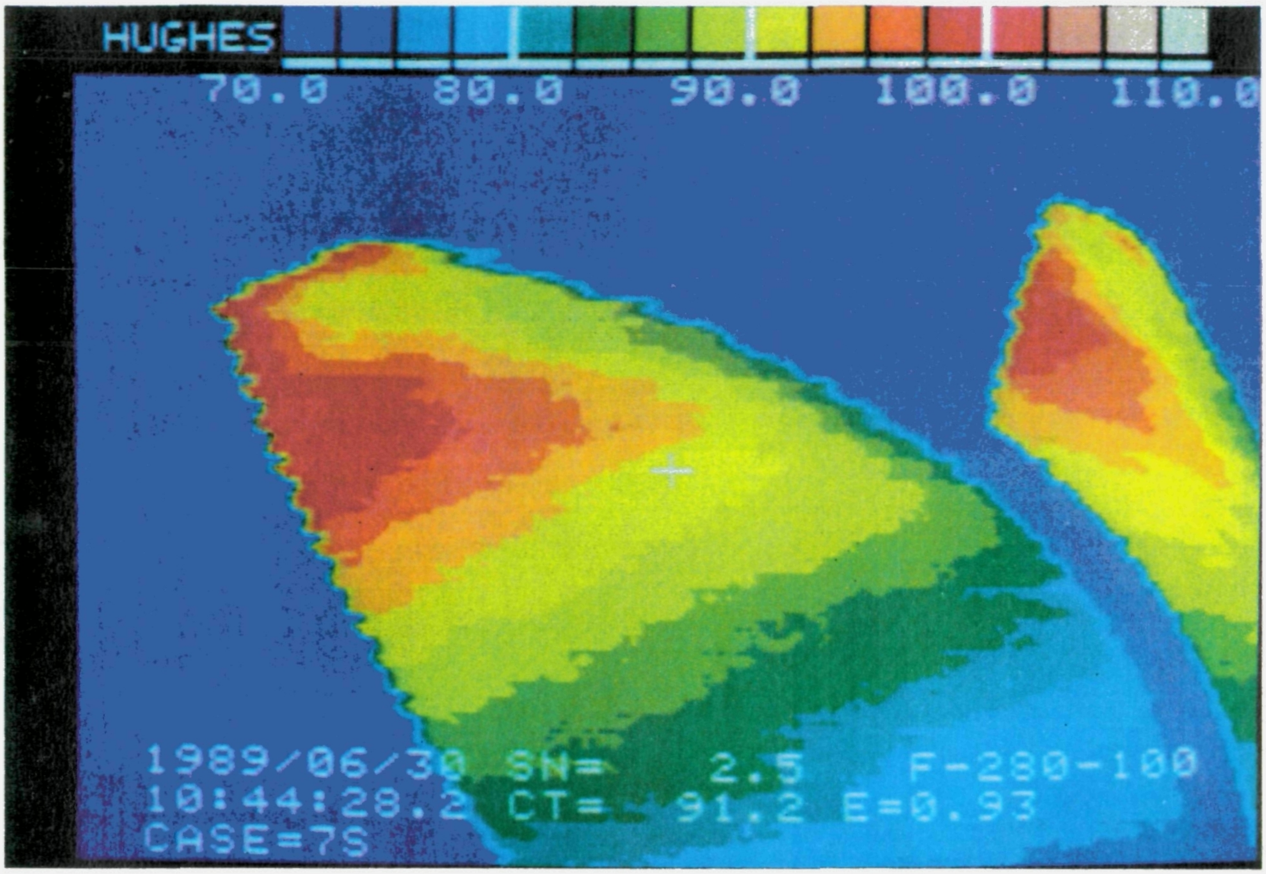
HUGHES
70.0 80.0 90.0 100.0 110.0
1989/06/30 SN= 2.5 F-280-100
10:44:28.2 CT= 91.2 E=0.93
CASE=7S

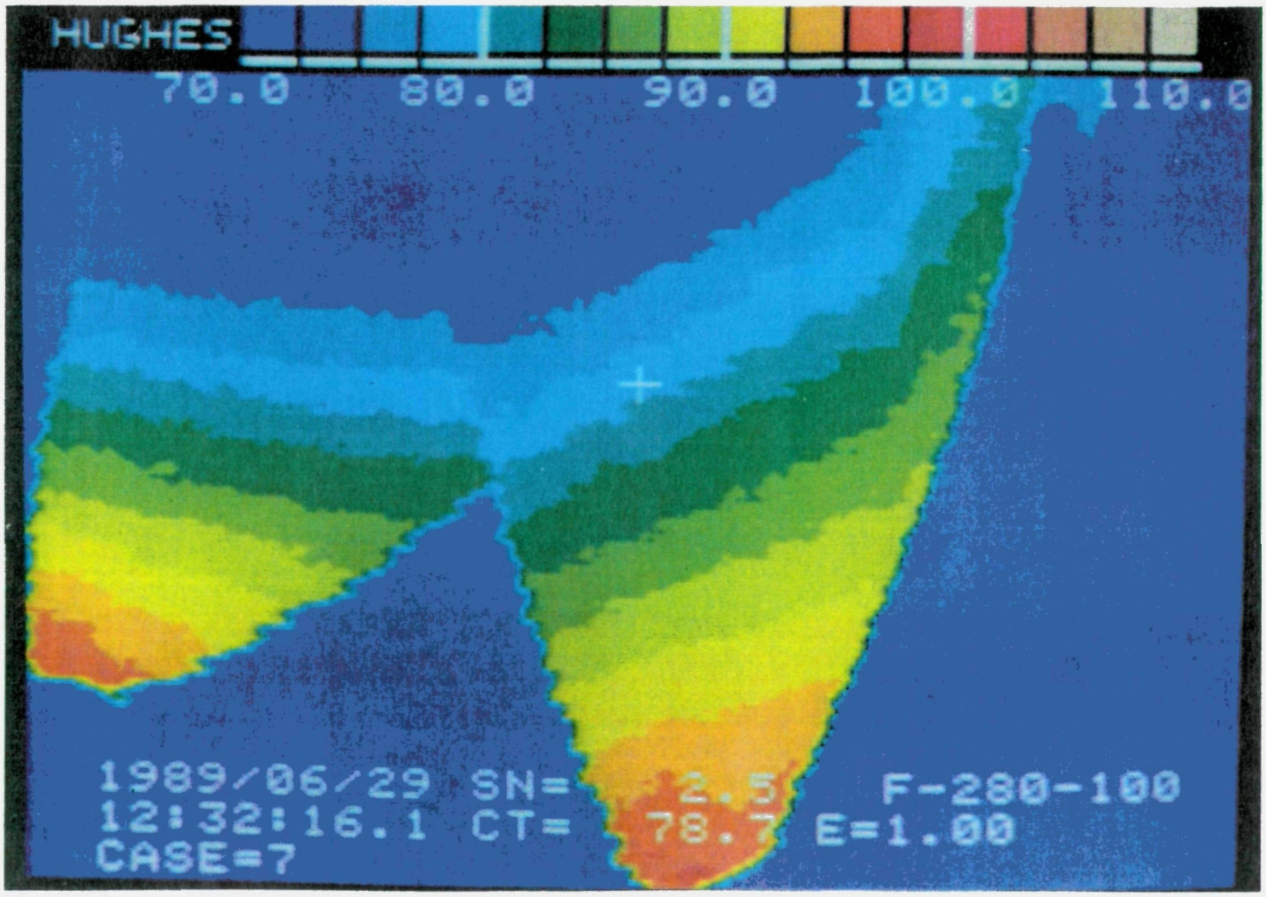
HUGHES
70.0 80.0 90.0 100.0 110.0
1989/06/29 SN= 2.5 F-280-100
12:32:16.1 CT= 78.7 E=1.00
CASE=7

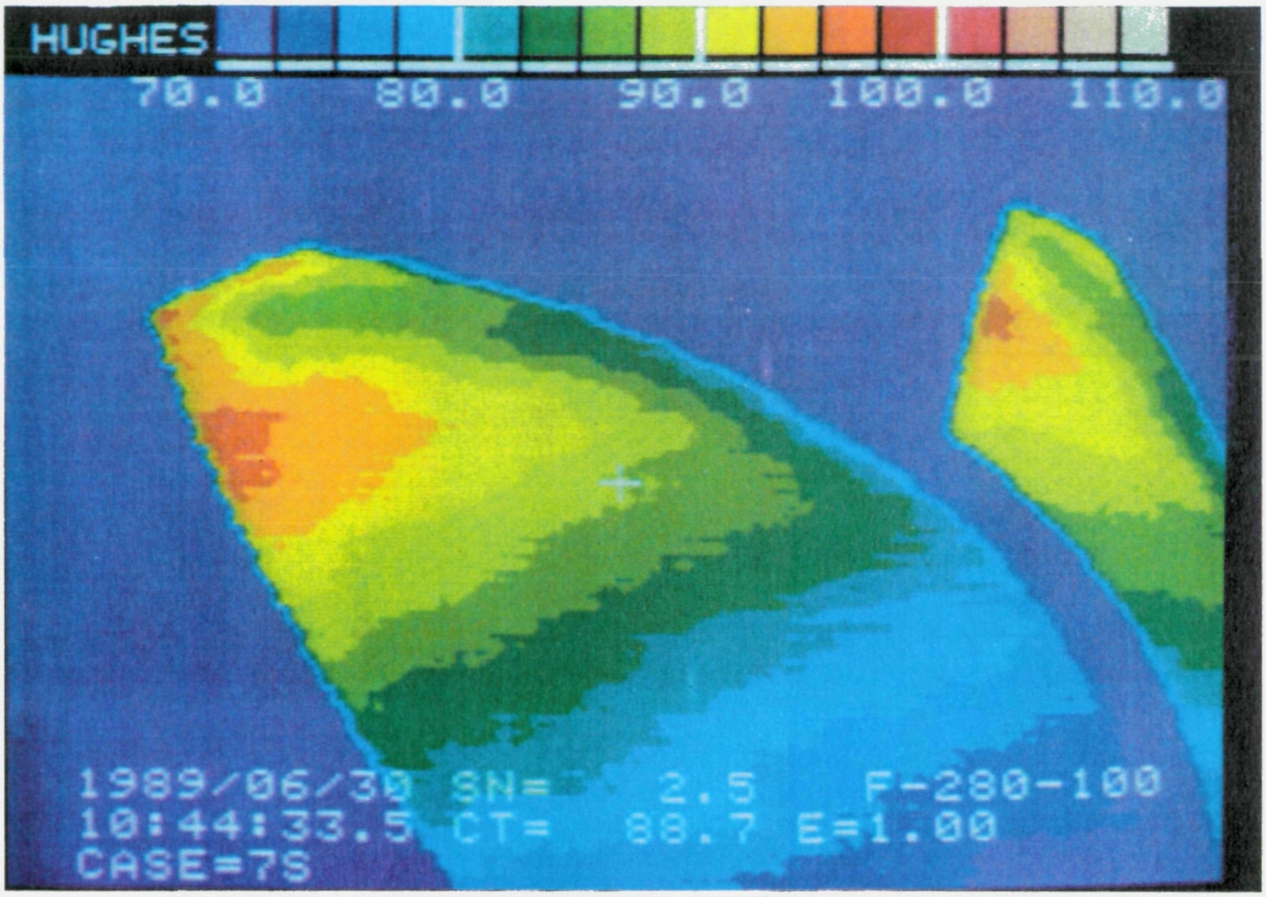
HUGHES
70.0 80.0 90.0 100.0 110.0
1989/06/30 SN= 2.5 F-280-100
10:44:33.5 CT= 88.7 E=1.00
CASE=7S

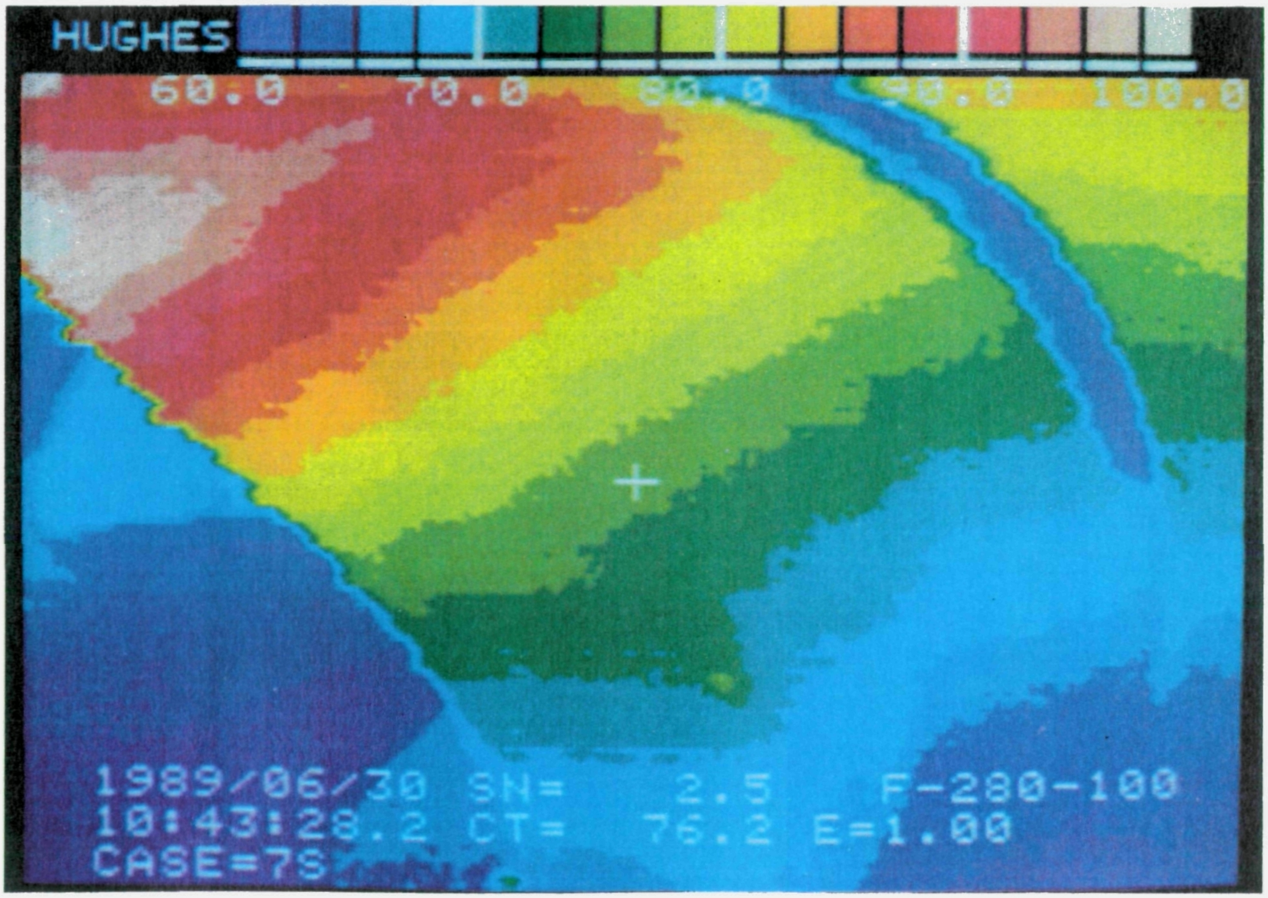
HUGHES
60.0 70.0 80.0 90.0 100.0
1989/06/30 SN= 2.5 F-280-100
10:43:28.2 CT= 76.2 E=1.00
CASE=7S

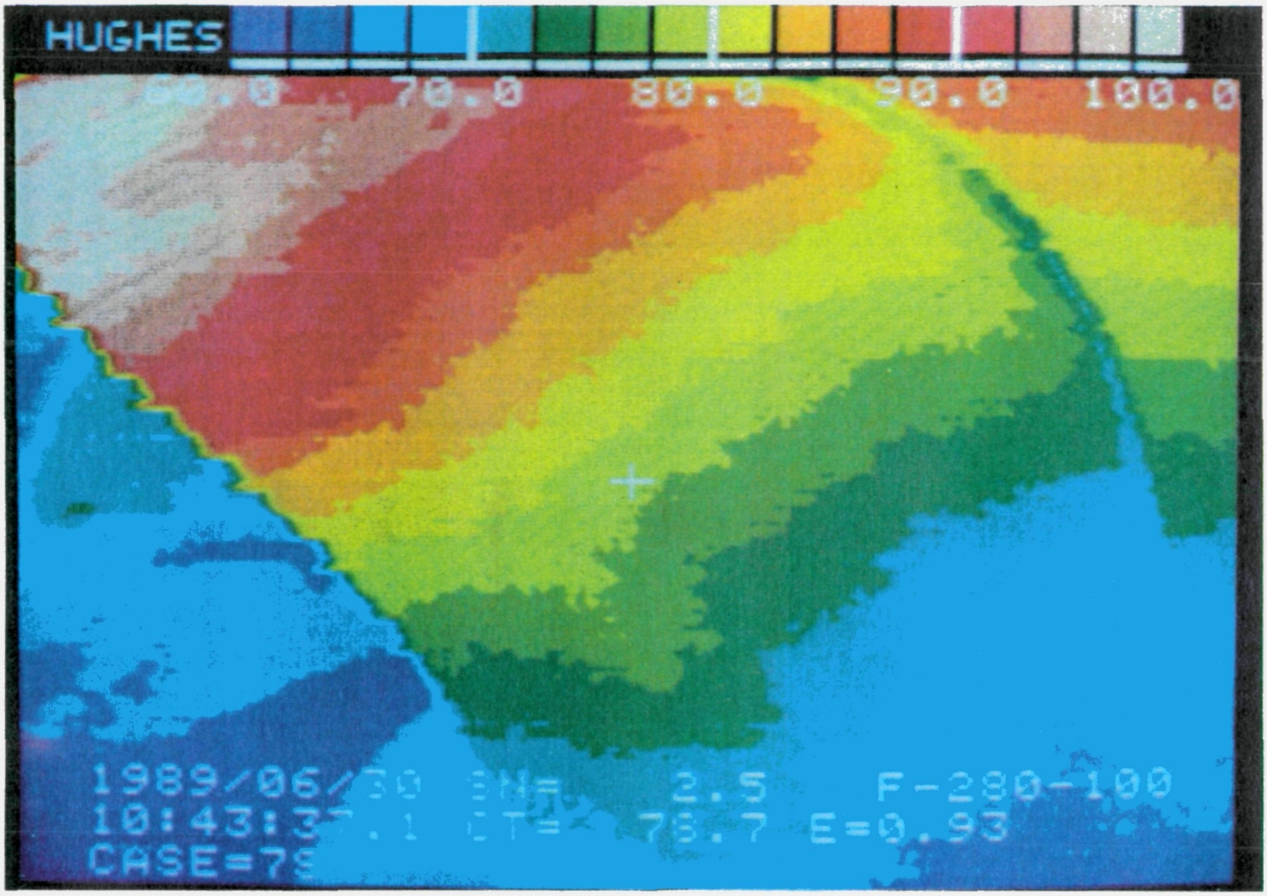

ORIGINAL PAGE
COLOR PHOTOGRAPH

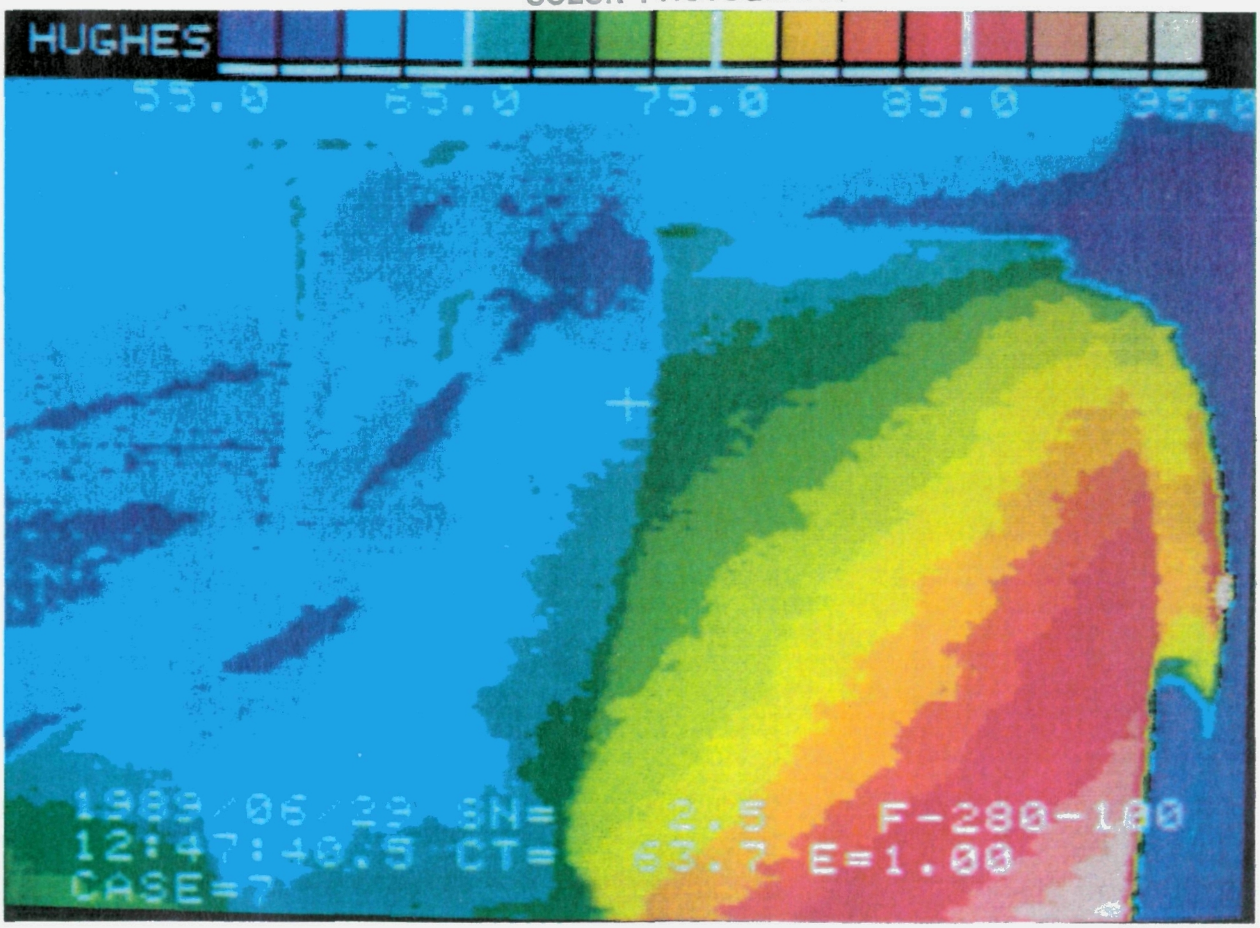

PAGE 80 INTENTIONALLY BLANK

PRECEDING PAGE BLANK NOT FILMED

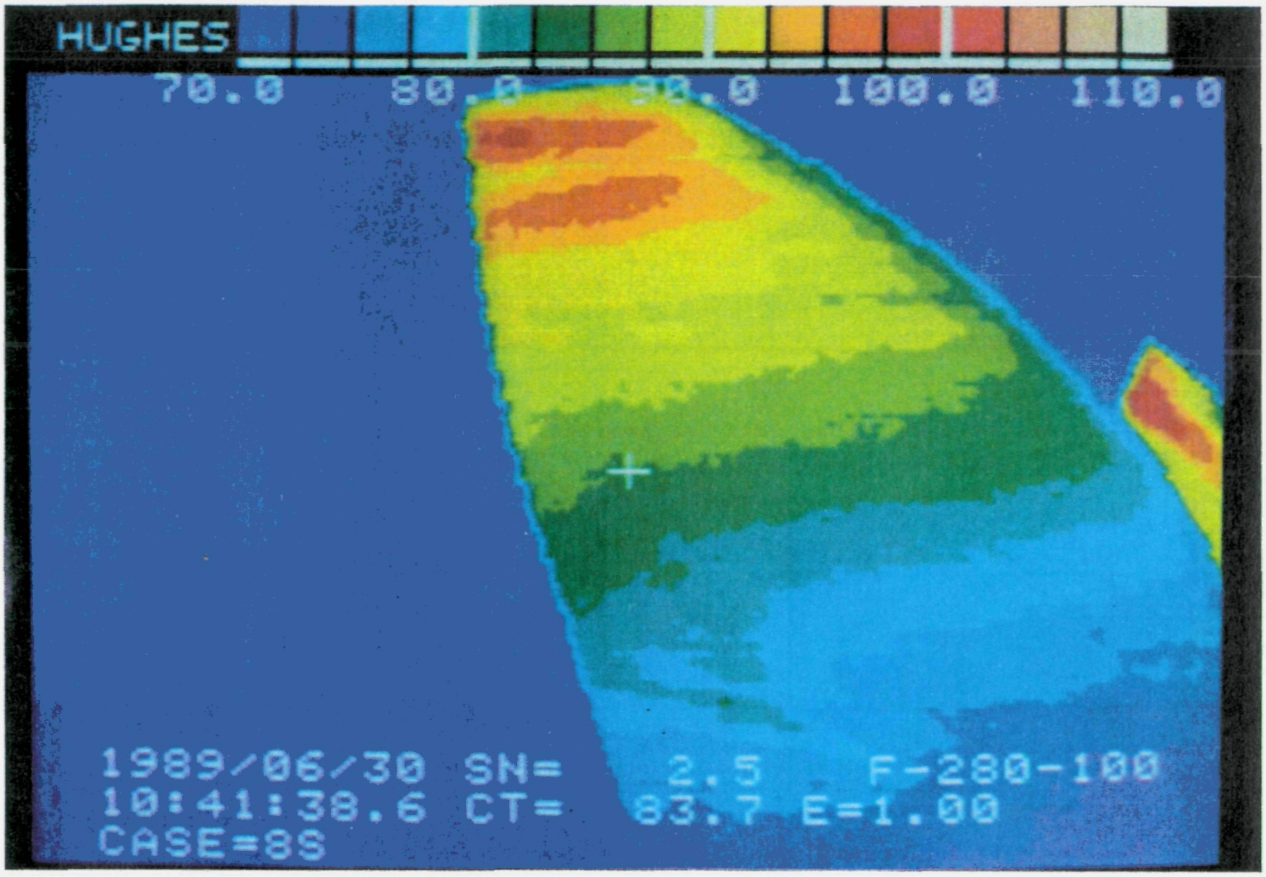

ORIGINAL PAGE
COLOR PHOTOGRAPH

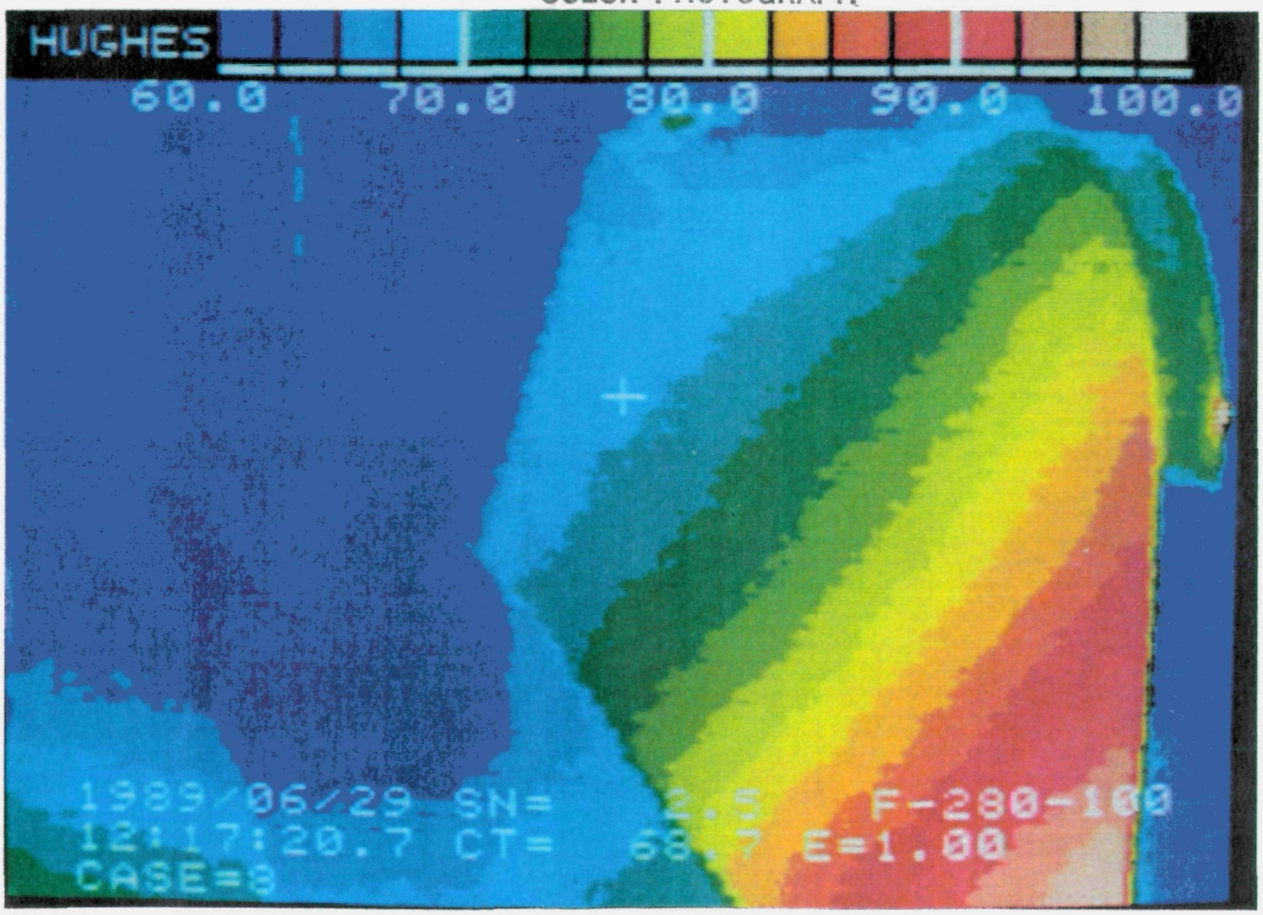

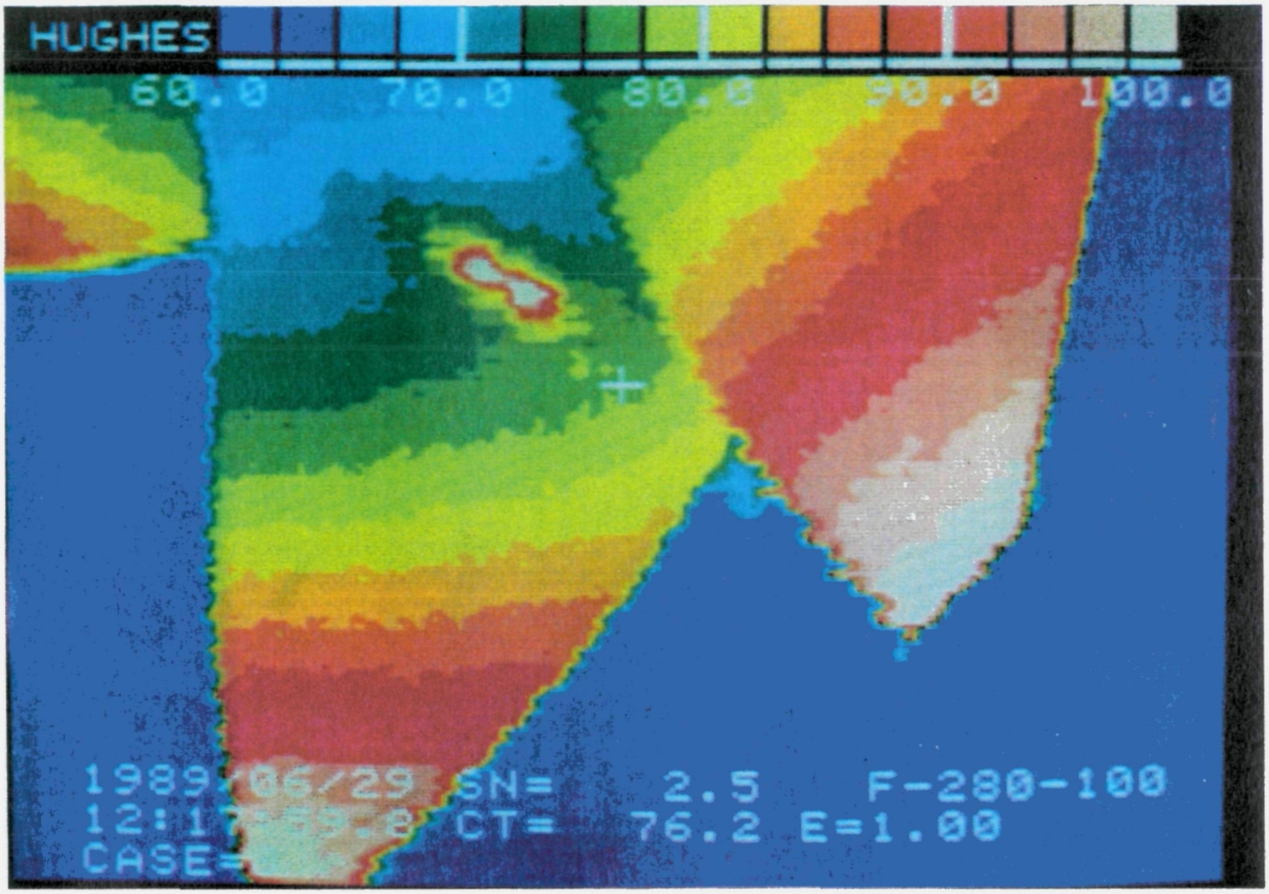

ORIGINAL PAGE
COLOR PHOTOGRAPH

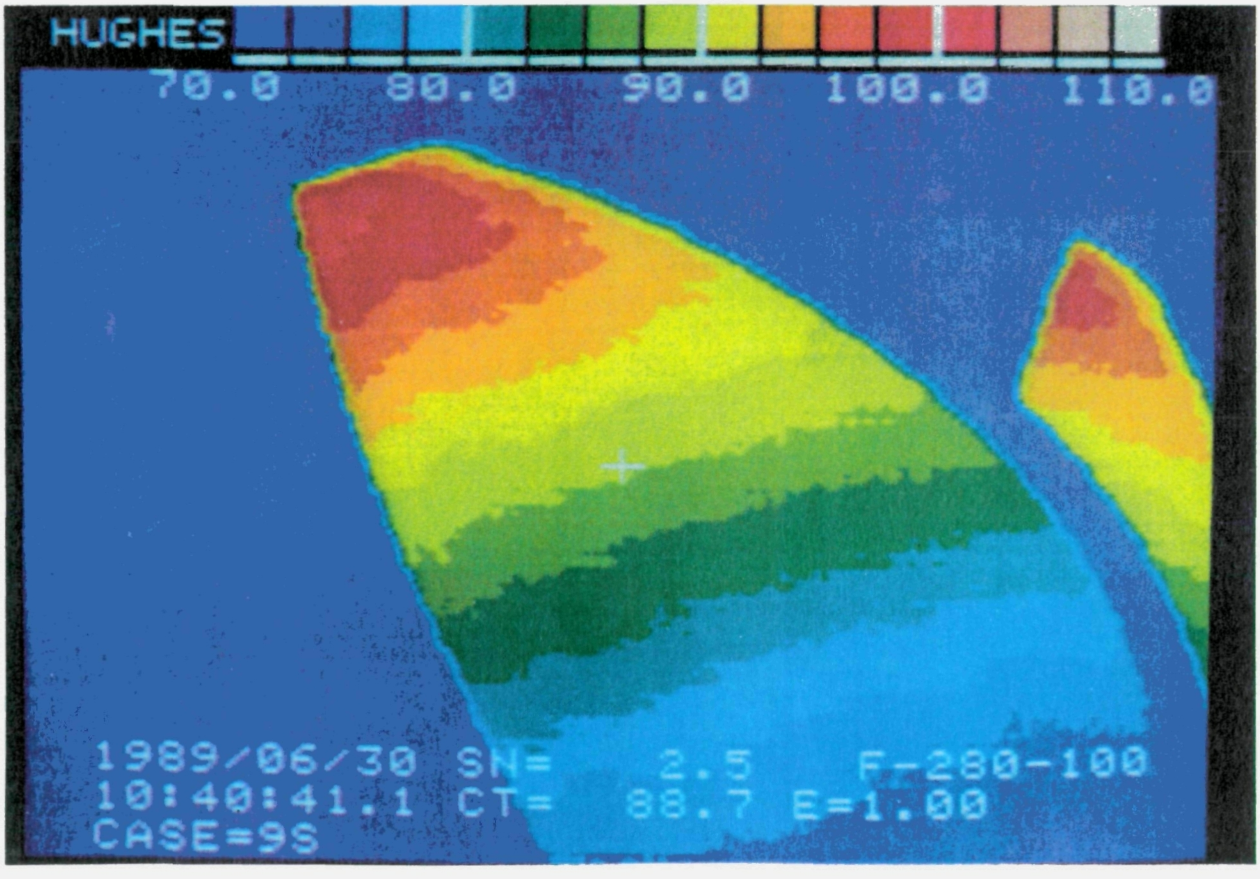

PAGE 84 INTENTIONALLY BLANK

PRECEDING PAGE BLANK NOT FILMED

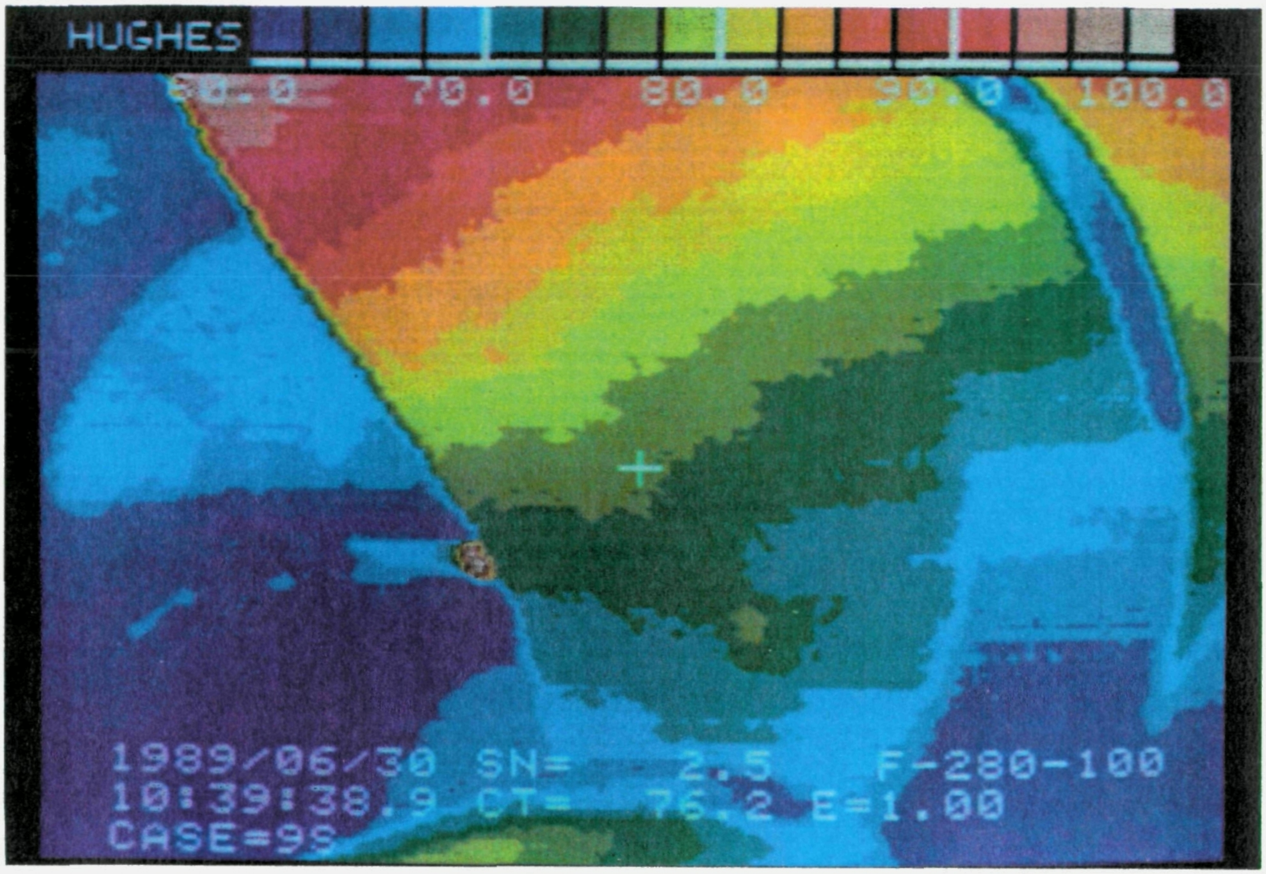

ORIGINAL PAGE
COLOR PHOTOGRAPH

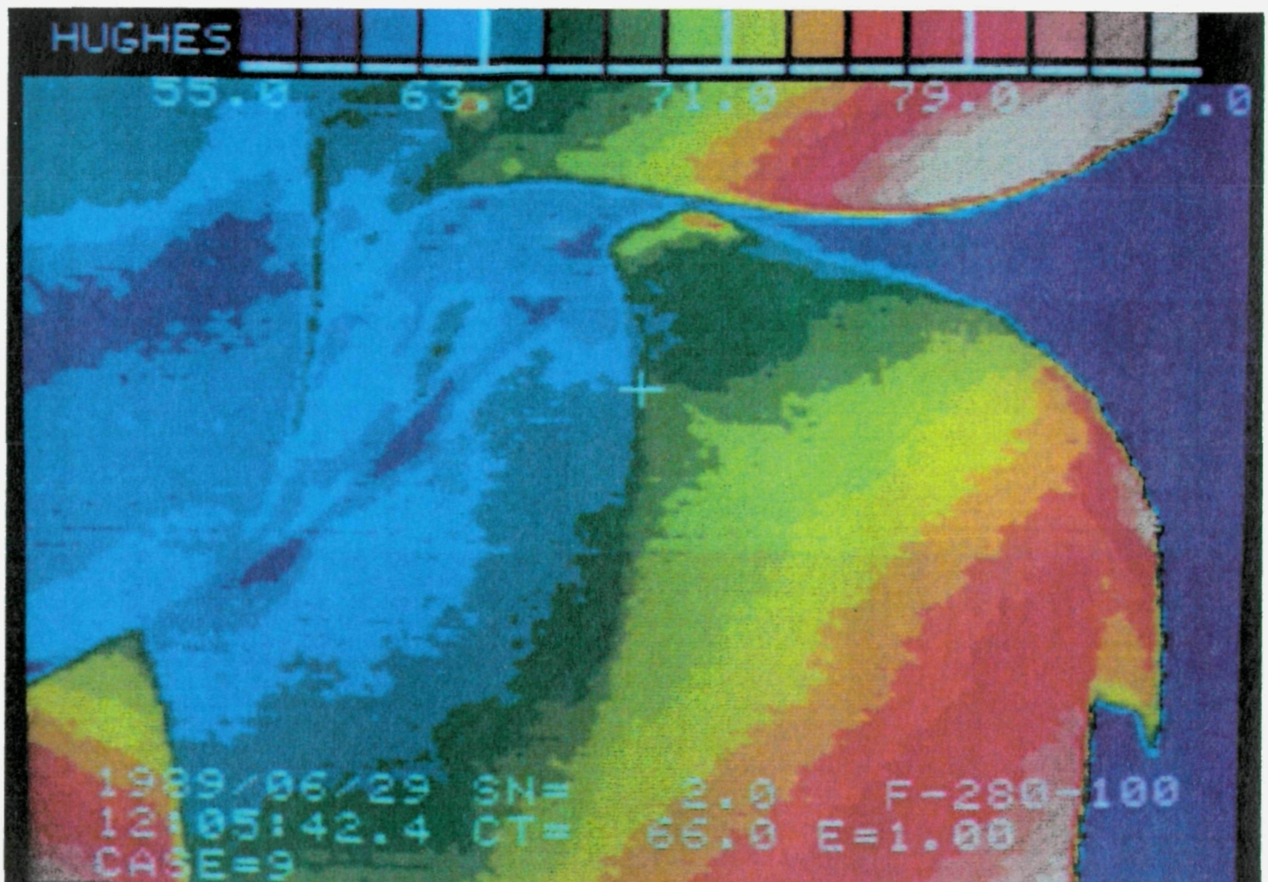

PAGE 86 INTENTIONALLY BLANK

PRECEDING PAGE BLANK NOT FILMED

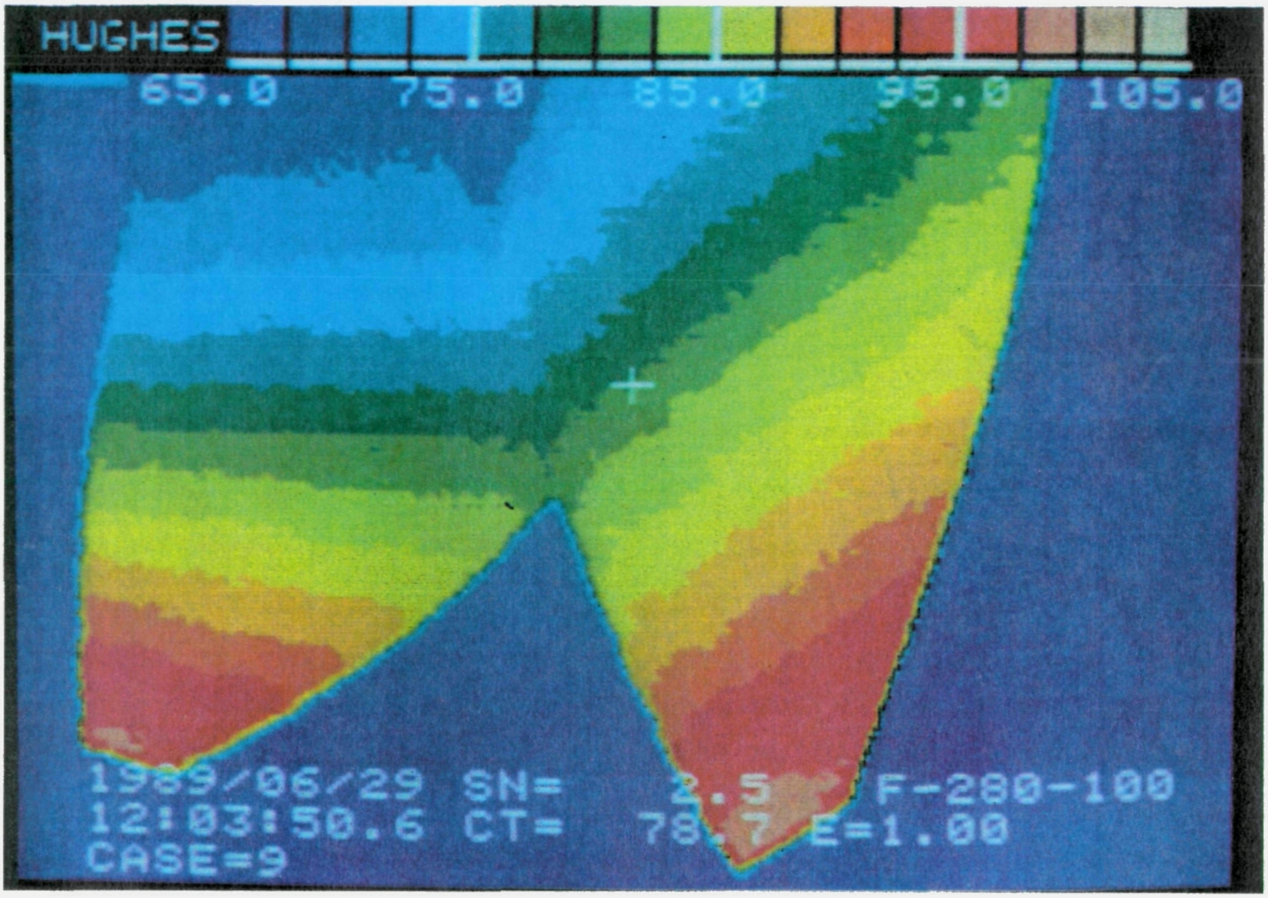
HUGHES
65.0
75.0
85.0
95.0
105.0
1989/06/29 SN= 2.5 F-280-100
12:03:50.6 CT= 78.7 E=1.00
CASE=9

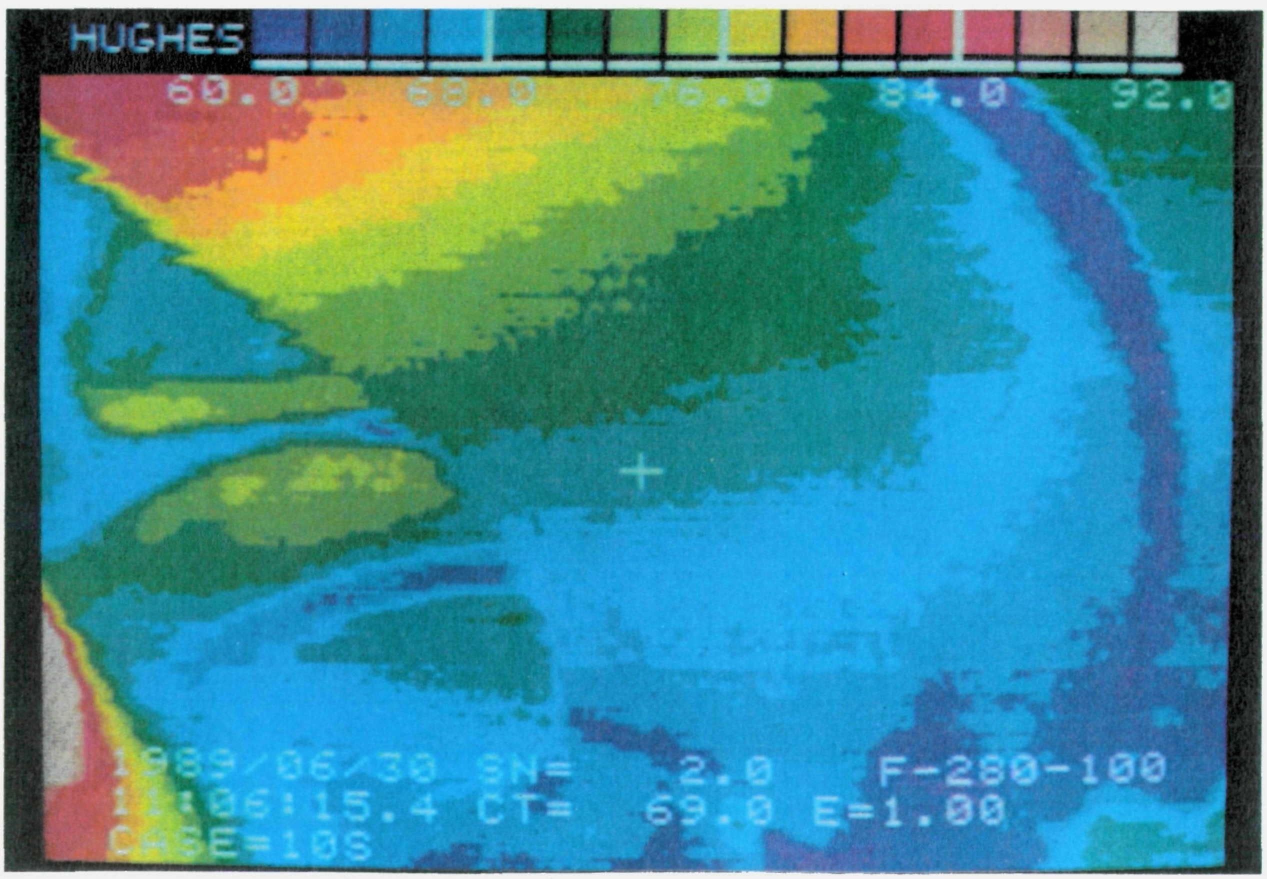
HUGHES
60.0
68.0
76.0
84.0
92.0
1989/06/30 SN= 2.0 F-280-100
11:06:15.4 CT= 69.0 E=1.00
CASE=10S

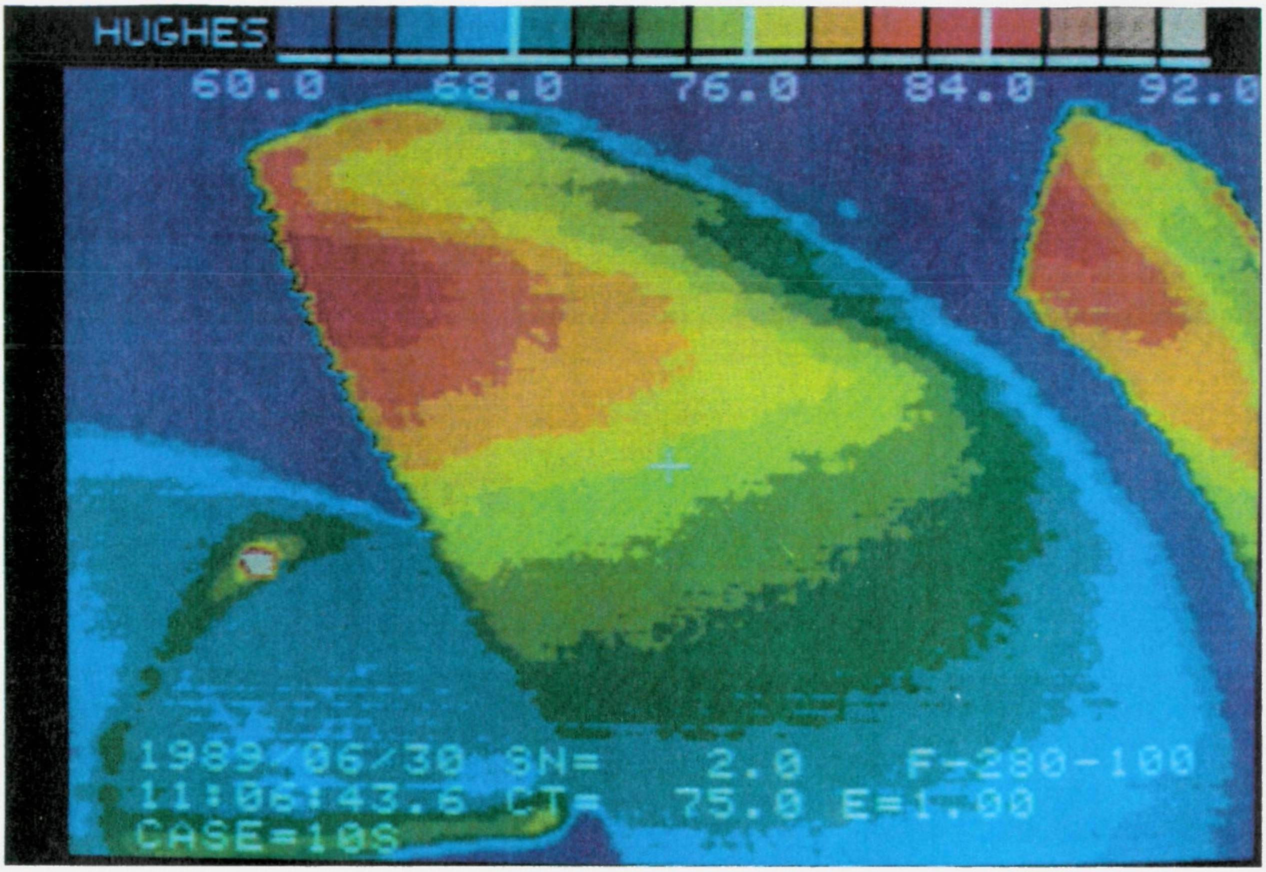
HUGHES
60.0 68.0 76.0 84.0 92.0
1989/06/30 SN= 2.0 F-280-100
11:06:43.6 CT= 75.0 E=1.00
CASE=10S

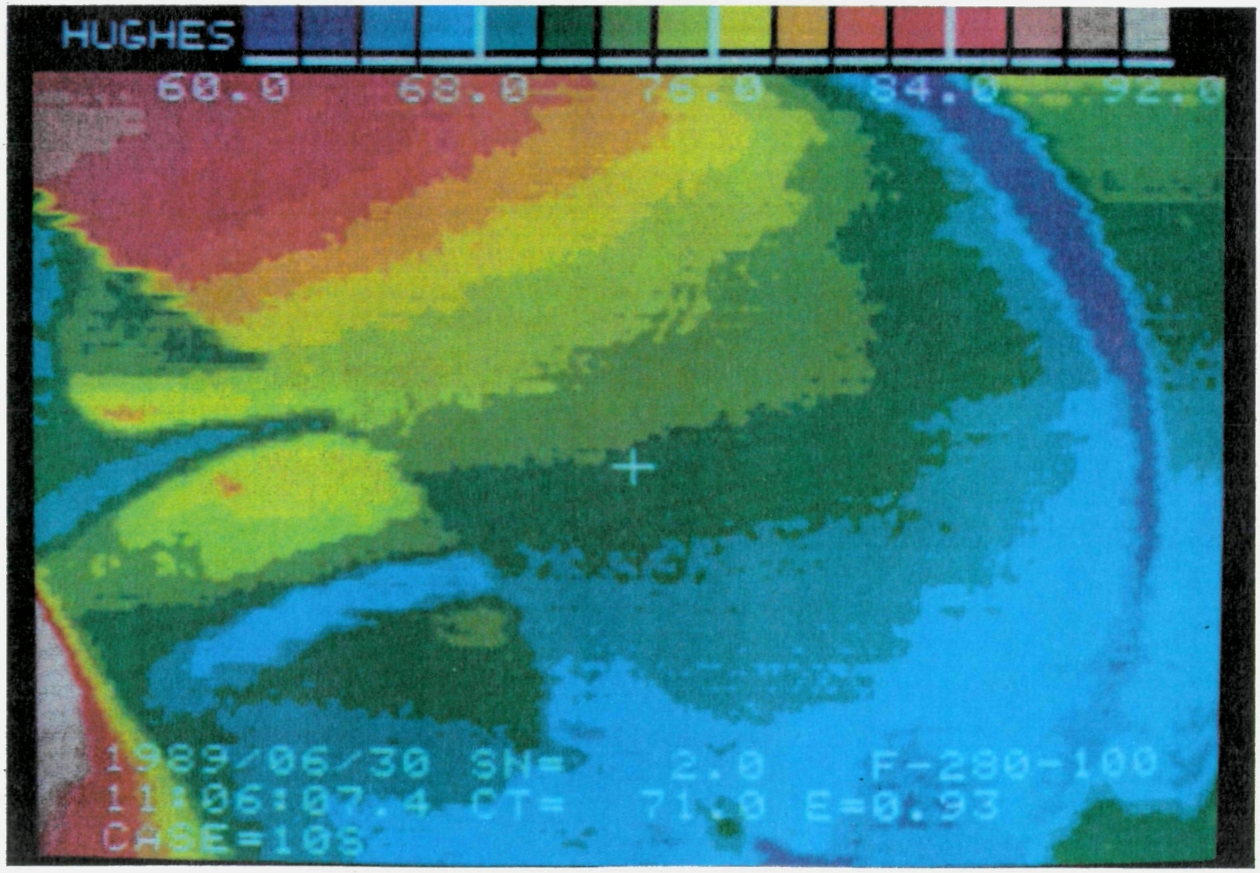
HUGHES
60.0 68.0 76.0 84.0 92.0
1989/06/30 SN= 2.0 F-280-100
11:06:07.4 CT= 71.0 E=0.93
CASE=10S

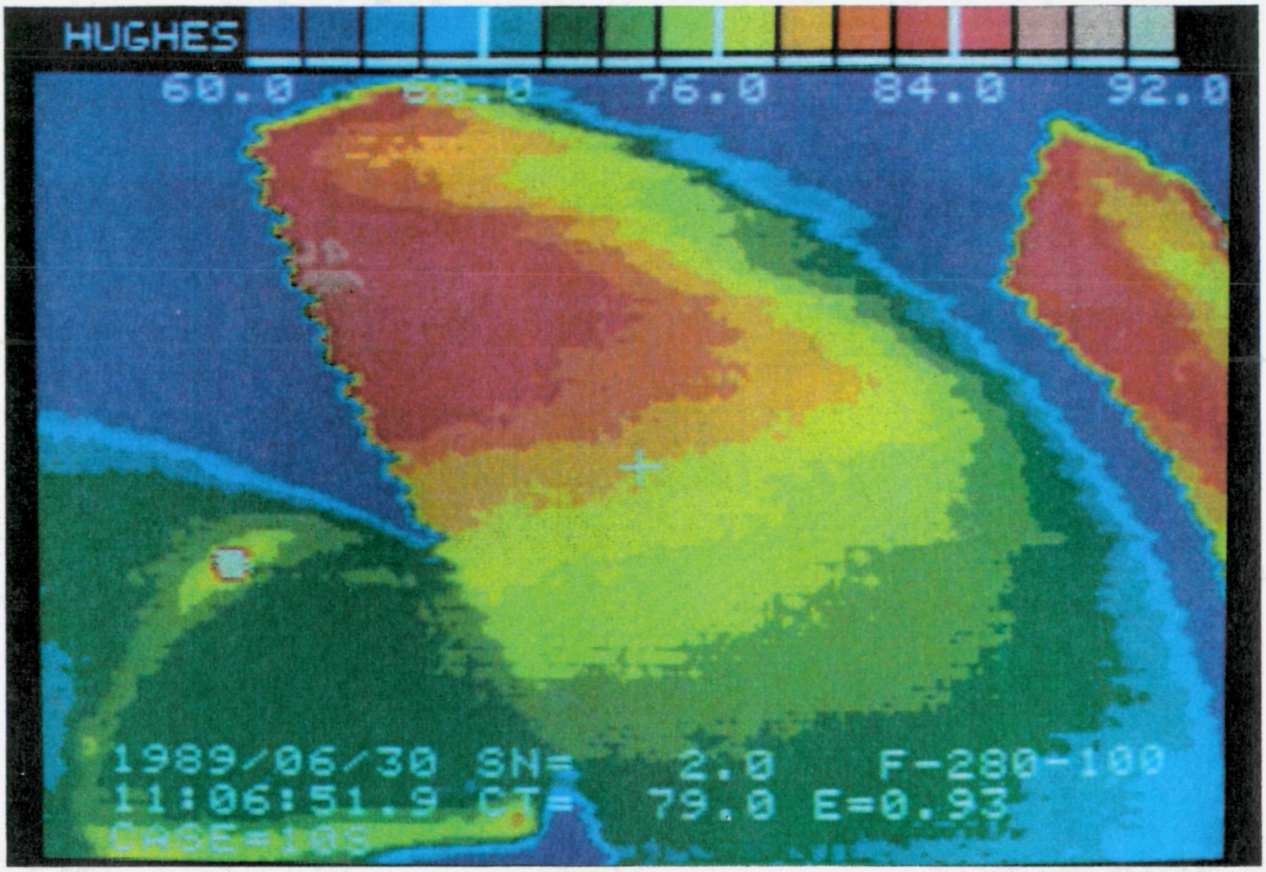

ORIGINAL PAGE
COLOR PHOTOGRAPH

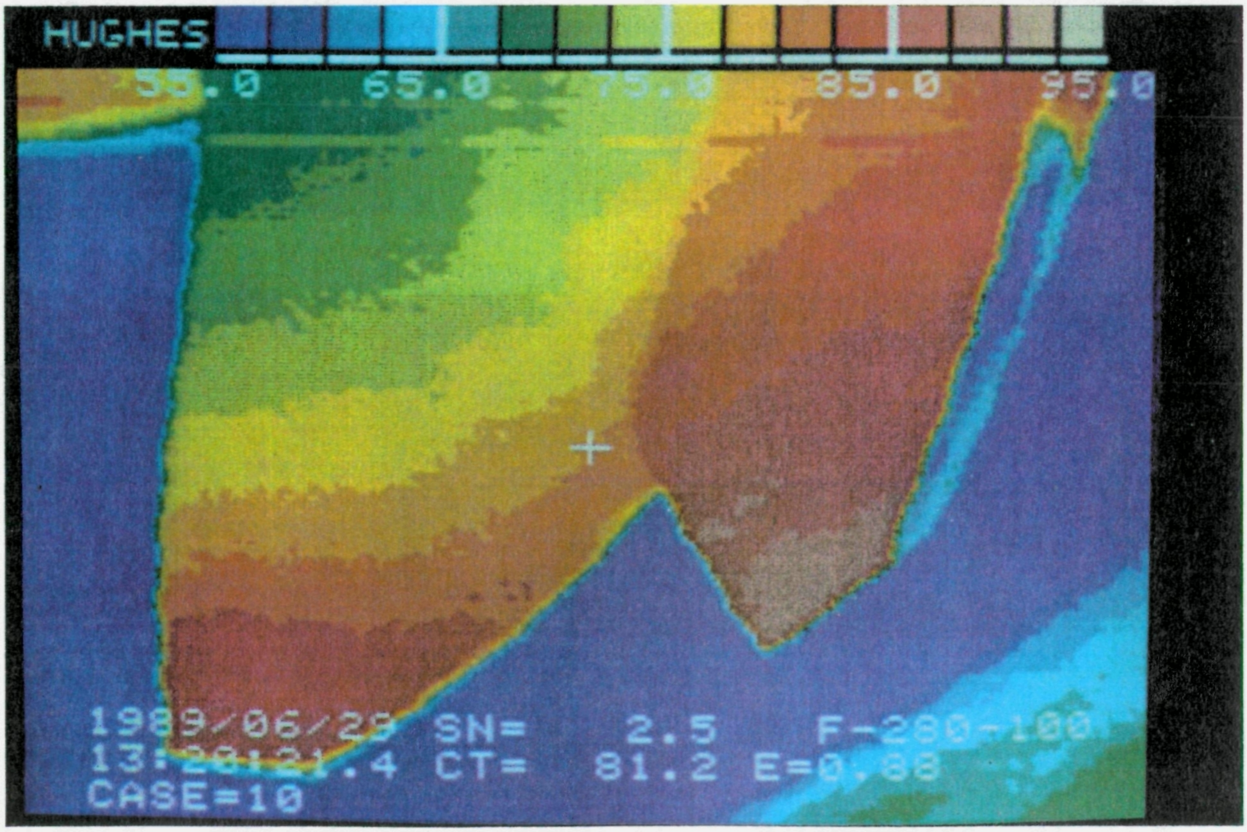

PAGE 92 INTENTIONALLY BLANK

PRECEDING PAGE BLANK NOT FILMED

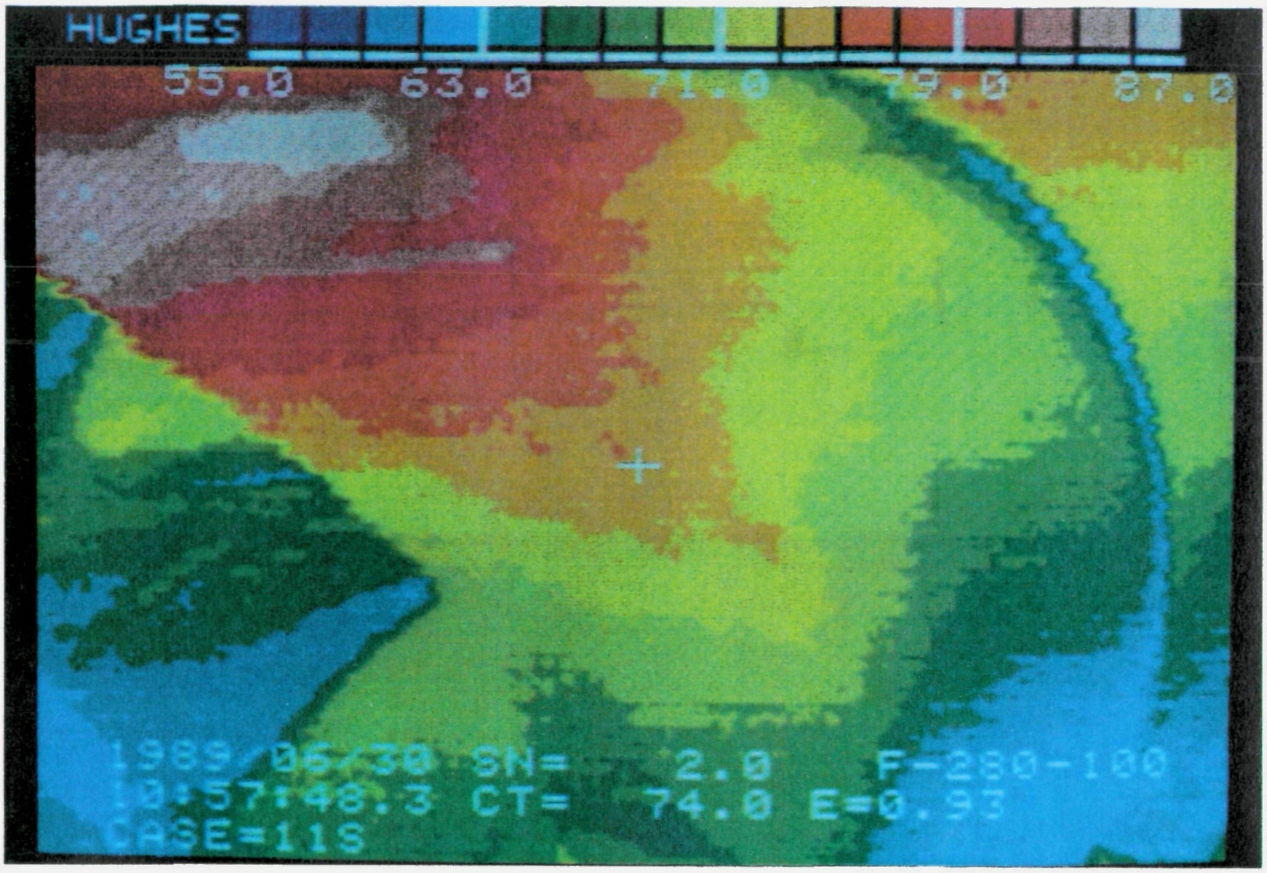
HUGHES
55.0 63.0 71.0 79.0 87.0
1989/06/30 SN= 2.0 F-280-100
10:57:48.3 CT= 74.0 E=0.93
CASE=11S

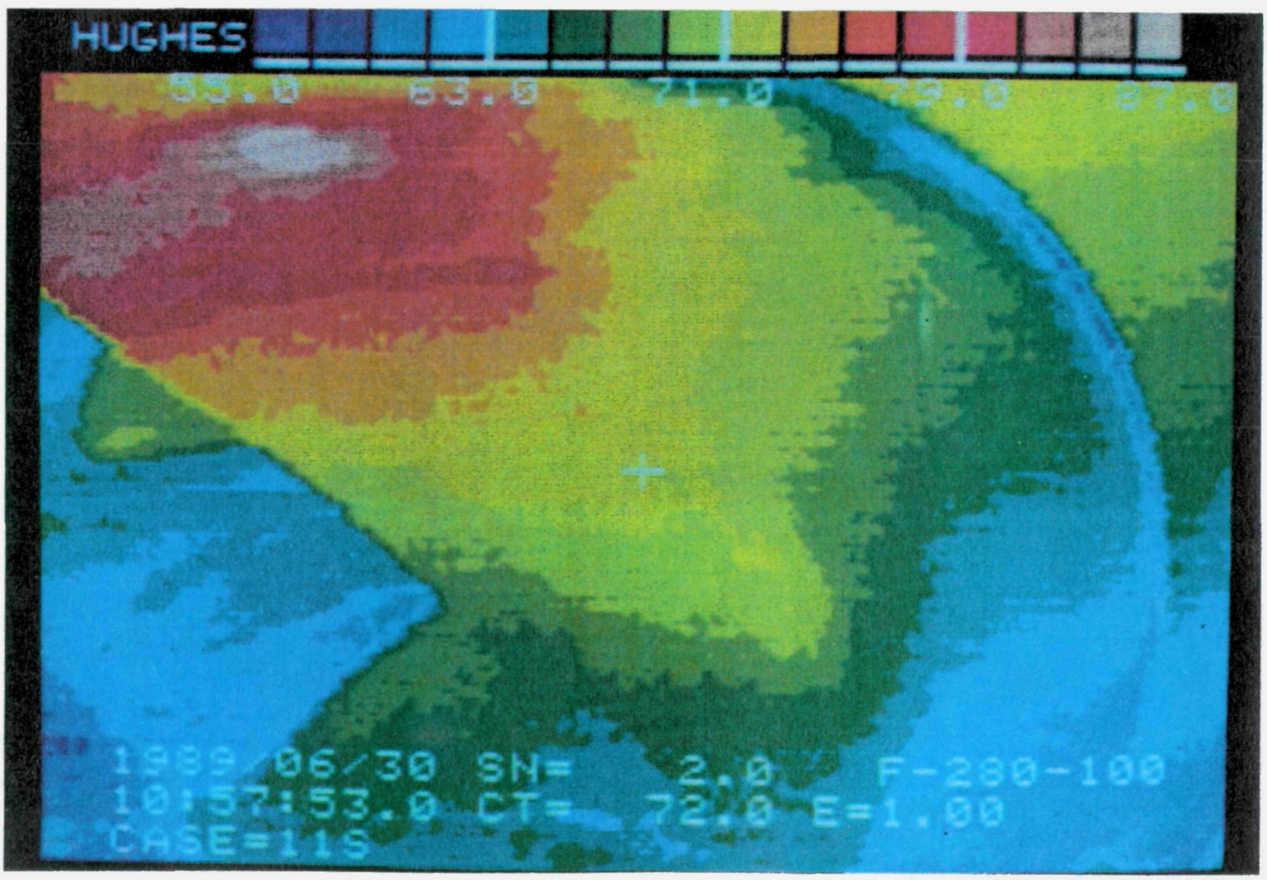
HUGHES
55.0 63.0 71.0 79.0 87.0
1989/06/30 SN= 2.0 F-280-100
10:57:53.0 CT= 72.0 E=1.00
CASE=11S

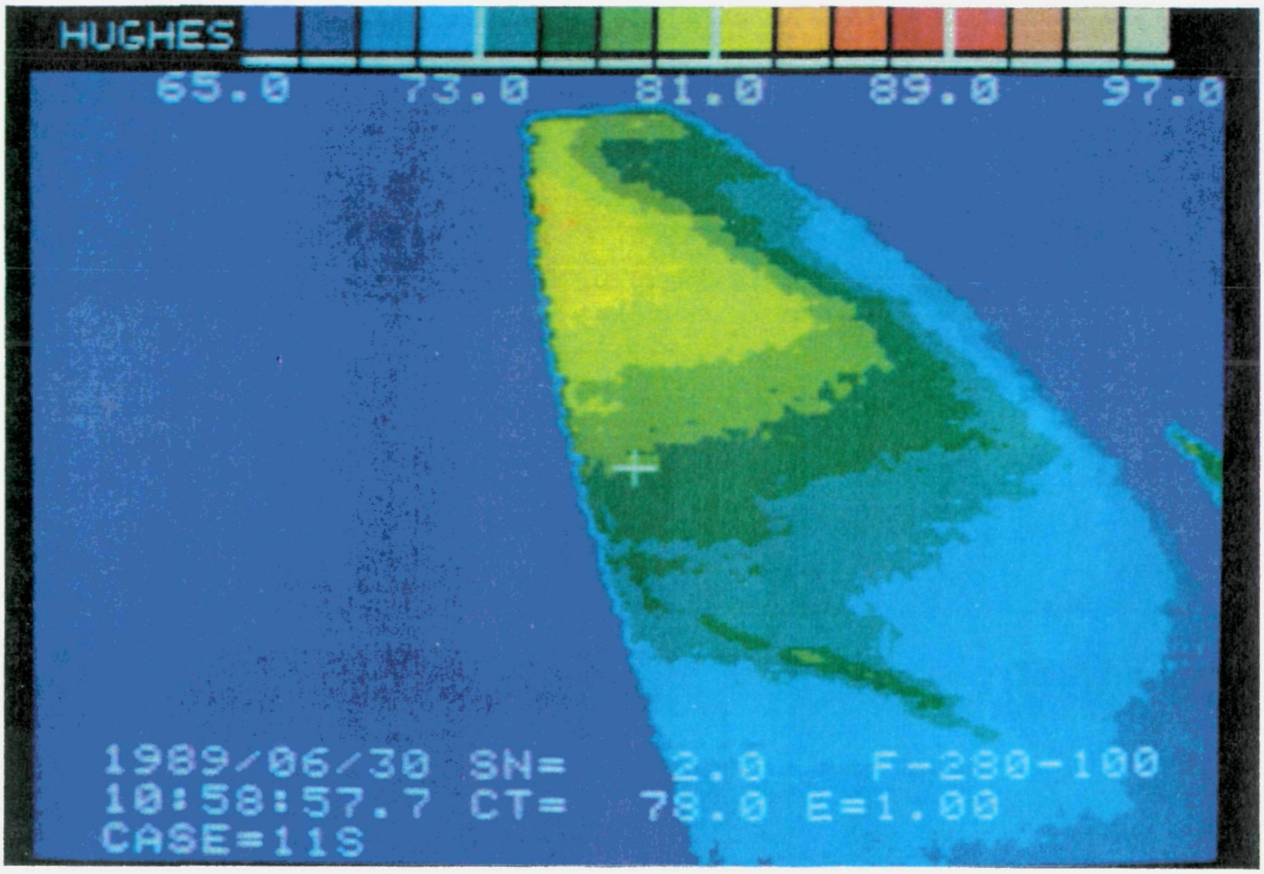

ORIGINAL PAGE
COLOR PHOTOGRAPH

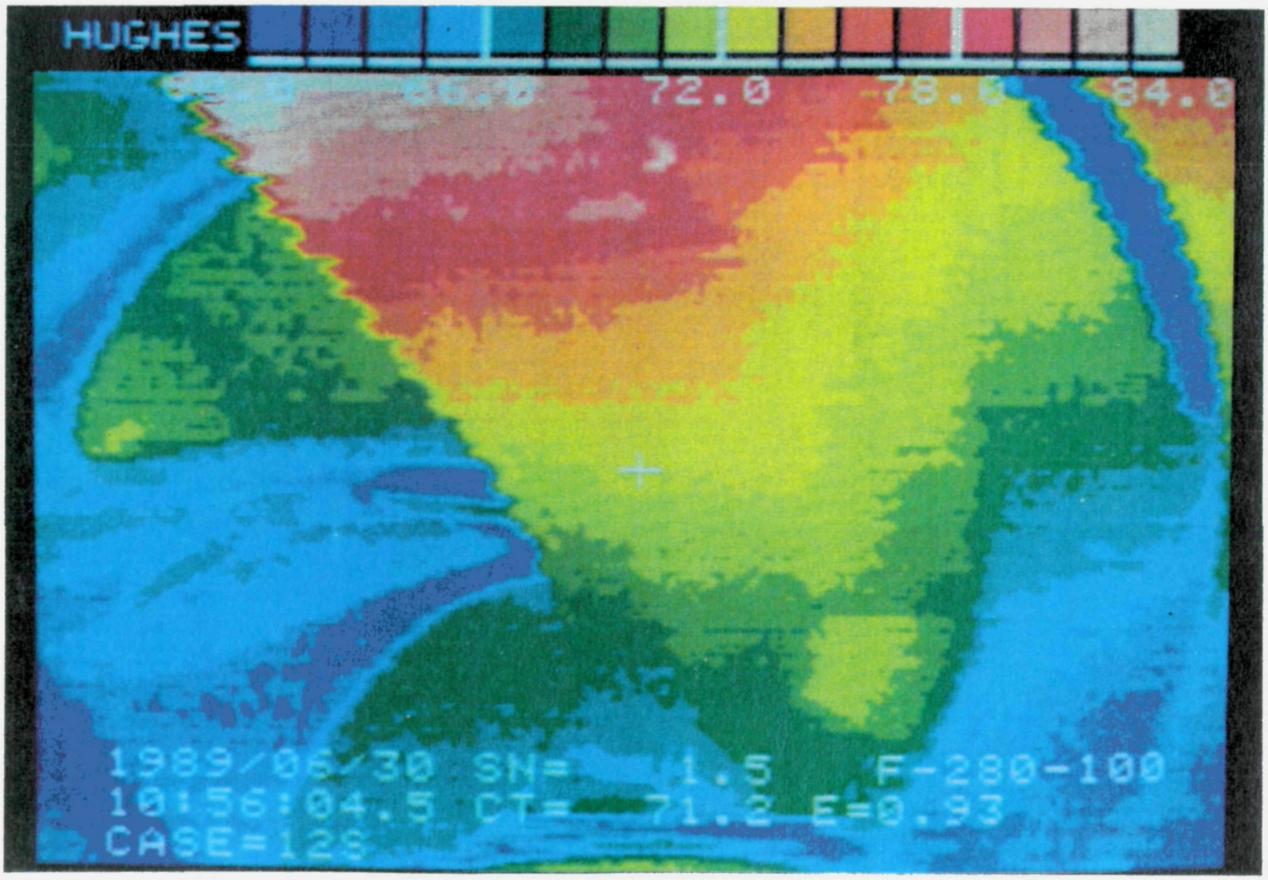

PAGE 96 INTENTIONALLY BLANK

PRECEDING PAGE BLANK NOT FILMED

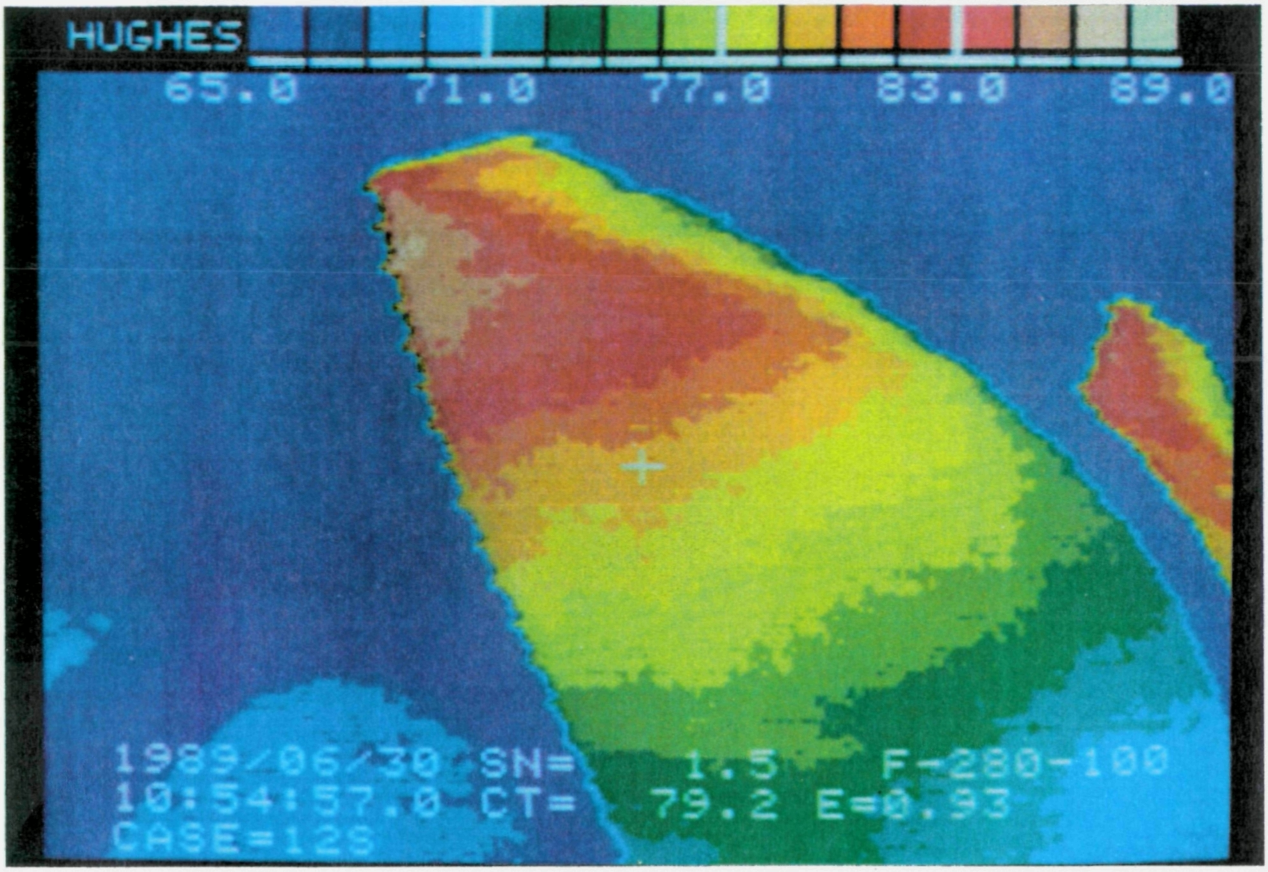

ORIGINAL PAGE
COLOR PHOTOGRAPH

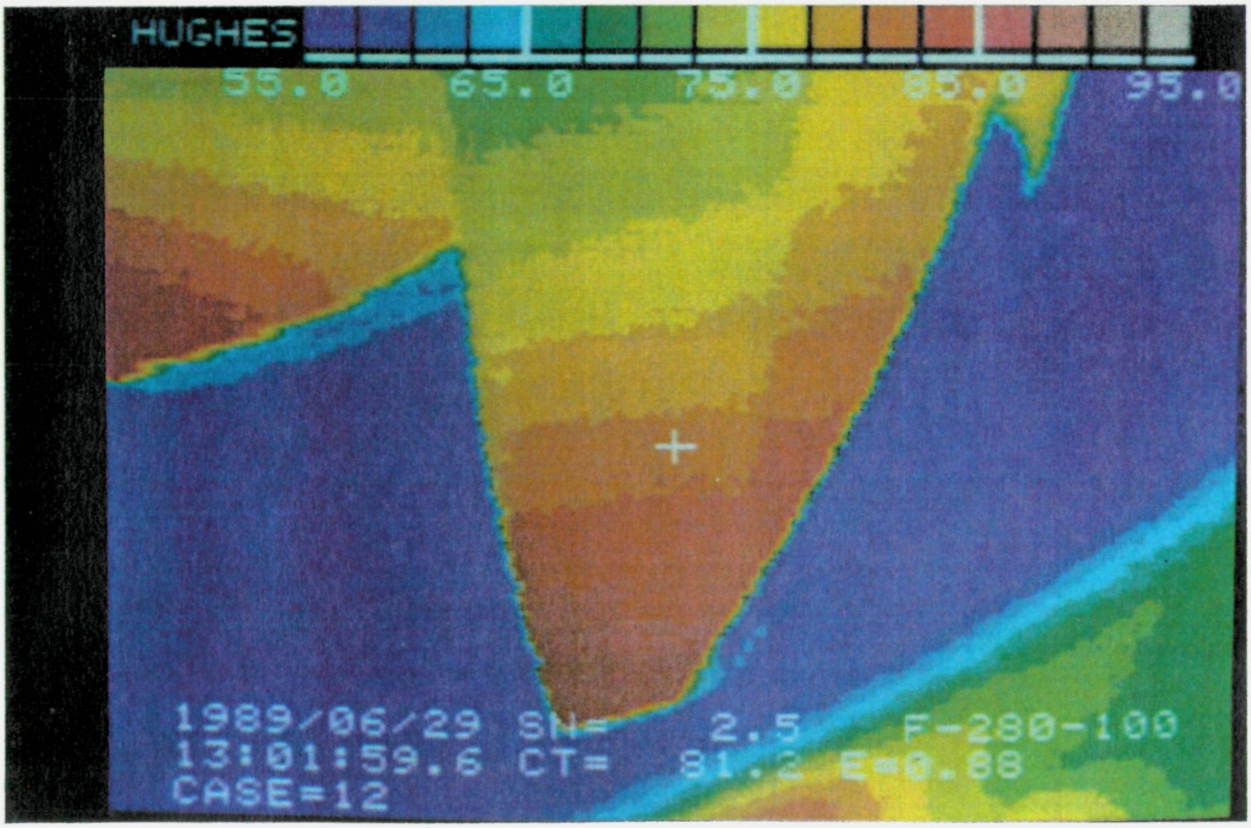

PRECEDING PAGE BLANK NOT FILMED

PAGE 98 INTENTIONALLY BLANK

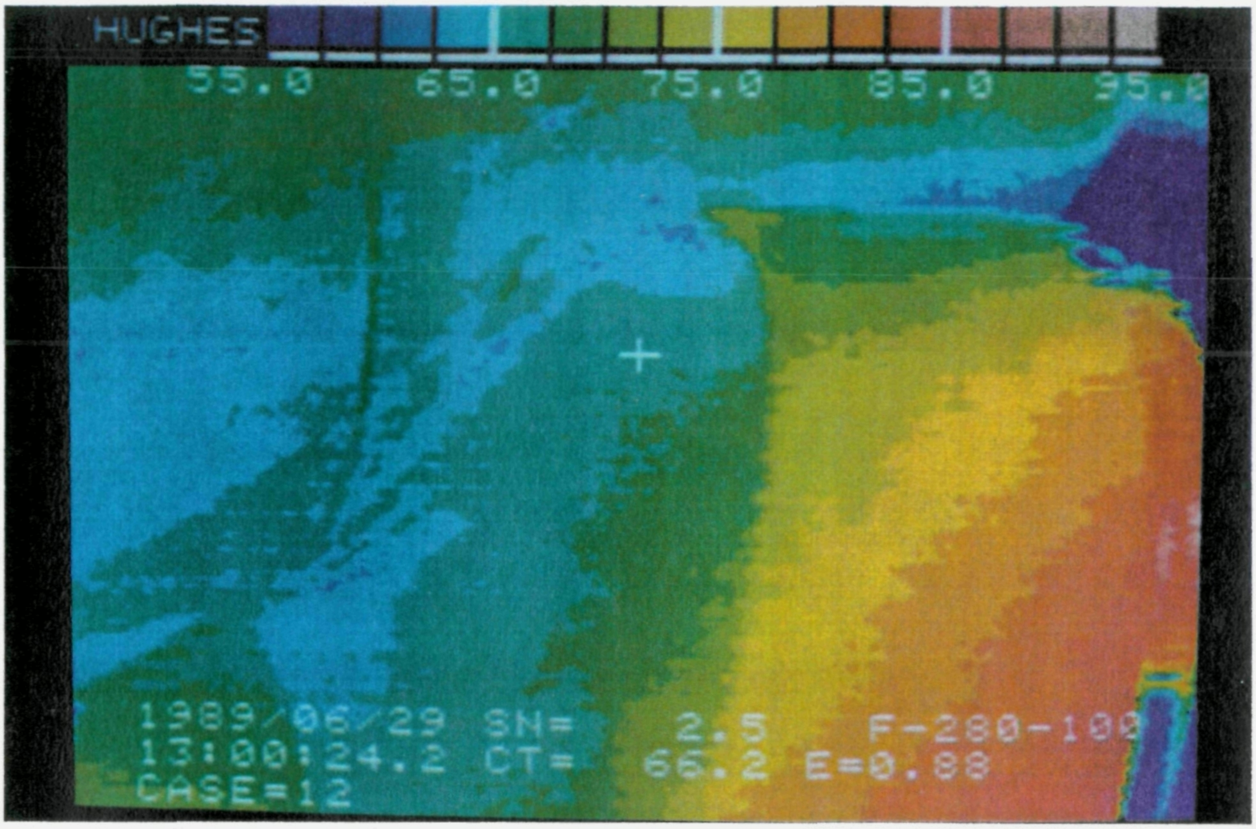
HUGHES
55.0 65.0 75.0 85.0 95.0
1989/06/29 SN= 2.5 F-280-100
13:00:24.2 CT= 66.2 E=0.88
CASE=12

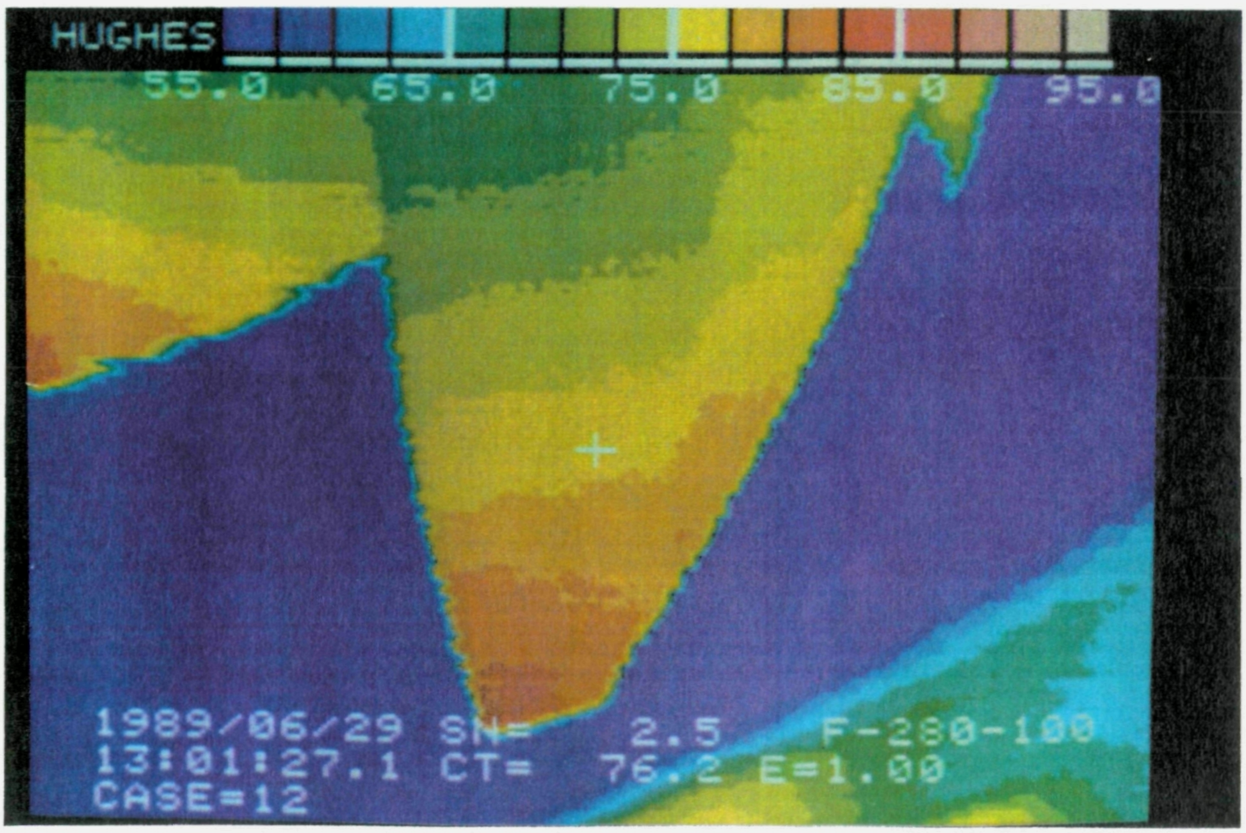
HUGHES
55.0 65.0 75.0 85.0 95.0
1989/06/29 SN= 2.5 F-280-100
13:01:27.1 CT= 76.2 E=1.00
CASE=12

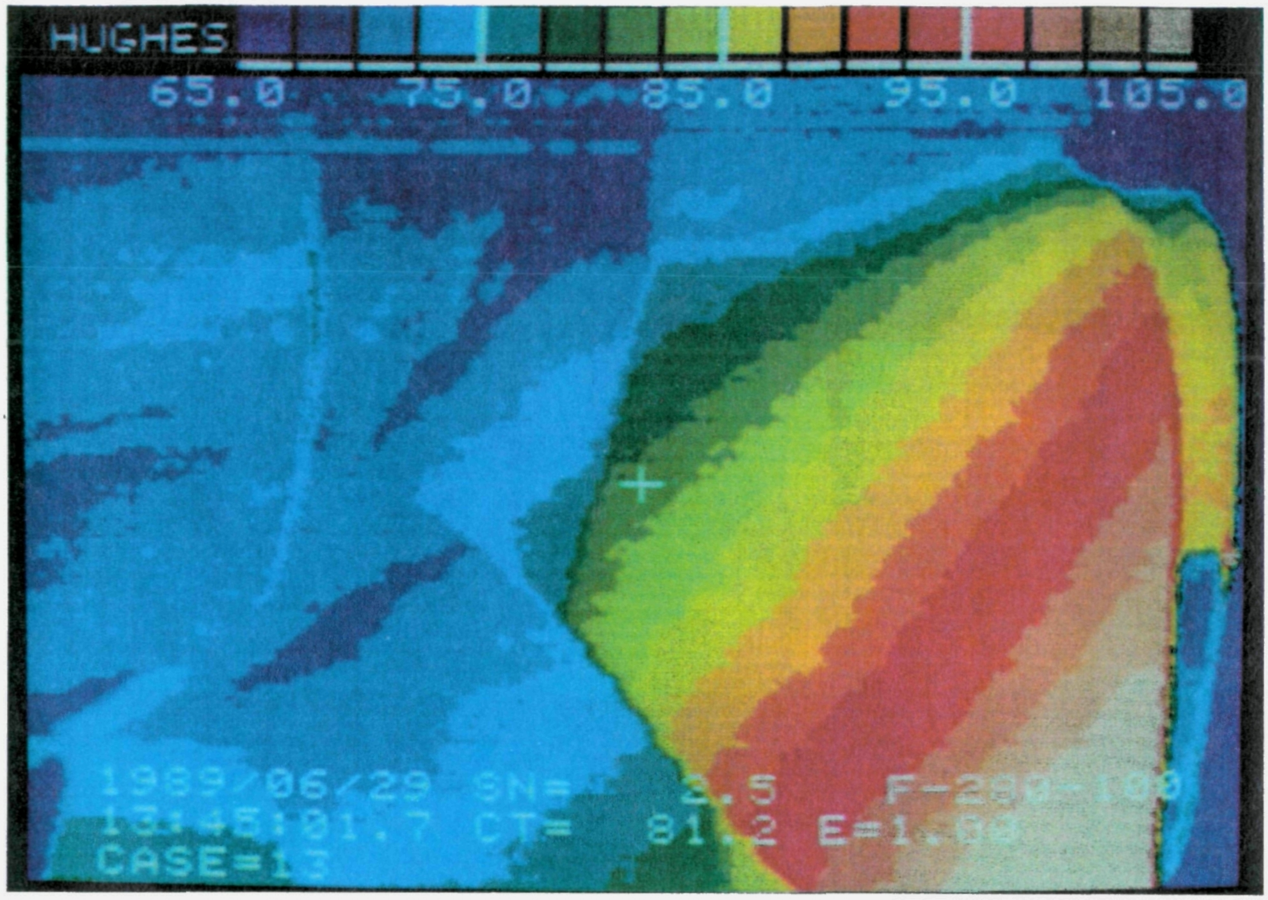
HUGHES
65.0 75.0 85.0 95.0 105.0
1989/06/29 SN= 2.5 F-280-100
13:45:01.7 CT= 81.2 E=1.00
CASE=13

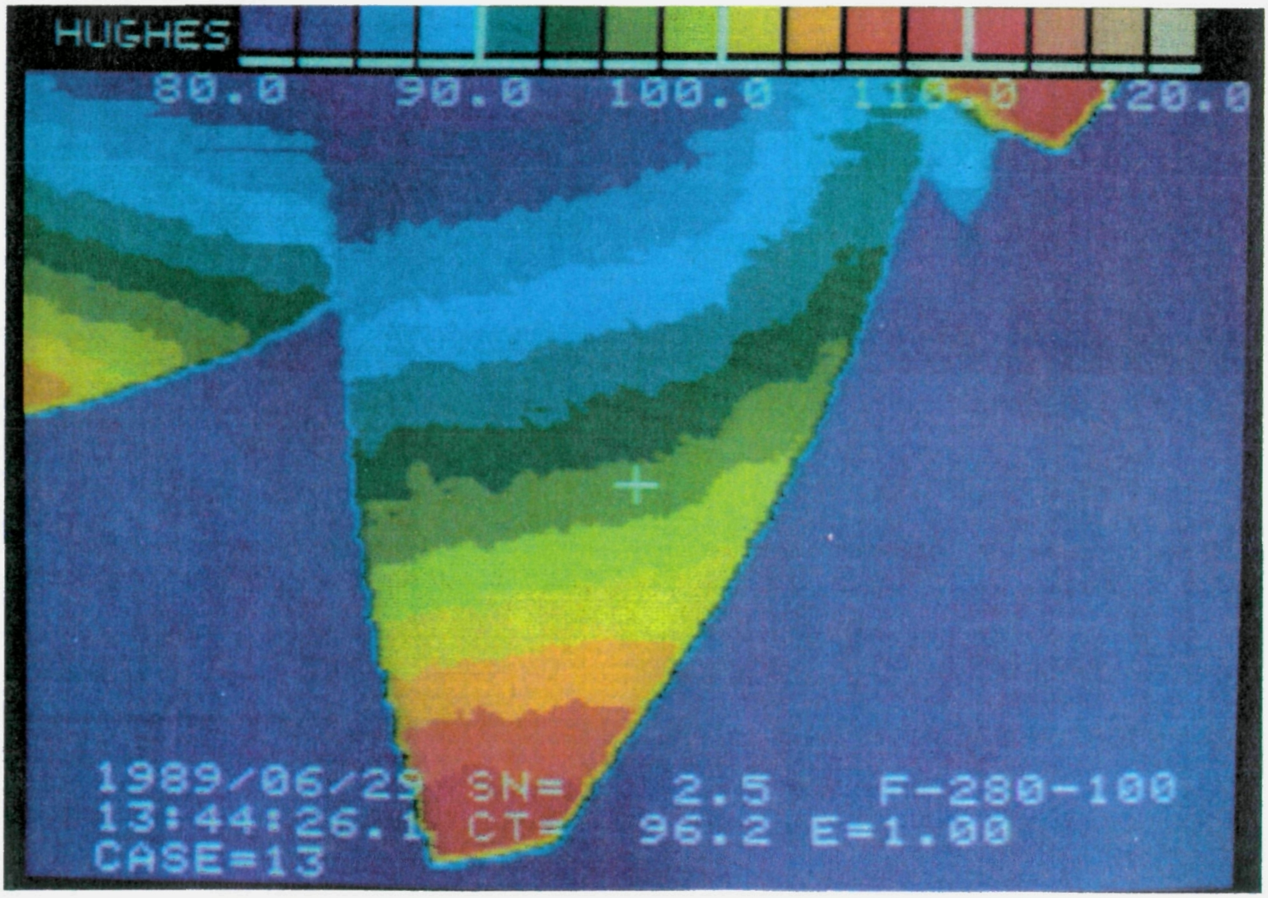
HUGHES
80.0 90.0 100.0 110.0 120.0
1989/06/29 SN= 2.5 F-280-100
13:44:26.1 CT= 96.2 E=1.00
CASE=13

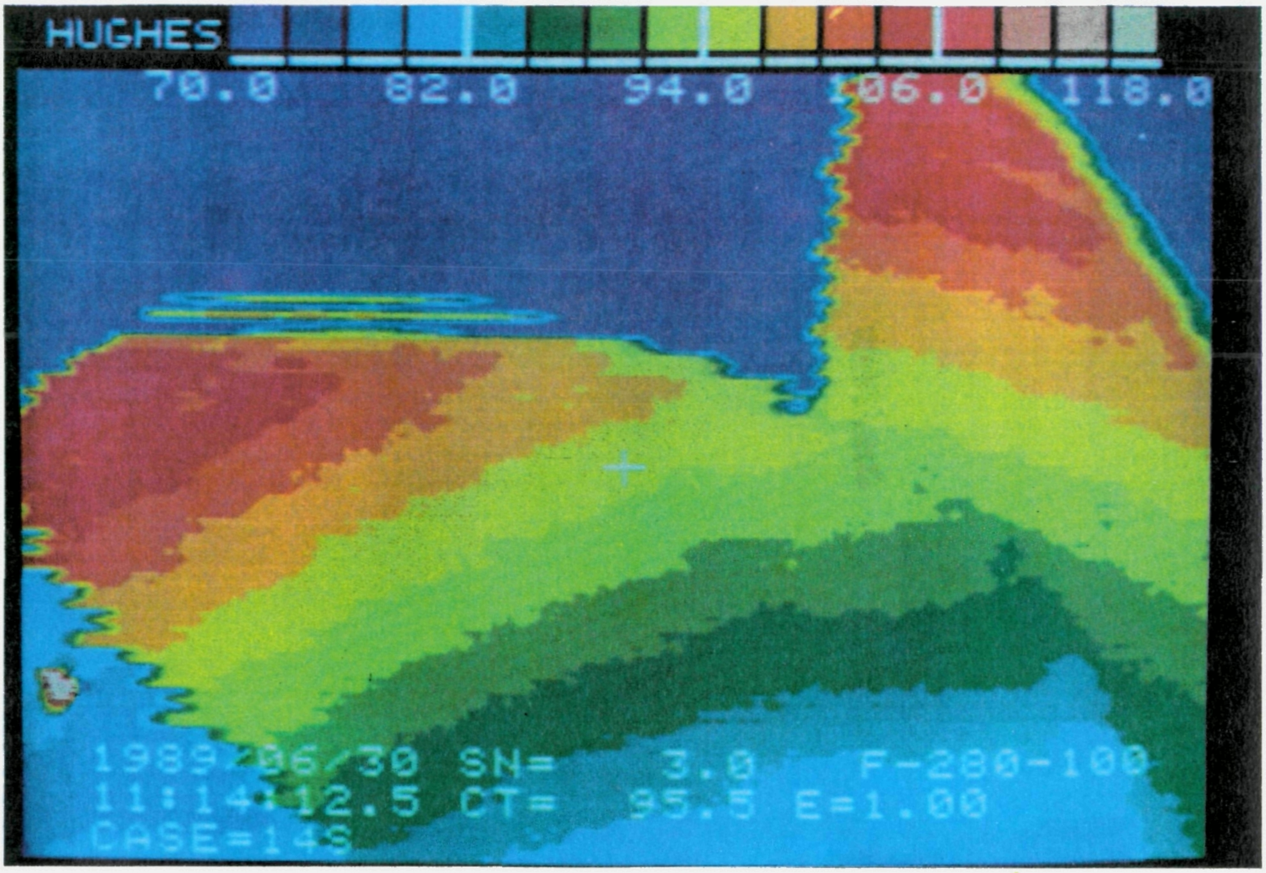

ORIGINAL PAGE
COLOR PHOTOGRAPH

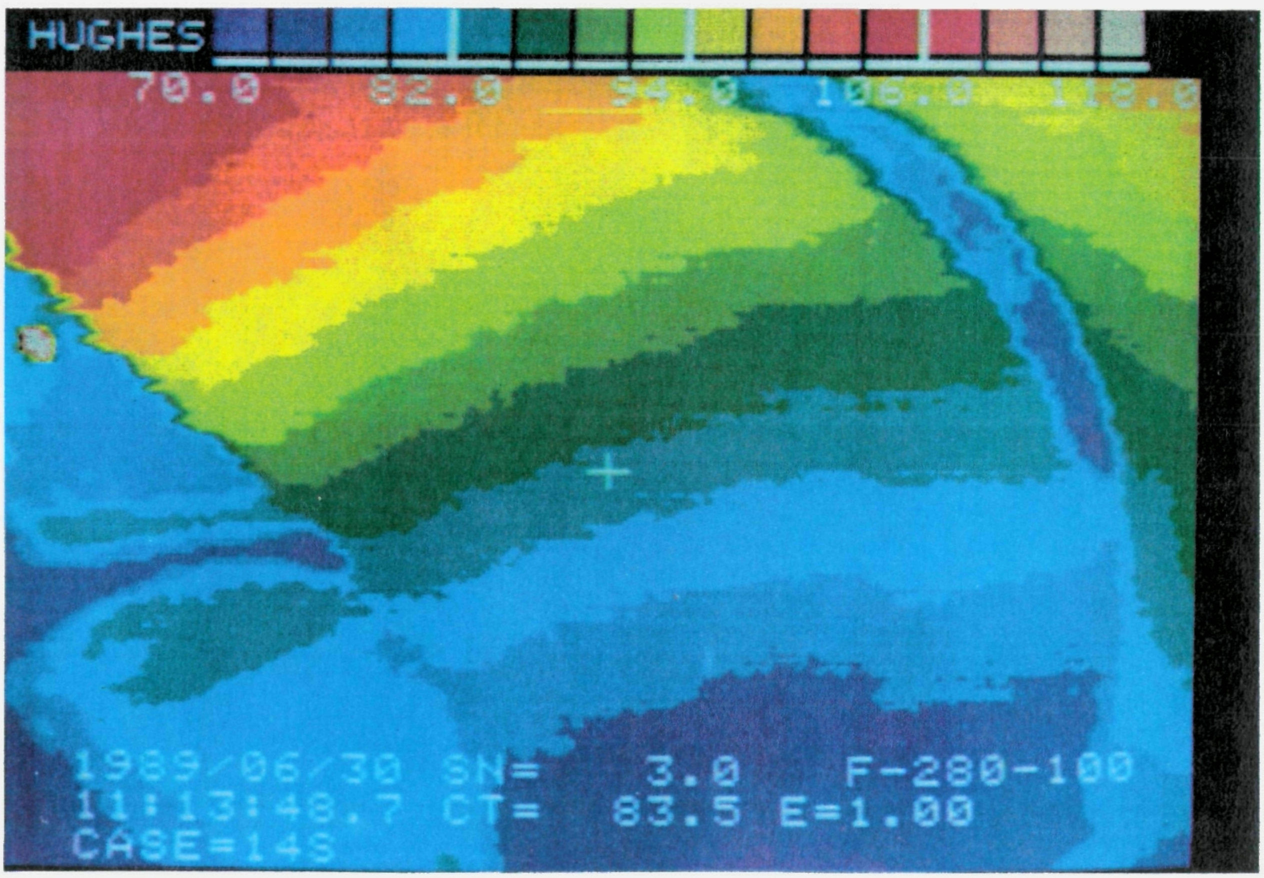

PAGE 104 INTENTIONALLY BLANK

PRECEDING PAGE BLANK NOT FILMED

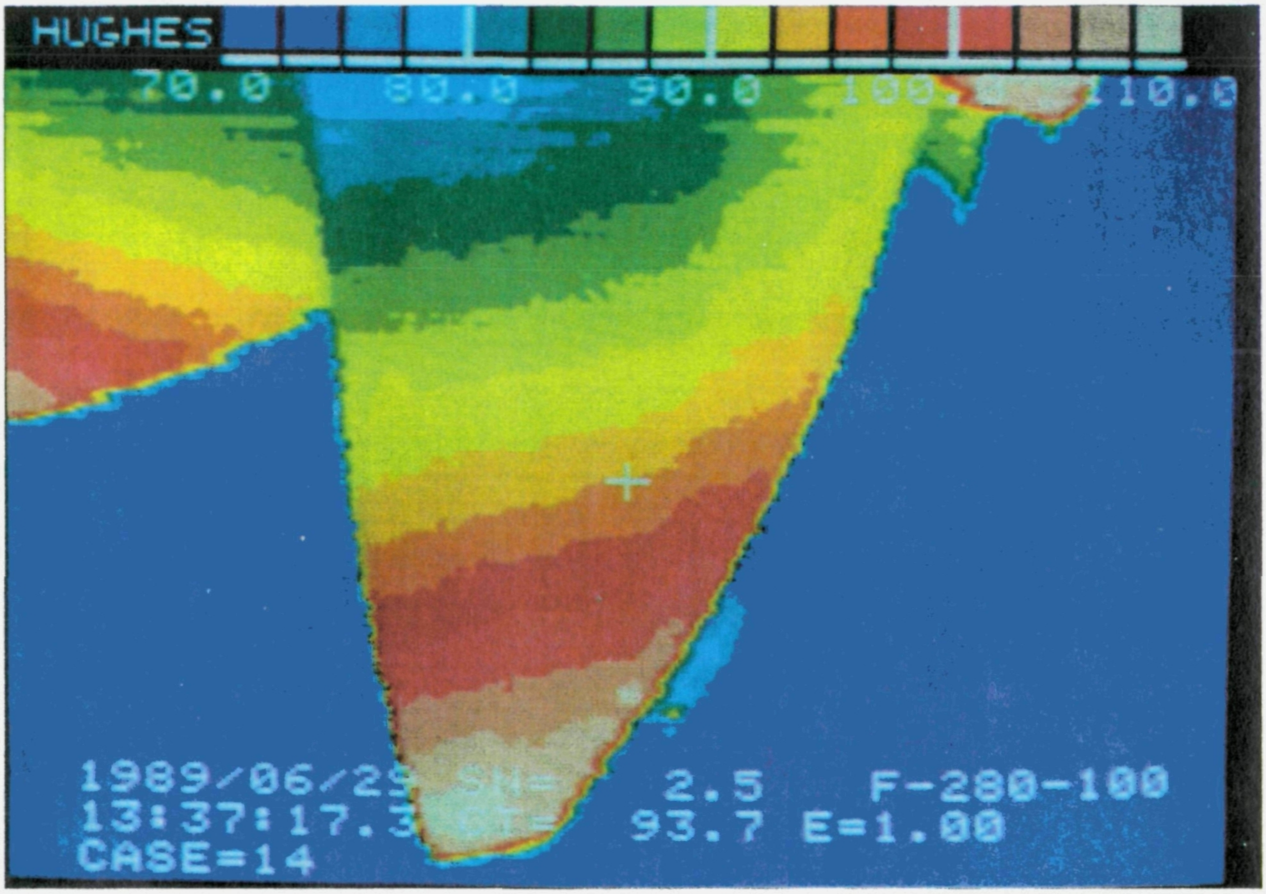

ORIGINAL PAGE
COLOR PHOTOGRAPH

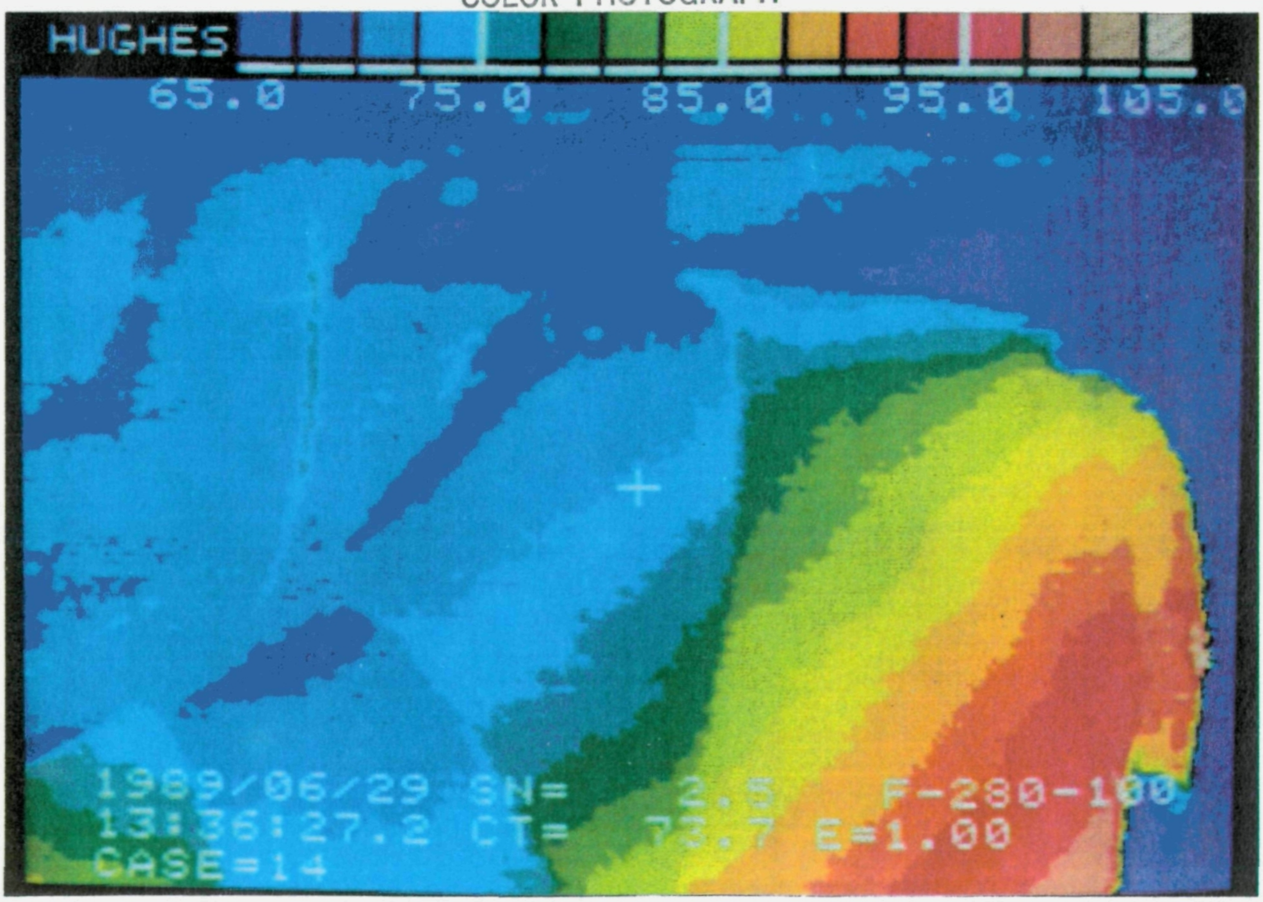

PAGE 106 INTENTIONALLY BLANK

PRECEDING PAGE BLANK NOT FILMED

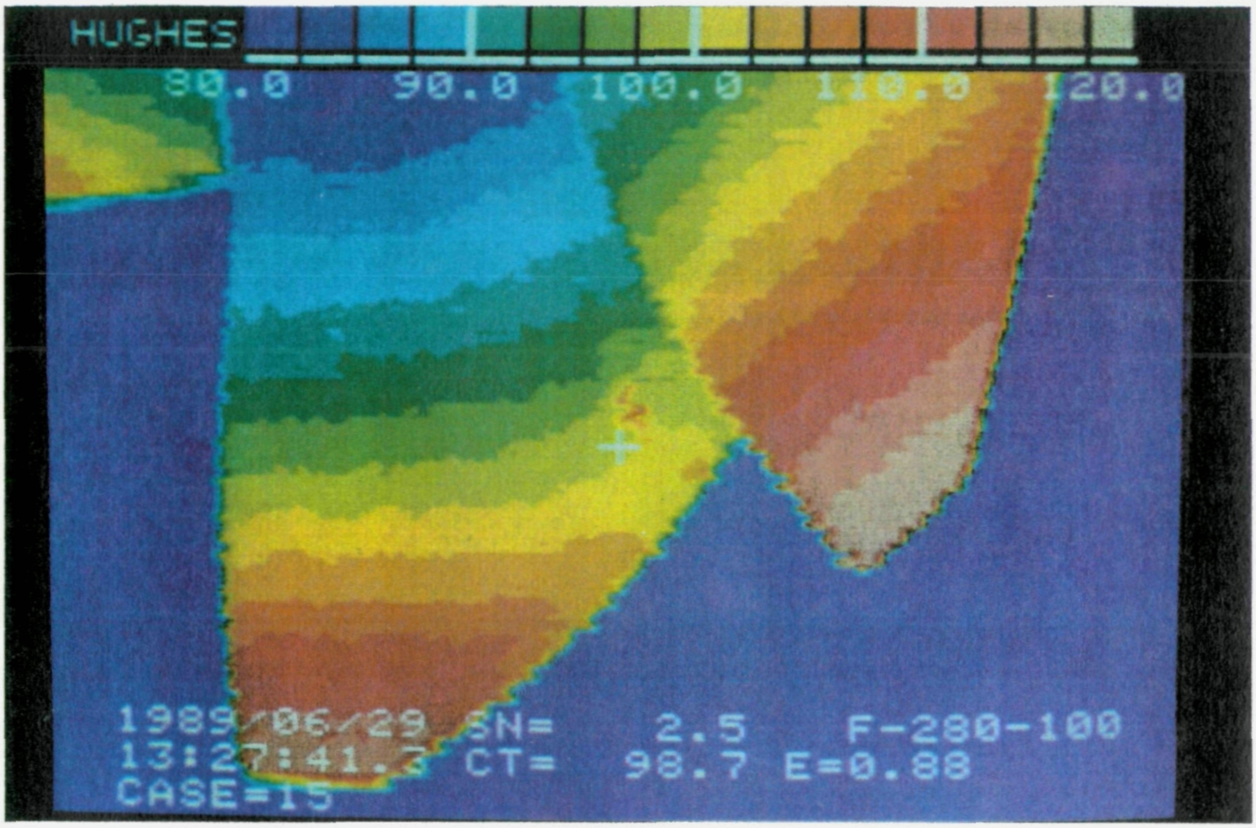

ORIGINAL PAGE
COLOR PHOTOGRAPH

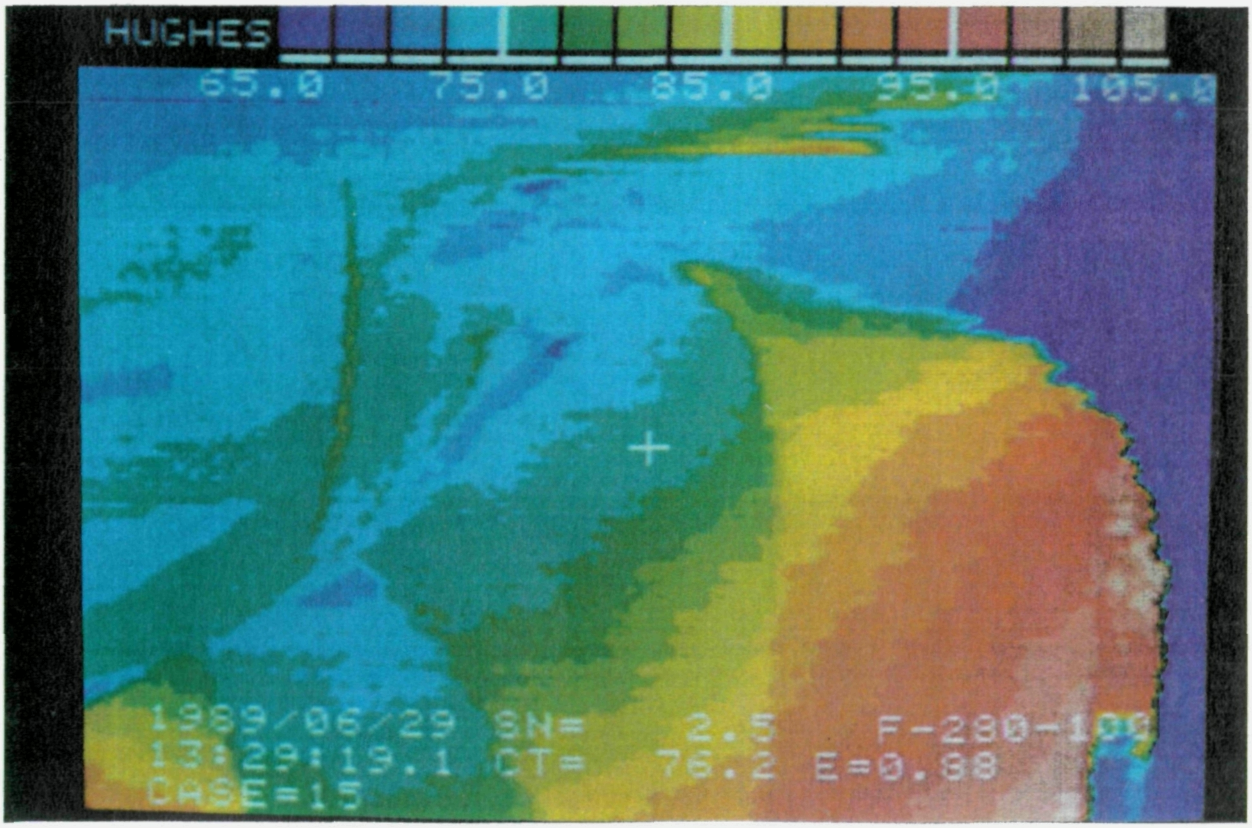

PAGE 108 INTENTIONALLY BLANK

PRECEDING PAGE BLANK NOT FILMED

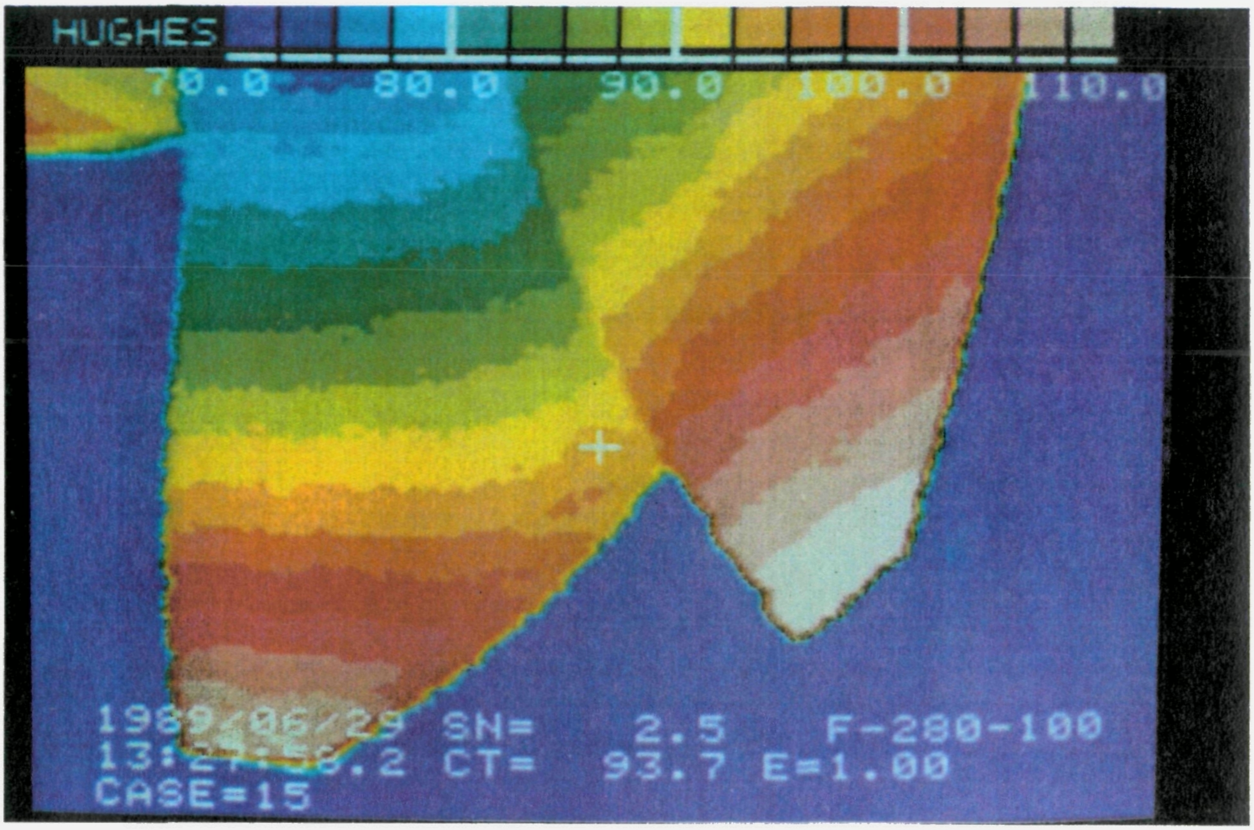

ORIGINAL PAGE
COLOR PHOTOGRAPH

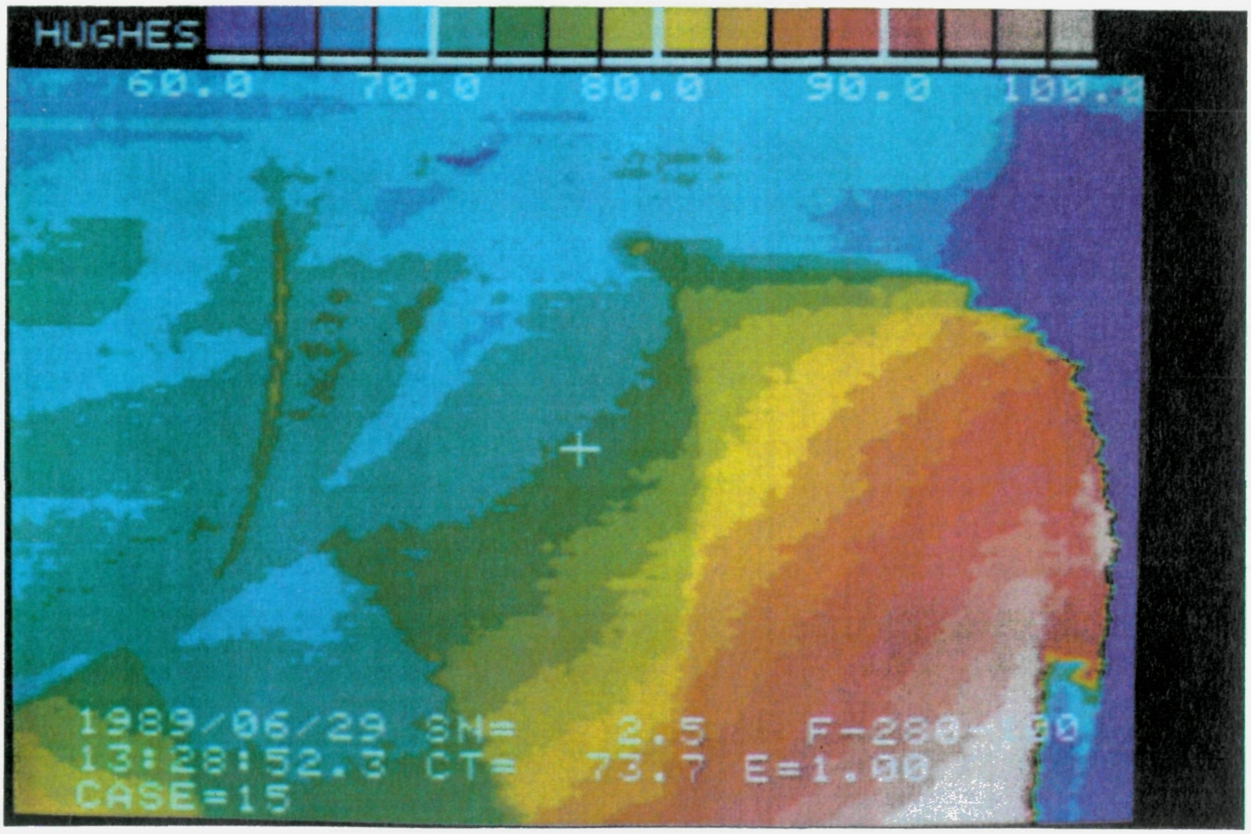

PAGE 110 INTENTIONALLY BLANK

PRECEDING PAGE BLANK NOT FILMED

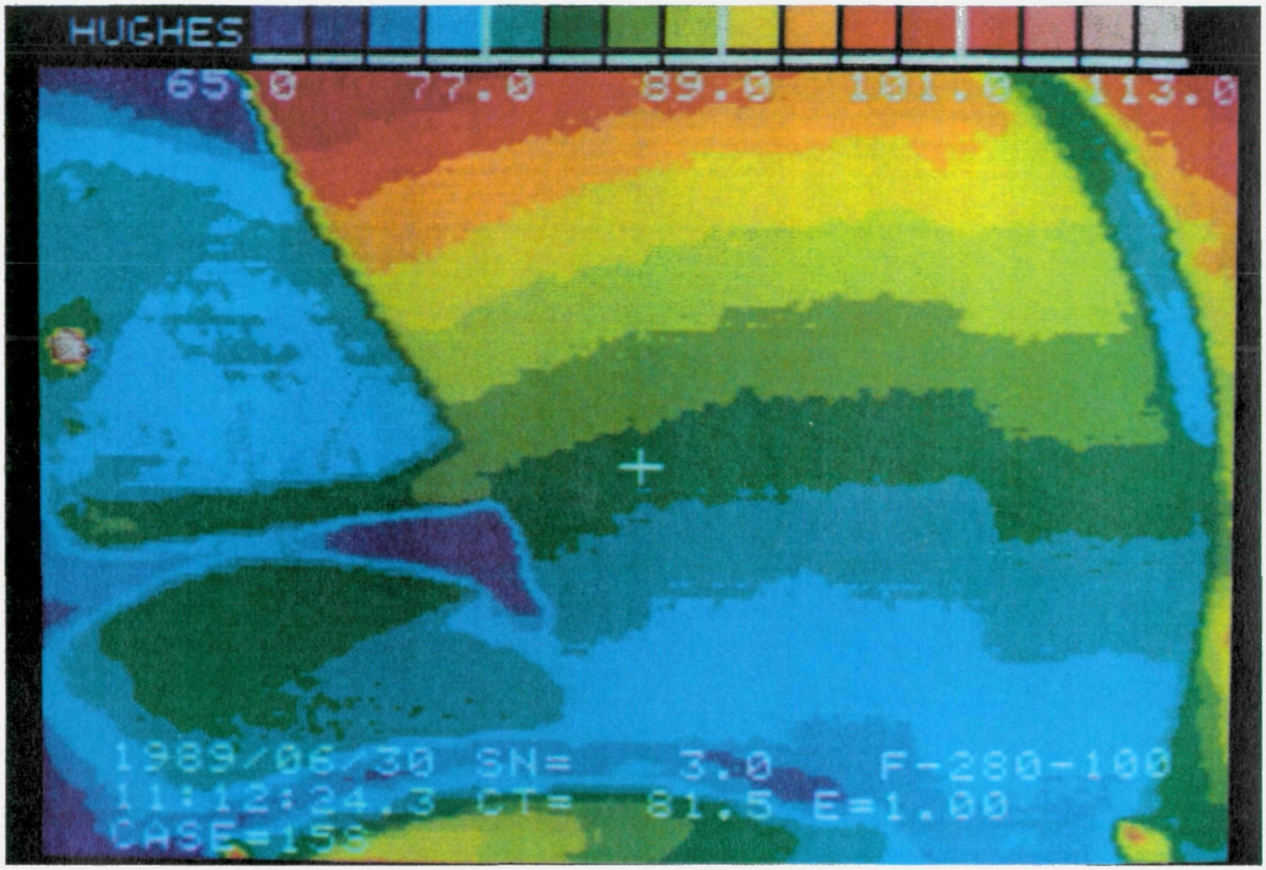
HUGHES
65.0 77.0 89.0 101.0 113.0
1989/06/30 SN= 3.0 F-280-100
11:12:24.3 CT= 81.5 E=1.00
CASE=15S

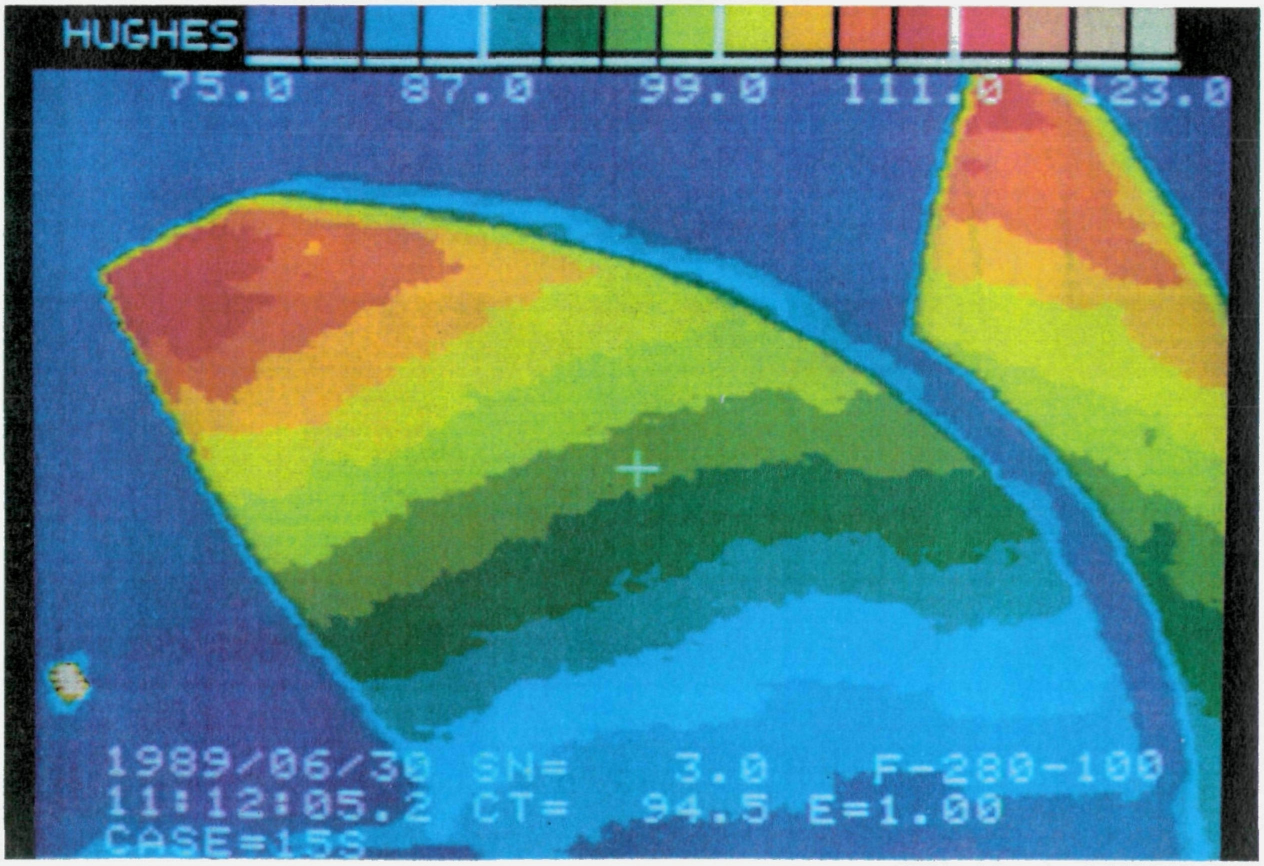
HUGHES
75.0 87.0 99.0 111.0 123.0
1989/06/30 SN= 3.0 F-280-100
11:12:05.2 CT= 94.5 E=1.00
CASE=15S

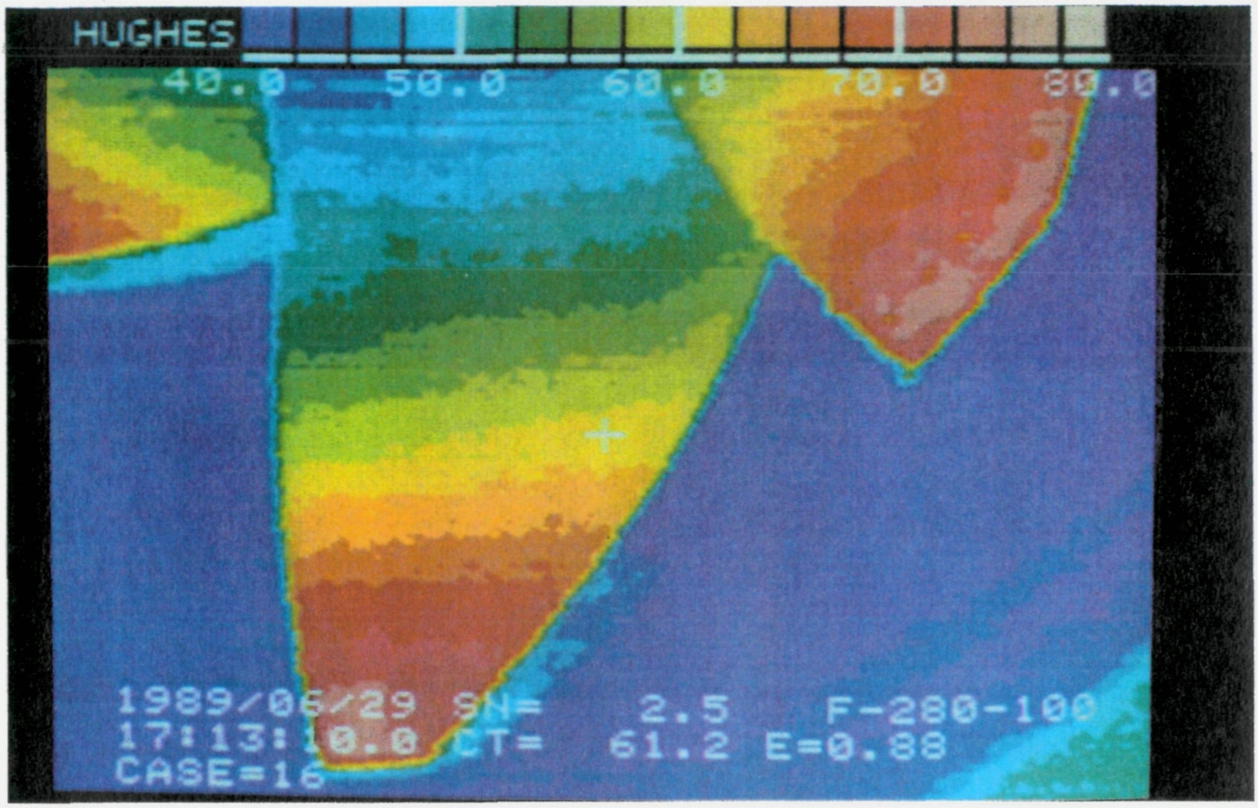

ORIGINAL PAGE
COLOR PHOTOGRAPH

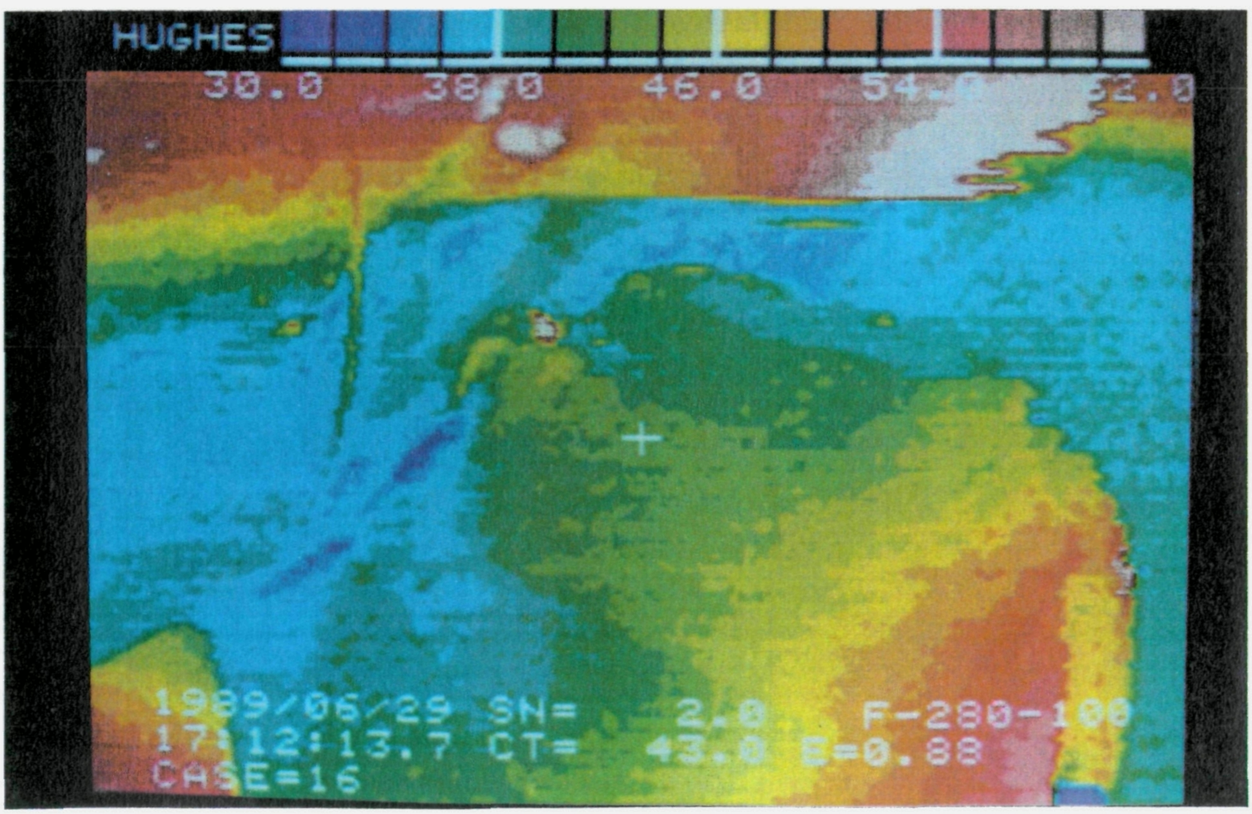

PRECEDING PAGE BLANK NOT FILMED

PAGE 114 INTENTIONALLY BLANK

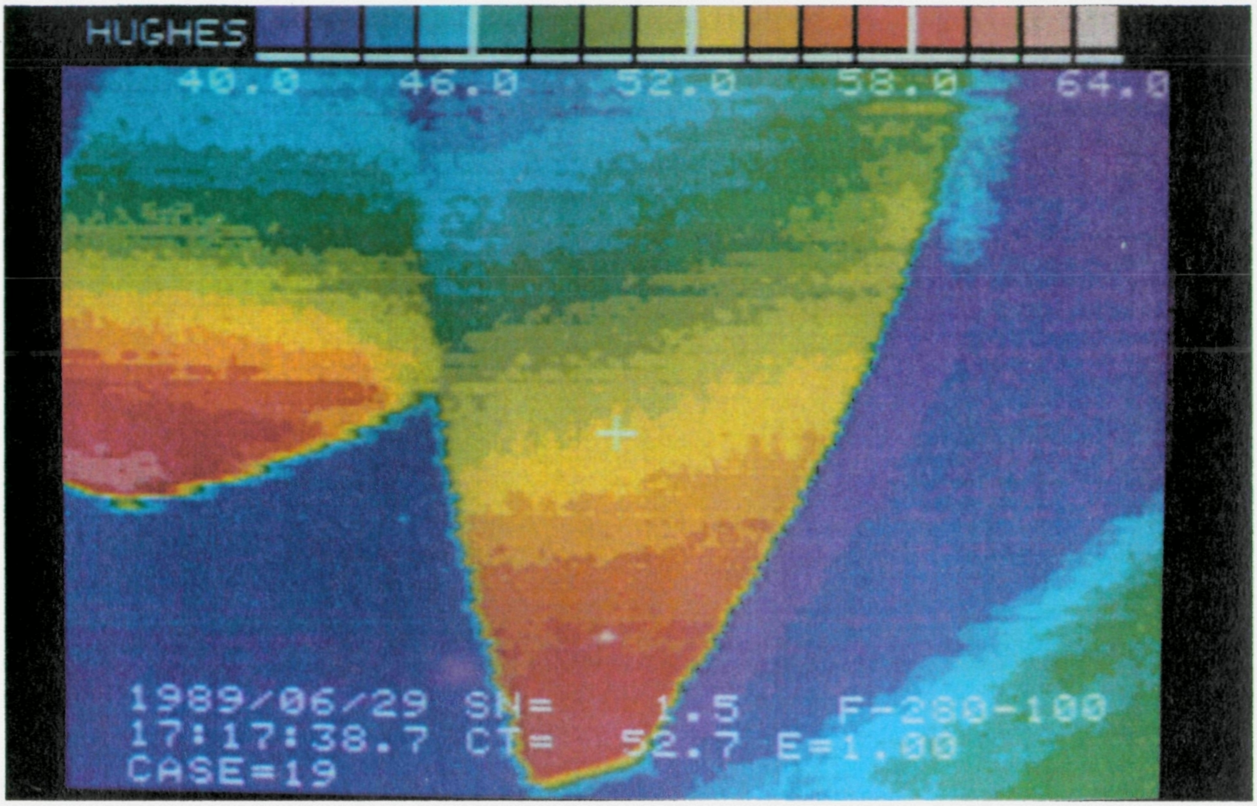

ORIGINAL PAGE
COLOR PHOTOGRAPH

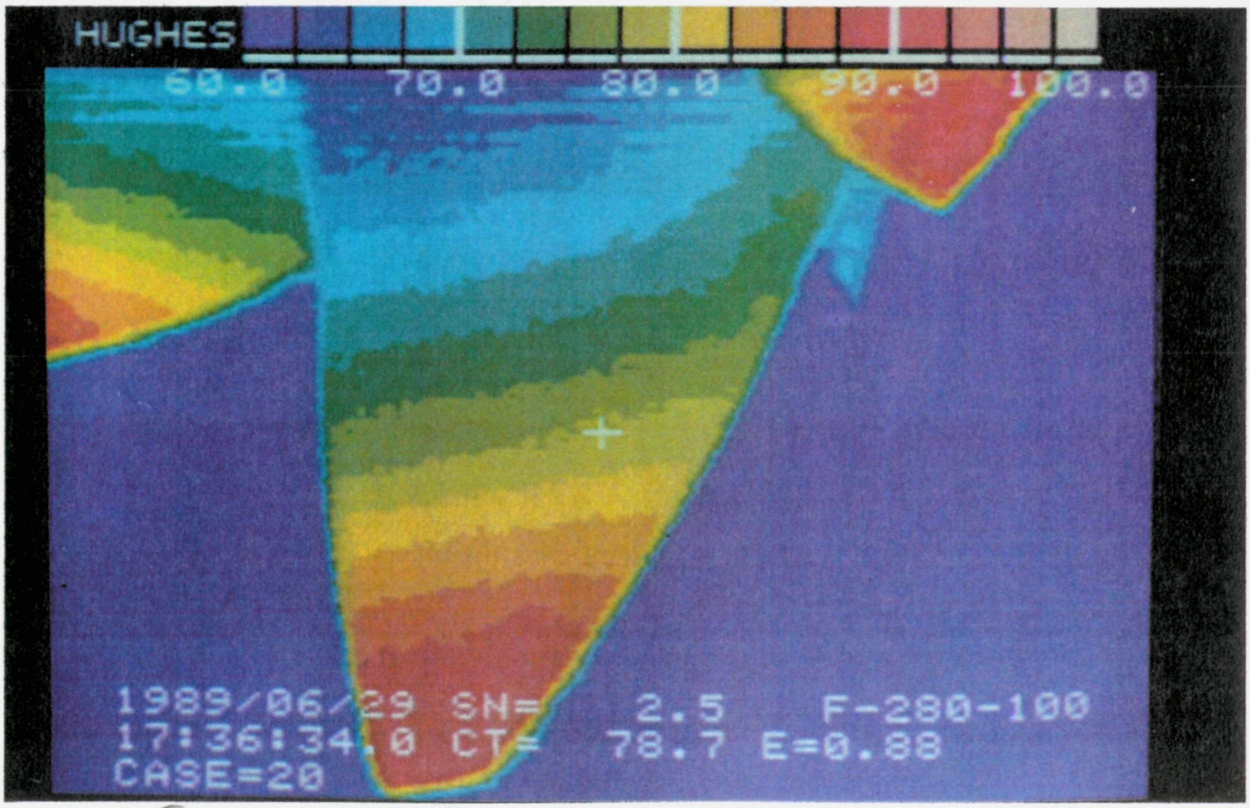

MISSING 116–117

PRECEDING PAGE BLANK NOT FILMED

PAGE 118 INTENTIONALLY BLANK

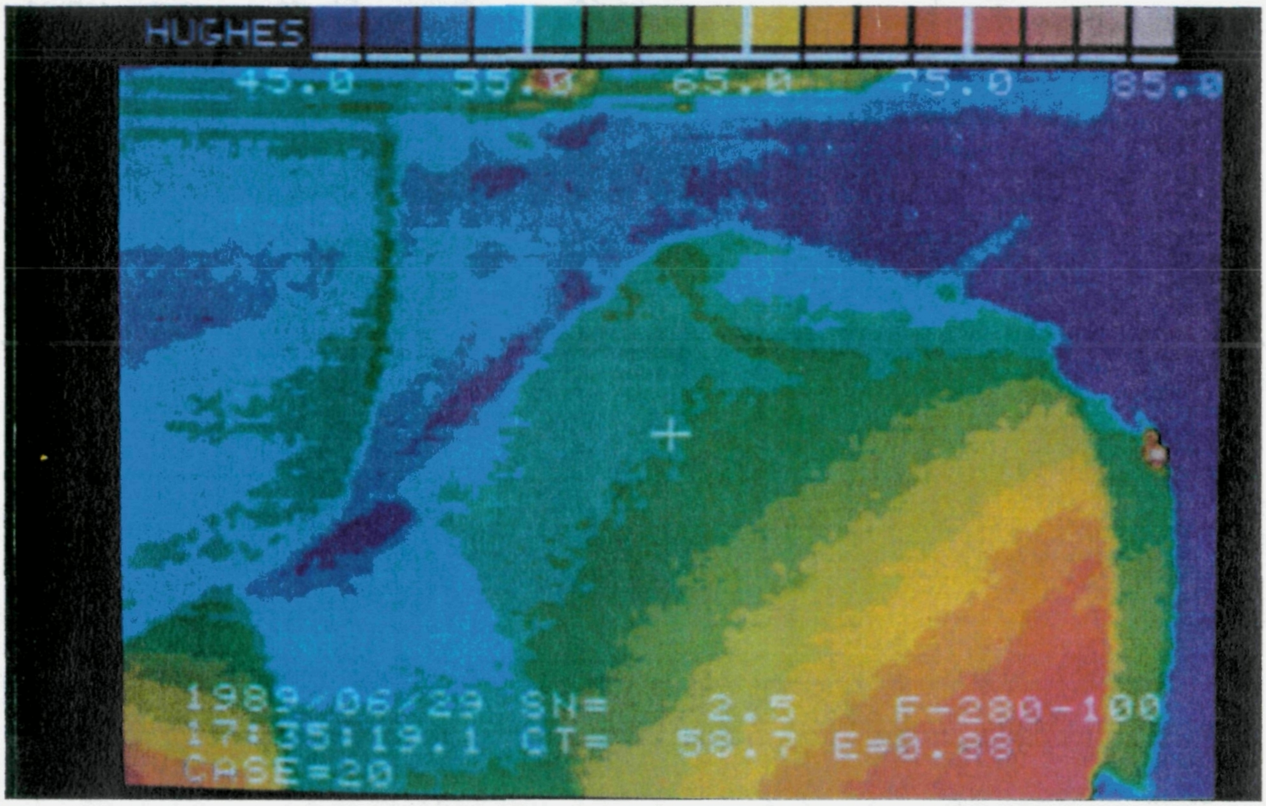

ORIGINAL PAGE
COLOR PHOTOGRAPH

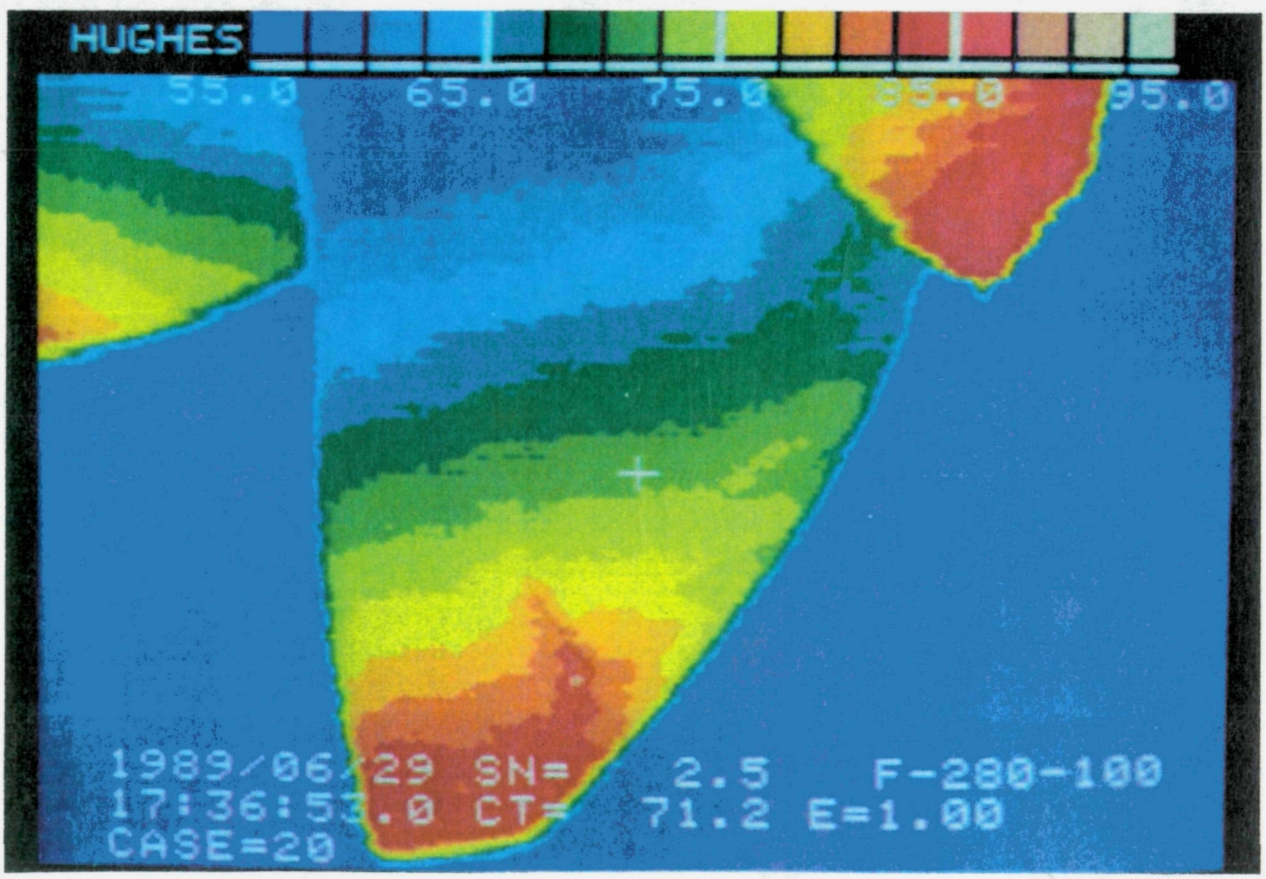

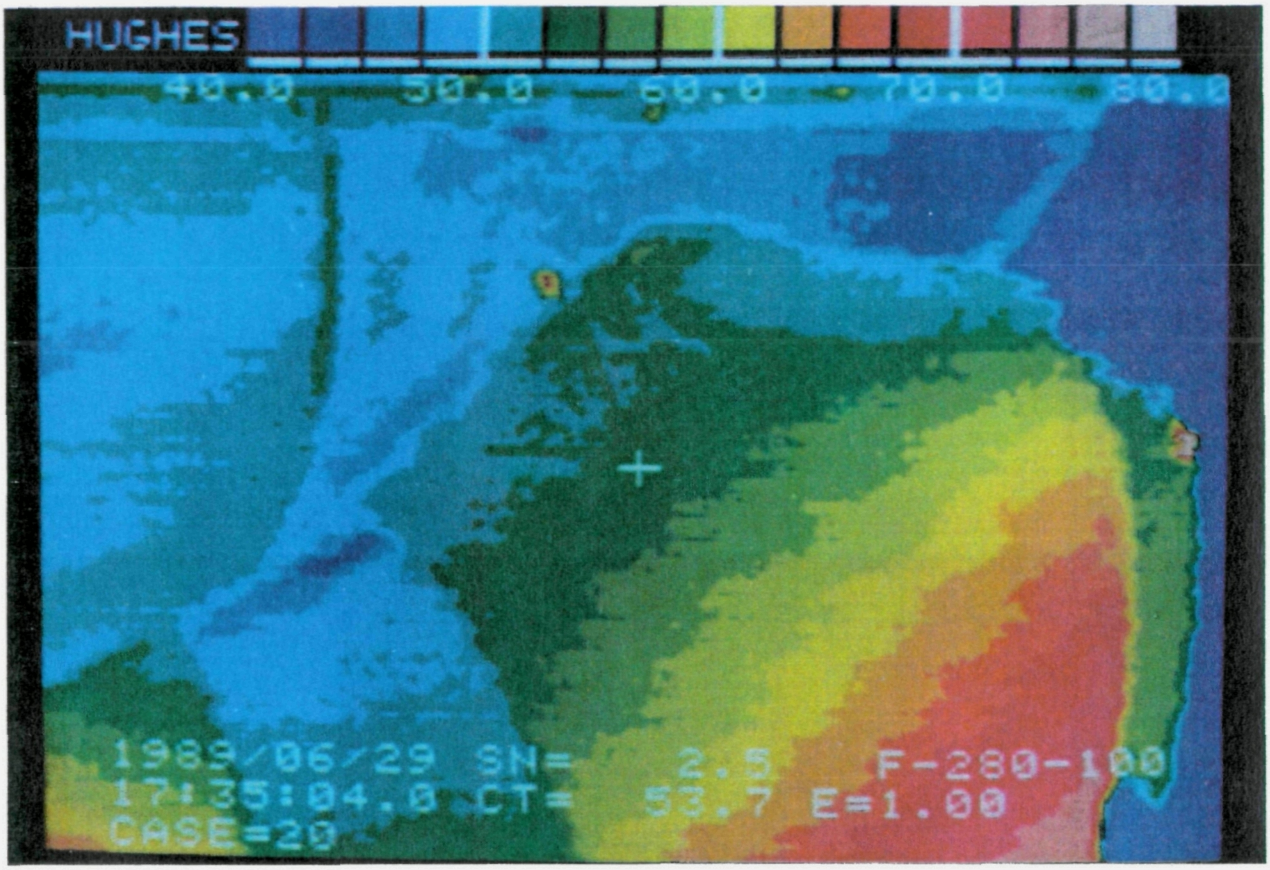

ORIGINAL PAGE
COLOR PHOTOGRAPH

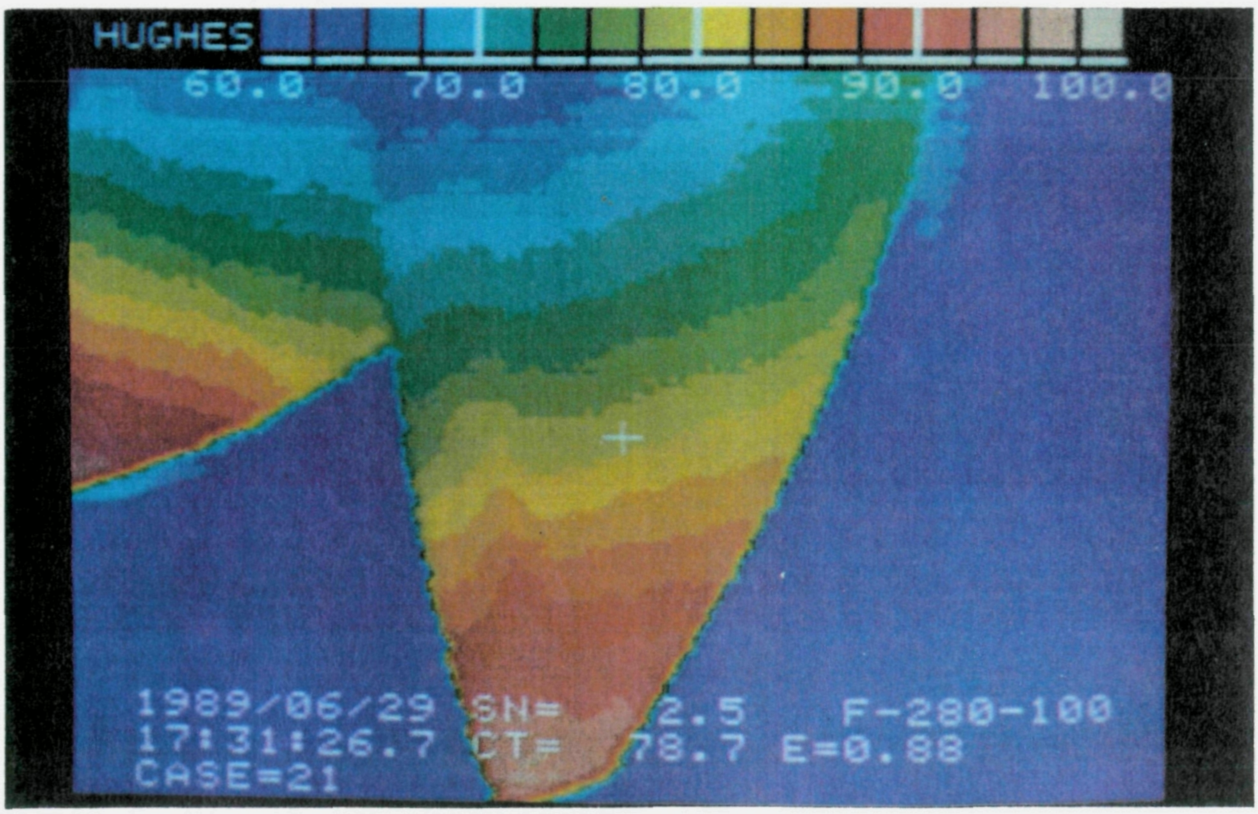

PAGE 122 INTENTIONALLY BLANK

PRECEDING PAGE BLANK NOT FILMED

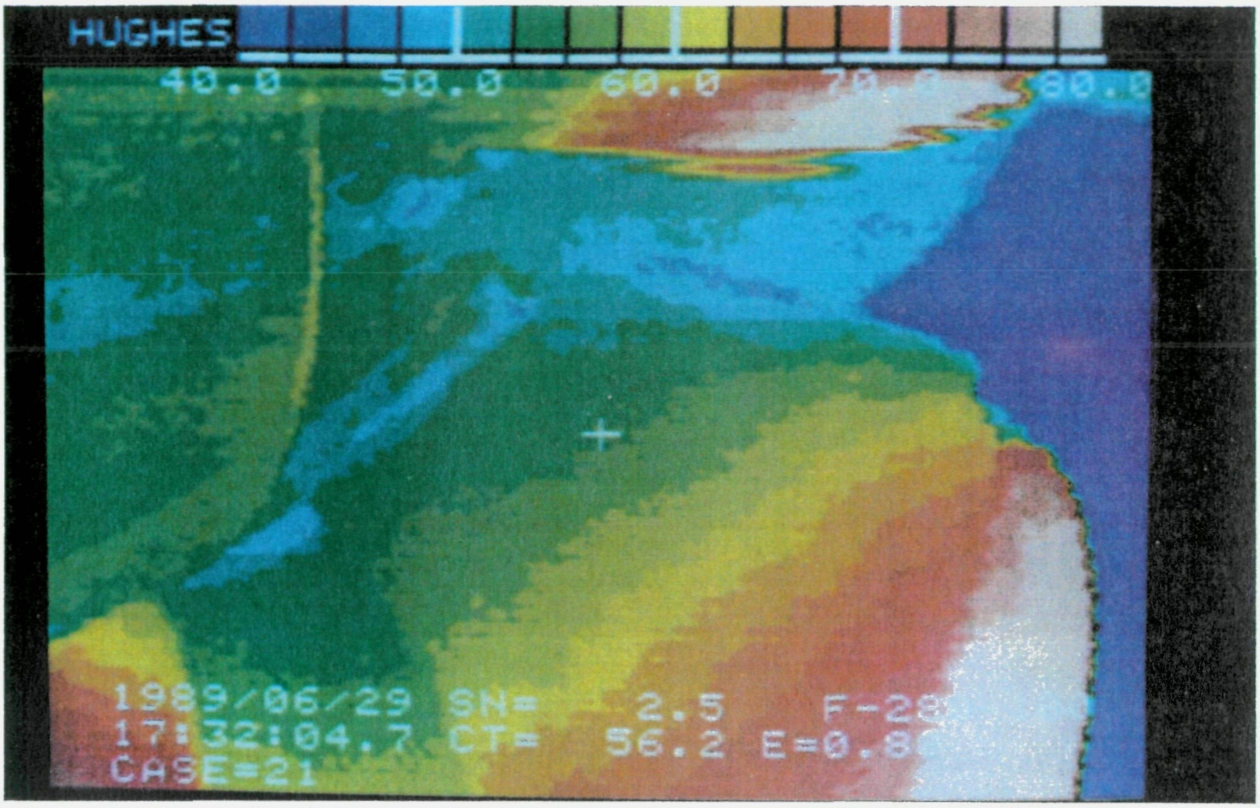

ORIGINAL PAGE
COLOR PHOTOGRAPH

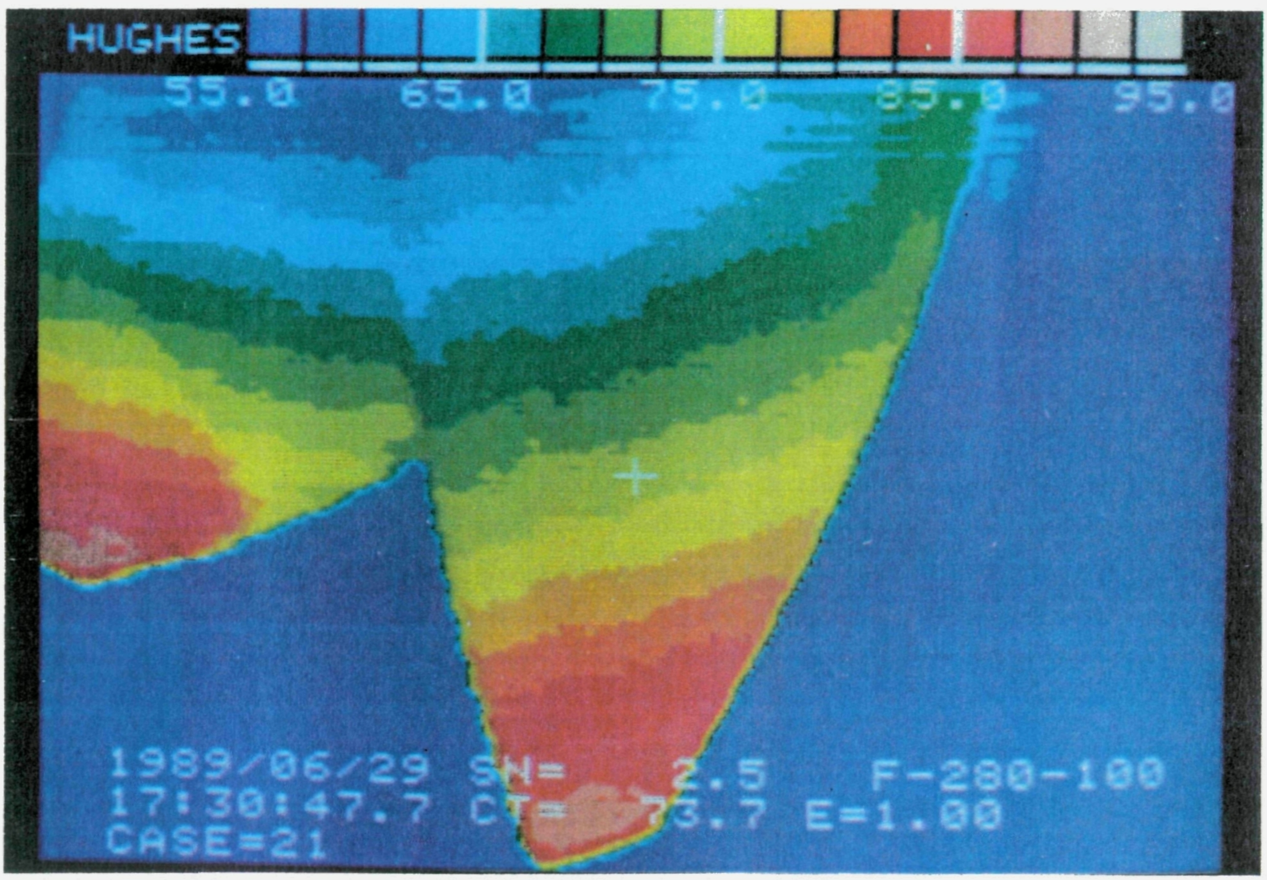

PRECEDING PAGE BLANK NOT FILMED

PAGE 124 INTENTIONALLY BLANK

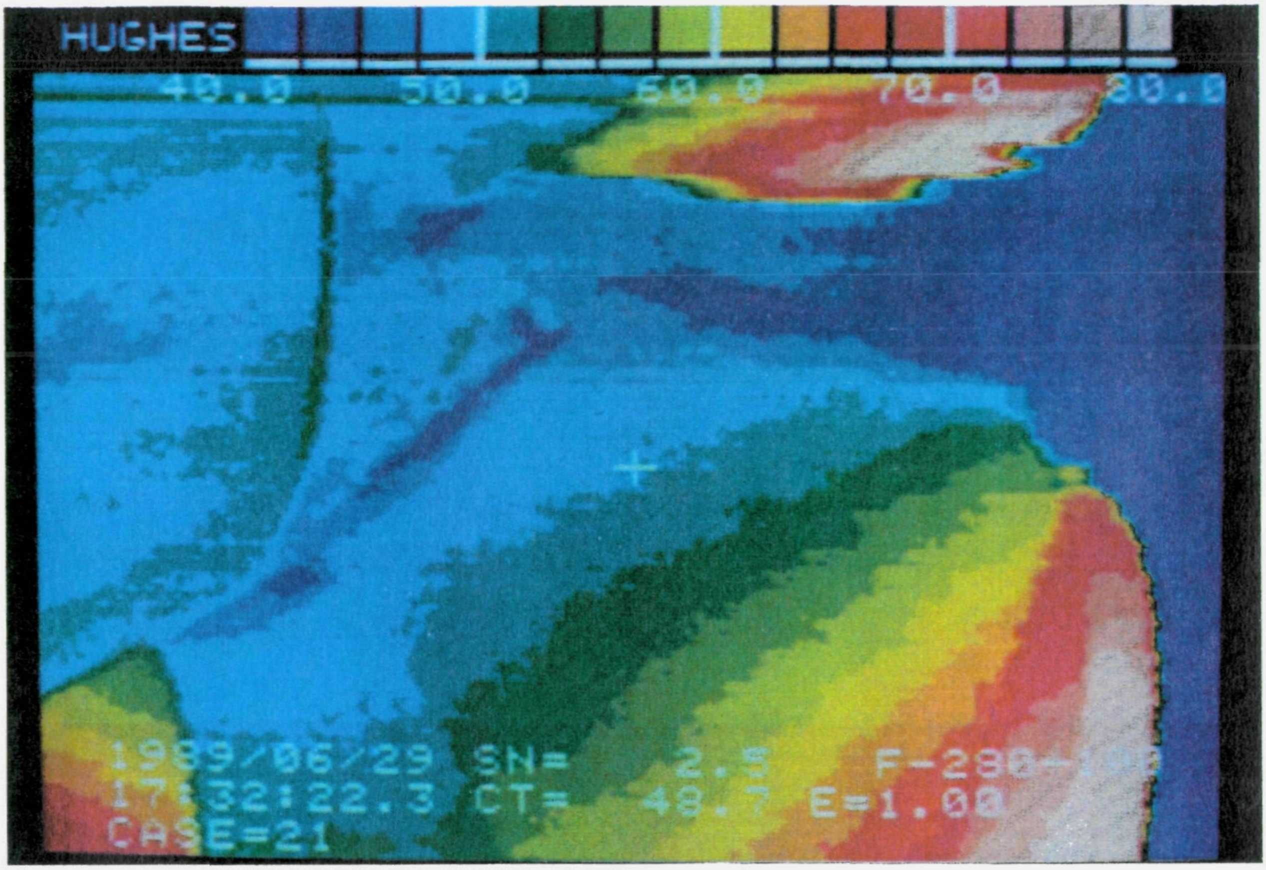

ORIGINAL PAGE
COLOR PHOTOGRAPH

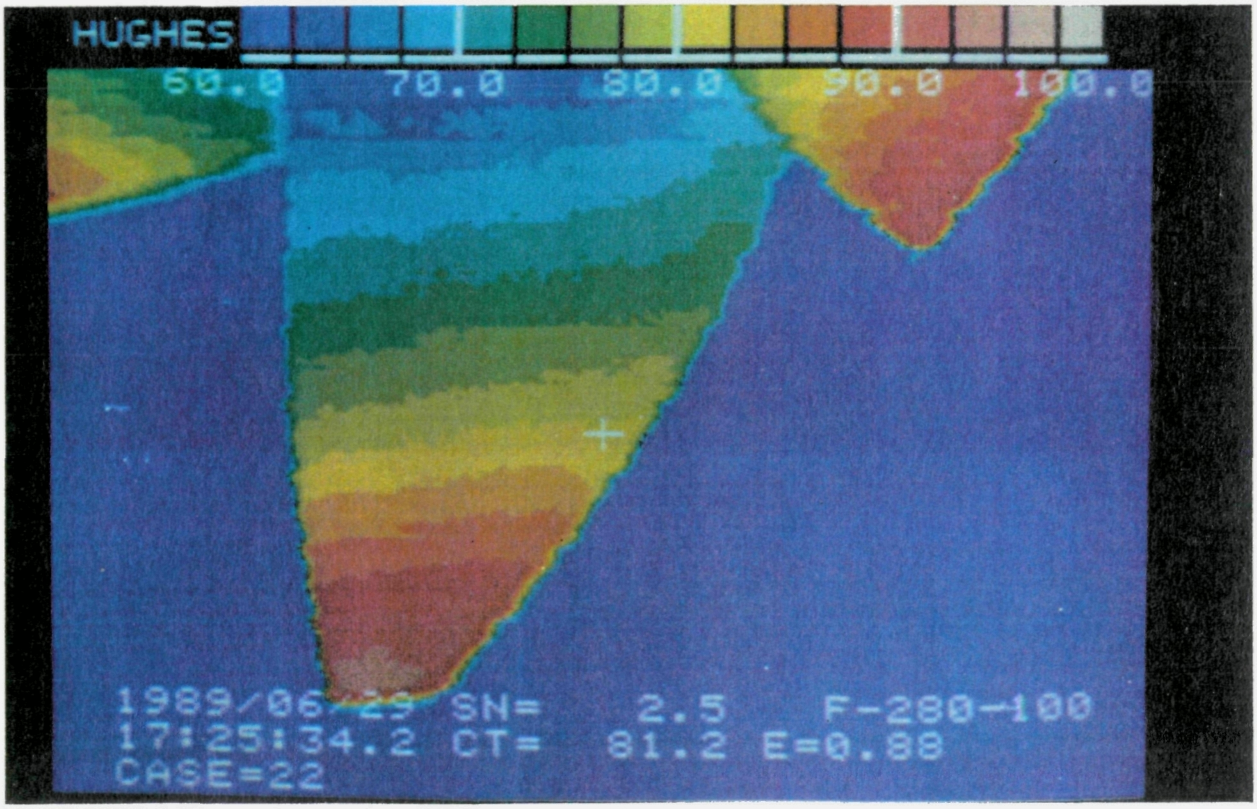

PAGE 126 INTENTIONALLY BLANK

PRECEDING PAGE BLANK NOT FILMED

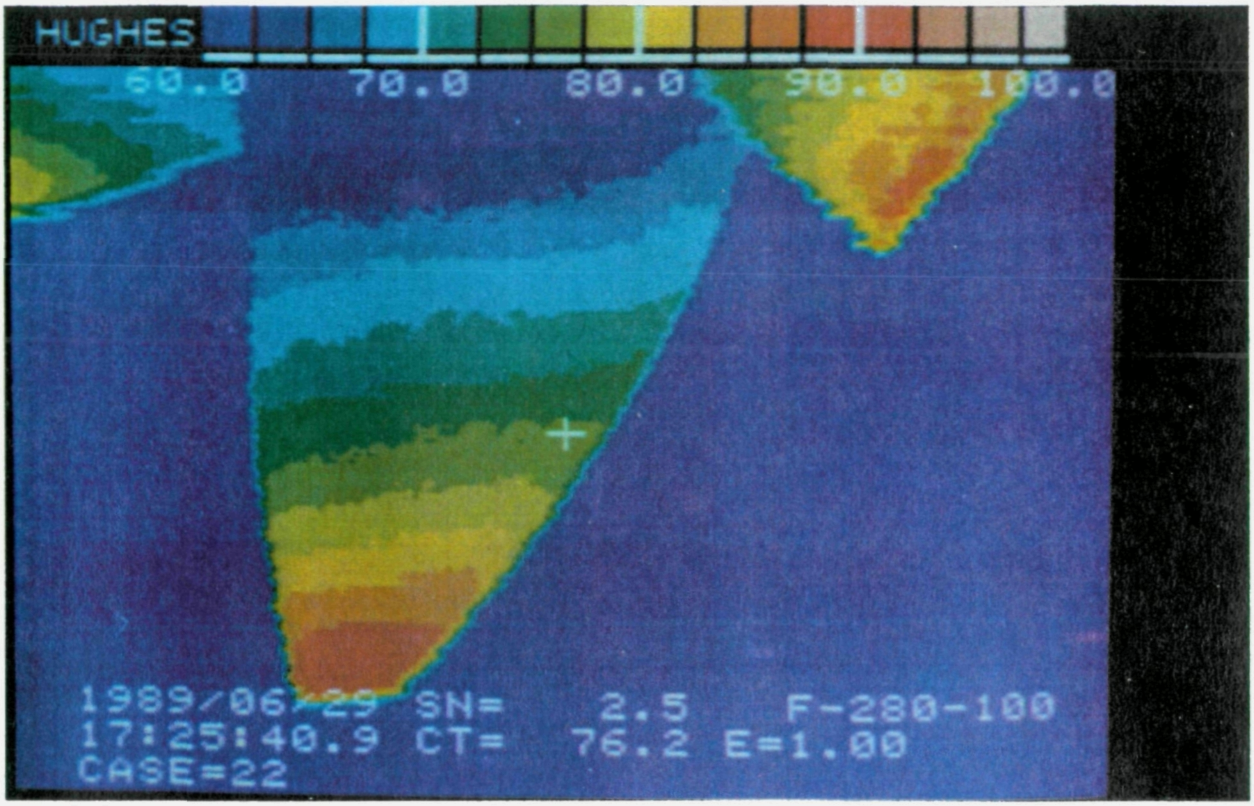

ORIGINAL PAGE
COLOR PHOTOGRAPH

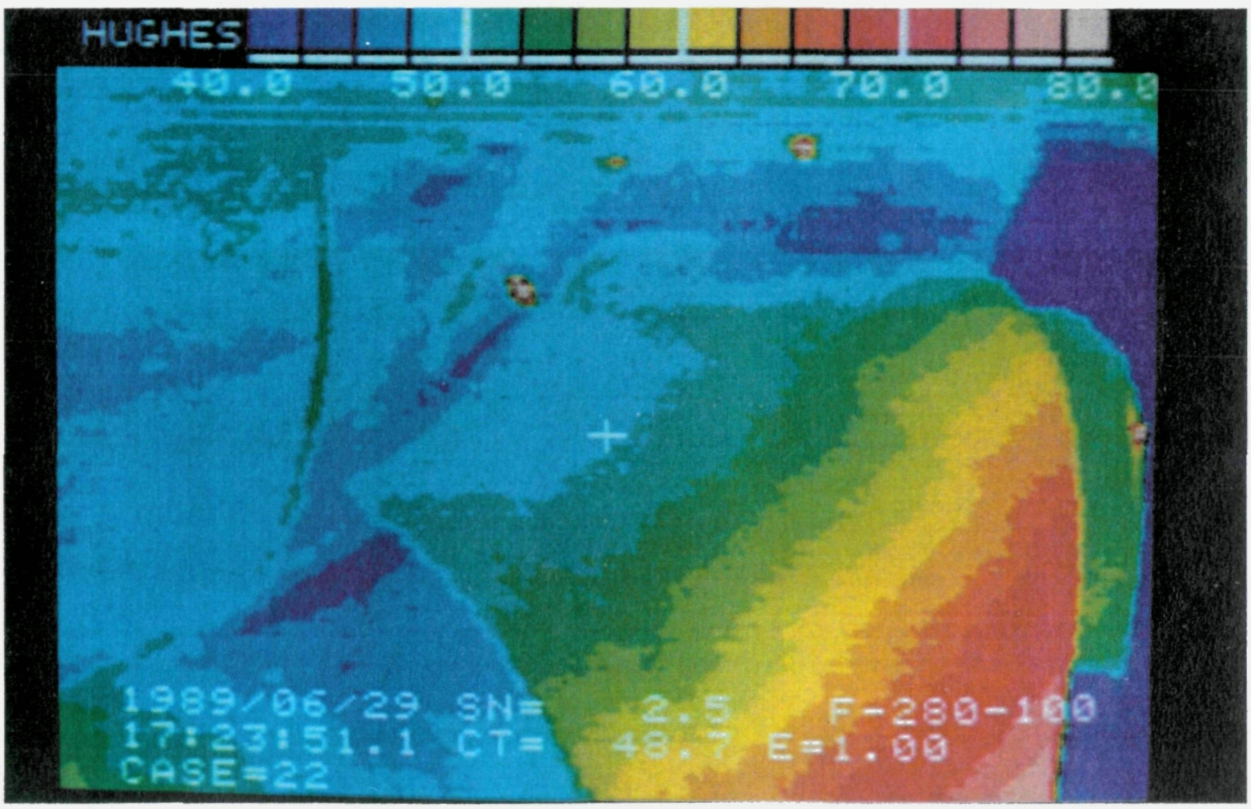

PAGE 128 INTENTIONALLY BLANK

PRECEDING PAGE BLANK NOT FILMED

APPENDIX B

UNCERTAINTY ANALYSIS

The equations used to reduce the flight test data for the blade pressure transducers were determined from three independent processes.

1. The systematic pressure gain and offset was determined for each transducer from ground test data recorded on the test aircraft. With the system fully assembled and checked out and the aircraft prepared for flight, calibration pressures were applied directly to each transducer while the system responses were recorded on a data tape.

2. Pressure gain and offset corrections for temperature sensitivity were determined for each transducer from a post-test blade calibration conducted in a laboratory test chamber at Hamilton Standard. With the blade configured with a sub-atmospheric pressure diaphragm, data was acquired at three different temperatures while pressure was varied over the transducer range.

3. Attenuation corrections for low-pass filters used in the data reduction process were determined from laboratory calibration data. The filters were used to attenuate FM band-edge noise, but the higher P-order data frequencies (>600 Hz) were within the attenuation region.

Systematic Pressure Gain and Offset

Two data points were recorded on the test aircraft, a point near 4 PSIA and the barometric pressure. The temperature was sufficiently constant to use the average. The only equation available was that of a straight line intersecting the two points, e.g., $y = m x + b$ @ temperature t. And in the terms of this system,

$$P_i = \overline{m}_c V_{P_i} + P_{o_c}, \ @\ t \qquad 1)$$

where, P_i = incremental pressure, in PSIA

$\overline{m}_c$ = average rate of change, in $\Delta P/\Delta V$

V_{P_i} = measured voltage @ P_i, in Volts

P_{o_c} = pressure offset @ $V_{P_i} = 0$, in PSIA

From tape reel #124, transducer location C7-7 and transducer S/N 39TD,

$$\overline{m}_c = \frac{\Delta P}{\Delta V} = \frac{P_2 - P_1}{V_{P_2} - V_{P_1}} = \frac{14.344 - 4.22}{0.831 - (-0.266)}$$

$$\overline{m}_c = 9.2288 \text{ PSI/Volt @ } 75.5^{o}F$$

$$P_{o_c} = P_2 - \overline{m}_c V_{P_2} = 6.675 \text{ PSIA @ } 75.5^{o}F$$

Note: $\overline{m}_c$ includes a systematic gain function

Pressure Gain and Offset Temperature Corrections

Expanding equation 1) to include a function of temperature,

$$P_i = \overline{m}_c V_{P_i}\ f(t) + P_{o_c}\ g(t) \qquad 2)$$

where, $f(t)$ = a function of temperature acting on $\overline{m}_c$

$g(t)$ = a function of temperature acting on P_{o_c}

From the post-test calibration data for the same transducer, using equation 1),

$$14 = 0.9264 \times 7.455 + P_o \text{ @ } t = 89.4^oF$$

$$\overline{m}\ V_{P_i} = 6.9063,\ P_o = 7.0937$$

$$14 = 0.8814 \times 8.252 + P_o \text{ @ } t = 26.5^oF$$

$$\overline{m}\ V_{P_i} = 7.2733,\ P_o = 6.7267$$

$$14 = 0.8620 \times 8.614 + P_o \text{ @ } t = -24.8^oF$$

$$\overline{m}\ V_{P_i} = 7.4253,\ P_o = 6.5747$$

and it was evident that both f(t) and g(t) must be non-linear, bi-directional and converge to 1.0 @ 75.5^{o}F. With only three conditions available, the best solution was the quadratic form,

$$f(t) = [1 + C_1(t-t_o) + C_2(t-t_o)^2]$$

$$g(t) = [1 + d_1(t-t_o) + d_2(t-t_o)^2]$$

And in terms of the data

$$\overline{m} = \overline{m}_1\ f(t),\ t_o = 75.5 \qquad 3)$$

$$P_o = P_{o_1}\ g(t),\ t_o = 75.5 \qquad 4)$$

Evaluating equation 3)

$$0.9264 = \overline{m}_1\ [1 + C_1\ (89.4 - 75.5) + C_2\ (89.4 - 75.5)^2] \qquad 3a)$$

$$0.8814 = \overline{m}_1\ [1 + C_1\ (26.5 - 75.5) + C_2\ (26.5 - 75.5)^2] \qquad 3b)$$

$$0.8620 = \overline{m}_1\ [1 + C_1\ (-24.8 - 75.5) + C_2\ (-24.8 - 75.5)^2] \qquad 3c)$$

With three equations in three unknowns, a simultaneous solution was achievable as follows:

Dividing 3b) by 3a) and simplifying,

$$0.95142\ (1 + 13.9C_1 + 193.21C_2) = 1 - 49C_1 + 2401C_2$$

$$-0.04858 = -62.225C_1 + 2217.2C_2 \qquad \text{3d)}$$

Dividing 3c) by 3a) and simplifying,

$$0.93048\ (1 + 13.9C_1 + 193.21C_2) = 1 - 100.3C_1 + 10060C_2$$

$$-0.069516 = -113.23C_1 + 9880.2C_2 \qquad \text{3e)}$$

Factoring 3d) by 113.23/-62.225

$$0.08840 = 113.23C_1 - 4034.6C_2 \qquad \text{3f)}$$

Adding 3e) and 3f) and solving for C_2

$$0.018884 = 5845.6C_2,\ C_2 = 3.23 * 10^{-6}$$

Substituting for C_2 in equation 3d)

$$-62.225C_1 = -0.05574,\ C_1 = 8.958 * 10^{-4}$$

Also, substituting for C_2 in equation 3e)

$$-113.23C_1 = -0.10143,\ C_1 = 8.958 * 10^{-4}$$

From equation 3a)

$$0.9264 = \overline{m}_1\ (1 + 0.01245 + 0.000624)$$

$$\overline{m}_1 = 0.9144\ @\ 75.5^oF$$

Evaluating equation 4)

$$7.0937 = P_{o_1}[1 + d_1\ (89.4 - 75.5) + d_2\ (89.4 - 75.5)^2] \qquad \text{4a)}$$

$$6.7267 = P_{o_1}[1 + d_1\ (26.5 - 75.5) + d_2\ (26.5 - 75.5)^2] \qquad \text{4b)}$$

$$6.5747 = P_{o_1}[1 + d_1\ (-24.8 - 75.5) + d_2\ (-24.8 - 75.5)^2] \qquad \text{4c)}$$

Dividing 4b) by 4a) and simplifying,

$$0.94826\ (1 + 13.9d_1 + 193.21d_2) = 1 - 49d_1 + 2401d_2$$

$$-0.051736 = -62.18d_1 + 2217.8d_2 \qquad \text{4d)}$$

Dividing 4c) by 4a) and simplifying,

$$0.92684\ (1 + 13.9d_1 + 193.21d_2) = 1 - 100.3d_1 + 10060d_2$$

$$-0.07316 = -113.18d_1 + 9880.9d_2 \qquad \text{4e)}$$

Factoring 4d) by 113.18/-62.18

$$0.09417 = 113.18d_1 - 4036.8d_2 \qquad \text{4f)}$$

Adding 4e) and 4f) and solving for d_2

$$0.02101 = 5844.1d_2, \; d_2 = 3.595 * 10^{-6}$$

Substituting for d_2 in equation 4d)

$$-62.18d_1 = -0.059709, \; d_1 = 9.603 * 10^{-4}$$

Also, substituting for d_2 in equation 4e)

$$-113.18d_1 = -0.10868, \; d_1 = 9.603 * 10^{-4}$$

From equation 4a)

$$7.0937 = P_{o_1} (1 + 0.013348 + 0.0006946)$$

$$P_{o_1} = 6.9955 \text{ PSIA @ } 75.5°F$$

Validation of Temperature Corrections

Figures B1 and B2 graphically depict $\overline{m}$ f(t) and P_o g(t) respectively. Table B1 indicates the comparisons of the calculated pressures to the pressures applied during the post-test calibration. Since f(t) and g(t) are functions of temperature only and are defined and applied as factors, they translate directly to equation 2).

Filter Attenuation Correction

Combinations of eight 1KHz low-pass filters were used during the flight test data reduction process. The calibration data sets for all eight were normalized and merged to a single data set. That data was fitted with a fifth order polynomial to be used to correct the test data. Figure B3 graphically depicts the filter characteristics and Figure B4 depicts the deviations of the eight filters from the polynomial. The correction is the reciprocal of the polynomial.

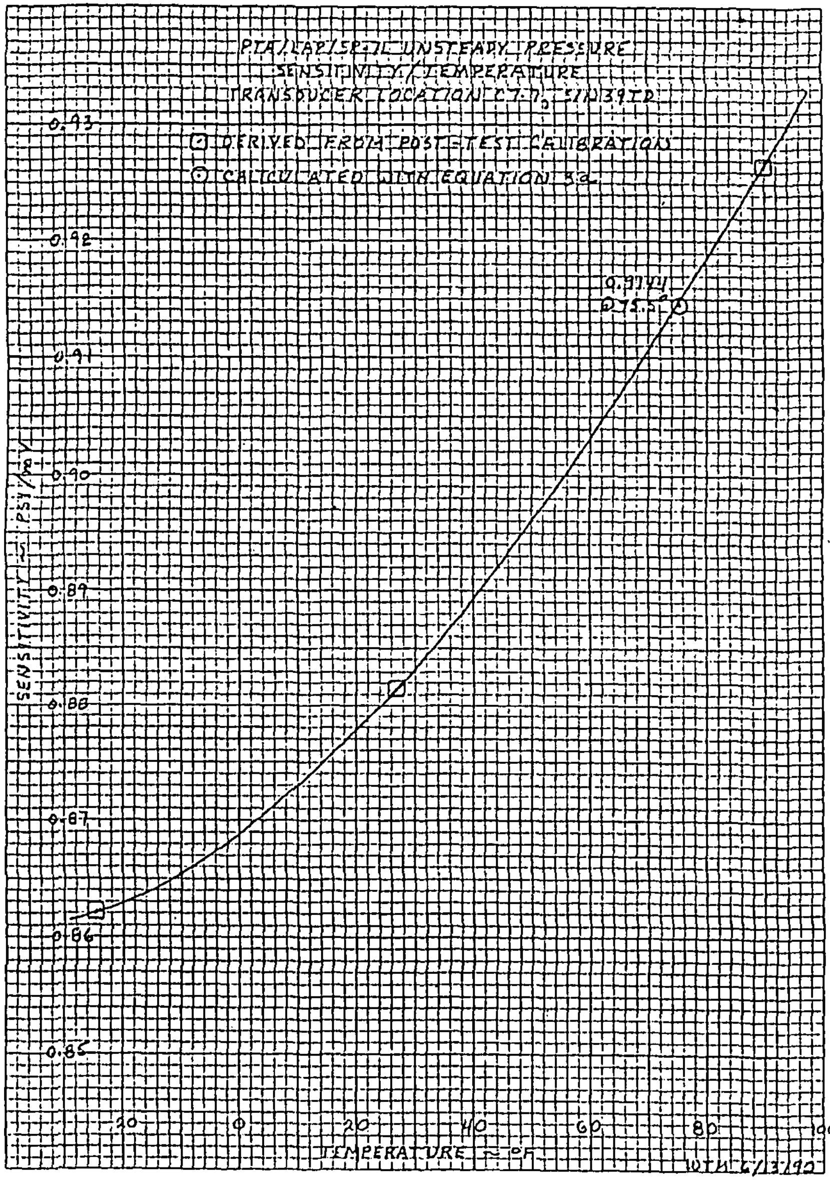

FIGURE B1

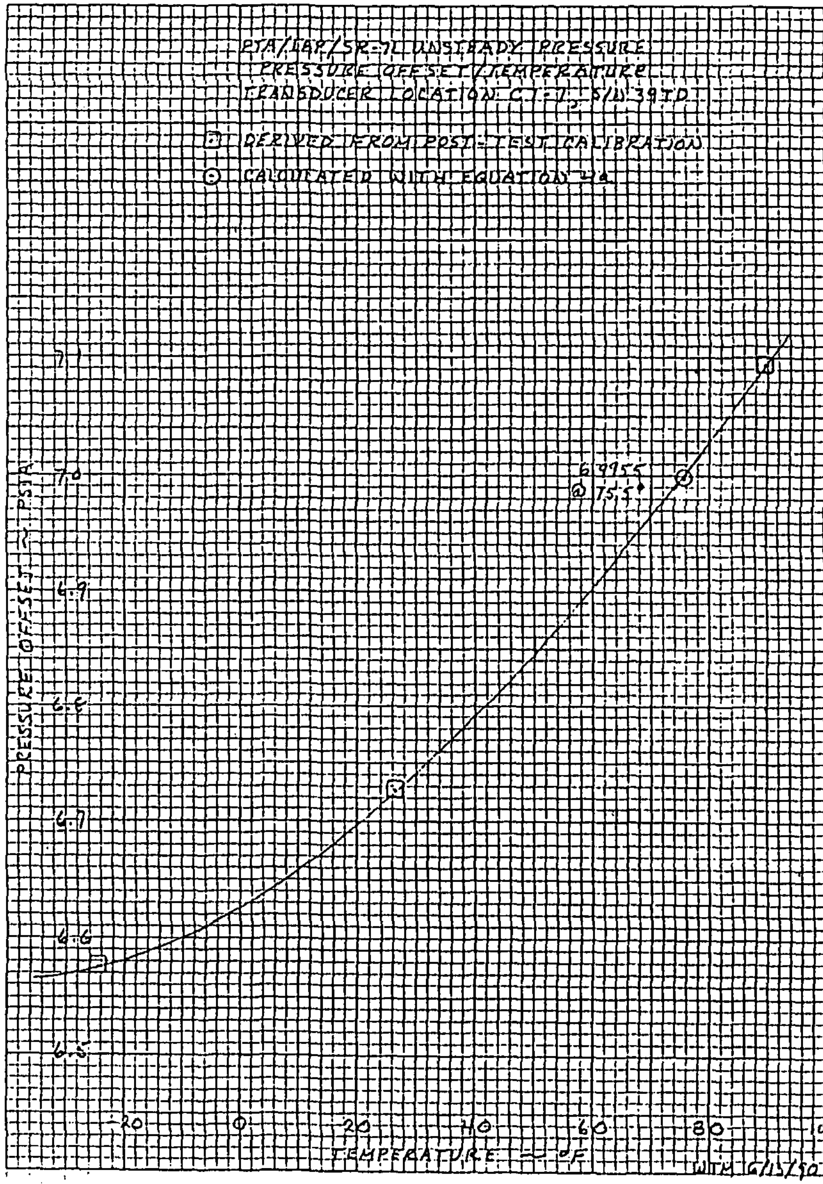

FIGURE B2

S/N 39TD

UNKNOWNS

C1= 8.969064E-04　　C2= 3.241249E-06

D1= 9.590462E-04　　D2= 3.583406E-06

M(75.5)= .9144531

P(75.5)= 6.995395

PSIA;	TEMP	VPI	M(BAR)	PO	Deviation
14	89.4	7.455	.9264263	7.093492	0.0
10	89.4	3.166	.9264263	7.066935	+0.0266
6	89.4	-1.152	.9264263	7.067243	+0.0262
2	89.4	-5.498	.9264263	7.093492	0.0
6	89.4	-1.153	.9264263	7.06817	+0.0253
10	89.4	3.166	.9264263	7.066935	+0.0266
14	89.4	7.455	.9264263	7.093492	0.0
14	26.5	8.252	.8813809	6.726845	0.0
10	26.5	3.738	.8813809	6.705399	+0.0214
6	26.5	-.804	.8813809	6.70863	+0.0182
2	26.5	-5.363	.8813809	6.726845	0.0
6	26.5	-.805	.8813809	6.709512	+0.0173
10	26.5	3.737	.8813809	6.70628	+0.0206
14	26.5	8.25	.8813809	6.728608	-0.0018
14	-24.8	8.614	.862007	6.574671	0.0
10	-24.8	4	.862007	6.551972	+0.0227
6	-24.8	-.642	.862007	6.553409	+0.0213
2	-24.8	-5.307	.862007	6.574671	0.0
6	-24.8	-.645	.862007	6.555995	+0.0187
10	-24.8	3.999	.862007	6.552834	+0.0218
14	-24.8	8.61	.862007	6.57812	-0.0034

$$M(BAR) = \frac{14 - 2}{\text{Delta VPI}}$$

; Po = PSIA - (M * VPI);

to = 75.5

Table B1

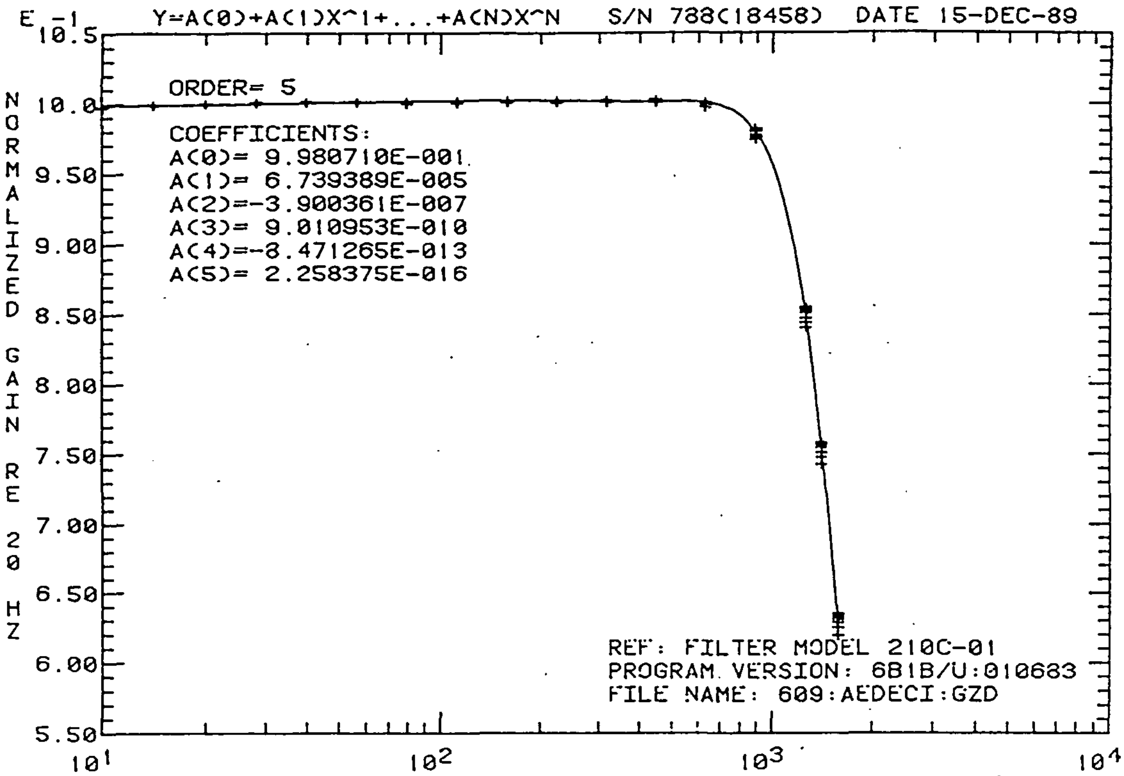

FIGURE B3

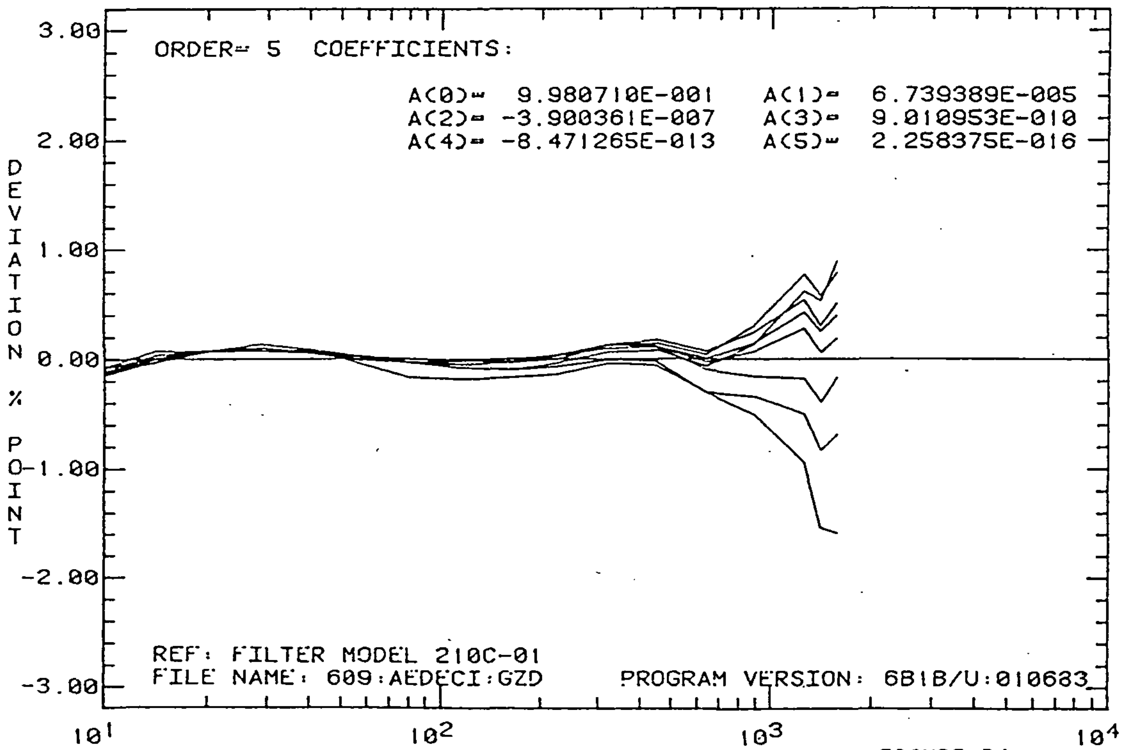

FIGURE B4

C2

Uncertainty Analysis - Instrumented SR-7L Blade

This analysis is based on a post-test calibration of the SR-7L blade with 30 pressure transducers and 30 channels of passive and active circuitry installed integrally within the blade.

The calibration was performed in a test chamber capable of controlling temperature uniform and stable over the planned range -25^{0} to 90^{0}F. Calibrated temperature sensors were installed in the vicinity of each transducer station.

The blade was configured with a thin diaphragm, standoffs and tubing to enable the simultaneous application of pressure to all 30 channels. Calibration data was accumulated with a high accuracy data acquisition system.

The calibration data was used to determine the characteristics of the transducers and circuitry as installed in the blade. It was noted the characteristics changed significantly when compared to the initial uninstalled calibration data.

The characteristics evaluated included gain, offset, non-linearity, hysteresis, repeatability, temperature affect on gain and temperature affect on offset. Also evaluated were the contributing uncertainties of the calibration equipment used and the uncertainties of the calibration temperature environment.

Equations were determined as previously described and each calibration point was calculated using those equations. The deviation of the calculated pressure from the applied pressure was then determined. It was intended the uncertainty associated with the blade instrumentation be based on the statistical mean and standard deviation for the steady pressure measurements. However, the end points of the post-test blade calibration were 2 and 14 PSIA, while the end points of the system calibration in the field were 4 and 14.7 PSIA.

Since the non-linearity was maximum near mid-range, the slope of the two end point straight lines were different. This difference, in effect, results in the statistical data being unreasonably conservative. The relationship of the non-linearity and the two slopes is shown in Figure B5.

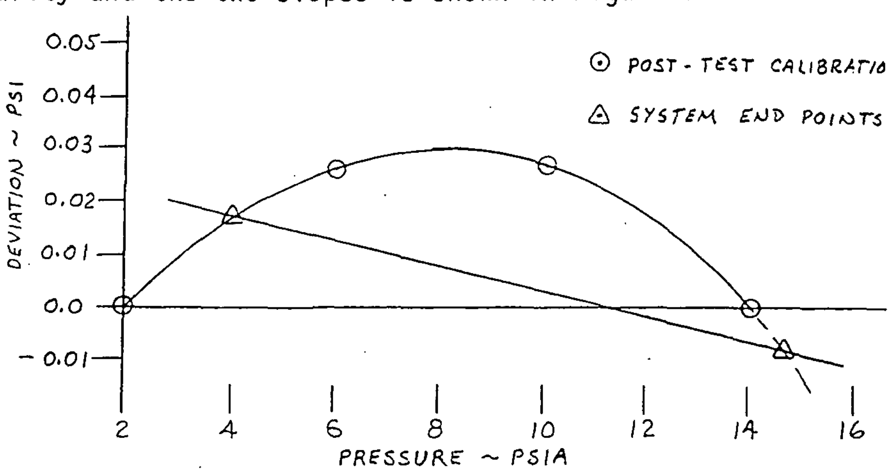

FIGURE B5

Of several other methods evaluated, the method considered most representative of the deviations as they apply to the final reduced data was to take one-half the maximum deviation as a systematic uncertainty and the remaining half as a random uncertainty. The uncertainties associated with the calibration were then combined with the random half of the deviation by the method of root-sum-square (RSS).

For transducer S/N 39TD the maximum deviation was +0.0266 PSI. Taking half, the systematic part of the uncertainty (Up) is +0.0133 PSI. The other half combined with the following calibration uncertainties is the estimate of the random part of Up.

Common to all channels and referred to pressure

Uncertainty of applied pressure	±0.0045 PSI
Uncertainty of measured voltage	±0.0005 PSI
Uncertainty of temperature measurement	±0.0069 PSI
Uncertainty of thermal gradients	±0.0069 PSI
Uncertainty of thermal repeatability	±0.0097 PSI
Half of maximum deviation S/N 39TD	±0.0133 PSI
Combined random uncertainty (RSS)	±0.0197 PSI

The systematic and random parts of the uncertainty Up for steady pressures are tabulated in Table B2 for each transducer.

The uncertainty of unsteady pressure measurements is a function of gain, but not offset. For small signals, the gain is increased/decreased by non-linearity. Since the test data was reduced based on the two point system calibration, an equation describing systematic non-linearity was not available. A representative uncertainty was taken as the rate of change of a line tangent to the deviation curve at 12 PSIA. The uncertainty (Upac) expressed as a % of point is tabulated in Table B2 for each transducer.

Uncertainty Analysis* - Instrumented SR-7L Blade

Location	Transducer S/N	Uncertainty (Up) Systematic PSI	Random PSI	Uncertainty (Upac) % Point
C4-5	A07W	+0.0107	±0.0180	±0.54
C4-10	96YK	+0.0285	±0.0320	±1.43
C4-15	29TD	+0.0185	±0.0235	±0.88
C4-25	24TD	+0.0223	±0.0266	±1.11
C4-40	32TD	+0.0328	±0.0359	±1.64
C4-60	94YK	+0.0225	±0.0267	±1.13
C4-80	87YK	+0.0224	±0.0267	±1.12
C7-7	39TD	+0.0133	±0.0197	±0.67
C7-15	82YK	+0.0144	±0.0204	±0.72
C7-25	84YK	+0.0131	±0.0195	±0.65
C7-37	89YK	+0.0198	±0.0245	±0.99
C7-50	27TD	+0.0238	±0.0278	±1.19
C7-70	21TD	+0.0179	±0.0230	±0.90
C7-90	50YK	+0.0156	±0.0213	±0.78
C10-8	83YH	+0.0126	±0.0192	±0.63
C10-25	30TD	+0.0115	±0.0185	±0.58
C10-42	98YH	+0.0248	±0.0287	±1.24
C10-58	98YK	+0.0093	±0.0172	±0.47
C10-75	90YK	+0.0142	±0.0203	±0.71
C10-92	38TD	+0.0164	±0.0219	±0.82
F4-15	07TC	+0.0127	±0.0193	±0.64
F4-40	23TD	+0.0241	±0.0281	±1.20
F4-60	25TD	+0.0289	±0.0323	±1.44
F4-80	97YK	+0.0125	±0.0191	±0.63
F10-8	99YK	+0.0145	±0.0205	±0.72
F10-25	47YK	+0.0135	±0.0198	±0.68
F10-42	83YK	+0.0159	±0.0215	±0.79
F10-58	85YH	+0.0131	±0.0195	±0.65
F10-75	73YH	+0.0253	±0.0292	±1.27
F10-92	93YK	+0.0293	±0.0327	±1.47

*95% confidence level

TABLE B2

F 214.2

Uncertainty Analysis - Transducer Temperature

This analysis is based on a technical evaluation of blade surface temperature measurements, temperature gradient distributions and the uncertainty of temperature at the pressure transducer locations during the unsteady pressure flight test. The objective of this analysis is to determine the effect of temperature uncertainty on the pressure measurements.

The installed pressure transducer temperature sensitivity is typically 10% FS over the temperature range measured during the flight test. That temperature sensitivity was determined during the post-test calibration and was modeled in the data reduction equation for each transducer location at each test condition.

Temperature data was acquired by two methods during the flight test. Combinations of two Resistance Temperature Devices (RTD), of six available, were recorded during the various flights. Strobed Infrared Thermography was introduced on two added flights that provided real-time imaging and records in VHS format. The thermography flights were limited to 20,000 foot altitudes, however, due to an open window, unpressurized cabin configuration.

The temperature data was independently evaluated and, by analytical methods, a matrix of temperature at each transducer location was determined for each test condition. Associated with those temperatures is the best estimate of uncertainty that embraces all test conditions. The uncertainties are considered equivalent to a 95% confidence level and are tabulated in Table B3 for each transducer.

The temperature uncertainties were entered into the data reduction equations to determine the corresponding pressure uncertainties. Since the temperature correction applies partly to gain and partly to offset, the pressure uncertainties were determined separately for each. The resulting pressure uncertainties are also tabulated in Table B3 for each transducer.

Uncertainty Analysis* - Transducer Temperature

LOCATION	TRANSDUCER S/N	TEMPERATURE UNCERTAINTY DEGREE F	OFFSET UNCERTAINTY PSI	GAIN UNCERTAINTY % POINT
C4-5	A07W	±6.4	±0.053	±0.79
C4-10	96YK	±6.4	±0.004	±0.81
C4-15	29TD	±4.7	±0.037	±0.55
C4-25	24TD	±2.7	±0.013	±0.33
C4-40	32TD	±2.0	±0.009	±0.23
C4-60	94YK	±3.5	±0.021	±0.44
C4-80	87YK	±4.8	±0.046	±0.71
C7-7	39TD	±5.8	±0.049	±0.63
C7-15	82YK	±4.5	±0.051	±0.55
C7-25	84YK	±3.7	±0.025	±0.43
C7-37	89YK	±3.2	±0.036	±0.47
C7-50	27TD	±1.5	±0.006	±0.18
C7-70	21TD	±2.5	±0.014	±0.32
C7-90	50YK	±1.8	±0.017	±0.24
C10-8	83YH	±8.9	±0.092	±1.21
C10-25	30TD	±7.9	±0.142	±0.90
C10-42	98YH	±4.8	±0.055	±0.64
C10-58	98YK	±7.1	±0.033	±0.89
C10-75	90YK	±8.6	±0.141	±1.05
C10-92	38TD	±8.9	±0.096	±1.15
F4-15	07TC	±2.2	±0.014	±0.26
F4-40	23TD	±0.6	±0.004	±0.07
F4-60	25TD	±1.4	±0.008	±0.16
F4-80	97YK	±2.6	±0.019	±0.35
F10-8	99YK	±3.7	±0.048	±0.49
F10-25	47YK	±2.7	±0.020	±0.34
F10-42	83YK	±1.7	±0.015	±0.22
F10-58	85YH	±2.4	±0.035	±0.27
F10-75	73YH	±3.1	±0.029	±0.38
F10-92	93YK	±3.9	±0.037	±0.53

95% confidence level

TABLE B3

Uncertainty Analysis - Data Path

This analysis was based on a technical evaluation and certain component calibrations of the unsteady pressure flight test data path. The data path is defined as starting at the signal source, continuing through the recording system, reproduce system and ending with the analog to digital conversion. Since all uncertainties associated with the instrumented blade are treated separately, the signal source considered in this analysis was the connector at the input of the rotating electronics assembly.

The data path of a typical channel was as follows:

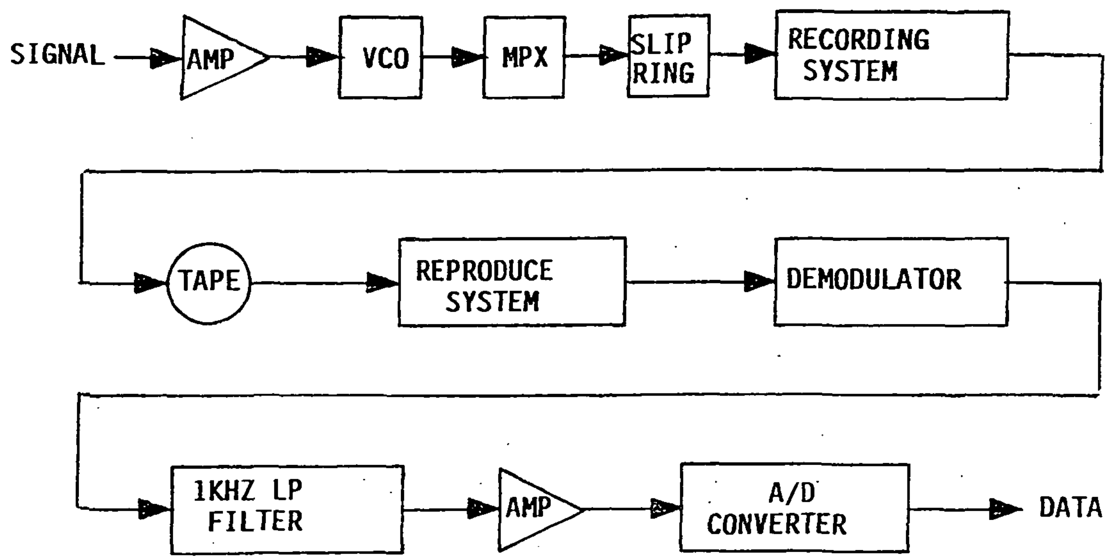

The preamplifier, voltage controlled oscillator (VCO) and multiplexer (MPX) define the data path through the rotating electronics. This part of the system, installed on the propeller bulkhead, was subject to cooling due to outside air temperature. There were a number of error sources associated with these components including; gain, offset, linearity, input bias current, temperature sensitivity and the inherent FM band-edge noise.

The recording system included a crystal oscillator to source a known frequency used in the data reduction process for tape speed compensation (TSC). The TSC was known to accurately correct for any constant or unsteady differences in record and reproduce tape speeds. There were no other identifiable error sources associated with the recording system or reproduce system.

The demodulator, low-pass filter and output amplifier were sources of additional errors including pass-band ripple. The analog to digital conversion utilized a 12 bit (0.025%) A/D converter. The data was digitized at 128 points per propeller revolution and averaged for approximately 1000 revolutions. As a result of the averaging, no uncertainty was considered reportable for that conversion.

A calibration facility was set up with the rotating components installed in a laboratory test chamber. The setup included all components except the slip ring, tape recorder and tape playback. Calibration signals were applied to the input of the preamplifier and measured at the output of the output amplifier.

Fifteen channels were calibrated at three input levels, seven frequencies and three temperatures ranging -65° to +85°F, totaling 945 data points. That data was normalized to a gain function and linearized to correct for the low-pass filter attenuation. The resulting data was then plotted on a single composite graph.

Since the gain and offset of each channel was established by the end-to-end calibration data, the boundaries of the plotted data were considered a statistical measure of the limits of uncertainty for each channel of the data path for all test conditions.

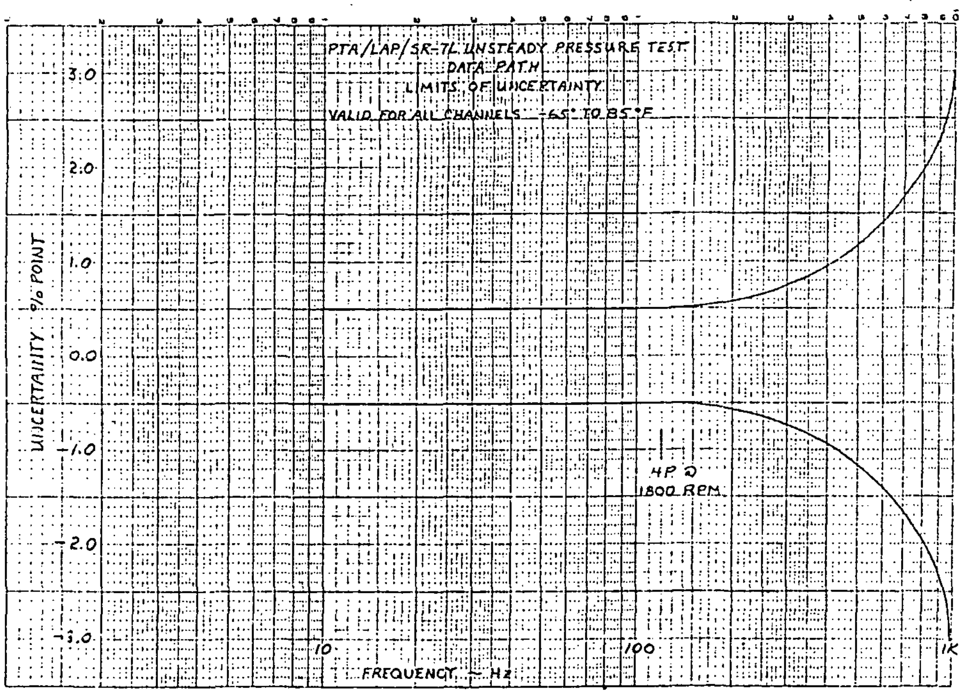

Summarizing the uncertainty in the defined data path:

Data Frequency	Uncertainty
DC to 140 Hz	± 0.5% Pt
@ 420 Hz	± 1.0% Pt
@ 600 Hz	± 1.4% Pt
@ 1050 Hz	± 3.5% Pt

S/N A07W

UNKNOWNS

C1= 1.105472E-03 C2= 3.1637E-06

D1= 1.057718E-03 D2= 3.829924E-06

M(75.5)= .8552706

P(75.5)= 6.609306

PSIA;	TEMP	VPI	M(BAR)	PO
14	89.4	8.388	.8689356	6.711369
10	89.4	3.809	.8689356	6.690225
6	89.4	-.794	.8689356	6.689935
2	89.4	-5.422	.8689356	6.711369
6	89.4	-.795	.8689356	6.690804
10	89.4	3.806	.8689356	6.692831
14	89.4	8.39	.8689356	6.70963
14	26.5	9.409	.8154389	6.327535
10	26.5	4.524	.8154389	6.310954
6	26.5	-.385	.8154389	6.313944
2	26.5	-5.307	.8154389	6.327535
6	26.5	-.38	.8154389	6.309867
10	26.5	4.523	.8154389	6.31177
14	26.5	9.405	.8154389	6.330797
14	-24.8	9.95	.78766	6.162783
10	-24.8	4.897	.78766	6.142829
6	-24.8	-.185	.78766	6.145717
2	-24.8	-5.285	.78766	6.162783
6	-24.8	-.184	.78766	6.144929
10	-24.8	4.898	.78766	6.142041
14	-24.8	9.947	.78766	6.165146

$$M(BAR) = \frac{14 - 2}{\text{Delta VPI}}$$

$$f(t) = 1 + C_1 (t-t_o) + C_2 (t-t_o)^2$$

$$g(t) = 1 + D_1 (t-t_o) + D_2 (t-t_o)^2$$

; Po = PSIA - (M * VPI);

to = 75.5

S/N 96YK

UNKNOWNS

C1= 1.043856E-03 C2= 4.74849E-06

D1= 8.161904E-05 D2= -1.738441E-07

M(75.5)= .9898391

P(75.5)= 5.568038

PSIA;	TEMP	VPI	M(BAR)	PO
14	89.4	8.383	1.005109	5.574168
10	89.4	4.46	1.005109	5.517212
6	89.4	.474	1.005109	5.523578
2	89.4	-3.556	1.005109	5.574169
6	89.4	.472	1.005109	5.525589
10	89.4	4.459	1.005109	5.518218
14	89.4	8.383	1.005109	5.574168
14	26.5	8.897	.9504951	5.543446
10	26.5	4.745	.9504951	5.489901
6	26.5	.526	.9504951	5.50004
2	26.5	-3.728	.9504951	5.543446
6	26.5	.528	.9504951	5.498138
10	26.5	4.746	.9504951	5.488951
14	26.5	8.894	.9504951	5.546297
14	-24.8	9.092	.933489	5.512718
10	-24.8	4.867	.933489	5.456709
6	-24.8	.571	.933489	5.466978
2	-24.8	-3.763	.933489	5.512719
6	-24.8	.572	.933489	5.466044
10	-24.8	4.867	.933489	5.456709
14	-24.8	9.09	.933489	5.514585

$$M(BAR) = \frac{14 - 2}{\text{Delta VPI}}$$

; Po = PSIA - (M * VPI);

to = 75.5

S/N 29TD

UNKNOWNS

C1= 9.38951E-04 C2= 4.700824E-06

D1= 9.154583E-04 D2= 5.407172E-06

M(75.5)= .839466

P(75.5)= 6.556338

PSIA:	TEMP	VPI	M(BAR)	PO
14	89.4	8.639	.8511846	6.646616
10	89.4	3.981	.8511846	6.611434
6	89.4	-.722	.8511846	6.614555
2	89.4	-5.459	.8511846	6.646617
6	89.4	-.723	.8511846	6.615407
10	89.4	3.983	.8511846	6.609732
14	89.4	8.642	.8511846	6.644063
14	26.5	9.444	.8103181	6.347356
10	26.5	4.548	.8103181	6.314673
6	26.5	-.396	.8103181	6.320886
2	26.5	-5.365	.8103181	6.347356
6	26.5	-.396	.8103181	6.320886
10	26.5	4.547	.8103181	6.315484
14	26.5	9.441	.8103181	6.349787
14	-24.8	9.61	.8001067	6.310975
10	-24.8	4.653	.8001067	6.277103
6	-24.8	-.355	.8001067	6.284038
2	-24.8	-5.388	.8001067	6.310975
6	-24.8	-.358	.8001067	6.286438
10	-24.8	4.651	.8001067	6.278704
14	-24.8	9.609	.8001067	6.311775

$$M(BAR) = \frac{14 - 2}{\text{Delta VPI}}$$

; Po = PSIA - (M * VPI);

to = 75.5

S/N 24TD

UNKNOWNS

C1= 1.041007E-03 C2= 4.235185E-06

D1= 6.429793E-04 D2= 3.19566E-06

M(75.5)= .9136753

P(75.5)= 5.94689

PSIA;	TEMP	VPI	M(BAR)	-PO
14	89.4	8.62	.9276438	6.003711
10	89.4	4.355	.9276438	5.960111
6	89.4	.037	.9276438	5.965677
2	89.4	-4.316	.9276438	6.003711
6	89.4	.036	.9276438	5.966605
10	89.4	4.356	.9276438	5.959184
14	89.4	8.62	.9276438	6.003711
14	26.5	9.351	.8763602	5.805156
10	26.5	4.832	.8763602	5.765428
6	26.5	.259	.8763602	5.773023
2	26.5	-4.342	.8763602	5.805156
6	26.5	.261	.8763602	5.77127
10	26.5	4.833	.8763602	5.764551
14	26.5	9.348	.8763602	5.807785
14	-24.8	9.619	.8572041	5.754554
10	-24.8	5.003	.8572041	5.711408
6	-24.8	.329	.8572041	5.71798
2	-24.8	-4.38	.8572041	5.754554
6	-24.8	.328	.8572041	5.718837
10	-24.8	5.002	.8572041	5.712265
14	-24.8	9.618	.8572041	5.755411

$$M(BAR) = \frac{14 - 2}{\text{Delta VPI}}$$

; Po = PSIA - (M * VPI);

to = 75.5

S/N 32TD

UNKNOWNS

C1= 1.005434E-03   C2= 3.080917E-06

D1= 7.56611E-04   D2= 4.702651E-06

M(75.5)= .8741805

P(75.5)= 4.431848

PSIA;	TEMP	VPI	M(BAR)	PO
14	89.4	10.731	.8869179	4.482484
10	89.4	6.294	.8869179	4.417738
6	89.4	1.773	.8869179	4.427495
2	89.4	-2.799	.8869179	4.482483
6	89.4	1.771	.8869179	4.429268
10	89.4	6.295	.8869179	4.416852
14	89.4	10.73	.8869179	4.483371
14	26.5	11.56	.8375794	4.317582
10	26.5	6.859	.8375794	4.255043
6	26.5	2.068	.8375794	4.267886
2	26.5	-2.767	.8375794	4.317582
6	26.5	2.069	.8375794	4.267048
10	26.5	6.859	.8375794	4.255043
14	26.5	11.557	.8375794	4.320095
14	-24.8	11.923	.8131183	4.30519
10	-24.8	7.082	.8131183	4.241497
6	-24.8	2.147	.8131183	4.254235
2	-24.8	-2.835	.8131183	4.30519
6	-24.8	2.146	.8131183	4.255048
10	-24.8	7.081	.8131183	4.24231
14	-24.8	11.921	.8131183	4.306817

$$M(BAR) = \frac{14 - 2}{\text{Delta VPI}}$$

; Po = PSIA - (M * VPI);

to = 75.5

S/N 94YK

UNKNOWNS

C1= 1.115585E-03 C2= 3.377424E-06

D1= 8.603389E-04 D2= 6.259645E-06

M(75.5)= .9449607

P(75.5)= 5.024814

PSIA;	TEMP	VPI	M(BAR)	PO
14	89.4	9.278	.9602305	5.090981
10	89.4	5.158	.9602305	5.047131
6	89.4	.987	.9602305	5.052253
2	89.4	-3.219	.9602305	5.090982
6	89.4	.985	.9602305	5.054173
10	89.4	5.158	.9602305	5.047131
14	89.4	9.278	.9602305	5.090981
14	26.5	10.113	.9009686	4.888505
10	26.5	5.72	.9009686	4.84646
6	26.5	1.27	.9009686	4.85577
2	26.5	-3.206	.9009686	4.888505
6	26.5	1.271	.9009686	4.854869
10	26.5	5.723	.9009686	4.843757
14	26.5	10.116	.9009686	4.885802
14	-24.8	10.435	.8713331	4.907639
10	-24.8	5.895	.8713331	4.863491
6	-24.8	1.295	.8713331	4.871624
2	-24.8	-3.337	.8713331	4.907639
6	-24.8	1.294	.8713331	4.872495
10	-24.8	5.896	.8713331	4.86262
14	-24.8	10.436	.8713331	4.906768

$$M(BAR) = \frac{14 - 2}{\text{Delta VPI}}$$

; Po = PSIA - (M * VPI);

to = 75.5

S/N 87YK

UNKNOWNS

C1= 1.023839E-03   C2= 8.725357E-06

D1= 1.143079E-03   D2= 1.091506E-05

M(75.5)= .8886539

P(75.5)= 5.363889

PSIA;	TEMP	VPI	M(BAR)	PO
14	89.4	9.459	.9027987	5.460427
10	89.4	5.075	.9027987	5.418297
6	89.4	.64	.9027987	5.422209
2	89.4	-3.833	.9027987	5.460427
6	89.4	.64	.9027987	5.422209
10	89.4	5.078	.9027987	5.415588
14	89.4	9.463	.9027987	5.456816
14	26.5	10.196	.8626887	5.204025
10	26.5	5.607	.8626887	5.162904
6	26.5	.961	.8626887	5.170956
2	26.5	-3.714	.8626887	5.204026
6	26.5	.962	.8626887	5.170094
10	26.5	5.606	.8626887	5.163767
14	26.5	10.197	.8626887	5.203163
14	-24.8	9.895	.8754012	5.337905
10	-24.8	5.375	.8754012	5.294719
6	-24.8	.798	.8754012	5.30143
2	-24.8	-3.813	.8754012	5.337905
6	-24.8	.797	.8754012	5.302305
10	-24.8	5.373	.8754012	5.296469
14	-24.8	9.893	.8754012	5.339656

$$M(BAR) = \frac{14 - 2}{\text{Delta VPI}}$$

; Po = PSIA - (M * VPI);

to = 75.5

S/N 39TD

UNKNOWNS

C1= 8.969064E-04 C2= 3.241249E-06

D1= 9.590462E-04 D2= 3.583406E-06

M(75.5)= .9144531

P(75.5)= 6.995395

PSIA;	TEMP	VPI	M(BAR)	PO
14	89.4	7.455	.9264263	7.093492
10	89.4	3.166	.9264263	7.066935
6	89.4	-1.152	.9264263	7.067243
2	89.4	-5.498	.9264263	7.093492
6	89.4	-1.153	.9264263	7.06817
10	89.4	3.166	.9264263	7.066935
14	89.4	7.455	.9264263	7.093492
14	26.5	8.252	.8813809	6.726845
10	26.5	3.738	.8813809	6.705399
6	26.5	-.804	.8813809	6.70863
2	26.5	-5.363	.8813809	6.726845
6	26.5	-.805	.8813809	6.709512
10	26.5	3.737	.8813809	6.70628
14	26.5	8.25	.8813809	6.728608
14	-24.8	8.614	.862007	6.574671
10	-24.8	4	.862007	6.551972
6	-24.8	-.642	.862007	6.553409
2	-24.8	-5.307	.862007	6.574671
6	-24.8	-.645	.862007	6.555995
10	-24.8	3.999	.862007	6.552834
14	-24.8	8.61	.862007	6.57812

$$M(BAR) = \frac{14 - 2}{\text{Delta VPI}}$$

; Po = PSIA - (M * VPI);

to = 75.5

S/N 82YK

UNKNOWNS

C1= 9.919953E-04 C2= 3.641087E-06

D1= 1.473228E-03 D2= 4.071245E-06

M(75.5)= .9677312

P(75.5)= 6.374631

PSIA;	TEMP	VPI	M(BAR)	PO
14	89.4	7.629	.9817557	6.510185
10	89.4	3.584	.9817557	6.481387
6	89.4	-.492	.9817557	6.483024
2	89.4	-4.594	.9817557	6.510186
6	89.4	-.494	.9817557	6.484987
10	89.4	3.582	.9817557	6.483351
14	89.4	7.627	.9817557	6.512149
14	26.5	8.635	.9291521	5.976771
10	26.5	4.357	.9291521	5.951684
6	26.5	.044	.9291521	5.959117
2	26.5	-4.28	.9291521	5.976771
6	26.5	.043	.9291521	5.960046
10	26.5	4.355	.9291521	5.953543
14	26.5	8.631	.9291521	5.980489
14	-24.8	9.159	.9068924	5.693772
10	-24.8	4.777	.9068924	5.667775
6	-24.8	.358	.9068924	5.675333
2	-24.8	-4.073	.9068924	5.693772
6	-24.8	.36	.9068924	5.673519
10	-24.8	4.776	.9068924	5.668682
14	-24.8	9.154	.9068924	5.698307

$$M(BAR) = \frac{14 - 2}{\text{Delta VPI}}$$

; Po = PSIA - (M * VPI);

to = 75.5

S/N 84YK

UNKNOWNS

C1= 9.991998E-04 C2= 2.789268E-06

D1= 9.831027E-04 D2= 2.186993E-06

M(75.5)= .9658172

P(75.5)= 5.962379

PSIA;	TEMP	VPI	M(BAR)	PO
14	89.4	8.118	.9797518	6.046375
10	89.4	4.062	.9797518	6.020248
6	89.4	-.022	.9797518	6.021554
2	89.4	-4.13	.9797518	6.046375
6	89.4	-.025	.9797518	6.024494
10	89.4	4.062	.9797518	6.020248
14	89.4	8.115	.9797518	6.049314
14	26.5	8.966	.9249981	5.706468
10	26.5	4.665	.9249981	5.684884
6	26.5	.333	.9249981	5.691976
2	26.5	-4.007	.9249981	5.706468
6	26.5	.334	.9249981	5.691051
10	26.5	4.666	.9249981	5.683959
14	26.5	8.967	.9249981	5.705542
14	-24.8	9.479	.8961243	5.505638
10	-24.8	5.04	.8961243	5.483533
6	-24.8	.571	.8961243	5.488313
2	-24.8	-3.912	.8961243	5.505638
6	-24.8	.569	.8961243	5.490105
10	-24.8	5.04	.8961243	5.483533
14	-24.8	9.477	.8961243	5.50743

$$M(BAR) = \frac{14 - 2}{\text{Delta VPI}}$$

; Po = PSIA - (M * VPI);

to = 75.5

S/N 89YK

UNKNOWNS

C1= 1.131939E-03 C2= 5.504947E-06

D1= 1.067346E-03 D2= 8.843695E-06

M(75.5)= .9280301

P(75.5)= 6.43424

PSIA;	TEMP	VPI	M(BAR)	PO
14	89.4	7.905	.9436188	6.540693
10	89.4	3.707	.9436188	6.502005
6	89.4	-.534	.9436188	6.503892
2	89.4	-4.812	.9436188	6.540693
6	89.4	-.536	.9436188	6.50578
10	89.4	3.708	.9436188	6.501061
14	89.4	7.904	.9436188	6.541637
14	26.5	8.737	.888823	6.234353
10	26.5	4.277	.888823	6.198504
6	26.5	-.229	.888823	6.20354
2	26.5	-4.764	.888823	6.234353
6	26.5	-.233	.888823	6.207096
10	26.5	4.273	.888823	6.20206
14	26.5	8.732	.888823	6.238797
14	-24.8	8.789	.8740622	6.317868
10	-24.8	4.252	.8740622	6.283488
6	-24.8	-.326	.8740622	6.284944
2	-24.8	-4.94	.8740622	6.317867
6	-24.8	-.338	.8740622	6.295433
10	-24.8	4.237	.8740622	6.296598
14	-24.8	8.775	.8740622	6.330105

$$M(BAR) = \frac{14 - 2}{\text{Delta VPI}}$$

; Po = PSIA - (M * VPI);

to = 75.5

S/N 27TD

UNKNOWNS

C1= 8.908476E-04 C2= 4.321207E-06

D1= 4.577776E-04 D2= 1.805989E-06

M(75.5)= .863037

P(75.5)= 6.709321

PSIA;	TEMP	VPI	M(BAR)	PO
14	89.4	8.286	.8744444	6.754354
10	89.4	3.756	.8744444	6.715587
6	89.4	-.82	.8744444	6.717044
2	89.4	-5.437	.8744444	6.754354
6	89.4	-.823	.8744444	6.719668
10	89.4	3.75	.8744444	6.720834
14	89.4	8.284	.8744444	6.756103
14	26.5	8.884	.8343183	6.587916
10	26.5	4.137	.8343183	6.548425
6	26.5	-.665	.8343183	6.554822
2	26.5	-5.499	.8343183	6.587916
6	26.5	-.667	.8343183	6.55649
10	26.5	4.132	.8343183	6.552597
14	26.5	8.879	.8343183	6.592088
14	-24.8	9.08	.8234406	6.52316
10	-24.8	4.28	.8234406	6.475674
6	-24.8	-.584	.8234406	6.480889
2	-24.8	-5.493	.8234406	6.52316
6	-24.8	-.588	.8234406	6.484183
10	-24.8	4.275	.8234406	6.479792
14	-24.8	9.082	.8234406	6.521513

$$M(BAR) = \frac{14 - 2}{\text{Delta VPI}}$$

; Po = PSIA - (M * VPI);

to = 75.5

S/N 21TD

UNKNOWNS

C1= 1.001441E-03 C2= 4.326469E-06

D1= 6.766801E-04 D2= 1.822359E-06

M(75.5)= .890743

P(75.5)= 6.786743

PSIA;	TEMP	VPI	M(BAR)	PO
14	89.4	7.907	.9038867	6.852968
10	89.4	3.515	.9038867	6.822838
6	89.4	-.911	.9038867	6.823441
2	89.4	-5.369	.9038867	6.852968
6	89.4	-.914	.9038867	6.826152
10	89.4	3.511	.9038867	6.826454
14	89.4	7.905	.9038867	6.854775
14	26.5	8.652	.8562866	6.591408
10	26.5	4.013	.8562866	6.563722
6	26.5	-.664	.8562866	6.568574
2	26.5	-5.362	.8562866	6.591409
6	26.5	-.665	.8562866	6.56943
10	26.5	4.01	.8562866	6.566291
14	26.5	8.647	.8562866	6.59569
14	-24.8	8.987	.840042	6.450542
10	-24.8	4.268	.840042	6.414701
6	-24.8	-.499	.840042	6.419181
2	-24.8	-5.298	.840042	6.450542
6	-24.8	-.51	.840042	6.428421
10	-24.8	4.26	.840042	6.421421
14	-24.8	8.988	.840042	6.449703

$$M(BAR) = \frac{14 - 2}{\text{Delta VPI}}$$

; Po = PSIA - (M * VPI);

to = 75.5

S/N 50YK

UNKNOWNS

C1= 1.051493E-03 C2= 4.276334E-06

D1= 1.054341E-03 D2= 5.12663E-06

M(75.5)= .8757606

P(75.5)= 6.384765

PSIA;	TEMP	VPI	M(BAR)	PO
14	89.4	8.451	.8892841	6.48466
10	89.4	3.986	.8892841	6.455314
6	89.4	-.513	.8892841	6.456203
2	89.4	-5.043	.8892841	6.48466
6	89.4	-.516	.8892841	6.45887
10	89.4	3.988	.8892841	6.453535
14	89.4	8.451	.8892841	6.48466
14	26.5	9.369	.8396305	6.133501
10	26.5	4.633	.8396305	6.109992
6	26.5	-.136	.8396305	6.11419
2	26.5	-4.923	.8396305	6.133501
6	26.5	-.135	.8396305	6.11335
10	26.5	4.631	.8396305	6.111671
14	26.5	9.364	.8396305	6.137699
14	-24.8	9.696	.8210742	6.038864
10	-24.8	4.861	.8210742	6.008758
6	-24.8	-.016	.8210742	6.013137
2	-24.8	-4.919	.8210742	6.038864
6	-24.8	-.018	.8210742	6.01478
10	-24.8	4.858	.8210742	6.011221
14	-24.8	9.697	.8210742	6.038043

$$M(BAR) = \frac{14 - 2}{\text{Delta VPI}}$$

; Po = PSIA - (M * VPI);

to = 75.5

S/N 83YH

UNKNOWNS

C1= 1.108327E-03 C2= 3.974816E-06

D1= 1.072761E-03 D2= 4.465857E-06

M(75.5)= .947601

P(75.5)= 7.274751

PSIA;	TEMP	VPI	M(BAR)	PO
14	89.4	6.865	.9629273	7.389504
10	89.4	2.732	.9629273	7.369283
6	89.4	-1.422	.9629273	7.369283
2	89.4	-5.597	.9629273	7.389504
6	89.4	-1.425	.9629273	7.372171
10	89.4	2.734	.9629273	7.367357
14	89.4	6.863	.9629273	7.39143
14	26.5	7.766	.9051822	6.970356
10	26.5	3.367	.9051822	6.952251
6	26.5	-1.057	.9051822	6.956778
2	26.5	-5.491	.9051822	6.970356
6	26.5	-1.06	.9051822	6.959493
10	26.5	3.361	.9051822	6.957683
14	26.5	7.759	.9051822	6.976692
14	-24.8	8.159	.8801525	6.818835
10	-24.8	3.641	.8801525	6.795364
6	-24.8	-.91	.8801525	6.800939
2	-24.8	-5.475	.8801525	6.818835
6	-24.8	-.911	.8801525	6.801819
10	-24.8	3.643	.8801525	6.793604
14	-24.8	8.163	.8801525	6.815315

$$M(BAR) = \frac{14 - 2}{\text{Delta VPI}}$$

; Po = PSIA - (M * VPI);

to = 75.5

S/N 30TD

UNKNOWNS

C1= 9.344729E-04 C2= 3.102274E-06

D1= 1.584812E-03 D2= 7.488129E-06

M(75.5)= 1.083573

P(75.5)= 8.266134

PSIA;	TEMP	VPI	M(BAR)	PO
14	89.4	5.044	1.098298	8.460187
10	89.4	1.42	1.098298	8.440417
6	89.4	-2.222	1.098298	8.440417
2	89.4	-5.882	1.098298	8.460186
6	89.4	-2.222	1.098298	8.440417
10	89.4	1.422	1.098298	8.438221
14	89.4	5.044	1.098298	8.460187
14	26.5	5.976	1.042029	7.772838
10	26.5	2.155	1.042029	7.754429
6	26.5	-1.688	1.042029	7.758944
2	26.5	-5.54	1.042029	7.772838
6	26.5	-1.688	1.042029	7.758944
10	26.5	2.15	1.042029	7.759639
14	26.5	5.97	1.042029	7.77909
14	-24.8	6.325	1.01583	7.574875
10	-24.8	2.41	1.01583	7.551849
6	-24.8	-1.533	1.01583	7.557267
2	-24.8	-5.488	1.01583	7.574875
6	-24.8	-1.532	1.01583	7.556252
10	-24.8	2.409	1.01583	7.552866
14	-24.8	6.326	1.01583	7.573859

$$M(BAR) = \frac{14 - 2}{\text{Delta VPI}}$$

; Po = PSIA - (M * VPI);

to = 75.5

S/N 98YH

UNKNOWNS

C1= 1.12793E-03 C2= 3.244637E-06

D1= 1.14923E-03 D2= 5.463567E-06

M(75.5)= 1.139278

P(75.5)= 7.124901

PSIA;	TEMP	VPI	M(BAR)	PO
14	89.4	5.833	1.157854	7.246237
10	89.4	2.419	1.157854	7.199151
6	89.4	-1.038	1.157854	7.201853
2	89.4	-4.531	1.157854	7.246237
6	89.4	-1.04	1.157854	7.204168
10	89.4	2.418	1.157854	7.200309
14	89.4	5.832	1.157854	7.247395
14	26.5	6.619	1.085187	6.817146
10	26.5	2.973	1.085187	6.773738
6	26.5	-.72	1.085187	6.781335
2	26.5	-4.439	1.085187	6.817146
6	26.5	-.72	1.085187	6.781335
10	26.5	2.97	1.085187	6.776994
14	26.5	6.61	1.085187	6.826912
14	-24.8	6.973	1.047578	6.695242
10	-24.8	3.199	1.047578	6.6488
6	-24.8	-.625	1.047578	6.654736
2	-24.8	-4.482	1.047578	6.695242
6	-24.8	-.622	1.047578	6.651593
10	-24.8	3.202	1.047578	6.645657
14	-24.8	6.972	1.047578	6.69629

$$M(BAR) = \frac{14 - 2}{\text{Delta VPI}}$$

; Po = PSIA - (M * VPI);

to = 75.5

S/N 98YK

UNKNOWNS

C1= 9.390063E-04   C2= 4.224694E-06

D1= -1.708739E-04   D2= -2.496365E-06

M(75.5)= 1.09815

P(75.5)= 8.811223

PSIA;	TEMP	VPI	M(BAR)	PO
14	89.4	4.683	1.113379	8.786045
10	89.4	1.105	1.113379	8.769716
6	89.4	-2.487	1.113379	8.768974
2	89.4	-6.095	1.113379	8.786045
6	89.4	-2.489	1.113379	8.7712
10	89.4	1.107	1.113379	8.767489
14	89.4	4.683	1.113379	8.786045
14	26.5	4.881	1.058761	8.832186
10	26.5	1.113	1.058761	8.821599
6	26.5	-2.669	1.058761	8.825833
2	26.5	-6.453	1.058761	8.832186
6	26.5	-2.672	1.058761	8.82901
10	26.5	1.106	1.058761	8.82901
14	26.5	4.87	1.058761	8.843833
14	-24.8	5.05	1.041395	8.740953
10	-24.8	1.221	1.041395	8.728456
6	-24.8	-2.624	1.041395	8.732622
2	-24.8	-6.473	1.041395	8.740952
6	-24.8	-2.629	1.041395	8.737828
10	-24.8	1.209	1.041395	8.740953
14	-24.8	5.037	1.041395	8.754491

$$M(BAR) = \frac{14 - 2}{\text{Delta VPI}}$$

; Po = PSIA - (M * VPI);

to = 75.5

S/N 90YK

UNKNOWNS

C1= 8.906735E-04 C2= 4.165141E-06

D1= 1.496541E-03 D2= 8.492784E-06

M(75.5)= .9613505

P(75.5)= 7.249953

PSIA;	TEMP	VPI	M(BAR)	PO
14	89.4	6.763	.974026	7.412662
10	89.4	2.683	.974026	7.386688
6	89.4	-1.425	.974026	7.387987
2	89.4	-5.557	.974026	7.412663
6	89.4	-1.428	.974026	7.390909
10	89.4	2.683	.974026	7.386688
14	89.4	6.761	.974026	7.41461
14	26.5	7.679	.9290083	6.866145
10	26.5	3.398	.9290083	6.84323
6	26.5	-.917	.9290083	6.851901
2	26.5	-5.238	.9290083	6.866146
6	26.5	-.918	.9290083	6.852829
10	26.5	3.399	.9290083	6.842301
14	26.5	7.692	.9290083	6.854068
14	-24.8	7.883	.9157509	6.781136
10	-24.8	3.546	.9157509	6.752748
6	-24.8	-.829	.9157509	6.759158
2	-24.8	-5.221	.9157509	6.781136
6	-24.8	-.834	.9157509	6.763736
10	-24.8	3.544	.9157509	6.754579
14	-24.8	7.888	.9157509	6.776556

$$M(BAR) = \frac{14 - 2}{\text{Delta VPI}}$$

; Po = PSIA - (M * VPI);

to = 75.5

S/N 38TD

UNKNOWNS

C1= 9.861114E-04 C2= 3.936118E-06

D1= 1.039495E-03 D2= 4.609303E-06

M(75.5)= .9485859

P(75.5)= 7.323743

PSIA;	TEMP	VPI	M(BAR)	PO
14	89.4	6.821	.9623095	7.436087
10	89.4	2.691	.9623095	7.410425
6	89.4	-1.466	.9623095	7.410746
2	89.4	-5.649	.9623095	7.436087
6	89.4	-1.467	.9623095	7.411708
10	89.4	2.694	.9623095	7.407538
14	89.4	6.823	.9623095	7.434162
14	26.5	7.643	.9117155	7.031758
10	26.5	3.285	.9117155	7.005014
6	26.5	-1.114	.9117155	7.015651
2	26.5	-5.519	.9117155	7.031758
6	26.5	-1.115	.9117155	7.016563
10	26.5	3.277	.9117155	7.012308
14	26.5	7.631	.9117155	7.042699
14	-24.8	7.957	.892326	6.899762
10	-24.8	3.511	.892326	6.867043
6	-24.8	-.982	.892326	6.876264
2	-24.8	-5.491	.892326	6.899762
6	-24.8	-.984	.892326	6.878049
10	-24.8	3.508	.892326	6.86972
14	-24.8	7.953	.892326	6.903331

$$M(BAR) = \frac{14 - 2}{\text{Delta VPI}}$$

; Po = PSIA - (M * VPI);

to = 75.5

S/N 07TC

UNKNOWNS

C1= 1.086329E-03 C2= 2.731935E-06

D1= 8.726402E-04 D2= 3.449842E-06

M(75.5)= .8346899

P(75.5)= 6.375906

PSIA;	TEMP	VPI	M(BAR)	PO
14	89.3	8.899	.8476372	6.456876
10	89.3	4.21	.8476372	6.431447
6	89.3	-.513	.8476372	6.434838
2	89.3	-5.258	.8476372	6.456876
6	89.3	-.515	.8476372	6.436533
10	89.3	4.209	.8476372	6.432295
14	89.3	8.901	.8476372	6.455181
14	26.3	9.86	.7955977	6.155407
10	26.3	4.855	.7955977	6.137373
6	26.3	-.179	.7955977	6.142412
2	26.3	-5.223	.7955977	6.155406
6	26.3	-.18	.7955977	6.143208
10	26.3	4.856	.7955977	6.136578
14	26.3	9.865	.7955977	6.151429
14	-24.6	10.382	.7667732	6.039361
10	-24.6	5.19	.7667732	6.020447
6	-24.6	-.031	.7667732	6.02377
2	-24.6	-5.268	.7667732	6.039361
6	-24.6	-.033	.7667732	6.025303
10	-24.6	5.186	.7667732	6.023515
14	-24.6	10.376	.7667732	6.043962

$$M(BAR) = \frac{14 - 2}{\text{Delta VPI}}$$

; Po = PSIA - (M * VPI);

to = 75.5

S/N 23TD

UNKNOWNS

C1= 1.098888E-03 C2= 4.049162E-06

D1= 1.107102E-03 D2= 6.908331E-06

M(75.5)= .9700066

P(75.5)= 4.84641

PSIA;	TEMP	VPI	M(BAR)	PO
14	89.3	9.207	.9854644	4.926829
10	89.3	5.196	.9854644	4.879527
6	89.3	1.13	.9854644	4.886425
2	89.3	-2.97	.9854644	4.926829
6	89.3	1.128	.9854644	4.888396
10	89.3	5.196	.9854644	4.879527
14	89.3	9.21	.9854644	4.923873
14	26.3	10.071	.9270704	4.663473
10	26.3	5.802	.9270704	4.621137
6	26.3	1.478	.9270704	4.62979
2	26.3	-2.873	.9270704	4.663473
6	26.3	1.48	.9270704	4.627936
10	26.3	5.804	.9270704	4.619283
14	26.3	10.072	.9270704	4.662547
14	-24.6	10.364	.9026628	4.644802
10	-24.6	5.984	.9026628	4.598465
6	-24.6	1.542	.9026628	4.608094
2	-24.6	-2.93	.9026628	4.644802
6	-24.6	1.544	.9026628	4.606288
10	-24.6	5.986	.9026628	4.59666
14	-24.6	10.365	.9026628	4.6439

$$M(BAR) = \frac{14 - 2}{\text{Delta VPI}}$$

; Po = PSIA - (M * VPI);

to = 75.5

S/N 25TD

UNKNOWNS

C1= 1.017951E-03 C2= 3.464171E-06

D1= 9.000237E-04 D2= 6.260641E-06

M(75.5)= .9051717

P(75.5)= 5.111136

PSIA;	TEMP	VPI	M(BAR)	PO
14	89.3	9.602	.9184844	5.180712
10	89.3	5.308	.9184844	5.124684
6	89.3	.945	.9184844	5.132032
2	89.3	-3.463	.9184844	5.180712
6	89.3	.942	.9184844	5.134788
10	89.3	5.308	.9184844	5.124684
14	89.3	9.601	.9184844	5.181631
14	26.3	10.419	.8674281	4.962267
10	26.3	5.867	.8674281	4.910799
6	26.3	1.245	.8674281	4.920052
2	26.3	-3.415	.8674281	4.962267
6	26.3	1.247	.8674281	4.918317
10	26.3	5.869	.8674281	4.909064
14	26.3	10.42	.8674281	4.961399
14	-24.6	10.693	.8443569	4.971292
10	-24.6	6.021	.8443569	4.916127
6	-24.6	1.271	.8443569	4.926822
2	-24.6	-3.519	.8443569	4.971292
6	-24.6	1.275	.8443569	4.923445
10	-24.6	6.024	.8443569	4.913594
14	-24.6	10.694	.8443569	4.970448

$$M(BAR) = \frac{14 - 2}{\text{Delta VPI}}$$

; Po = PSIA - (M * VPI);

to = 75.5

S/N 97YK

UNKNOWNS

C1= 1.182127E-03 C2= 4.255065E-06

D1= 1.103684E-03 D2= 5.1898E-06

M(75.5)= .8548018

P(75.5)= 5.605931

PSIA;	TEMP	VPI	M(BAR)	PO
14	89.3	9.55	.8694392	5.696856
10	89.3	4.978	.8694392	5.671932
6	89.3	.373	.8694392	5.675699
2	89.3	-4.252	.8694392	5.696856
6	89.3	.37	.8694392	5.678308
10	89.3	4.977	.8694392	5.672801
14	89.3	9.548	.8694392	5.698594
14	26.3	10.601	.8138904	5.371948
10	26.3	5.712	.8138904	5.351058
6	26.3	.789	.8138904	5.357841
2	26.3	-4.143	.8138904	5.371948
6	26.3	.791	.8138904	5.356213
10	26.3	5.716	.8138904	5.347803
14	26.3	10.608	.8138904	5.366251
14	-24.6	11.039	.7900975	5.278114
10	-24.6	6.004	.7900975	5.256255
6	-24.6	.933	.7900975	5.262839
2	-24.6	-4.149	.7900975	5.278114
6	-24.6	.935	.7900975	5.261259
10	-24.6	6.008	.7900975	5.253095
14	-24.6	11.042	.7900975	5.275743

$$M(BAR) = \frac{14 - 2}{\text{Delta VPI}}$$

; Po = PSIA - (M * VPI);

to = 75.5

S/N 99YK

UNKNOWNS

C1= 1.066827E-03 C2= 3.731841E-06

D1= 1.234954E-03 D2= 5.697999E-06

M(75.5)= .9687368

P(75.5)= 7.478339

PSIA;	TEMP	VPI	M(BAR)	PO
14	89.3	6.492	.9836872	7.613903
10	89.3	2.455	.9836872	7.585048
6	89.3	-1.614	.9836872	7.587671
2	89.3	-5.707	.9836872	7.613903
6	89.3	-1.617	.9836872	7.590622
10	89.3	2.453	.9836872	7.587015
14	89.3	6.493	.9836872	7.612919
14	26.3	7.417	.9266409	7.127104
10	26.3	3.12	.9266409	7.108881
6	26.3	-1.199	.9266409	7.111042
2	26.3	-5.533	.9266409	7.127104
6	26.3	-1.196	.9266409	7.108263
10	26.3	3.129	.9266409	7.100541
14	26.3	7.426	.9266409	7.118764
14	-24.6	7.786	.9015101	6.980843
10	-24.6	3.37	.9015101	6.961911
6	-24.6	-1.072	.9015101	6.966419
2	-24.6	-5.525	.9015101	6.980843
6	-24.6	-1.066	.9015101	6.96101
10	-24.6	3.38	.9015101	6.952896
14	-24.6	7.794	.9015101	6.97363

$$M(BAR) = \frac{14 - 2}{\text{Delta VPI}}$$

; Po = PSIA - (M * VPI);

to = 75.5

S/N 47YK

UNKNOWNS

C1= 1.04712E-03 C2= 3.280354E-06

D1= 8.282974E-04 D2= 3.772956E-06

M(75.5)= .8961331

P(75.5)= 6.51365

PSIA;	TEMP	VPI	M(BAR)	PO
14	89.3	8.143	.9096422	6.592784
10	89.3	3.761	.9096422	6.578835
6	89.3	-.622	.9096422	6.565797
2	89.3	-5.049	.9096422	6.592783
6	89.3	-.622	.9096422	6.565797
10	89.3	3.802	.9096422	6.54154
14	89.3	8.141	.9096422	6.594603
14	26.3	8.975	.8570816	6.307693
10	26.3	4.322	.8570816	6.295693
6	26.3	-.358	.8570816	6.306835
2	26.3	-5.026	.8570816	6.307692
6	26.3	-.346	.8570816	6.29655
10	26.3	4.324	.8570816	6.29398
14	26.3	8.963	.8570816	6.317977
14	-24.6	9.355	.8316585	6.219835
10	-24.6	4.558	.8316585	6.2093
6	-24.6	-.257	.8316585	6.213736
2	-24.6	-5.074	.8316585	6.219835
6	-24.6	-.242	.8316585	6.201262
10	-24.6	4.577	.8316585	6.193499
14	-24.6	9.375	.8316585	6.203201

$$M(BAR) = \frac{14 - 2}{\text{Delta VPI}}$$

; Po = PSIA - (M * VPI);

to = 75.5

S/N 83YK

UNKNOWNS

C1= 1.143896E-03 C2= 2.351116E-06

D1= 1.084481E-03 D2= 4.22739E-06

M(75.5)= .8822705

P(75.5)= 6.151932

PSIA;	TEMP	VPI	M(BAR)	PO
14	89.3	8.645	.8965929	6.248954
10	89.3	4.219	.8965929	6.217275
6	89.3	-.246	.8965929	6.220562
2	89.3	-4.739	.8965929	6.248954
6	89.3	-.25	.8965929	6.224148
10	89.3	4.217	.8965929	6.219068
14	89.3	8.645	.8965929	6.248954
14	26.3	9.686	.8376378	5.88664
10	26.3	4.939	.8376378	5.862906
6	26.3	.155	.8376378	5.870166
2	26.3	-4.64	.8376378	5.88664
6	26.3	.153	.8376378	5.871841
10	26.3	4.94	.8376378	5.862069
14	26.3	9.688	.8376378	5.884965
14	-24.6	10.293	.8020318	5.744686
10	-24.6	5.336	.8020318	5.720358
6	-24.6	.34	.8020318	5.727309
2	-24.6	-4.669	.8020318	5.744687
6	-24.6	.339	.8020318	5.728111
10	-24.6	5.336	.8020318	5.720358
14	-24.6	10.291	.8020318	5.74629

$$M(BAR) = \frac{14 - 2}{\text{Delta VPI}}$$

; Po = PSIA - (M * VPI);

to = 75.5

S/N 85YH

UNKNOWNS

C1= 9.195752E-04 C2= 2.822584E-06

D1= 1.809689E-03 D2= 9.624122E-06

M(75.5)= .8688533

P(75.5)= 6.731016

PSIA;	TEMP	VPI	M(BAR)	PO
14	89.3	8.052	.8803462	6.911452
10	89.3	3.538	.8803462	6.885335
6	89.3	-1.009	.8803462	6.888269
2	89.3	-5.579	.8803462	6.911452
6	89.3	-1.011	.8803462	6.89003
10	89.3	3.538	.8803462	6.885335
14	89.3	8.055	.8803462	6.908811
14	26.3	9.23	.8354801	6.288519
10	26.3	4.462	.8354801	6.272088
6	26.3	-.33	.8354801	6.275708
2	26.3	-5.133	.8354801	6.288519
6	26.3	-.327	.8354801	6.273202
10	26.3	4.472	.8354801	6.263733
14	26.3	9.239	.8354801	6.280999
14	-24.6	9.637	.813449	6.160792
10	-24.6	4.743	.813449	6.141811
6	-24.6	-.179	.813449	6.145607
2	-24.6	-5.115	.813449	6.160791
6	-24.6	-.178	.813449	6.144794
10	-24.6	4.749	.813449	6.13693
14	-24.6	9.642	.813449	6.156724

$$M(BAR) = \frac{14 - 2}{\text{Delta VPI}}$$

; Po = PSIA - (M * VPI);

to = 75.5

S/N 93YK

UNKNOWNS

C1= 1.109778E-03 C2= 3.573072E-06

D1= 1.281164E-03 D2= 5.161262E-06

M(75.5)= .9151617

P(75.5)= 5.457423

PSIA;	TEMP	VPI	M(BAR)	PO
14	89.3	9.078	.9298001	5.559275
10	89.3	4.839	.9298001	5.500697
6	89.3	.528	.9298001	5.509066
2	89.3	-3.828	.9298001	5.559275
6	89.3	.526	.9298001	5.510925
10	89.3	4.839	.9298001	5.500697
14	89.3	9.082	.9298001	5.555555
14	26.3	10.1	.8731082	5.181606
10	26.3	5.569	.8731082	5.137661
6	26.3	.982	.8731082	5.142608
2	26.3	-3.644	.8731082	5.181606
6	26.3	.983	.8731082	5.141735
10	26.3	5.579	.8731082	5.128929
14	26.3	10.109	.8731082	5.173749
14	-24.6	10.588	.8462623	5.039774
10	-24.6	5.911	.8462623	4.997744
6	-24.6	1.184	.8462623	4.998025
2	-24.6	-3.592	.8462623	5.039774
6	-24.6	1.183	.8462623	4.998872
10	-24.6	5.919	.8462623	4.990973
14	-24.6	10.591	.8462623	5.037236

$$M(BAR) = \frac{14 - 2}{\text{Delta VPI}}$$

; Po = PSIA - (M * VPI);

to = 75.5

APPENDIX C

UNSTEADY DATA TABULATIONS

Available on diskette. Notify

Larry J. Heidelberg

NASA Lewis Research Center
Propulsion Systems Division
Mailstop 77-6 Room 129
21000 Brookpark Road
Cleveland, Ohio 44135

(216) 433-3859

APPENDIX D

STEADY PRESSURE PLOTS

APPENDIX D1

-1 DEGREE STEADY PRESSURE
DISTRIBUTION PLOTS

LAP/SR-7L Flight Test
Blade Surface Pressure Distribution

Record	: 37	Altitude (ft)	: 1986.
Condition	: 1A	Mach No.	: 0.307
Nacelle Tilt	: -1	True Airspeed (fps)	: 351.
Radial Sta	: .680	Tip Speed (fps)	: 624.
		Power Coeff.	: 1.484
		Blade Angle (deg)	: 44.63

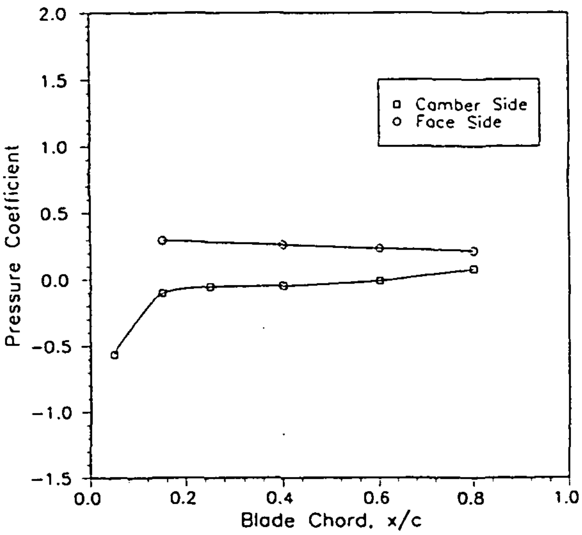

LAP/SR-7L Flight Test
Blade Surface Pressure Distribution

Record	: 37	Altitude (ft)	: 1986.
Condition	: 1A	Mach No.	: 0.307
Nacelle Tilt	: -1	True Airspeed (fps)	: 351.
Radial Sta	: .860	Tip Speed (fps)	: 624.
		Power Coeff.	: 1.484
		Blade Angle (deg)	: 44.63

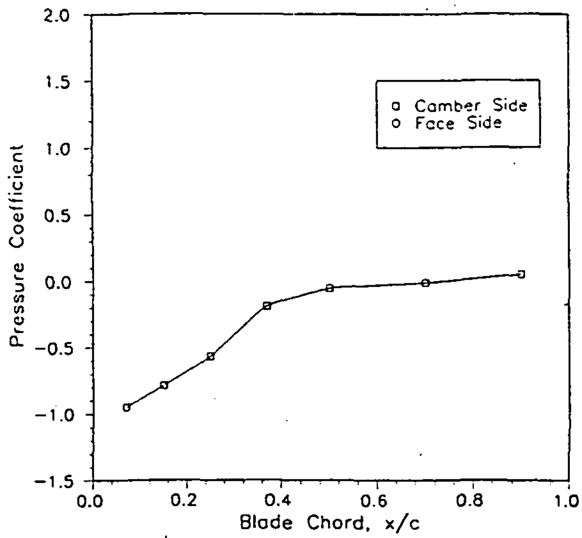

LAP/SR-7L Flight Test
Blade Surface Pressure Distribution

Record	: 37	Altitude (ft)	: 1986.
Condition	: 1A	Mach No.	: 0.307
Nacelle Tilt	: -1	True Airspeed (fps)	: 351.
Radial Sta	: .964	Tip Speed (fps)	: 624.
		Power Coeff.	: 1.484
		Blade Angle (deg)	: 44.63

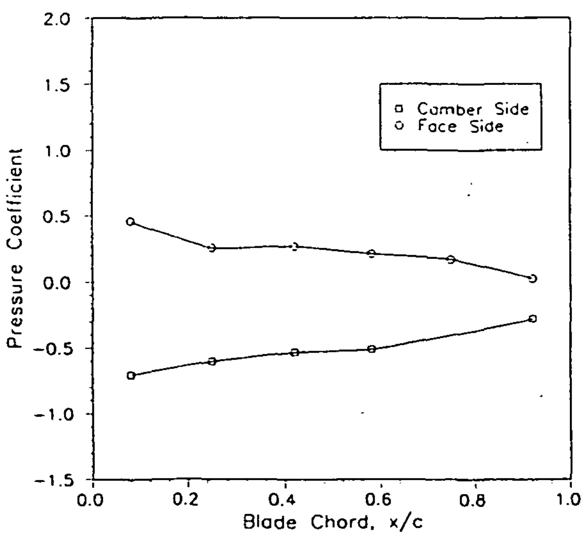

LAP/SR-7L Flight Test
Blade Surface Pressure Distribution

Record	: 39	Altitude (ft)	: 2042.
Condition	: 2A	Mach No.	: 0.309
Nacelle Tilt	: -1	True Airspeed (fps)	: 353.
Radial Sta	: .680	Tip Speed (fps)	: 631.
		Power Coeff.	: 2.103
		Blade Angle (deg)	: 47.28

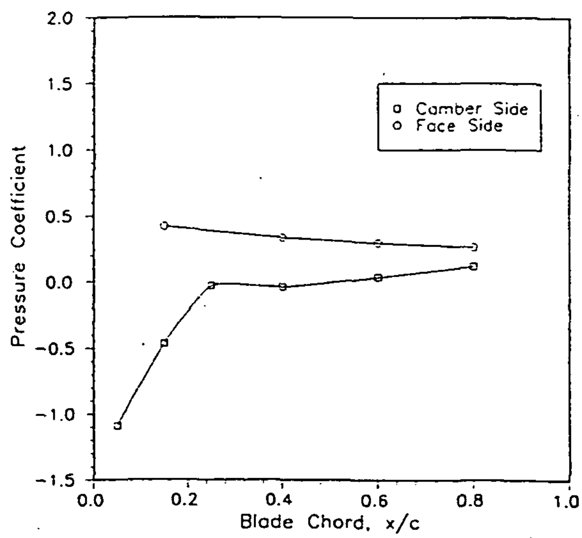

LAP/SR-7L Flight Test
Blade Surface Pressure Distribution

Record : 39
Condition : 2A
Nacelle Tilt : -1
Radial Sta : .860

Altitude (ft) : 2042.
Mach No. : 0.309
True Airspeed (fps) : 353.
Tip Speed (fps) : 631.
Power Coeff. : 2.103
Blade Angle (deg): 47.28

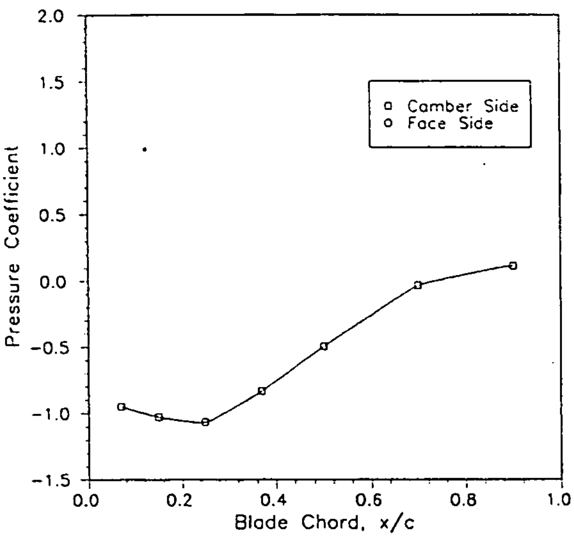

LAP/SR-7L Flight Test
Blade Surface Pressure Distribution

Record : 39
Condition : 2A
Nacelle Tilt : -1
Radial Sta : .964

Altitude (ft) : 2042.
Mach No. : 0.309
True Airspeed (fps) : 353.
Tip Speed (fps) : 631.
Power Coeff. : 2.103
Blade Angle (deg): 47.28

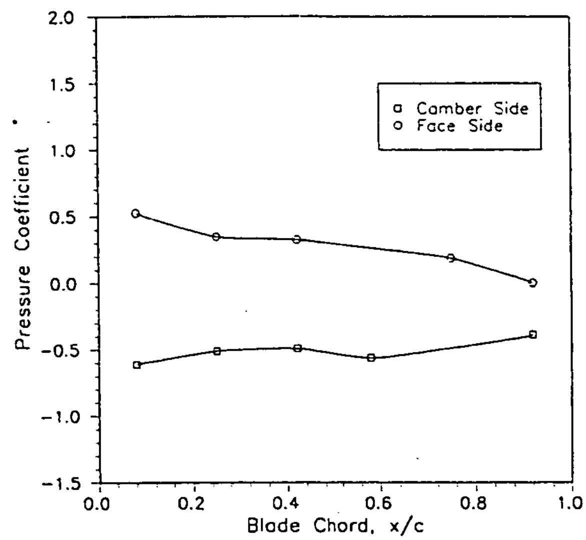

LAP/SR-7L Flight Test
Blade Surface Pressure Distribution

Record : 40
Condition : 3A
Nacelle Tilt : -1
Radial Sta : .680

Altitude (ft) : 1993.
Mach No. : 0.307
True Airspeed (fps) : 350.
Tip Speed (fps) : 704.
Power Coeff. : 1.006
Blade Angle (deg): 39.96

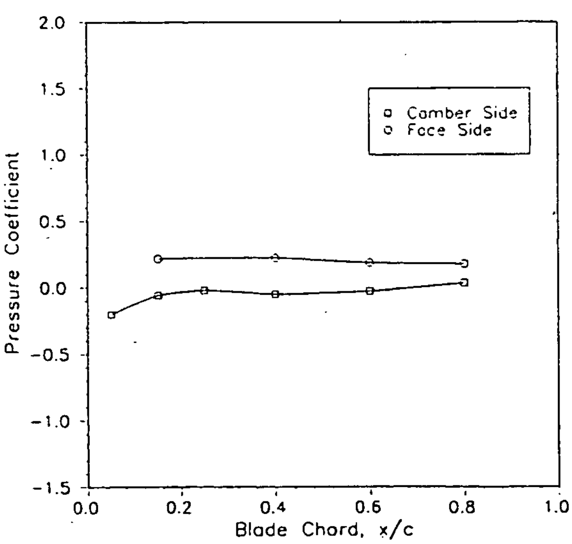

LAP/SR-7L Flight Test
Blade Surface Pressure Distribution

Record : 40
Condition : 3A
Nacelle Tilt : -1
Radial Sta : .860

Altitude (ft) : 1993.
Mach No. : 0.307
True Airspeed (fps) : 350.
Tip Speed (fps) : 704.
Power Coeff. : 1.006
Blade Angle (deg): 39.96

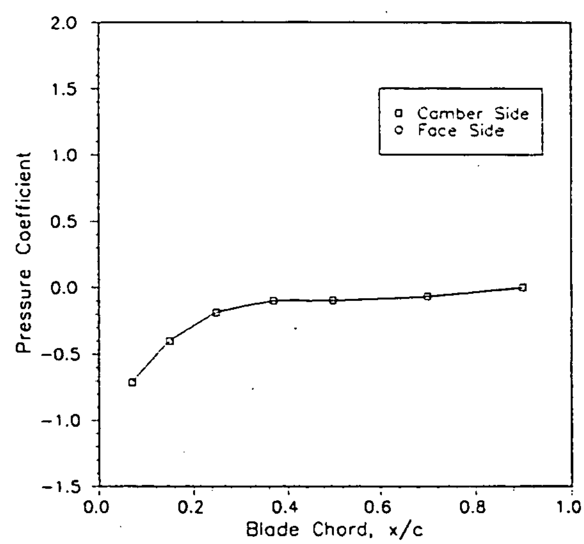

LAP/SR-7L Flight Test
Blade Surface Pressure Distribution

Record : 40
Condition : 3A
Nacelle Tilt : −1
Radial Sta : .964

Altitude (ft) : 1993.
Mach No. : 0.307
True Airspeed (fps) : 350.
Tip Speed (fps) : 704.
Power Coeff. : 1.006
Blade Angle (deg): 39.96

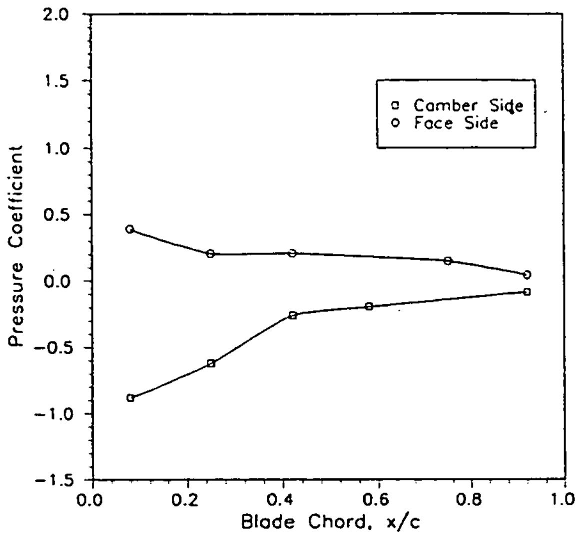

LAP/SR-7L Flight Test
Blade Surface Pressure Distribution

Record : 41
Condition : 5A
Nacelle Tilt : −1
Radial Sta : .680

Altitude (ft) : 2308.
Mach No. : 0.312
True Airspeed (fps) : 356.
Tip Speed (fps) : 703.
Power Coeff. : 1.639
Blade Angle (deg): 39.96

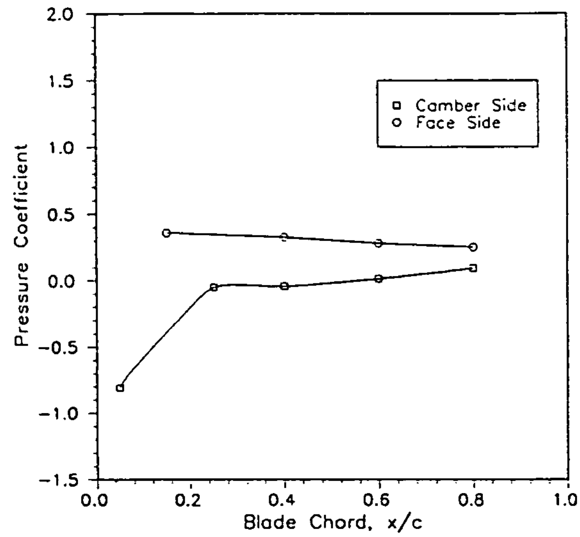

LAP/SR-7L Flight Test
Blade Surface Pressure Distribution

Record : 41
Condition : 5A
Nacelle Tilt : −1
Radial Sta : .860

Altitude (ft) : 2308.
Mach No. : 0.312
True Airspeed (fps) : 356.
Tip Speed (fps) : 703.
Power Coeff. : 1.639
Blade Angle (deg): 39.96

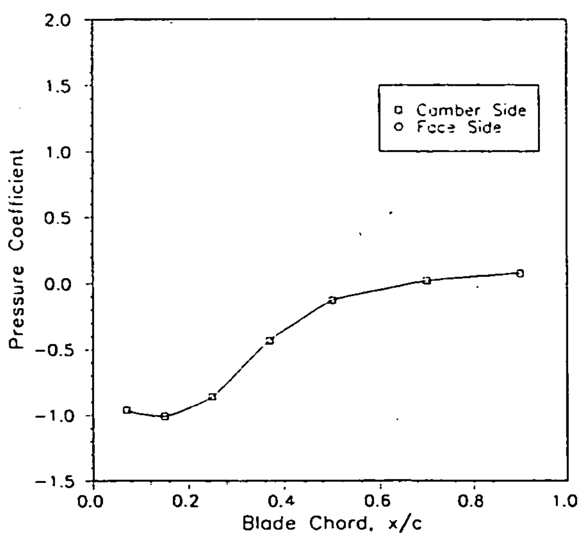

LAP/SR-7L Flight Test
Blade Surface Pressure Distribution

Record : 41
Condition : 5A
Nacelle Tilt : −1
Radial Sta : .964

Altitude (ft) : 2308.
Mach No. : 0.312
True Airspeed (fps) : 356.
Tip Speed (fps) : 703.
Power Coeff. : 1.639
Blade Angle (deg): 39.96

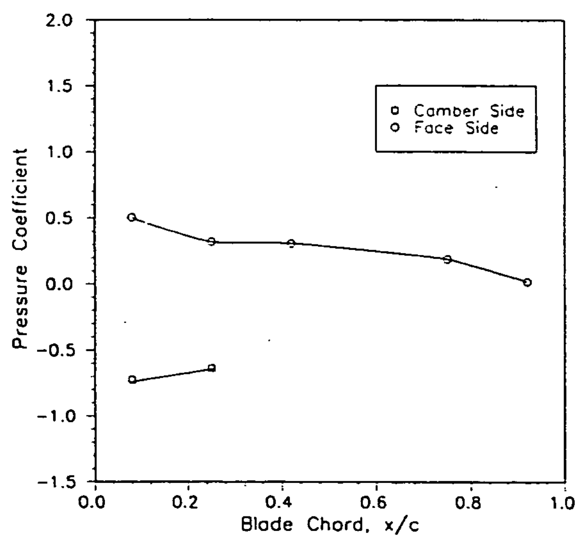

LAP/SR-7L Flight Test
Blade Surface Pressure Distribution

Record	: 43	Altitude (ft)	: 2042.
Condition	: 7A	Mach No.	: 0.316
Nacelle Tilt	: -1	True Airspeed (fps)	: 360.
Radial Sta	: .680	Tip Speed (fps)	: 797.
		Power Coeff.	: 0.691
		Blade Angle (deg)	: 39.94

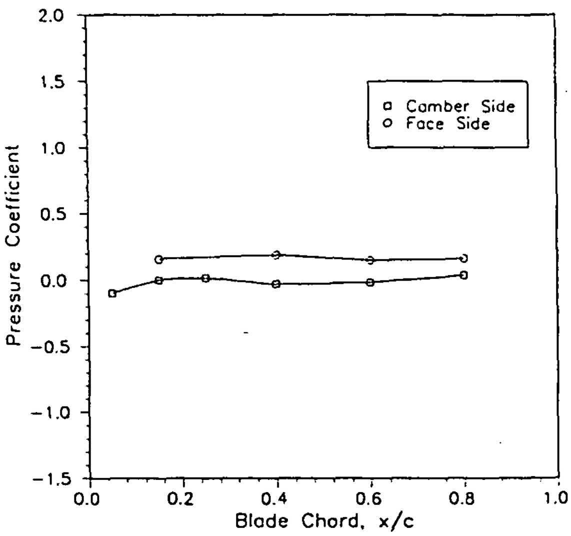

LAP/SR-7L Flight Test
Blade Surface Pressure Distribution

Record	: 43.	Altitude (ft)	: 2042.
Condition	: 7A	Mach No.	: 0.316
Nacelle Tilt	: -1	True Airspeed (fps)	: 360.
Radial Sta	: .860	Tip Speed (fps)	: 797.
		Power Coeff.	: 0.691
		Blade Angle (deg)	: 39.94

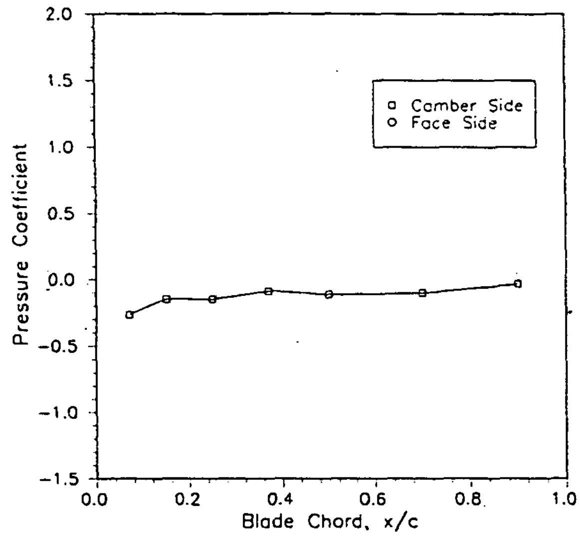

LAP/SR-7L Flight Test
Blade Surface Pressure Distribution

Record	: 43	Altitude (ft)	: 2042.
Condition	: 7A	Mach No.	: 0.316
Nacelle Tilt	: -1	True Airspeed (fps)	: 360.
Radial Sta	: .964	Tip Speed (fps)	: 797.
		Power Coeff.	: 0.691
		Blade Angle (deg)	: 39.94

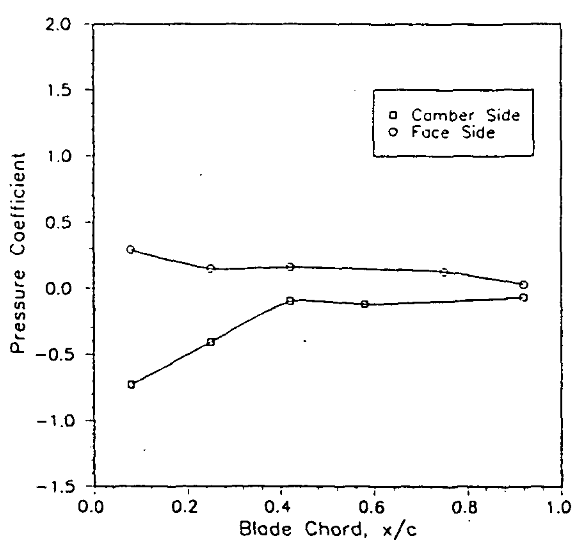

LAP/SR-7L Flight Test
Blade Surface Pressure Distribution

Record	: 44	Altitude (ft)	: 2177.
Condition	: 9A	Mach No.	: 0.308
Nacelle Tilt	: -1	True Airspeed (fps)	: 352.
Radial Sta	: .680	Tip Speed (fps)	: 790.
		Power Coeff.	: 1.122
		Blade Angle (deg)	: 39.91

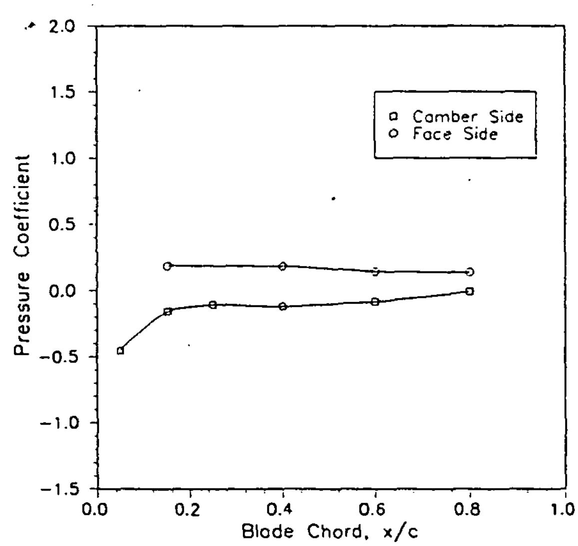

LAP/SR-7L Flight Test
Blade Surface Pressure Distribution

Record : 44
Condition : 9A
Nacelle Tilt : −1
Radial Sta : .860

Altitude (ft) : 2177.
Mach No. : 0.308
True Airspeed (fps) : 352.
Tip Speed (fps) : 790.
Power Coeff. : 1.122
Blade Angle (deg): 39.91

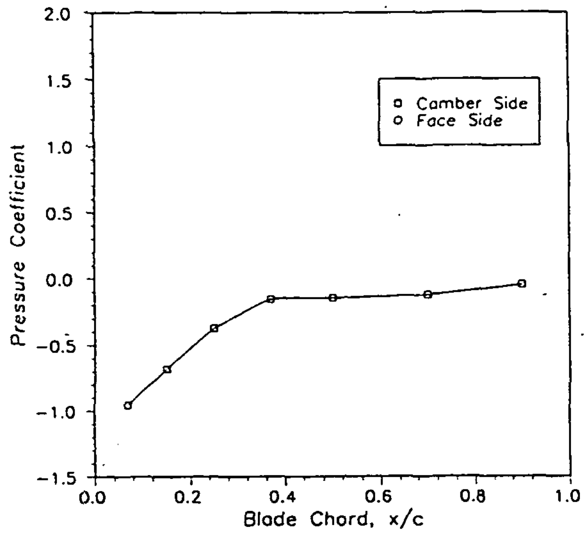

LAP/SR-7L Flight Test
Blade Surface Pressure Distribution

Record : 44
Condition : 9A
Nacelle Tilt : −1
Radial Sta : .964

Altitude (ft) : 2177.
Mach No. : 0.308
True Airspeed (fps) : 352.
Tip Speed (fps) : 790.
Power Coeff. : 1.122
Blade Angle (deg): 39.91

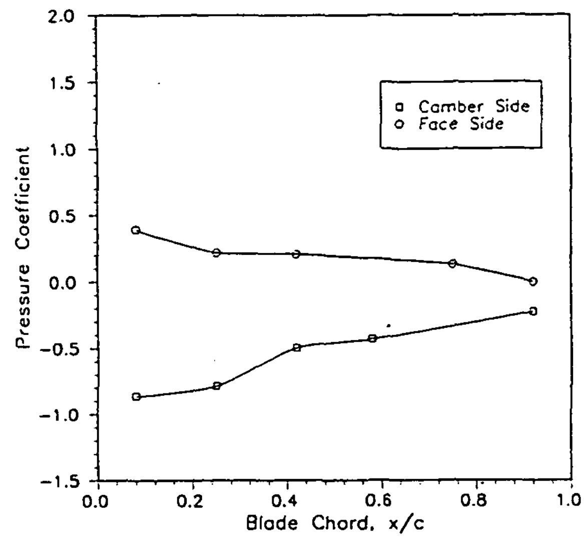

LAP/SR-7L Flight Test
Blade Surface Pressure Distribution

Record : 36
Condition : 10A
Nacelle Tilt : −1
Radial Sta : .680

Altitude (ft) : 1974.
Mach No. : 0.308
True Airspeed (fps) : 351.
Tip Speed (fps) : 622.
Power Coeff. : 0.953
Blade Angle (deg): 39.86

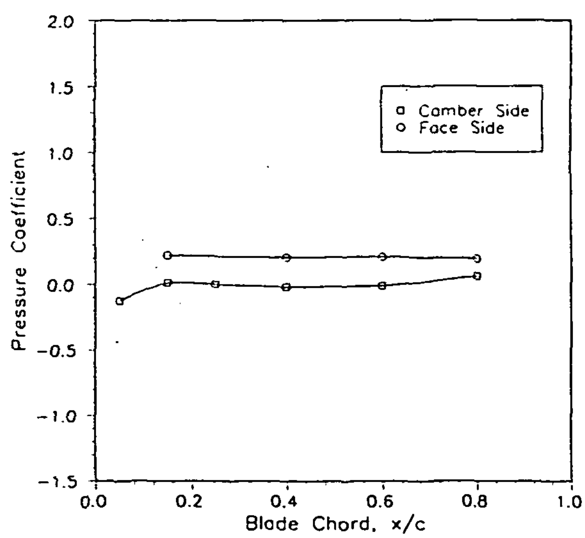

LAP/SR-7L Flight Test
Blade Surface Pressure Distribution

Record : 36
Condition : 10A
Nacelle Tilt : −1
Radial Sta : .860

Altitude (ft) : 1974.
Mach No. : 0.308
True Airspeed (fps) : 351.
Tip Speed (fps) : 622.
Power Coeff. : 0.953
Blade Angle (deg): 39.86

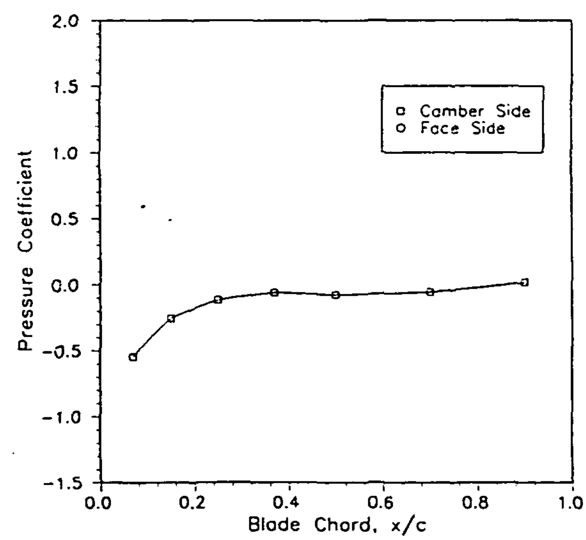

LAP/SR-7L Flight Test
Blade Surface Pressure Distribution

Record : 36
Condition : 10A
Nacelle Tilt : -1
Radial Sta : .964

Altitude (ft) : 1974.
Mach No. : 0.308
True Airspeed (fps) : 351.
Tip Speed (fps) : 622.
Power Coeff. : 0.953
Blade Angle (deg): 39.86

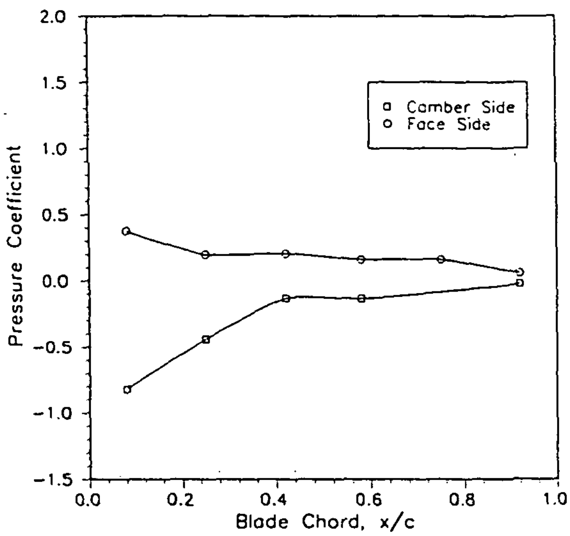

LAP/SR-7L Flight Test
Blade Surface Pressure Distribution

Record : 38
Condition : 11A
Nacelle Tilt : -1
Radial Sta : .680

Altitude (ft) : 1883.
Mach No. : 0.307
True Airspeed (fps) : 350.
Tip Speed (fps) : 623.
Power Coeff. : 1.890
Blade Angle (deg). 46.72

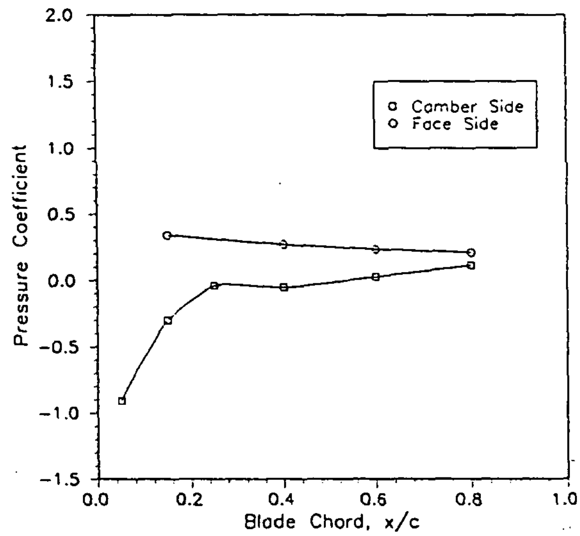

LAP/SR-7L Flight Test
Blade Surface Pressure Distribution

Record : 38
Condition : 11A
Nacelle Tilt : -1
Radial Sta : .860

Altitude (ft) : 1883.
Mach No. : 0.307
True Airspeed (fps) : 350.
Tip Speed (fps) : 623.
Power Coeff. : 1.890
Blade Angle (deg): 46.72

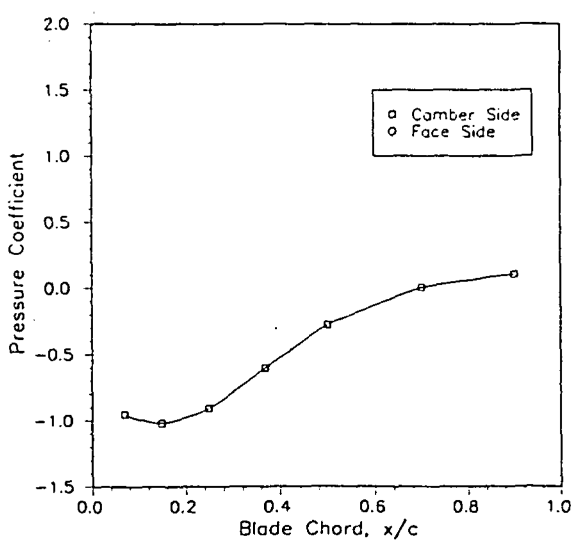

LAP/SR-7L Flight Test
Blade Surface Pressure Distribution

Record : 38
Condition : 11A
Nacelle Tilt : -1
Radial Sta : .964

Altitude (ft) : 1883.
Mach No. : 0.307
True Airspeed (fps) : 350.
Tip Speed (fps) : 623.
Power Coeff. : 1.890
Blade Angle (deg): 46.72

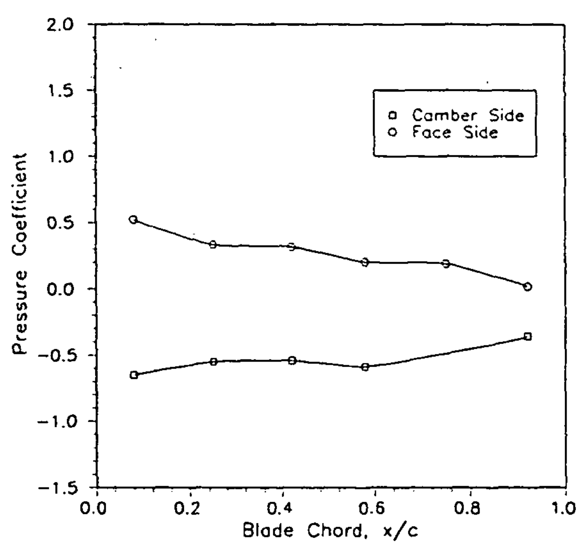

LAP/SR-7L Flight Test
Blade Surface Pressure Distribution

Record : 47
Condition : 1B
Nacelle Tilt : -1
Radial Sta : .680

Altitude (ft) : 35393.
Mach No. : 0.807
True Airspeed (fps) : 816.
Tip Speed (fps) : 623.
Power Coeff. : 0.723
Blade Angle (deg): 52.39

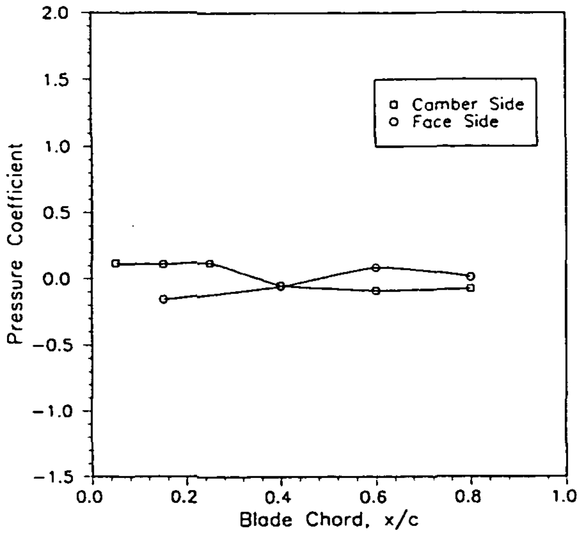

LAP/SR-7L Flight Test
Blade Surface Pressure Distribution

Record : 47
Condition : 1B
Nacelle Tilt : -1
Radial Sta : .860

Altitude (ft) : 35393.
Mach No. : 0.807
True Airspeed (fps) : 816.
Tip Speed (fps) : 623.
Power Coeff. : 0.723
Blade Angle (deg): 52.39

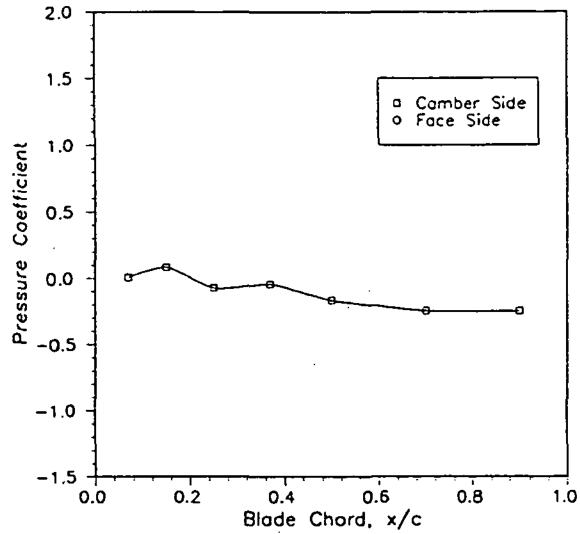

LAP/SR-7L Flight Test
Blade Surface Pressure Distribution

Record : 47
Condition : 1B
Nacelle Tilt : -1
Radial Sta : .964

Altitude (ft) : 35393.
Mach No. : 0.807
True Airspeed (fps) : 816.
Tip Speed (fps) : 623.
Power Coeff. : 0.723
Blade Angle (deg): 52.39

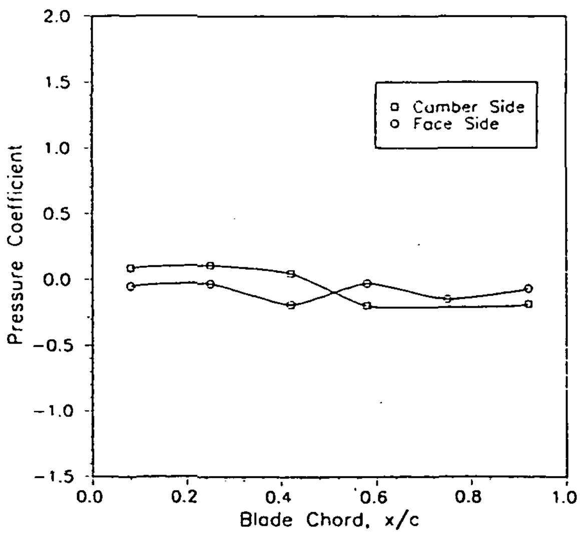

LAP/SR-7L Flight Test
Blade Surface Pressure Distribution

Record : 48
Condition : 2B
Nacelle Tilt : -1
Radial Sta : .680

Altitude (ft) : 35415.
Mach No. : 0.808
True Airspeed (fps) : 817.
Tip Speed (fps) : 623.
Power Coeff. : 1.682
Blade Angle (deg): 54.93

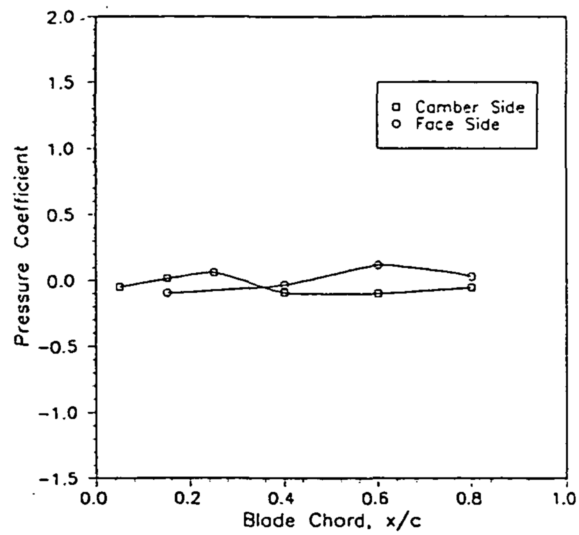

LAP/SR-7L Flight Test
Blade Surface Pressure Distribution

Record	: 48	Altitude (ft)	: 35415.
Condition	: 28	Mach No.	: 0.808
Nacelle Tilt	: −1	True Airspeed (fps)	: 817.
Radial Sta	: .860	Tip Speed (fps)	: 623.
		Power Coeff.	: 1.682
		Blade Angle (deg)	: 54.93

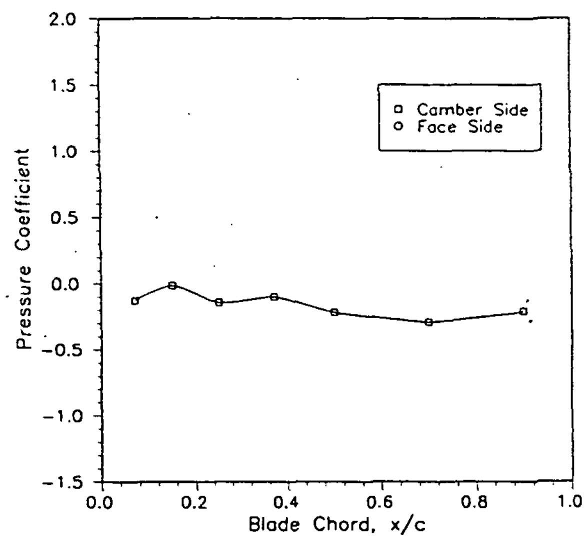

LAP/SR-7L Flight Test
Blade Surface Pressure Distribution

Record	: 48	Altitude (ft)	: 35415.
Condition	: 28	Mach No.	: 0.808
Nacelle Tilt	: −1	True Airspeed (fps)	: 817.
Radial Sta	: .964	Tip Speed (fps)	: 623.
		Power Coeff.	: 1.682
		Blade Angle (deg)	: 54.93

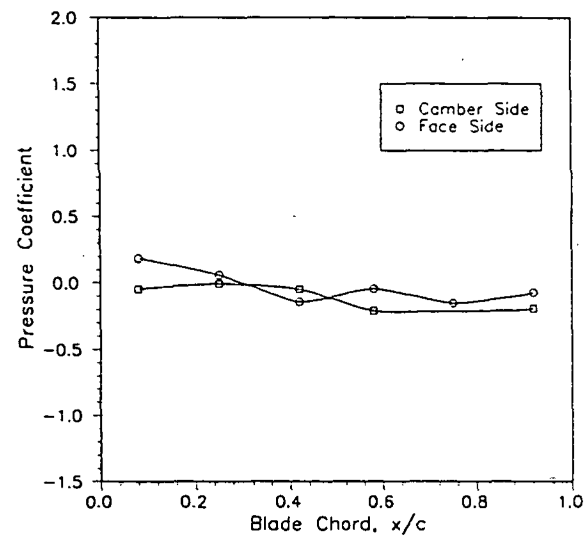

LAP/SR-7L Flight Test
Blade Surface Pressure Distribution

Record	: 49	Altitude (ft)	: 35420.
Condition	: 38	Mach No.	: 0.807
Nacelle Tilt	: −1	True Airspeed (fps)	: 815.
Radial Sta	: .680	Tip Speed (fps)	: 623.
		Power Coeff.	: 2.775
		Blade Angle (deg)	: 58.23

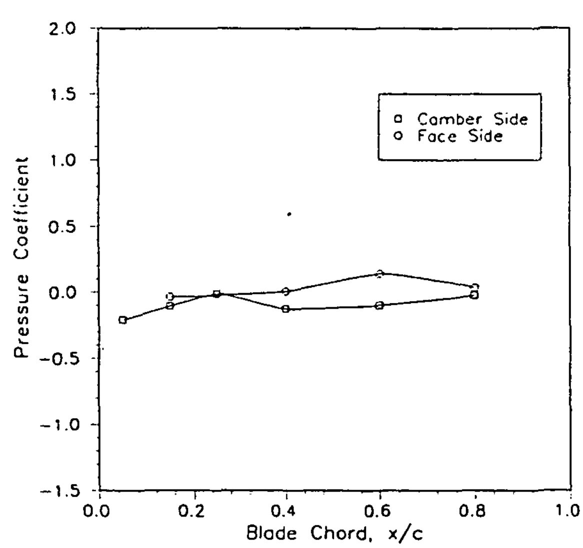

LAP/SR-7L Flight Test
Blade Surface Pressure Distribution

Record	: 49	Altitude (ft)	: 35420.
Condition	: 38	Mach No.	: 0.807
Nacelle Tilt	: −1	True Airspeed (fps)	: 815.
Radial Sta	: .860	Tip Speed (fps)	: 623.
		Power Coeff.	: 2.775
		Blade Angle (deg)	: 58.23

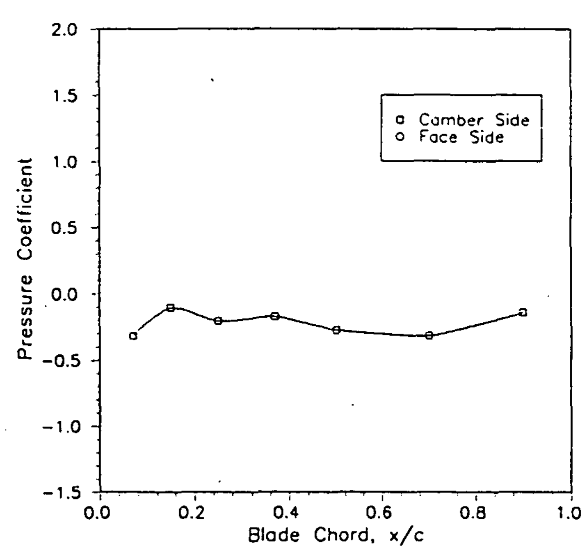

LAP/SR-7L Flight Test
Blade Surface Pressure Distribution

Record	: 49	Altitude (ft)	: 35420.
Condition	: 3B	Mach No.	: 0.807
Nacelle Tilt	: −1	True Airspeed (fps)	: 815.
Radial Sta	: .964	Tip Speed (fps)	: 623.
		Power Coeff.	: 2.775
		Blade Angle (deg)	: 58.23

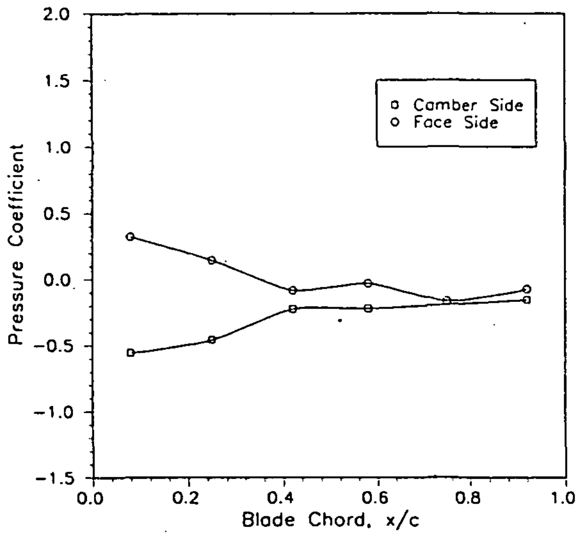

LAP/SR-7L Flight Test
Blade Surface Pressure Distribution

Record	: 50	Altitude (ft)	: 35399.
Condition	: 4B	Mach No.	: 0.809
Nacelle Tilt	: −1	True Airspeed (fps)	: 820.
Radial Sta	: .680	Tip Speed (fps)	: 624.
		Power Coeff.	: 3.134
		Blade Angle (deg)	: 59.12

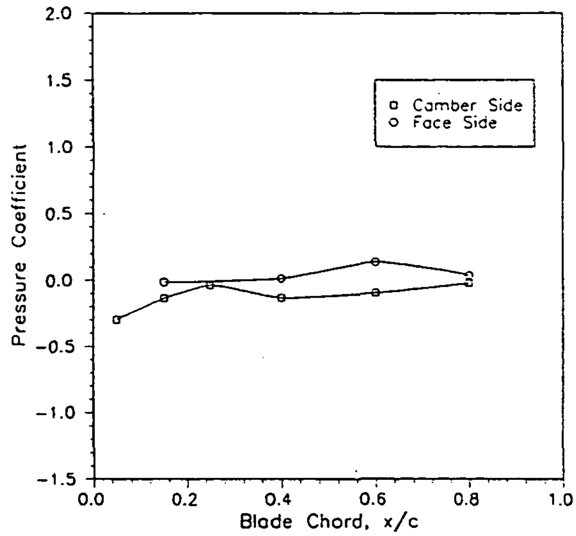

LAP/SR-7L Flight Test
Blade Surface Pressure Distribution

Record	: 50	Altitude (ft)	: 35399.
Condition	: 4B	Mach No.	: 0.809
Nacelle Tilt	: −1	True Airspeed (fps)	: 820.
Radial Sta	: .860	Tip Speed (fps)	: 624.
		Power Coeff.	: 3.134
		Blade Angle (deg)	: 59.12

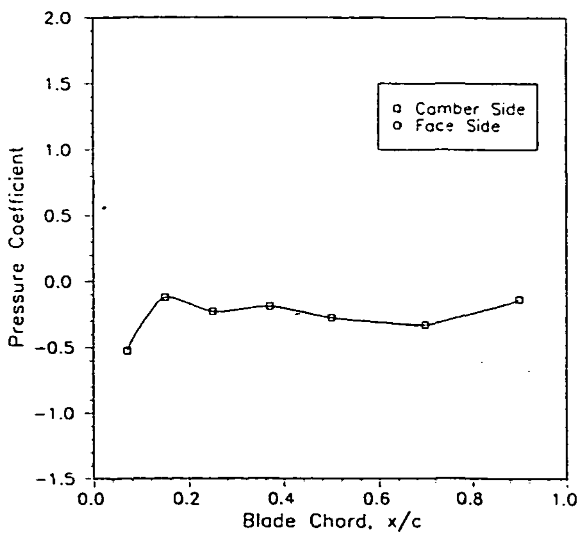

LAP/SR-7L Flight Test
Blade Surface Pressure Distribution

Record	: 50	Altitude (ft)	: 35399.
Condition	: 4B	Mach No.	: 0.809
Nacelle Tilt	: −1	True Airspeed (fps)	: 820.
Radial Sta	: .964	Tip Speed (fps)	: 624.
		Power Coeff.	: 3.134
		Blade Angle (deg)	: 59.12

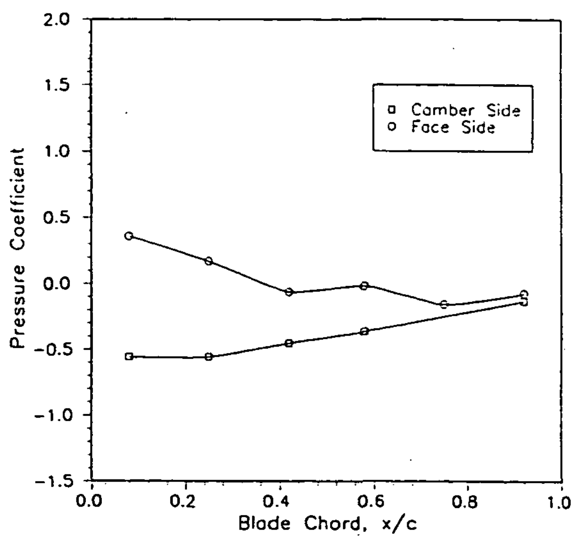

LAP/SR-7L Flight Test
Blade Surface Pressure Distribution

Record	: 51	Altitude (ft)	: 35411.
Condition	: 11B	Mach No.	: 0.816
Nacelle Tilt	: −1	True Airspeed (fps)	: 827.
Radial Sta	: .680	Tip Speed (fps)	: 696.
		Power Coeff.	: 0.589
		Blade Angle (deg)	: 56.99

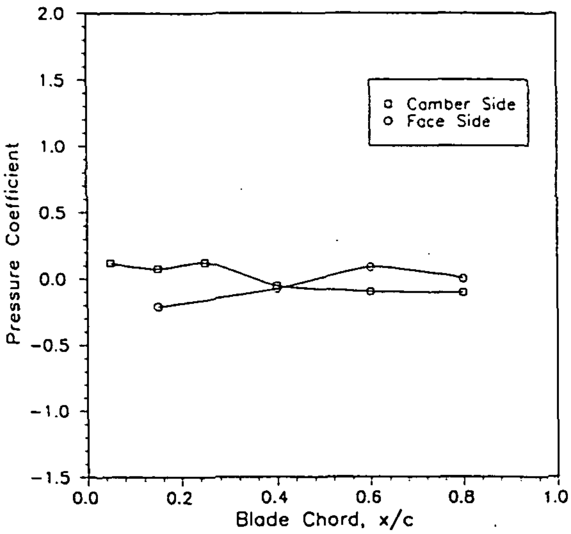

LAP/SR-7L Flight Test
Blade Surface Pressure Distribution

Record	: 51	Altitude (ft)	: 35411.
Condition	: 11B	Mach No.	: 0.816
Nacelle Tilt	: −1	True Airspeed (fps)	: 827.
Radial Sta	: .860	Tip Speed (fps)	: 696.
		Power Coeff.	: 0.589
		Blade Angle (deg)	: 56.99

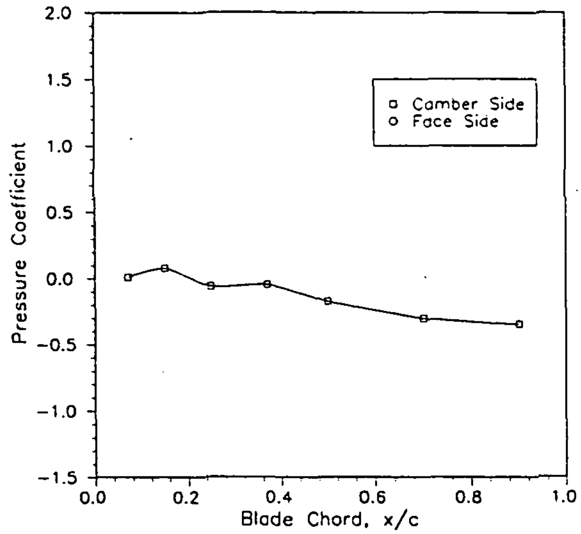

LAP/SR-7L Flight Test
Blade Surface Pressure Distribution

Record	: 51	Altitude (ft)	: 35411.
Condition	: 11B	Mach No.	: 0.816
Nacelle Tilt	: −1	True Airspeed (fps)	: 827.
Radial Sta	: .964	Tip Speed (fps)	: 696.
		Power Coeff.	: 0.589
		Blade Angle (deg)	: 56.99

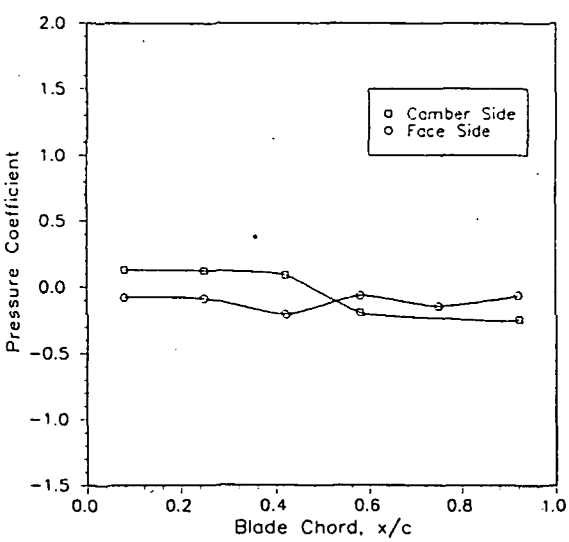

LAP/SR-7L Flight Test
Blade Surface Pressure Distribution

Record	: 52	Altitude (ft)	: 35396.
Condition	: 12B	Mach No.	: 0.806
Nacelle Tilt	: −1	True Airspeed (fps)	: 817.
Radial Sta	: .680	Tip Speed (fps)	: 698.
		Power Coeff.	: 1.326
		Blade Angle (deg)	: 57.00

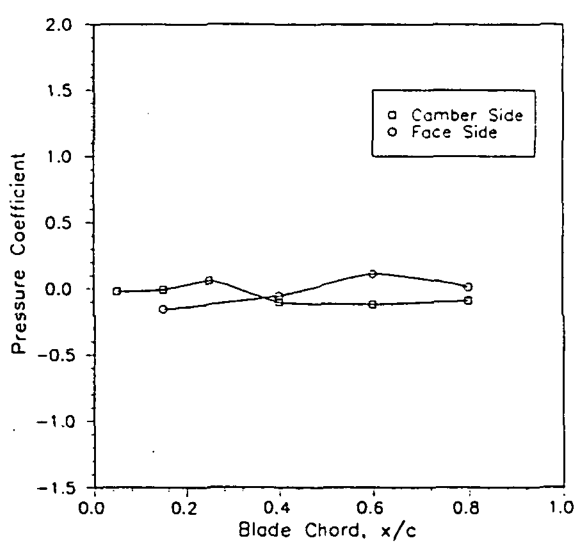

LAP/SR-7L Flight Test
Blade Surface Pressure Distribution

Record : 52
Condition : 128
Nacelle Tilt : −1
Radial Sta : .860

Altitude (ft) : 35396.
Mach No. : 0.806
True Airspeed (fps) : 817.
Tip Speed (fps) : 698.
Power Coeff. : 1.326
Blade Angle (deg): 57.00

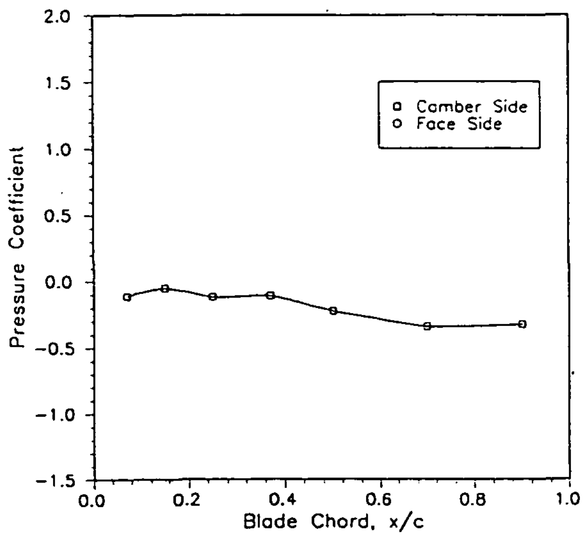

LAP/SR-7L Flight Test
Blade Surface Pressure Distribution

Record : 52
Condition : 128
Nacelle Tilt : −1
Radial Sta : .964

Altitude (ft) : 35396.
Mach No. : 0.806
True Airspeed (fps) : 817.
Tip Speed (fps) : 698.
Power Coeff. : 1.326
Blade Angle (deg): 57.00

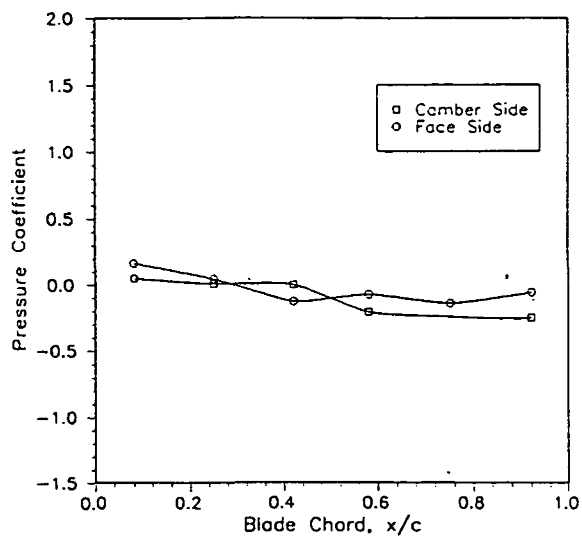

LAP/SR-7L Flight Test
Blade Surface Pressure Distribution

Record : 53
Condition : 138
Nacelle Tilt : −1
Radial Sta : .680

Altitude (ft) : 35383.
Mach No. : 0.806
True Airspeed (fps) : 816.
Tip Speed (fps) : 701.
Power Coeff. : 2.057
Blade Angle (deg): 57.03

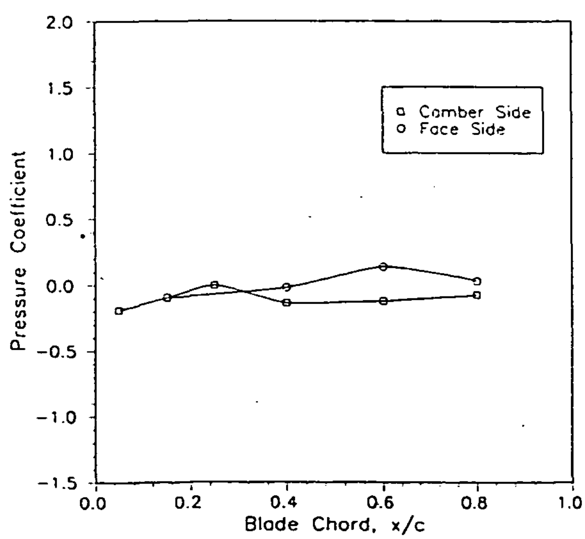

LAP/SR-7L Flight Test
Blade Surface Pressure Distribution

Record : 53
Condition : 138
Nacelle Tilt : −1
Radial Sta : .860

Altitude (ft) : 35383.
Mach No. : 0.806
True Airspeed (fps) : 816.
Tip Speed (fps) : 701.
Power Coeff. : 2.057
Blade Angle (deg): 57.03

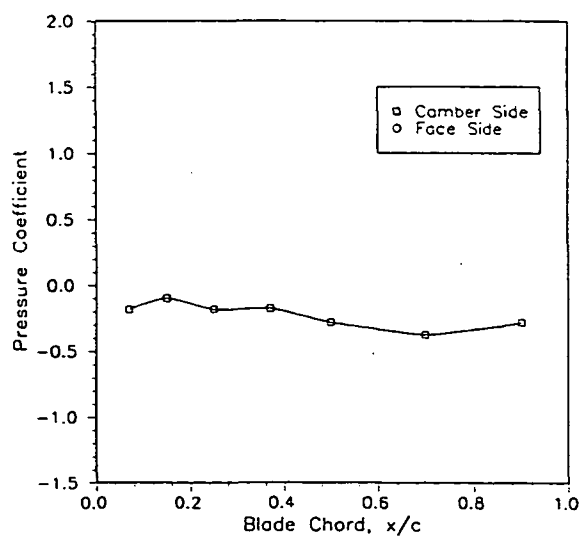

LAP/SR-7L Flight Test
Blade Surface Pressure Distribution

Record : 53
Condition : 13B
Nacelle Tilt : -1
Radial Sta : .964

Altitude (ft) : 35383.
Mach No. : 0.806
True Airspeed (fps) : 816.
Tip Speed (fps) : 701.
Power Coeff. : 2.057
Blade Angle (deg): 57.03

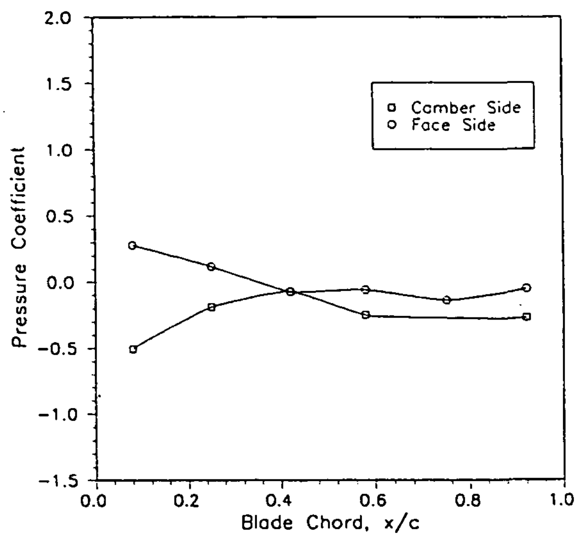

LAP/SR-7L Flight Test
Blade Surface Pressure Distribution

Record : 54
Condition : 14B
Nacelle Tilt : -1
Radial Sta : .680

Altitude (ft) : 35399.
Mach No. : 0.810
True Airspeed (fps) : 818.
Tip Speed (fps) : 702.
Power Coeff. : 2.395
Blade Angle (deg): 56.99

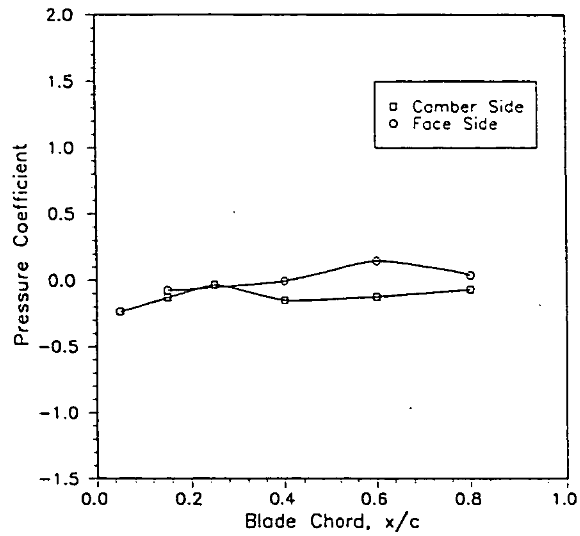

LAP/SR-7L Flight Test
Blade Surface Pressure Distribution

Record : 54
Condition : 14B
Nacelle Tilt : -1
Radial Sta : .860

Altitude (ft) : 35399.
Mach No. : 0.810
True Airspeed (fps) : 818.
Tip Speed (fps) : 702.
Power Coeff. : 2.395
Blade Angle (deg): 56.99

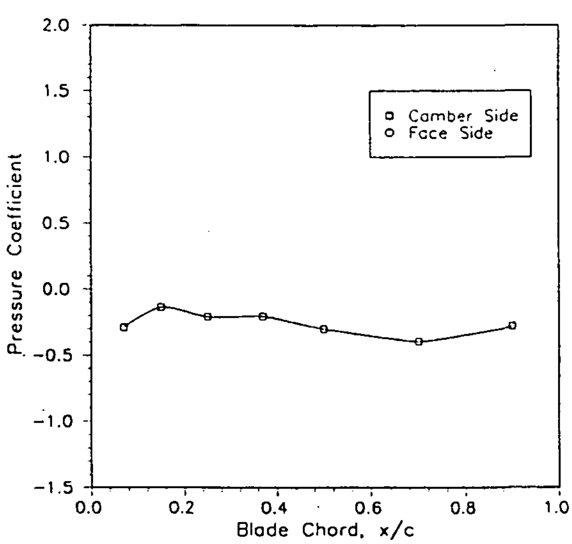

LAP/SR-7L Flight Test
Blade Surface Pressure Distribution

Record : 54
Condition : 14B
Nacelle Tilt : -1
Radial Sta : .964

Altitude (ft) : 35399.
Mach No. : 0.810
True Airspeed (fps) : 818.
Tip Speed (fps) : 702.
Power Coeff. : 2.395
Blade Angle (deg): 56.99

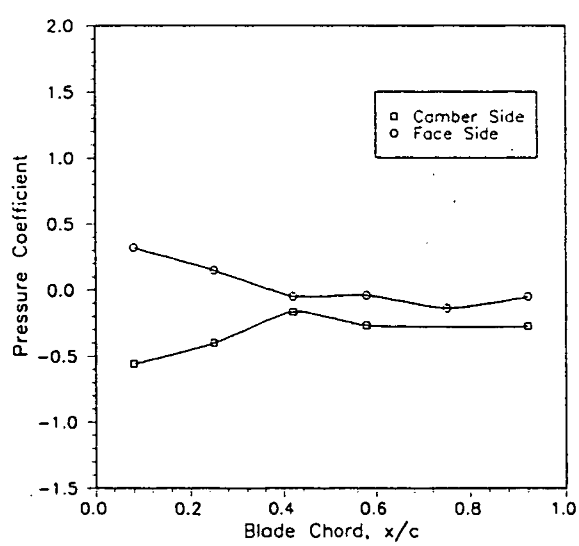

LAP/SR-7L Flight Test
Blade Surface Pressure Distribution

Record : 56
Condition : 22B
Nacelle Tilt : −1
Radial Sta : .680

Altitude (ft) : 35436.
Mach No. : 0.814
True Airspeed (fps) : 822.
Tip Speed (fps) : 798.
Power Coeff. : 0.935
Blade Angle (deg): 56.97

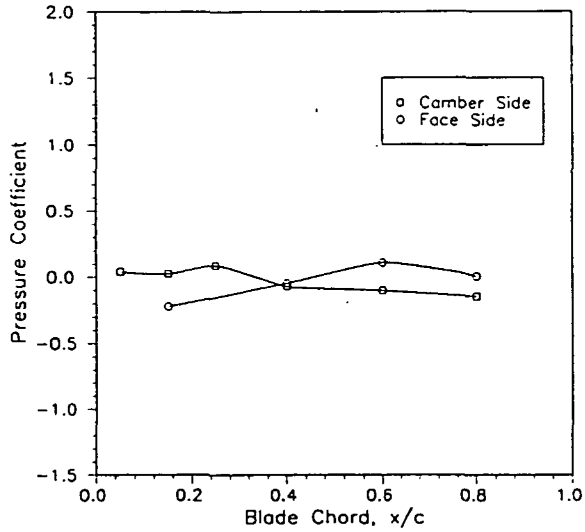

LAP/SR-7L Flight Test
Blade Surface Pressure Distribution

Record : 56
Condition : 22B
Nacelle Tilt : −1
Radial Sta : .860

Altitude (ft) : 35436.
Mach No. : 0.814
True Airspeed (fps) : 822.
Tip Speed (fps) : 798.
Power Coeff. : 0.935
Blade Angle (deg): 56.97

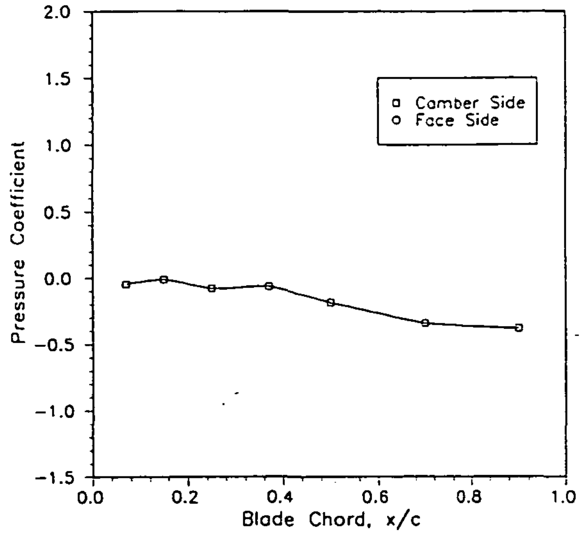

LAP/SR-7L Flight Test
Blade Surface Pressure Distribution

Record : 56
Condition : 22B
Nacelle Tilt : −1
Radial Sta : .964

Altitude (ft) : 35436.
Mach No. : 0.814
True Airspeed (fps) : 822.
Tip Speed (fps) : 798.
Power Coeff. : 0.935
Blade Angle (deg): 56.97

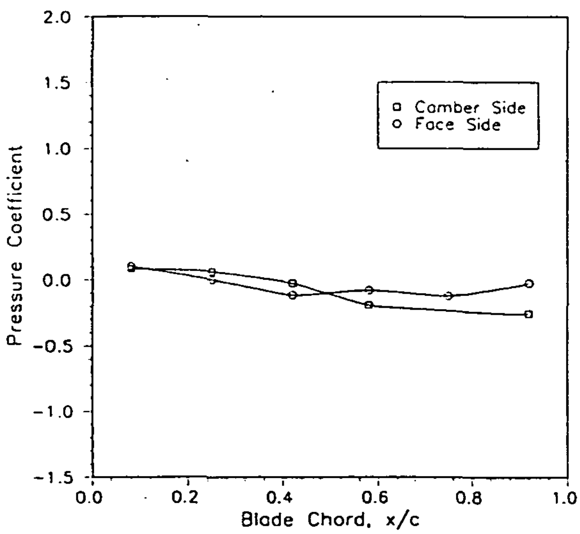

LAP/SR-7L Flight Test
Blade Surface Pressure Distribution

Record : 57
Condition : 23B
Nacelle Tilt : −1
Radial Sta : .680

Altitude (ft) : 35408.
Mach No. : 0.810
True Airspeed (fps) : 819.
Tip Speed (fps) : 799.
Power Coeff. : 1.496
Blade Angle (deg): 56.97

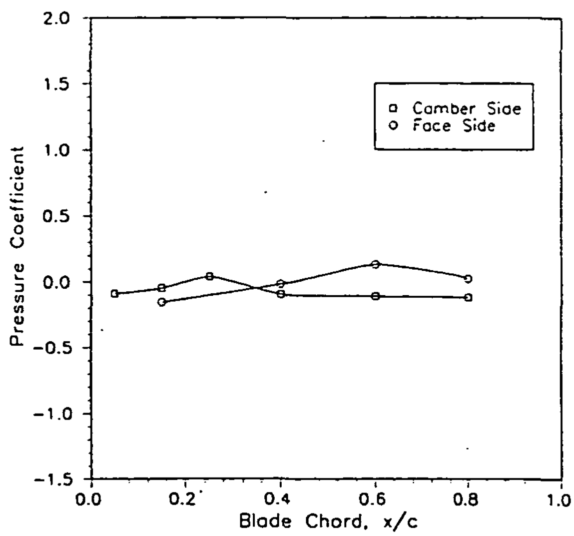

LAP/SR-7L Flight Test
Blade Surface Pressure Distribution

Record : 57
Condition : 23B
Nacelle Tilt : −1
Radial Sta : .860

Altitude (ft) : 35408.
Mach No. : 0.810
True Airspeed (fps) : 819.
Tip Speed (fps) : 799.
Power Coeff. : 1.496
Blade Angle (deg): 56.97

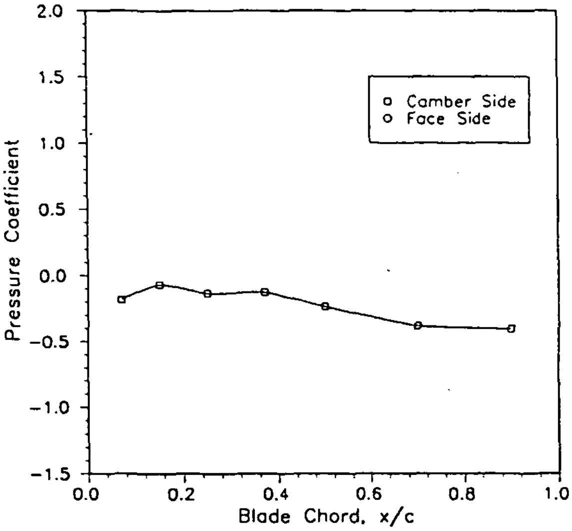

LAP/SR-7L Flight Test
Blade Surface Pressure Distribution

Record : 57
Condition : 23B
Nacelle Tilt : −1
Radial Sta : .964

Altitude (ft) : 35408.
Mach No. : 0.810
True Airspeed (fps) : 819.
Tip Speed (fps) : 799.
Power Coeff. : 1.496
Blade Angle (deg): 56.97

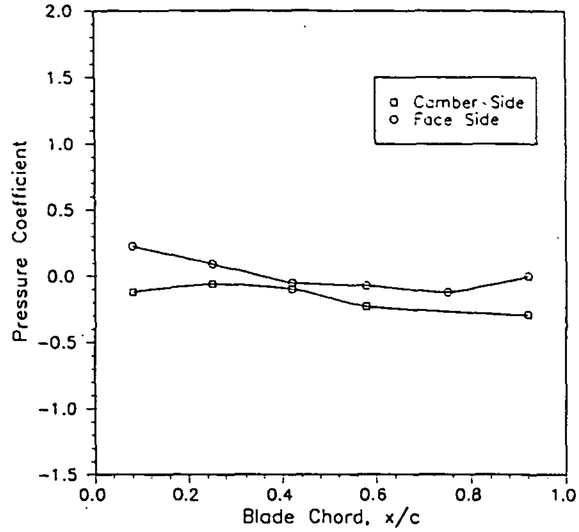

LAP/SR-7L Flight Test
Blade Surface Pressure Distribution

Record : 58
Condition : 24B
Nacelle Tilt : −1
Radial Sta : .680

Altitude (ft) : 35419.
Mach No. : 0.812
True Airspeed (fps) : 819.
Tip Speed (fps) : 800.
Power Coeff. : 1.734
Blade Angle (deg): 56.97

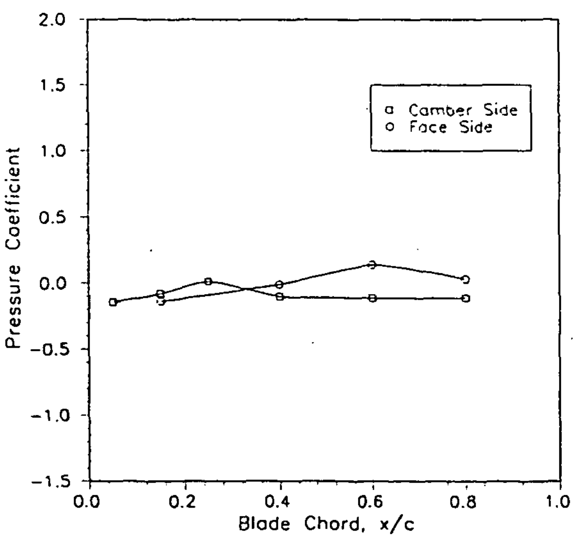

LAP/SR-7L Flight Test
Blade Surface Pressure Distribution

Record : 58
Condition : 24B
Nacelle Tilt : −1
Radial Sta : .860

Altitude (ft) : 35419.
Mach No. : 0.812
True Airspeed (fps) : 819.
Tip Speed (fps) : 800.
Power Coeff. : 1.734
Blade Angle (deg): 56.97

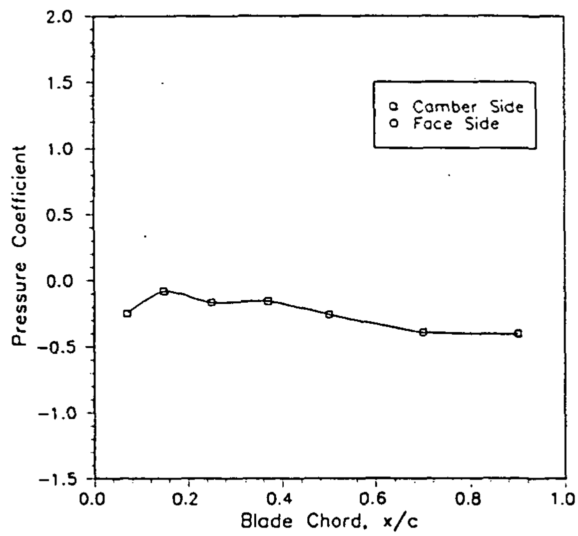

LAP/SR-7L Flight Test
Blade Surface Pressure Distribution

Record : 58
Condition : 24B
Nacelle Tilt : -1
Radial Sta : .964

Altitude (ft) : 35419.
Mach No. : 0.812
True Airspeed (fps) : 819.
Tip Speed (fps) : 800.
Power Coeff. : 1.734
Blade Angle (deg): 56.97

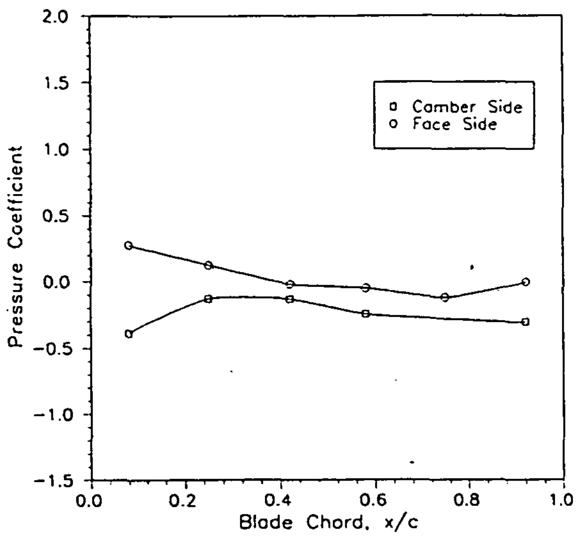

LAP/SR-7L Flight Test
Blade Surface Pressure Distribution

Record : 61
Condition : 1C
Nacelle Tilt : -1
Radial Sta : .860

Altitude (ft) : 23338.
Mach No. : 0.603
True Airspeed (fps) : 636.
Tip Speed (fps) : 634.
Power Coeff. : 1.520
Blade Angle (deg): 56.16

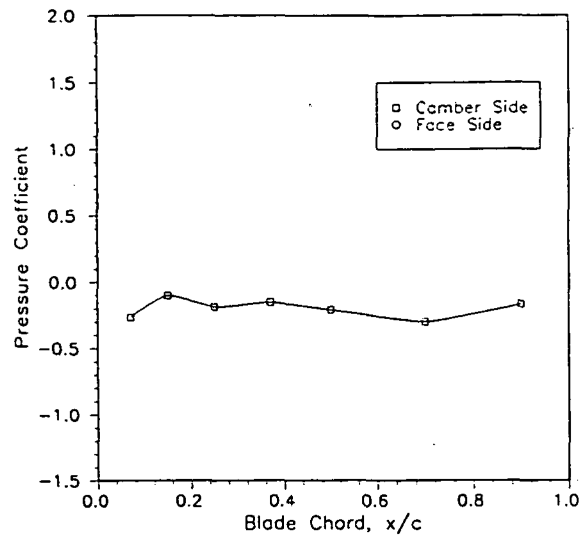

LAP/SR-7L Flight Test
Blade Surface Pressure Distribution

Record : 61
Condition : 1C
Nacelle Tilt : -1
Radial Sta : .964

Altitude (ft) : 23338.
Mach No. : 0.603
True Airspeed (fps) : 636.
Tip Speed (fps) : 634.
Power Coeff. : 1.520
Blade Angle (deg): 56.16

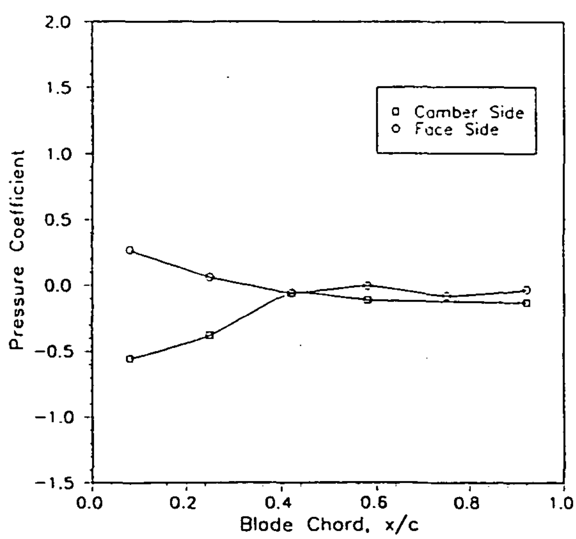

LAP/SR-7L Flight Test
Blade Surface Pressure Distribution

Record : 61
Condition : 1C
Nacelle Tilt : -1
Radial Sta : .680

Altitude (ft) : 23338.
Mach No. : 0.603
True Airspeed (fps) : 636.
Tip Speed (fps) : 634.
Power Coeff. : 1.520
Blade Angle (deg): 56.16

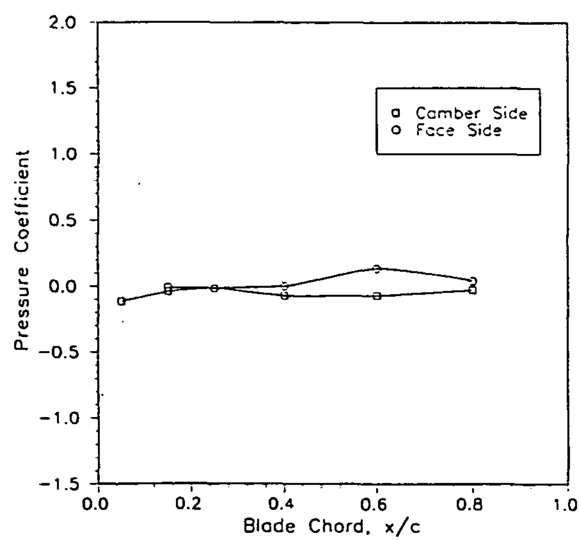

LAP/SR-7L Flight Test
Blade Surface Pressure Distribution

Record : 60
Condition : 2C
Nacelle Tilt : -1
Radial Sta : .680

Altitude (ft) : 31357.
Mach No. : 0.696
True Airspeed (fps) : 716.
Tip Speed (fps) : 713.
Power Coeff. : 1.521
Blade Angle (deg): 56.95

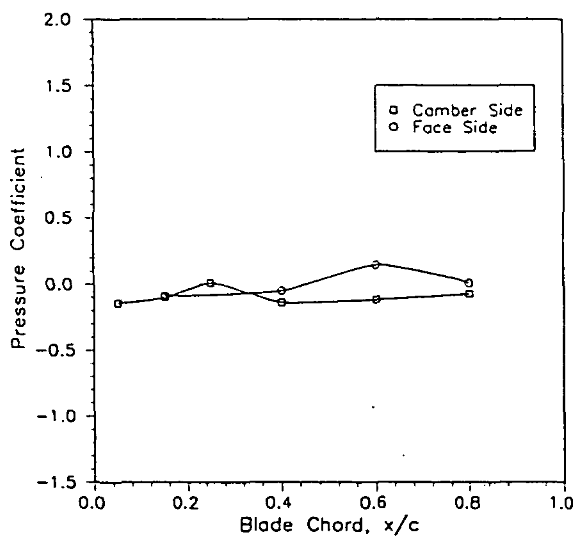

LAP/SR-7L Flight Test
Blade Surface Pressure Distribution

Record : 60
Condition : 2C
Nacelle Tilt : -1
Radial Sta : .860

Altitude (ft) : 31357.
Mach No. : 0.696
True Airspeed (fps) : 716.
Tip Speed (fps) : 713.
Power Coeff. : 1.521
Blade Angle (deg): 56.95

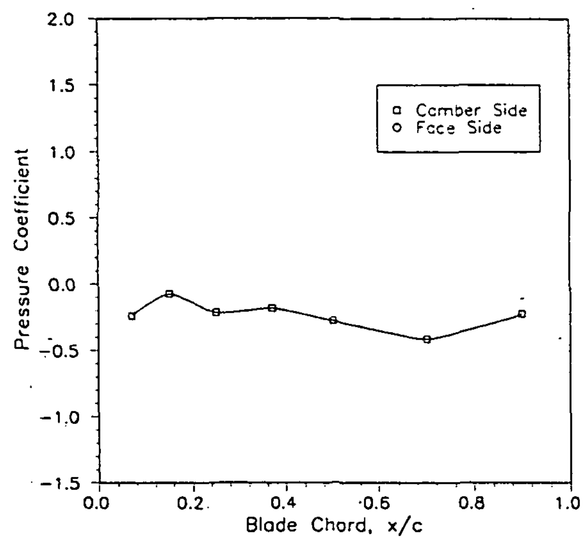

LAP/SR-7L Flight Test
Blade Surface Pressure Distribution

Record : 60
Condition : 2C
Nacelle Tilt : -1
Radial Sta : .964

Altitude (ft) : 31357.
Mach No. : 0.696
True Airspeed (fps) : 716.
Tip Speed (fps) : 713.
Power Coeff. : 1.521
Blade Angle (deg): 56.95

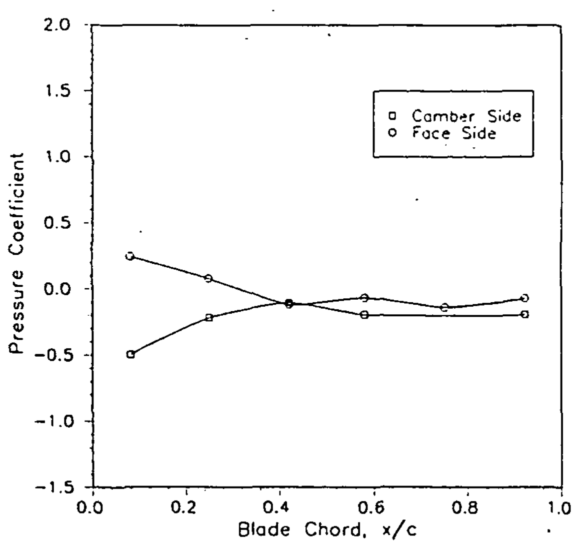

LAP/SR-7L Flight Test
Blade Surface Pressure Distribution

Record : 59
Condition : 3C
Nacelle Tilt : -1
Radial Sta : .680

Altitude (ft) : 38472.
Mach No. : 0.811
True Airspeed (fps) : 814.
Tip Speed (fps) : 798.
Power Coeff. : 1.600
Blade Angle (deg): 56.97

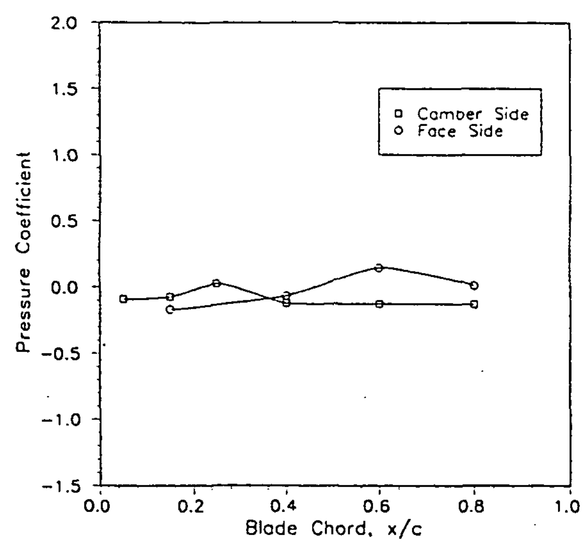

LAP/SR-7L Flight Test
Blade Surface Pressure Distribution

Record	: 59	Altitude (ft)	: 38472.
Condition	: 3C	Mach No.	: 0.811
Nacelle Tilt	: −1	True Airspeed (fps)	: 814.
Radial Sta	: .860	Tip Speed (fps)	: 798.
		Power Coeff.	: 1.600
		Blade Angle (deg)	: 56.97

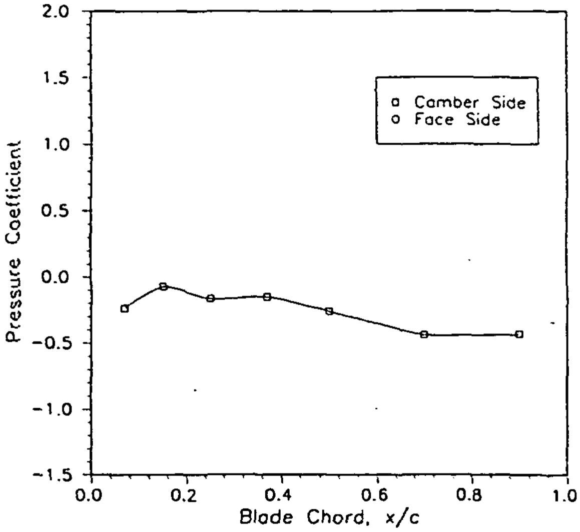

LAP/SR-7L Flight Test
Blade Surface Pressure Distribution

Record	: 59	Altitude (ft)	: 38472.
Condition	: 3C	Mach No.	: 0.811
Nacelle Tilt	: −1	True Airspeed (fps)	: 814.
Radial Sta	: .964	Tip Speed (fps)	: 798.
		Power Coeff.	: 1.600
		Blade Angle (deg)	: 56.97

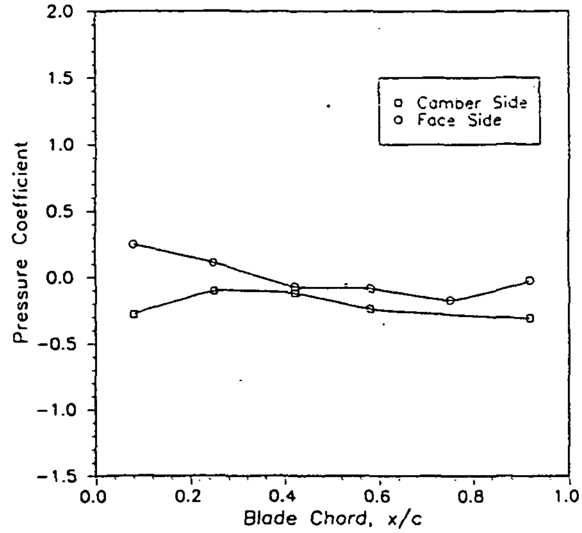

APPENDIX D2

+2 DEGREE STEADY PRESSURE
DISTRIBUTION PLOTS

LAP/SR-7L Flight Test
Blade Surface Pressure Distribution

Record	: 109	Altitude (ft)	: 1993.
Condition	: 1A	Mach No.	: 0.310
Nacelle Tilt	: 2	True Airspeed (fps)	: 357.
Radial Sta	: .680	Tip Speed (fps)	: 622.
		Power Coeff.	: 1.536
		Blade Angle (deg)	: 43.98

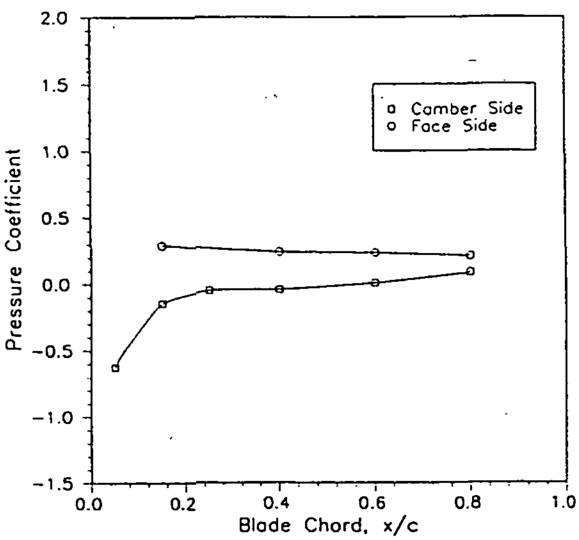

LAP/SR-7L Flight Test
Blade Surface Pressure Distribution

Record	: 109	Altitude (ft)	: 1993.
Condition	: 1A	Mach No.	: 0.310
Nacelle Tilt	: 2	True Airspeed (fps)	: 357.
Radial Sta	: .860	Tip Speed (fps)	: 622.
		Power Coeff.	: 1.536
		Blade Angle (deg)	: 43.98

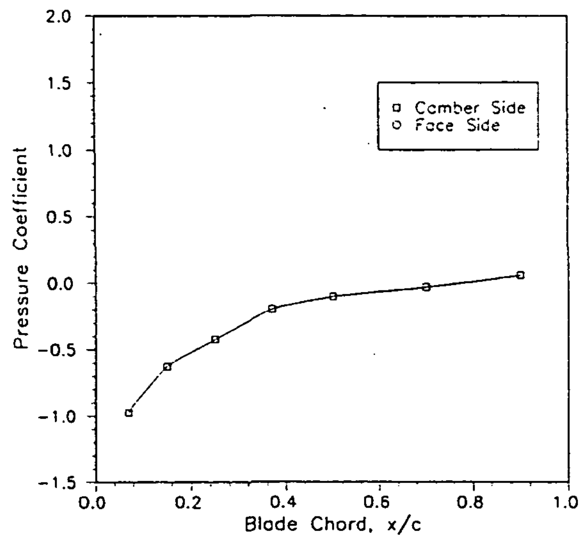

LAP/SR-7L Flight Test
Blade Surface Pressure Distribution

Record	: 109	Altitude (ft)	: 1993.
Condition	: 1A	Mach No.	: 0.310
Nacelle Tilt	: 2	True Airspeed (fps)	: 357.
Radial Sta	: .964	Tip Speed (fps)	: 622.
		Power Coeff.	: 1.536
		Blade Angle (deg)	: 43.98

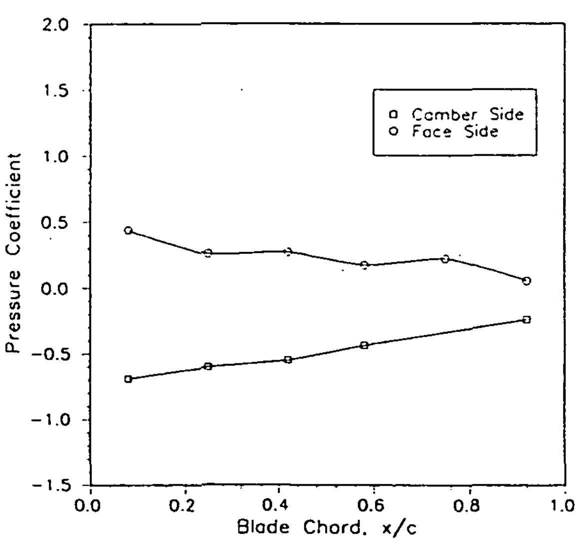

LAP/SR-7L Flight Test
Blade Surface Pressure Distribution

Record	: 111	Altitude (ft)	: 2054.
Condition	: 2A	Mach No.	: 0.311
Nacelle Tilt	: 2	True Airspeed (fps)	: 359.
Radial Sta	: .680	Tip Speed (fps)	: 622.
		Power Coeff.	: 2.116
		Blade Angle (deg)	: 48.51

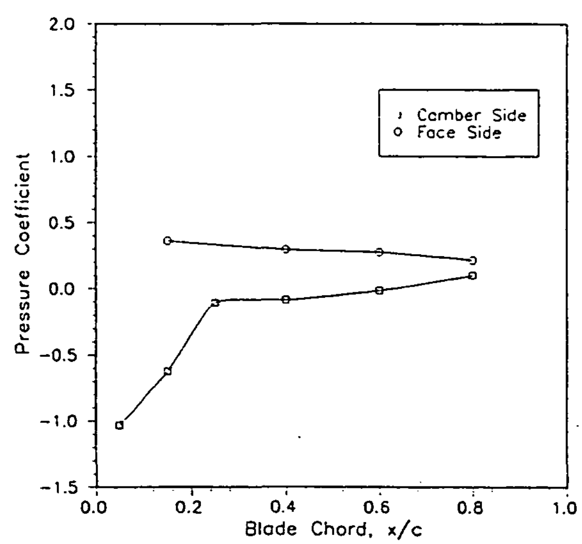

LAP/SR-7L Flight Test
Blade Surface Pressure Distribution

Record	: 111	Altitude (ft)	: 2054.
Condition	: 2A	Mach No.	: 0.311
Nacelle Tilt	: 2	True Airspeed (fps)	: 359.
Radial Sta	: .860	Tip Speed (fps)	: 622.
		Power Coeff.	: 2.116
		Blade Angle (deg)	: 48.51

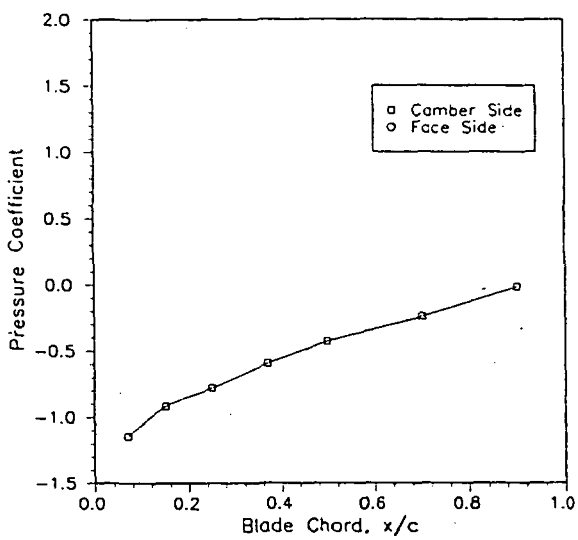

LAP/SR-7L Flight Test
Blade Surface Pressure Distribution

Record	: 111	Altitude (ft)	: 2054.
Condition	: 2A	Mach No.	: 0.311
Nacelle Tilt	: 2	True Airspeed (fps)	: 359.
Radial Sta	: .964	Tip Speed (fps)	: 622.
		Power Coeff.	: 2.116
		Blade Angle (deg)	: 48.51

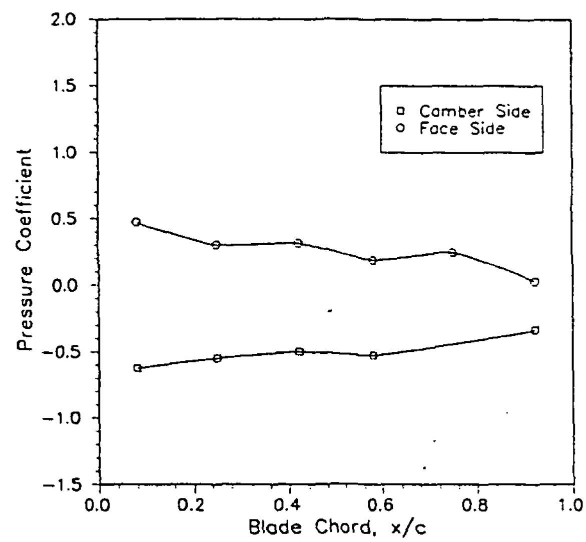

LAP/SR-7L Flight Test
Blade Surface Pressure Distribution

Record	: 113	Altitude (ft)	: 2011.
Condition	: 3A	Mach No.	: 0.313
Nacelle Tilt	: 2	True Airspeed (fps)	: 361.
Radial Sta	: .680	Tip Speed (fps)	: 704.
		Power Coeff.	: 1.034
		Blade Angle (deg)	: 40.11

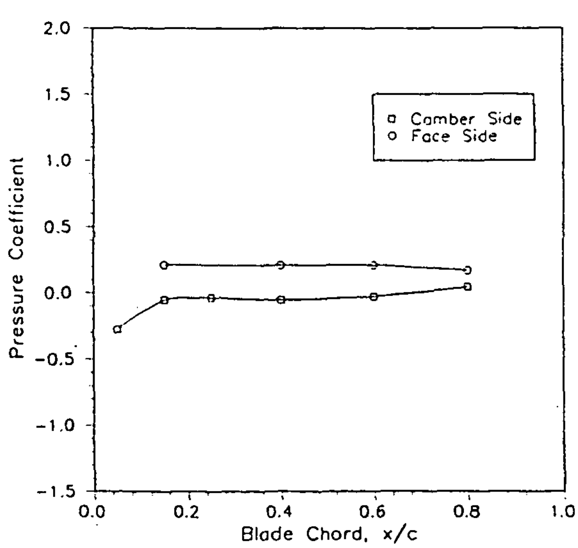

LAP/SR-7L Flight Test
Blade Surface Pressure Distribution

Record	: 113	Altitude (ft)	: 2011.
Condition	: 3A	Mach No.	: 0.313
Nacelle Tilt	: 2	True Airspeed (fps)	: 361.
Radial Sta	: .860	Tip Speed (fps)	: 704.
		Power Coeff.	: 1.034
		Blade Angle (deg)	: 40.11

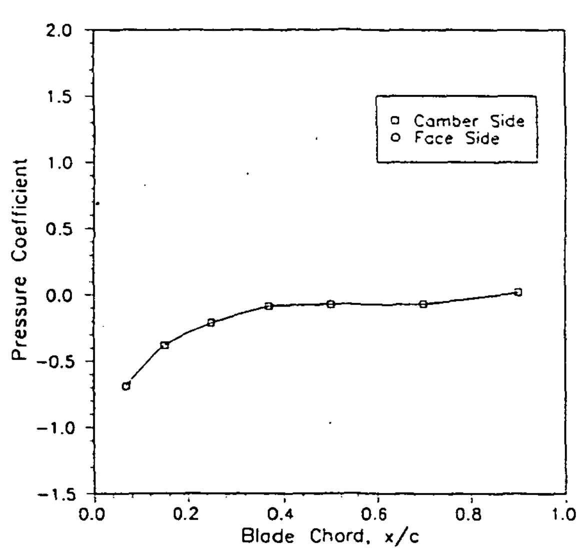

LAP/SR-7L Flight Test
Blade Surface Pressure Distribution

Record	: 113	Altitude (ft)	: 2011.
Condition	: 3A	Mach No.	: 0.313
Nacelle Tilt	: 2	True Airspeed (fps)	: 361.
Radial Sta	: .964	Tip Speed (fps)	: 704.
		Power Coeff.	: 1.034
		Blade Angle (deg)	: 40.11

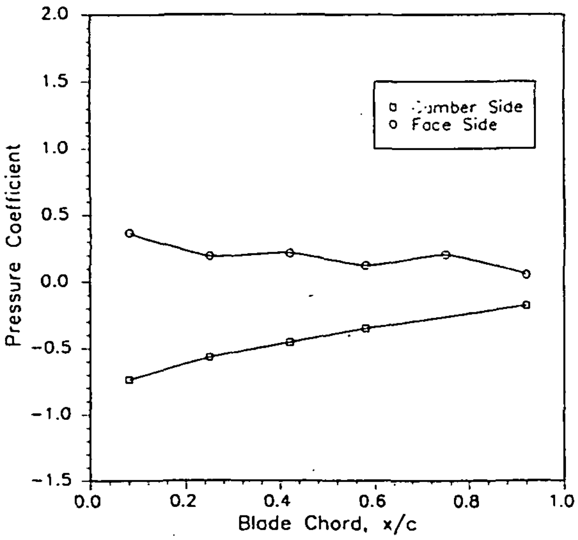

LAP/SR-7L Flight Test
Blade Surface Pressure Distribution

Record	: 114	Altitude (ft)	: 2055.
Condition	: 5A	Mach No.	: 0.315
Nacelle Tilt	: 2	True Airspeed (fps)	: 363.
Radial Sta	: .680	Tip Speed (fps)	: 704.
		Power Coeff.	: 1.508
		Blade Angle (deg)	: 40.11

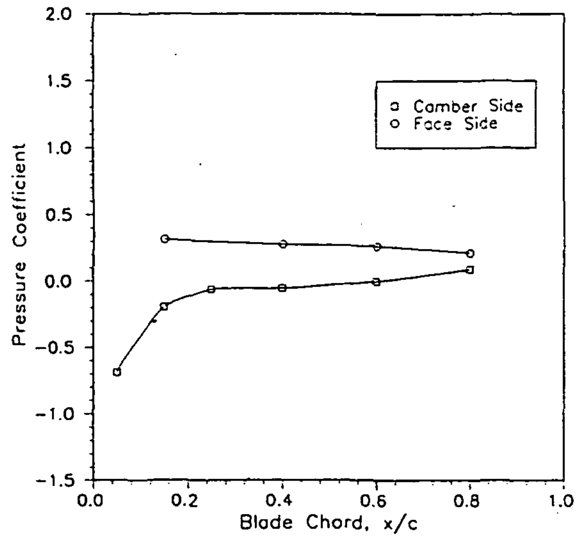

LAP/SR-7L Flight Test
Blade Surface Pressure Distribution

Record	: 114	Altitude (ft)	: 2055.
Condition	: 5A.	Mach No.	: 0.315
Nacelle Tilt	: 2	True Airspeed (fps)	: 363.
Radial Sta	: .860	Tip Speed (fps)	: 704.
		Power Coeff.	: 1.508
		Blade Angle (deg)	: 40.11

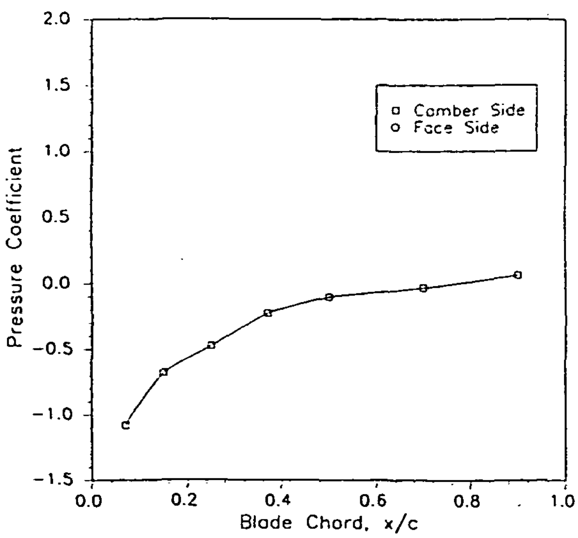

LAP/SR-7L Flight Test
Blade Surface Pressure Distribution

Record	: 114	Altitude (ft)	: 2055.
Condition	: 5A	Mach No.	: 0.315
Nacelle Tilt	: 2	True Airspeed (fps)	: 363.
Radial Sta	: .964	Tip Speed (fps)	: 704.
		Power Coeff.	: 1.508
		Blade Angle (deg)	: 40.11

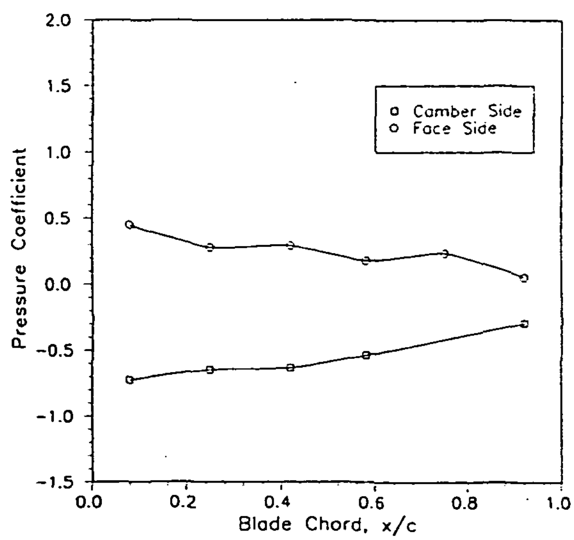

LAP/SR-7L Flight Test
Blade Surface Pressure Distribution

Record	: 117	Altitude (ft)	: 2111.
Condition	: 6A	Mach No.	: 0.315
Nacelle Tilt	: 2	True Airspeed (fps)	: 364.
Radial Sta	: .680	Tip Speed (fps)	: 798.
		Power Coeff.	: 1.059
		Blade Angle (deg)	: 40.14

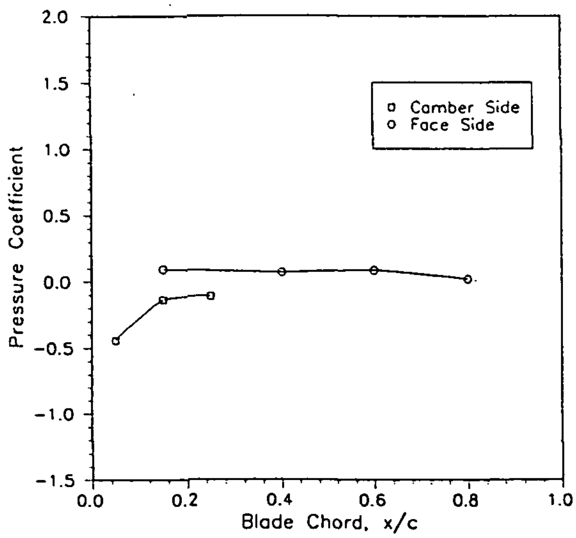

LAP/SR-7L Flight Test
Blade Surface Pressure Distribution

Record	: 117	Altitude (ft)	: 2111.
Condition	: 6A	Mach No.	: 0.315
Nacelle Tilt	: 2	True Airspeed (fps)	: 364.
Radial Sta	: .860	Tip Speed (fps)	: 798.
		Power Coeff.	: 1.059
		Blade Angle (deg)	: 40.14

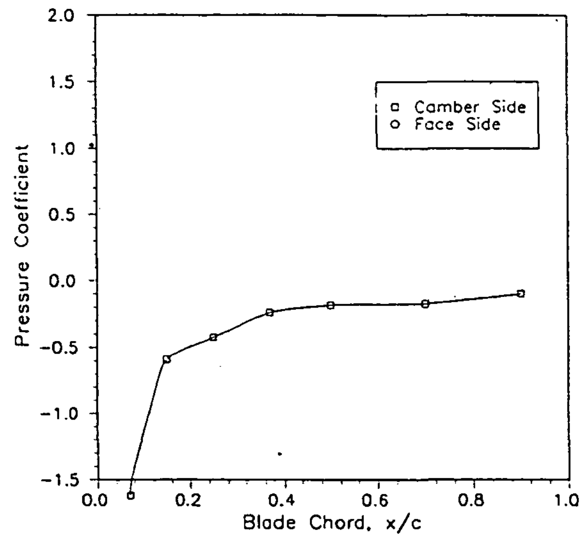

LAP/SR-7L Flight Test
Blade Surface Pressure Distribution

Record	: 117	Altitude (ft)	: 2111.
Condition	: 6A	Mach No.	: 0.315
Nacelle Tilt	: 2	True Airspeed (fps)	: 364.
Radial Sta	: .964	Tip Speed (fps)	: 798.
		Power Coeff.	: 1.059
		Blade Angle (deg)	: 40.14

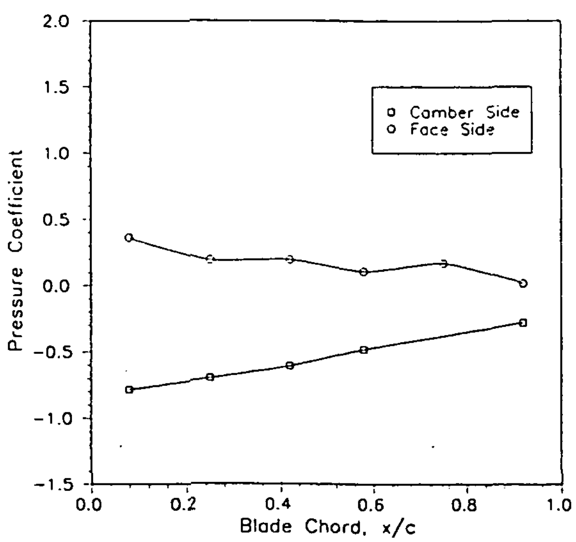

LAP/SR-7L Flight Test
Blade Surface Pressure Distribution

Record	: 115	Altitude (ft)	: 1982.
Condition	: 7A	Mach No.	: 0.315
Nacelle Tilt	: 2	True Airspeed (fps)	: 363.
Radial Sta	: .680	Tip Speed (fps)	: 799.
		Power Coeff.	: 0.705
		Blade Angle (deg)	: 40.11

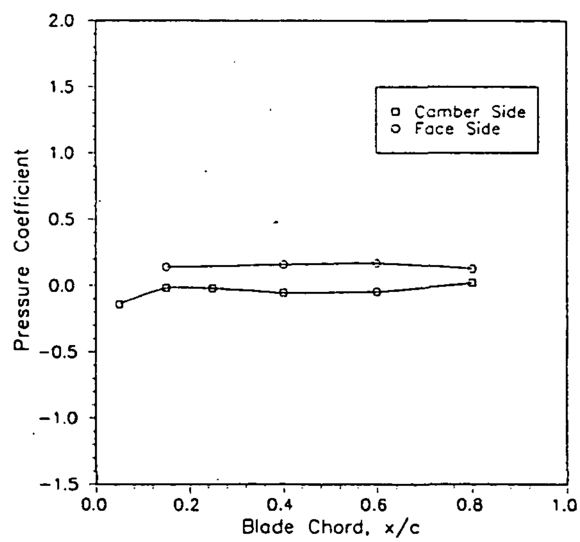

LAP/SR-7L Flight Test
Blade Surface Pressure Distribution

Record : 115
Condition : 7A
Nacelle Tilt : 2
Radial Sta : .860

Altitude (ft) : 1982.
Mach No. : 0.315
True Airspeed (fps) : 363.
Tip Speed (fps) : 799.
Power Coeff. : 0.705
Blade Angle (deg): 40.11

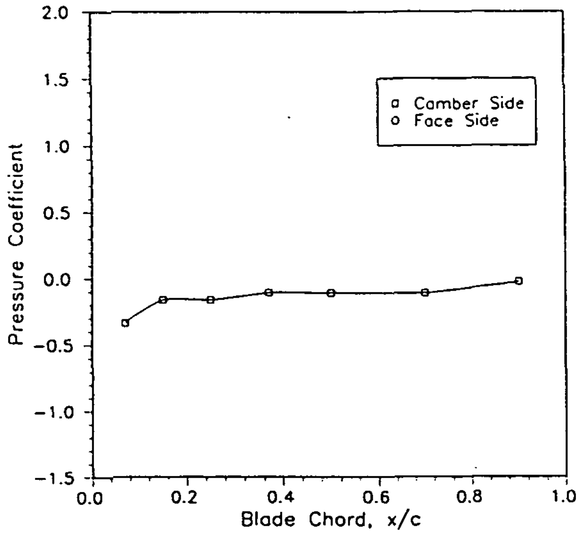

LAP/SR-7L Flight Test
Blade Surface Pressure Distribution

Record : 115
Condition : 7A
Nacelle Tilt : 2
Radial Sta : .964

Altitude (ft) : 1982.
Mach No. : 0.315
True Airspeed (fps) : 363.
Tip Speed (fps) : 799.
Power Coeff. : 0.705
Blade Angle (deg): 40.11

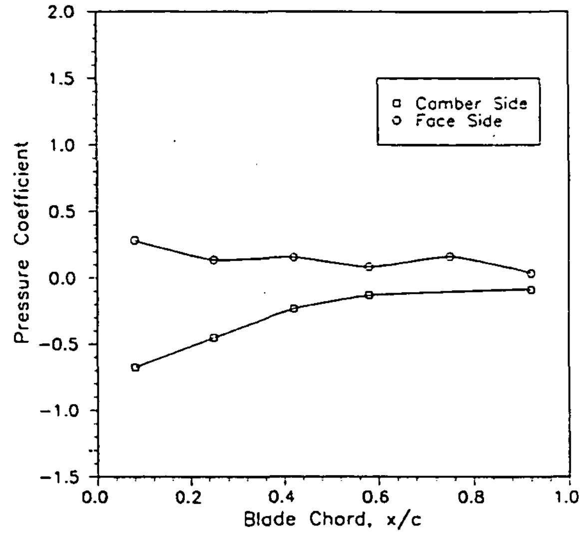

LAP/SR-7L Flight Test
Blade Surface Pressure Distribution

Record : 107
Condition : 10A
Nacelle Tilt : 2
Radial Sta : .680

Altitude (ft) : 2001.
Mach No. : 0.310
True Airspeed (fps) : 358.
Tip Speed (fps) : 623.
Power Coeff. : 0.975
Blade Angle (deg): 39.39

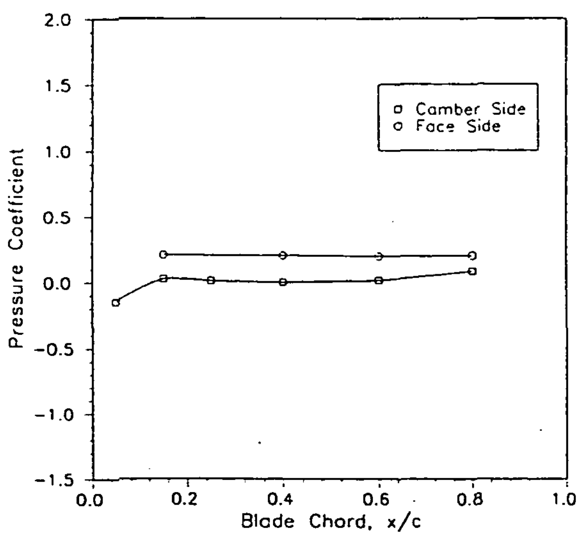

LAP/SR-7L Flight Test
Blade Surface Pressure Distribution

Record : 107
Condition : 10A
Nacelle Tilt : 2
Radial Sta : .860

Altitude (ft) : 2001.
Mach No. : 0.310
True Airspeed (fps) : 358.
Tip Speed (fps) : 623.
Power Coeff. : 0.975
Blade Angle (deg): 39.39

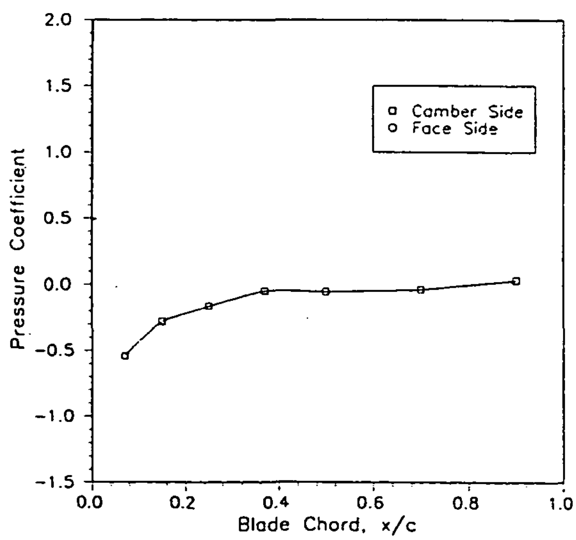

LAP/SR-7L Flight Test
Blade Surface Pressure Distribution

Record : 107
Condition : 10A
Nacelle Tilt : 2
Radial Sta : .964

Altitude (ft) : 2001.
Mach No. : 0.310
True Airspeed (fps) : 358.
Tip Speed (fps) : 623.
Power Coeff. : 0.975
Blade Angle (deg) : 39.39

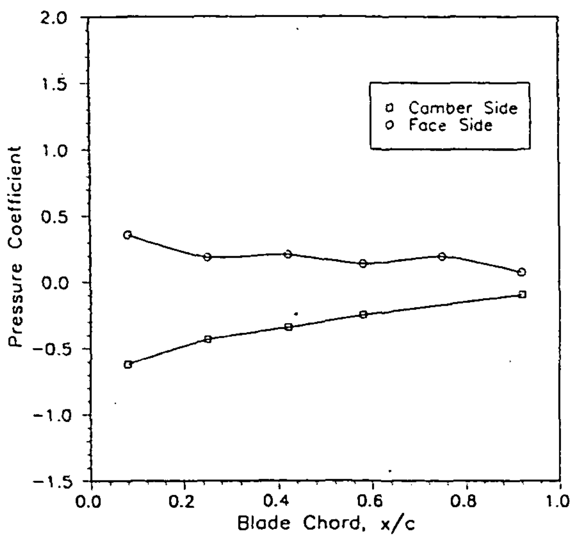

LAP/SR-7L Flight Test
Blade Surface Pressure Distribution

Record : 110
Condition : 11A
Nacelle Tilt : 2
Radial Sta : .680

Altitude (ft) : 2026.
Mach No. : 0.310
True Airspeed (fps) : 357.
Tip Speed (fps) : 623.
Power Coeff. : 1.950
Blade Angle (deg) : 47.57

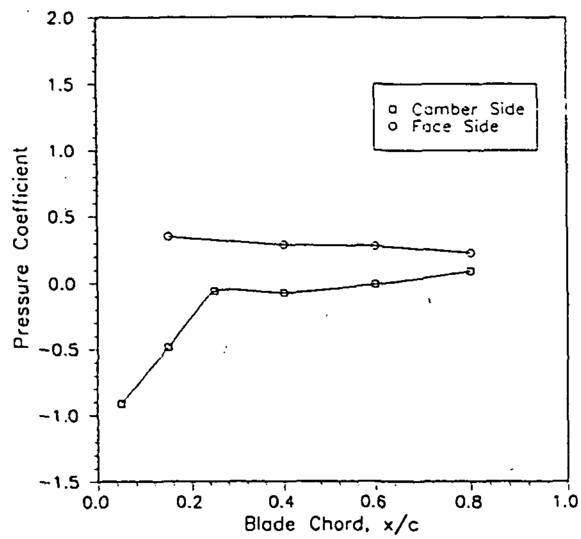

LAP/SR-7L Flight Test
Blade Surface Pressure Distribution

Record : 110
Condition : 11A
Nacelle Tilt : 2
Radial Sta : .860

Altitude (ft) : 2026.
Mach No. : 0.310
True Airspeed (fps) : 357.
Tip Speed (fps) : 623.
Power Coeff. : 1.950
Blade Angle (deg) : 47.57

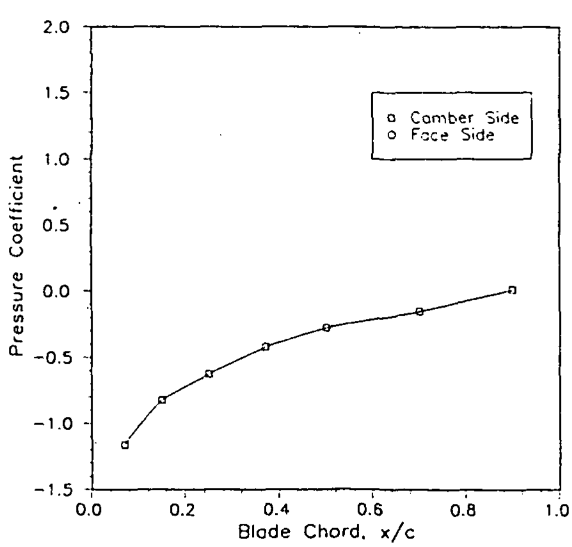

LAP/SR-7L Flight Test
Blade Surface Pressure Distribution

Record : 110
Condition : 11A
Nacelle Tilt : 2
Radial Sta : .964

Altitude (ft) : 2026.
Mach No. : 0.310
True Airspeed (fps) : 357.
Tip Speed (fps) : 623.
Power Coeff. : 1.950
Blade Angle (deg) : 47.57

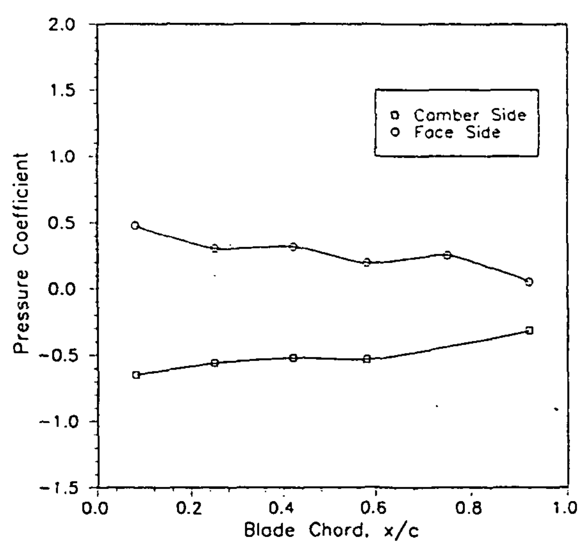

LAP/SR-7L Flight Test
Blade Surface Pressure Distribution

Record : 123
Condition : 1B
Nacelle Tilt : 2
Radial Sta : .680

Altitude (ft) : 35502.
Mach No. : 0.822
True Airspeed (fps) : 824.
Tip Speed (fps) : 626.
Power Coeff. : 3.372
Blade Angle (deg): 58.98

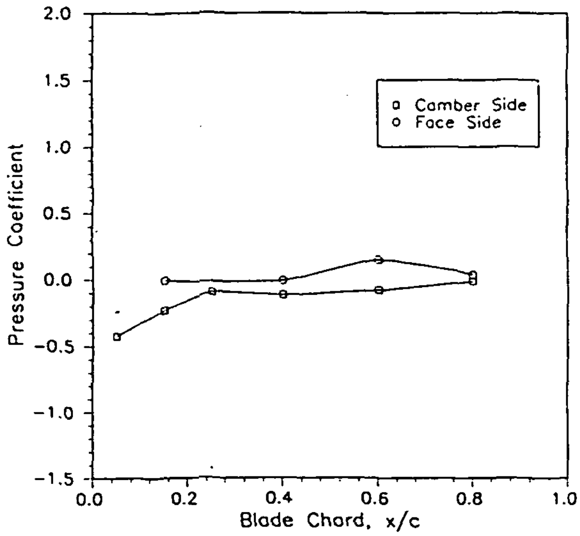

LAP/SR-7L Flight Test
Blade Surface Pressure Distribution

Record : 123
Condition : 1B
Nacelle Tilt : 2
Radial Sta : .860

Altitude (ft) : 35502.
Mach No. : 0.822
True Airspeed (fps) : 824.
Tip Speed (fps) : 626.
Power Coeff. : 3.372
Blade Angle (deg): 58.98

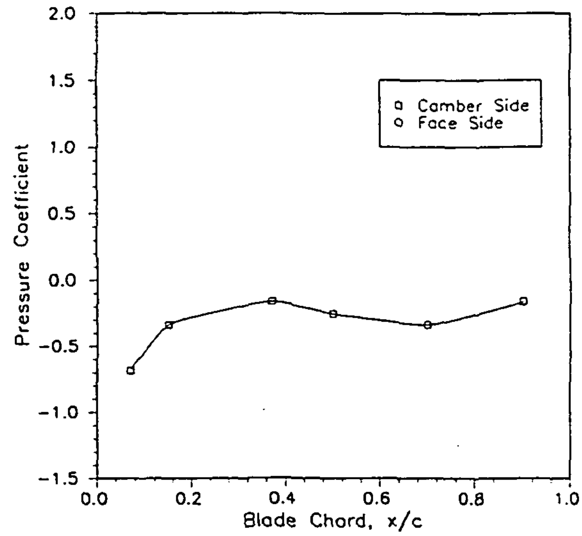

LAP/SR-7L Flight Test
Blade Surface Pressure Distribution

Record : 123
Condition : 1B
Nacelle Tilt : 2
Radial Sta : .964

Altitude (ft) : 35502.
Mach No. : 0.822
True Airspeed (fps) : 824.
Tip Speed (fps) : 626.
Power Coeff. : 3.372
Blade Angle (deg): 58.98

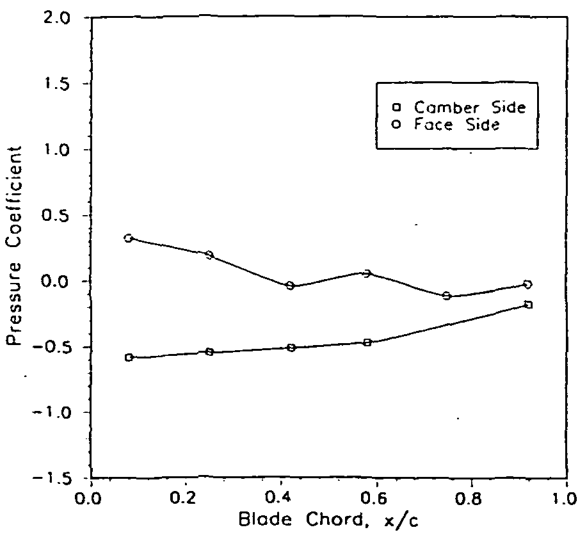

LAP/SR-7L Flight Test
Blade Surface Pressure Distribution

Record : 132
Condition : 3B
Nacelle Tilt : 2
Radial Sta : .680

Altitude (ft) : 35455.
Mach No. : 0.816
True Airspeed (fps) : 820.
Tip Speed (fps) : 702.
Power Coeff. : 1.221
Blade Angle (deg): 56.60

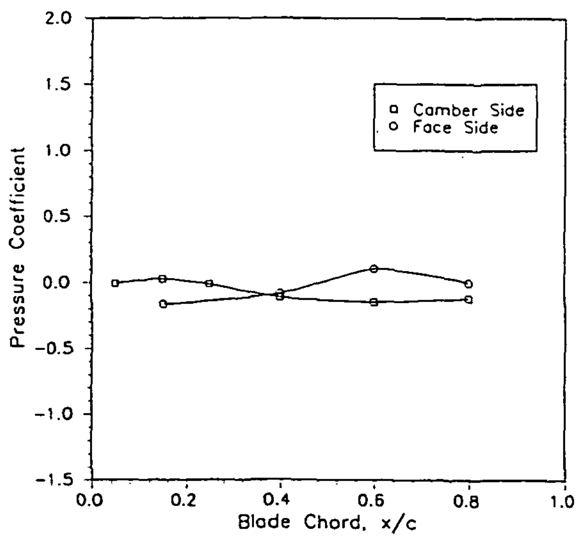

LAP/SR-7L Flight Test
Blade Surface Pressure Distribution

Record : 132
Condition : 3B
Nacelle Tilt : 2
Radial Sta : .860

Altitude (ft) : 35455.
Mach No. : 0.816
True Airspeed (fps) : 820.
Tip Speed (fps) : 702.
Power Coeff. : 1.221
Blade Angle (deg): 56.60

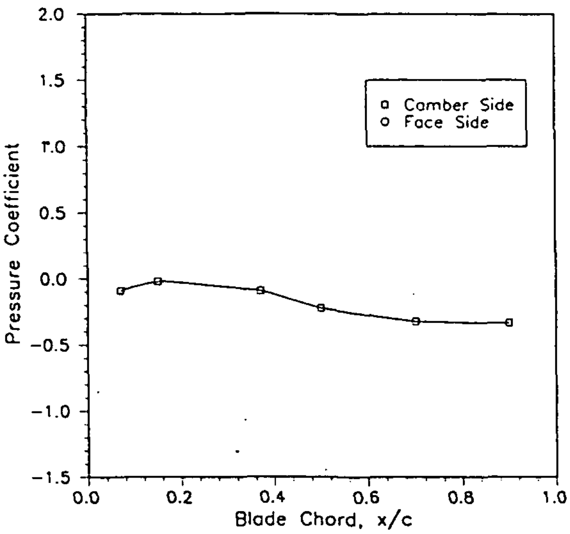

LAP/SR-7L Flight Test
Blade Surface Pressure Distribution

Record : 132
Condition : 3B
Nacelle Tilt : 2
Radial Sta : .964

Altitude (ft) : 35455.
Mach No. : 0.816
True Airspeed (fps) : 820.
Tip Speed (fps) : 702.
Power Coeff. : 1.221
Blade Angle (deg): 56.60

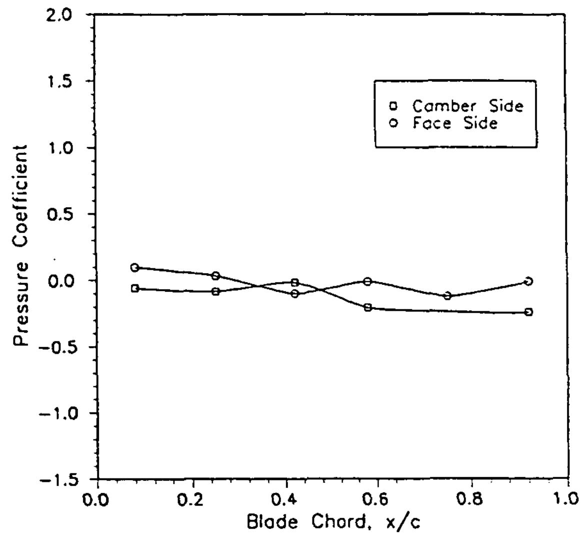

LAP/SR-7L Flight Test
Blade Surface Pressure Distribution

Record : 133
Condition : 4B
Nacelle Tilt : 2
Radial Sta : .680

Altitude (ft) : 35415.
Mach No. : 0.819
True Airspeed (fps) : 823.
Tip Speed (fps) : 701.
Power Coeff. : 2.007
Blade Angle (deg): 56.60

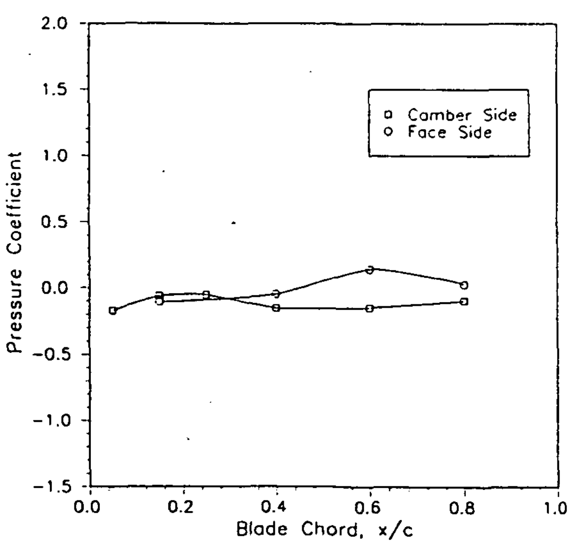

LAP/SR-7L Flight Test
Blade Surface Pressure Distribution

Record : 133
Condition : 4B
Nacelle Tilt : 2
Radial Sta : .860

Altitude (ft) : 35415.
Mach No. : 0.819
True Airspeed (fps) : 823.
Tip Speed (fps) : 701.
Power Coeff. : 2.007
Blade Angle (deg): 56.60

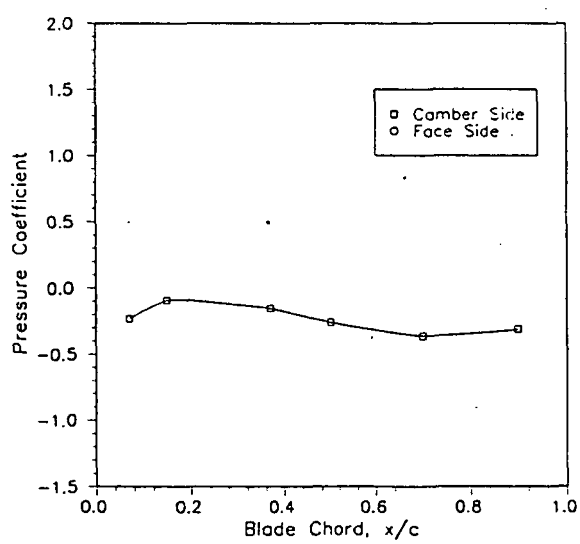

LAP/SR-7L Flight Test
Blade Surface Pressure Distribution

Record	: 133	Altitude (ft)	: 35415.
Condition	: 4B	Mach No.	: 0.819
Nacelle Tilt	: 2	True Airspeed (fps)	: 823.
Radial Sta	: .964	Tip Speed (fps)	: 701.
		Power Coeff.	: 2.007
		Blade Angle (deg)	: 56.60

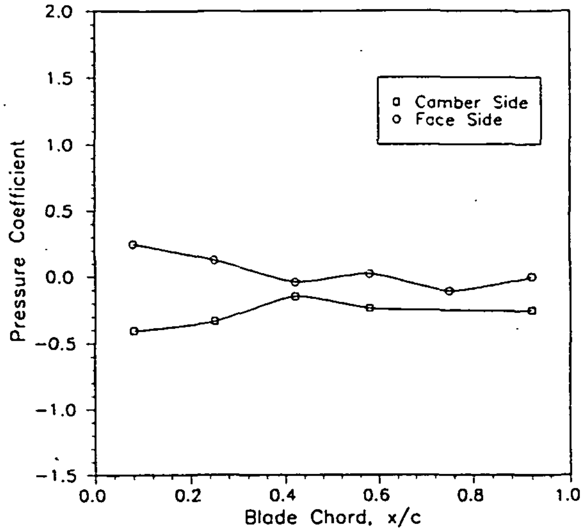

LAP/SR-7L Flight Test
Blade Surface Pressure Distribution

Record	: 134	Altitude (ft)	: 35446.
Condition	: 5B	Mach No.	: 0.816
Nacelle Tilt	: 2	True Airspeed (fps)	: 819.
Radial Sta	: .680	Tip Speed (fps)	: 702.
		Power Coeff.	: 2.517
		Blade Angle (deg)	: 56.58

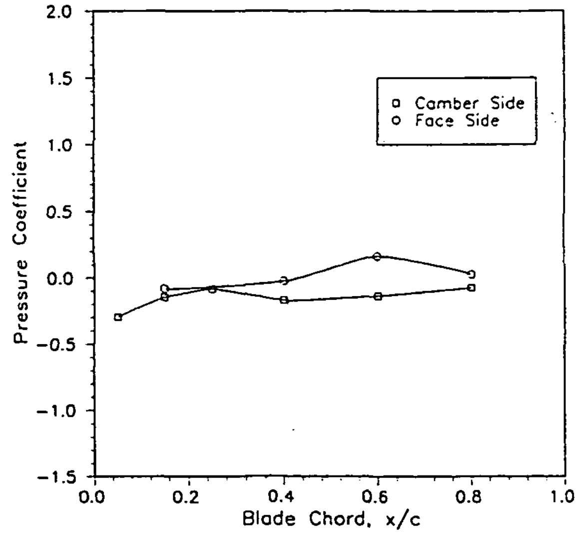

LAP/SR-7L Flight Test
Blade Surface Pressure Distribution

Record	: 134	Altitude (ft)	: 35446.
Condition	: 5B	Mach No.	: 0.816
Nacelle Tilt	: 2	True Airspeed (fps)	: 819.
Radial Sta	: .860	Tip Speed (fps)	: 702.
		Power Coeff.	: 2.517
		Blade Angle (deg)	: 56.58

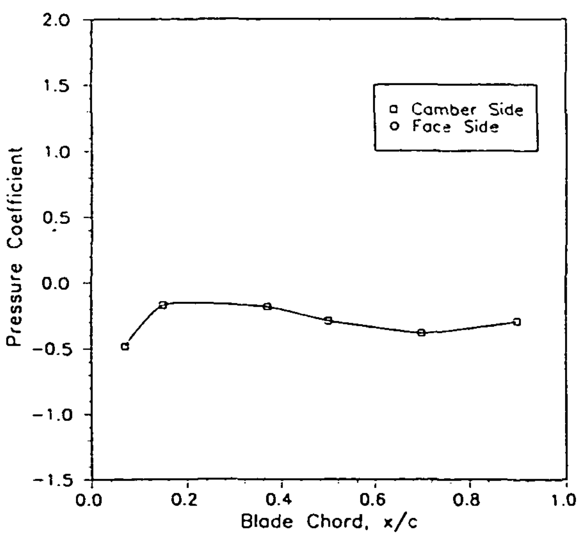

LAP/SR-7L Flight Test
Blade Surface Pressure Distribution

Record	: 134	Altitude (ft)	: 35446.
Condition	: 5B	Mach No.	: 0.816
Nacelle Tilt	: 2	True Airspeed (fps)	: 819.
Radial Sta	: .964	Tip Speed (fps)	: 702.
		Power Coeff.	: 2.517
		Blade Angle (deg)	: 56.58

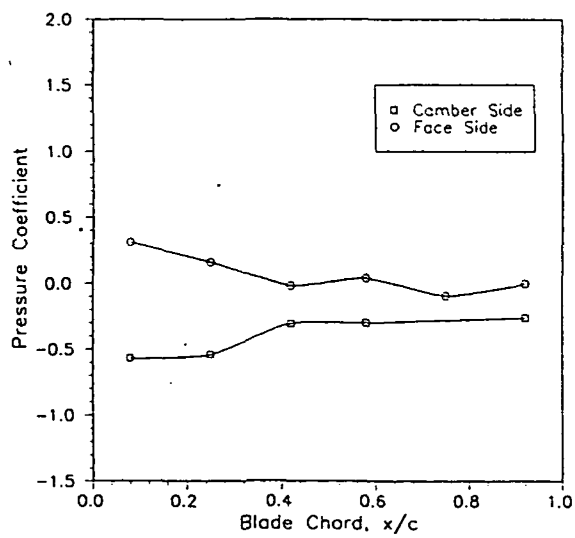

LAP/SR-7L Flight Test
Blade Surface Pressure Distribution

Record	: 136	Altitude (ft)	: 35456.
Condition	: 7B	Mach No.	: 0.820
Nacelle Tilt	: 2	True Airspeed (fps)	: 823.
Radial Sta	: .680	Tip Speed (fps)	: 797.
		Power Coeff.	: 0.886
		Blade Angle (deg)	: 56.67

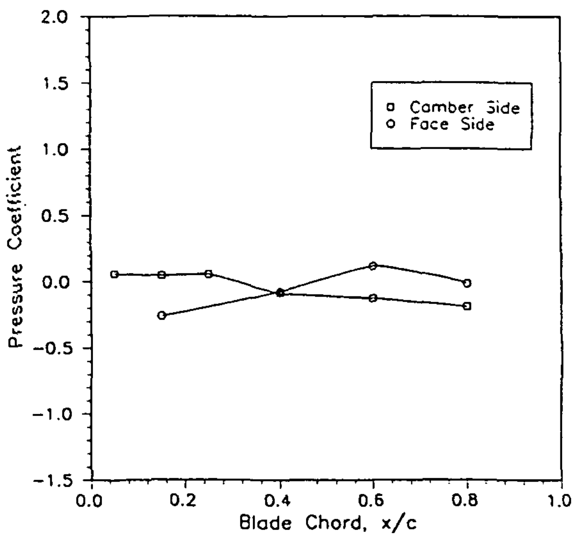

LAP/SR-7L Flight Test
Blade Surface Pressure Distribution

Record	: 136	Altitude (ft)	: 35456.
Condition	: 7B	Mach No.	: 0.820
Nacelle Tilt	: 2	True Airspeed (fps)	: 823.
Radial Sta	: .860	Tip Speed (fps)	: 797.
		Power Coeff.	: 0.886
		Blade Angle (deg)	: 56.67

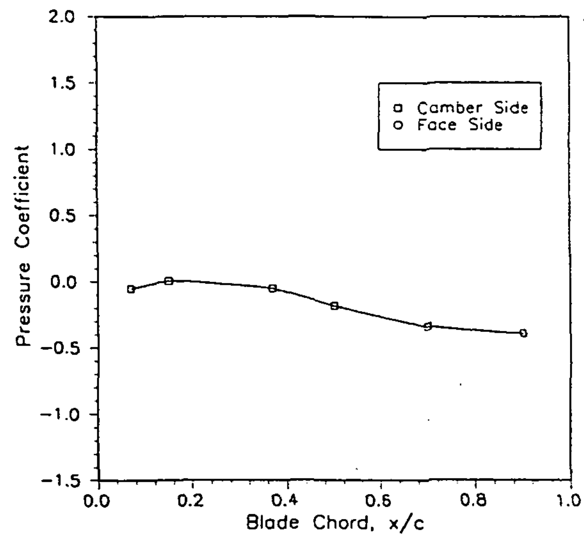

LAP/SR-7L Flight Test
Blade Surface Pressure Distribution

Record	: 136	Altitude (ft)	: 35456.
Condition	: 7B	Mach No.	: 0.820
Nacelle Tilt	: 2	True Airspeed (fps)	: 823.
Radial Sta	: .964	Tip Speed (fps)	: 797.
		Power Coeff.	: 0.886
		Blade Angle (deg)	: 56.67

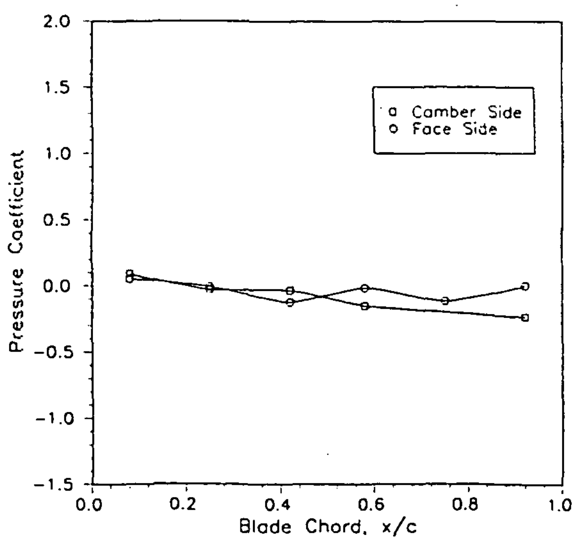

LAP/SR-7L Flight Test
Blade Surface Pressure Distribution

Record	: 137	Altitude (ft)	: 35412.
Condition	: 8B	Mach No.	: 0.815
Nacelle Tilt	: 2	True Airspeed (fps)	: 819.
Radial Sta	: .680	Tip Speed (fps)	: 796.
		Power Coeff.	: 1.486
		Blade Angle (deg)	: 56.68

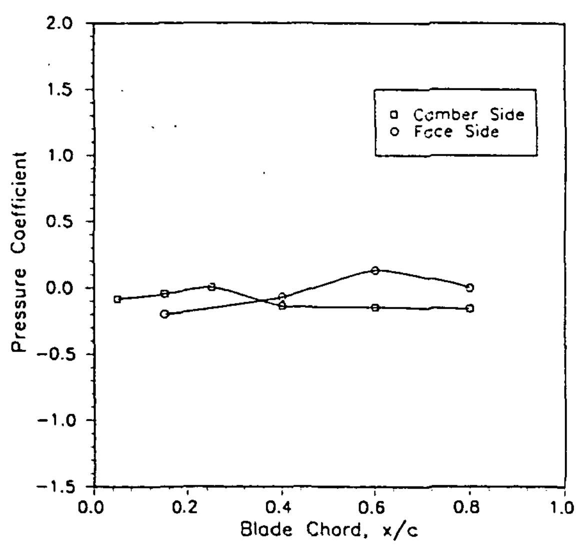

LAP/SR-7L Flight Test
Blade Surface Pressure Distribution

Record : 137
Condition : 88
Nacelle Tilt : 2
Radial Sta : .860

Altitude (ft) : 35412.
Mach No. : 0.815
True Airspeed (fps) : 819.
Tip Speed (fps) : 796.
Power Coeff. : 1.486
Blade Angle (deg): 56.68

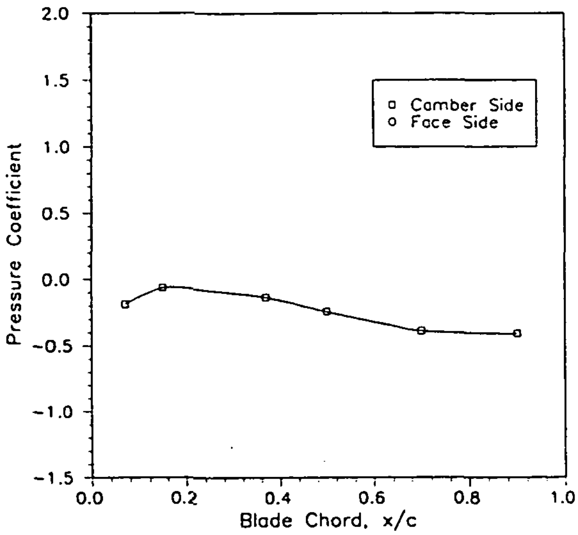

LAP/SR-7L Flight Test
Blade Surface Pressure Distribution

Record : 137
Condition : 88
Nacelle Tilt : 2
Radial Sta : .964

Altitude (ft) : 35412.
Mach No. : 0.815
True Airspeed (fps) : 819.
Tip Speed (fps) : 796.
Power Coeff. : 1.486
Blade Angle (deg): 56.68

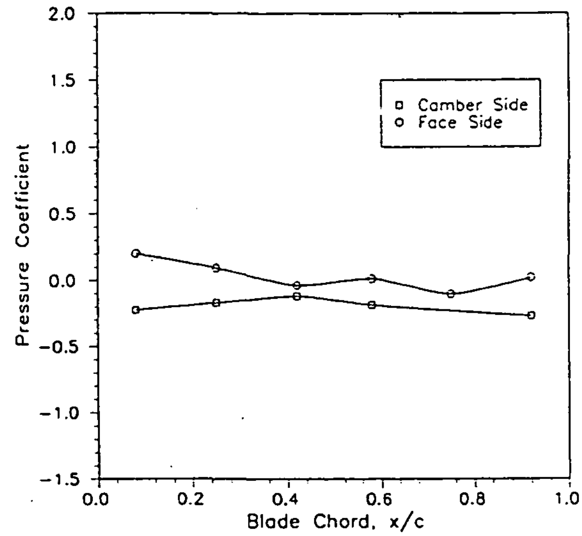

LAP/SR-7L Flight Test
Blade Surface Pressure Distribution

Record : 138
Condition : 98
Nacelle Tilt : 2
Radial Sta : .680

Altitude (ft) : 35418.
Mach No. : 0.816
True Airspeed (fps) : 820.
Tip Speed (fps) : 796.
Power Coeff. : 1.836
Blade Angle (deg): 56.67

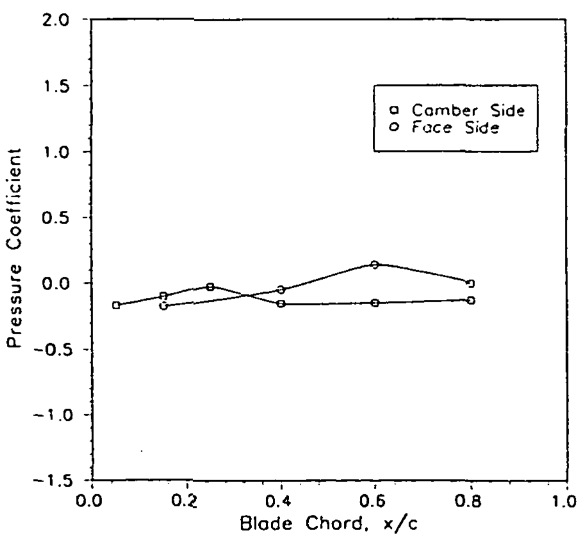

LAP/SR-7L Flight Test
Blade Surface Pressure Distribution

Record : 138
Condition : 98
Nacelle Tilt : 2
Radial Sta : .860

Altitude (ft) : 35418.
Mach No. : 0.816
True Airspeed (fps) : 820.
Tip Speed (fps) : 796.
Power Coeff. : 1.836
Blade Angle (deg): 56.67

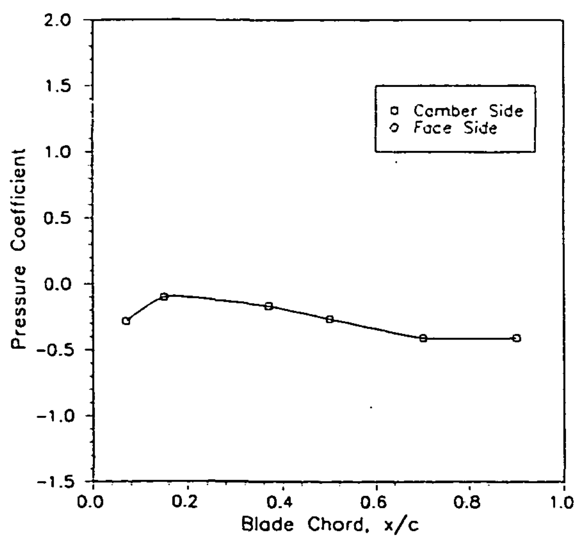

LAP/SR-7L Flight Test
Blade Surface Pressure Distribution

Record : 138
Condition : 9B
Nacelle Tilt : 2
Radial Sta : .964

Altitude (ft) : 35418.
Mach No. : 0.816
True Airspeed (fps) : 820.
Tip Speed (fps) : 796.
Power Coeff. : 1.836
Blade Angle (deg): 56.67

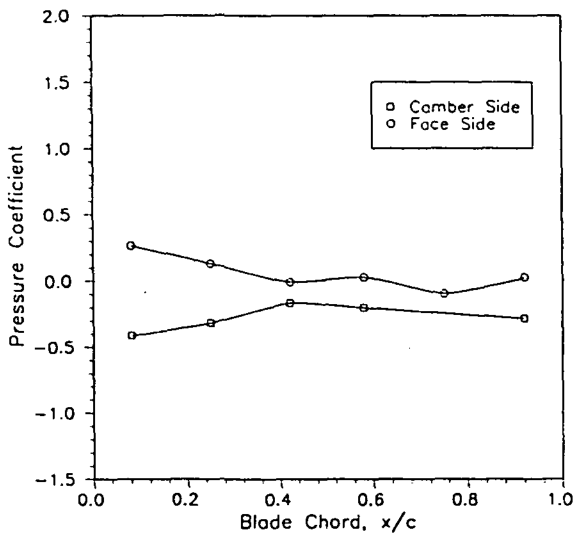

LAP/SR-7L Flight Test
Blade Surface Pressure Distribution

Record : 120
Condition : 10B
Nacelle Tilt : 2
Radial Sta : .680

Altitude (ft) : 35031.
Mach No. : 0.816
True Airspeed (fps) : 820.
Tip Speed (fps) : 625.
Power Coeff. : 0.739
Blade Angle (deg): 53.05

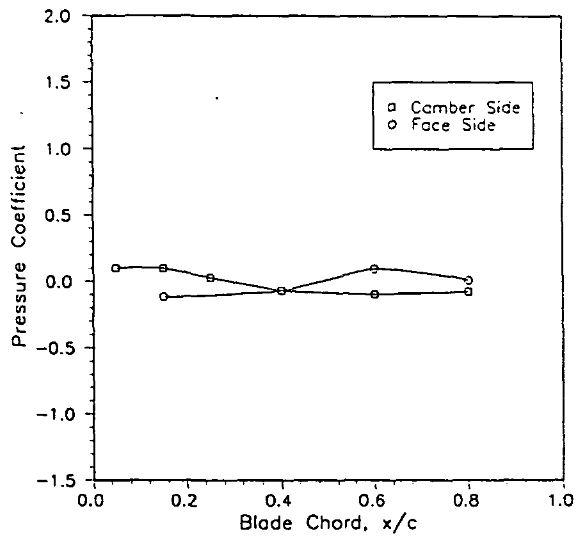

LAP/SR-7L Flight Test
Blade Surface Pressure Distribution

Record : 120
Condition : 10B
Nacelle Tilt : 2
Radial Sta : .860

Altitude (ft) : 35031.
Mach No. : 0.816
True Airspeed (fps) : 820.
Tip Speed (fps) : 625.
Power Coeff. : 0.739
Blade Angle (deg): 53.05

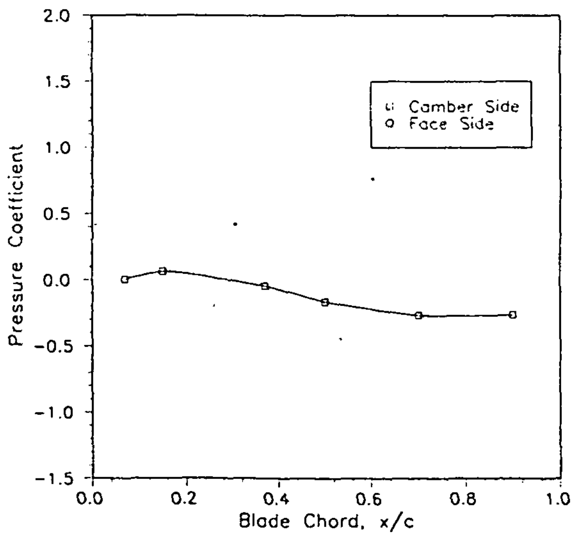

LAP/SR-7L Flight Test
Blade Surface Pressure Distribution

Record : 120
Condition : 10B
Nacelle Tilt : 2
Radial Sta : .964

Altitude (ft) : 35031.
Mach No. : 0.816
True Airspeed (fps) : 820.
Tip Speed (fps) : 625.
Power Coeff. : 0.739
Blade Angle (deg): 53.05

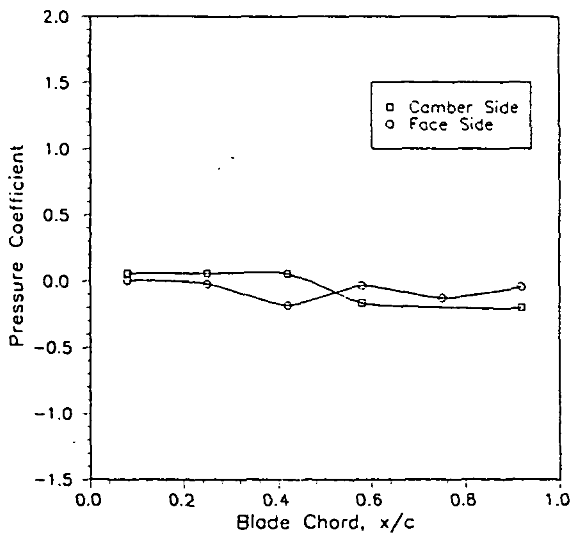

LAP/SR-7L Flight Test
Blade Surface Pressure Distribution

Record : 121
Condition : 118
Nacelle Tilt : 2
Radial Sta : .680

Altitude (ft) : 35528.
Mach No. : 0.823
True Airspeed (fps) : 825.
Tip Speed (fps) : 625.
Power Coeff. : 1.690
Blade Angle (deg): 54.53

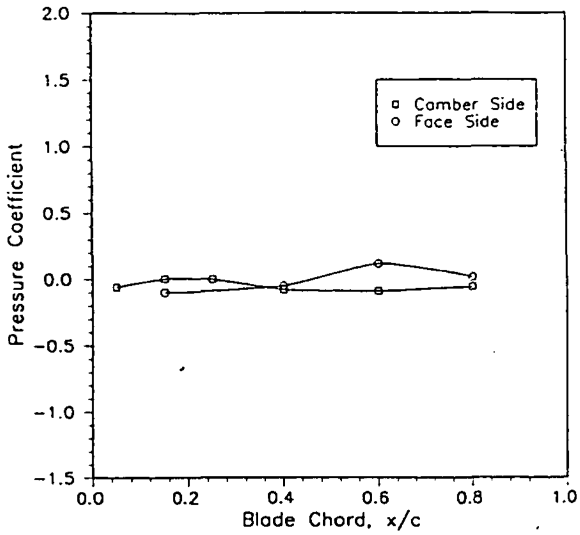

LAP/SR-7L Flight Test
Blade Surface Pressure Distribution

Record : 121
Condition : 118
Nacelle Tilt : 2
Radial Sta : .860

Altitude (ft) : 35528.
Mach No. : 0.823
True Airspeed (fps) : 825.
Tip Speed (fps) : 625.
Power Coeff. : 1.690
Blade Angle (deg): 54.53

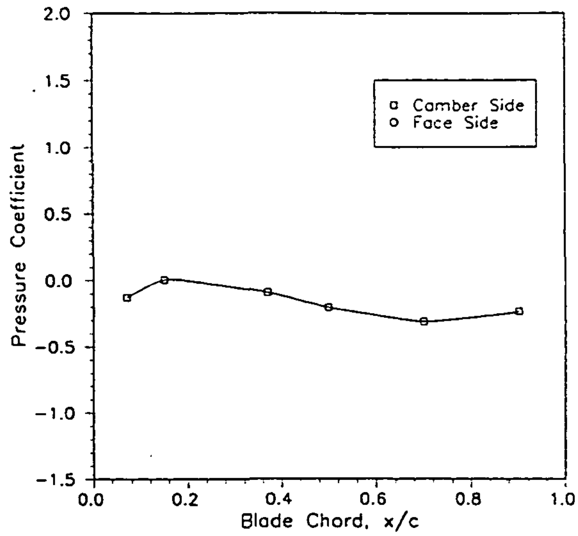

LAP/SR-7L Flight Test
Blade Surface Pressure Distribution

Record : 121
Condition : 118
Nacelle Tilt : 2
Radial Sta : .964

Altitude (ft) : 35528.
Mach No. : 0.823
True Airspeed (fps) : 825.
Tip Speed (fps) : 625.
Power Coeff. : 1.690
Blade Angle (deg): 54.53

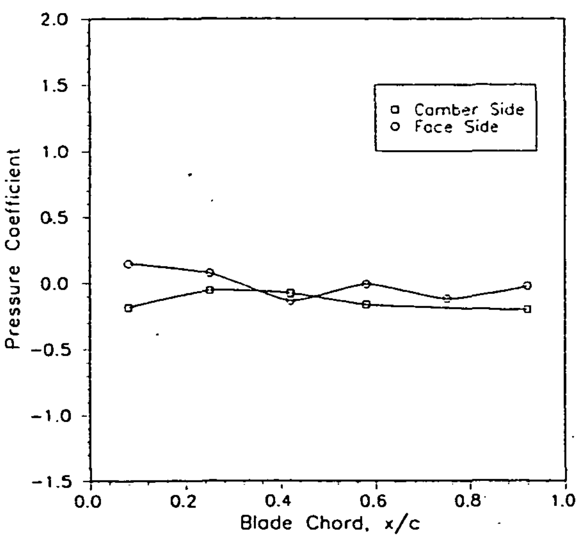

LAP/SR-7L Flight Test
Blade Surface Pressure Distribution

Record : 122
Condition : 128
Nacelle Tilt : 2
Radial Sta : .680

Altitude (ft) : 35507.
Mach No. : 0.820
True Airspeed (fps) : 822.
Tip Speed (fps) : 625.
Power Coeff. : 2.726
Blade Angle (deg): 57.34

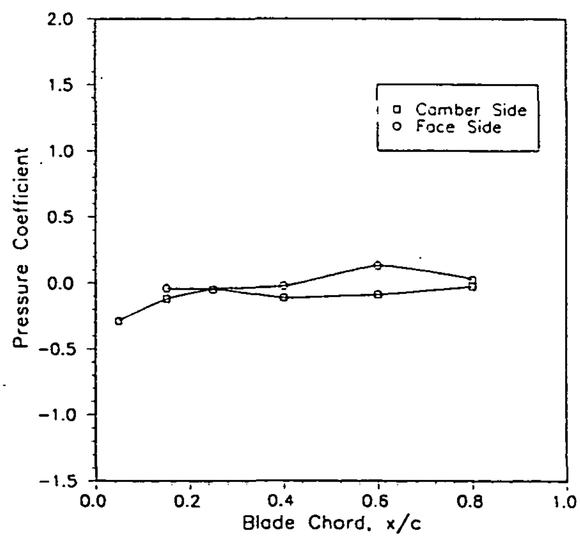

LAP/SR-7L Flight Test
Blade Surface Pressure Distribution

Record : 122
Condition : 12B
Nacelle Tilt : 2
Radial Sta : .860

Altitude (ft) : 35507.
Mach No. : 0.820
True Airspeed (fps) : 822.
Tip Speed (fps) : 625.
Power Coeff. : 2.726
Blade Angle (deg): 57.34

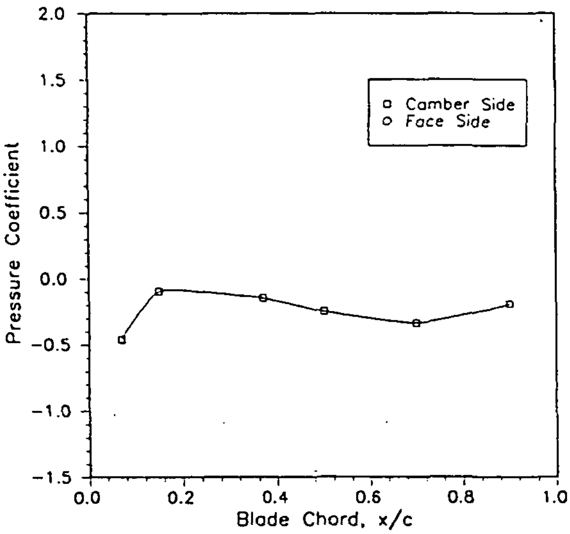

LAP/SR-7L Flight Test
Blade Surface Pressure Distribution

Record : 122
Condition : 12B
Nacelle Tilt : 2
Radial Sta : .964

Altitude (ft) : 35507.
Mach No. : 0.820
True Airspeed (fps) : 822.
Tip Speed (fps) : 625.
Power Coeff. : 2.726
Blade Angle (deg): 57.34

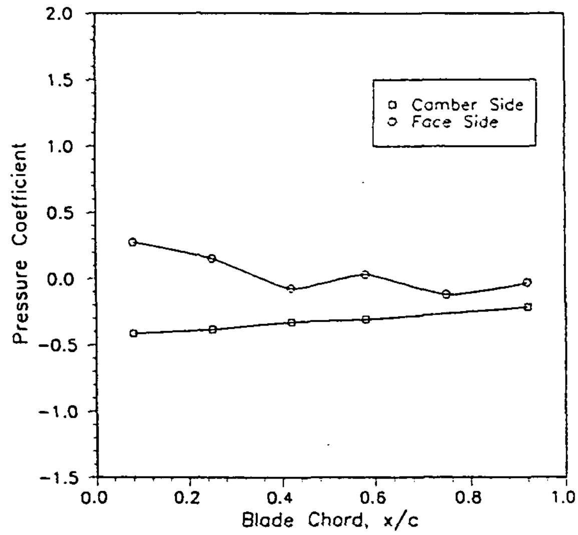

LAP/SR-7L Flight Test
Blade Surface Pressure Distribution

Record : 144
Condition : 1C
Nacelle Tilt : 2
Radial Sta : .680

Altitude (ft) : 22960.
Mach No. : 0.603
True Airspeed (fps) : 646.
Tip Speed (fps) : 635.
Power Coeff. : 1.475
Blade Angle (deg): 55.47

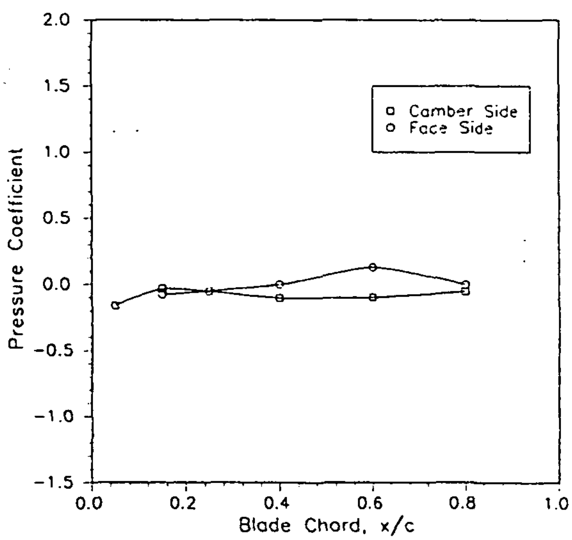

LAP/SR-7L Flight Test
Blade Surface Pressure Distribution

Record : 144
Condition : 1C
Nacelle Tilt : 2
Radial Sta : .860

Altitude (ft) : 22960.
Mach No. : 0.603
True Airspeed (fps) : 646.
Tip Speed (fps) : 635.
Power Coeff. : 1.475
Blade Angle (deg): 55.47

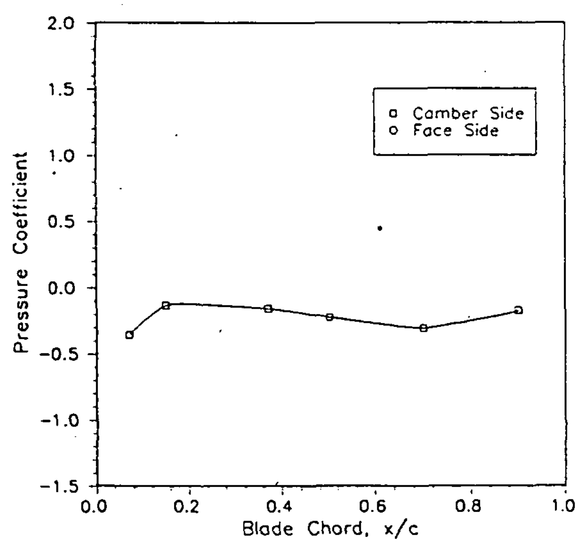

LAP/SR-7L Flight Test
Blade Surface Pressure Distribution

Record : 144
Condition : 1C
Nacelle Tilt : 2
Radial Sta : .964

Altitude (ft) : 22960.
Mach No. : 0.603
True Airspeed (fps) : 646.
Tip Speed (fps) : 635.
Power Coeff. : 1.475
Blade Angle (deg): 55.47

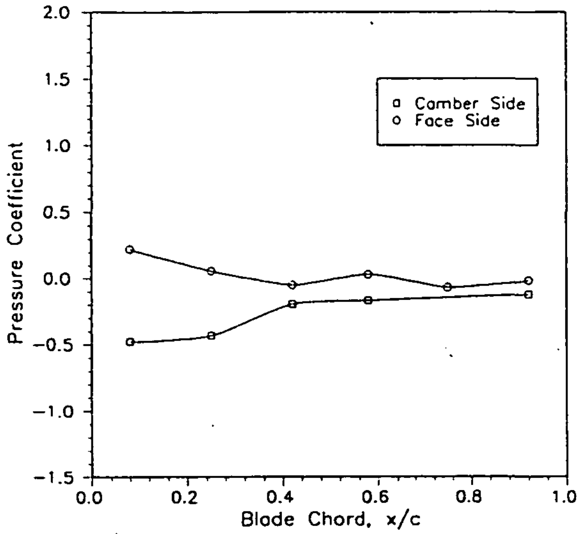

LAP/SR-7L Flight Test
Blade Surface Pressure Distribution

Record : 142
Condition : 2C
Nacelle Tilt : 2
Radial Sta : .680

Altitude (ft) : 31547.
Mach No. : 0.701
True Airspeed (fps) : 720.
Tip Speed (fps) : 712.
Power Coeff. : 1.533
Blade Angle (deg): 56.63

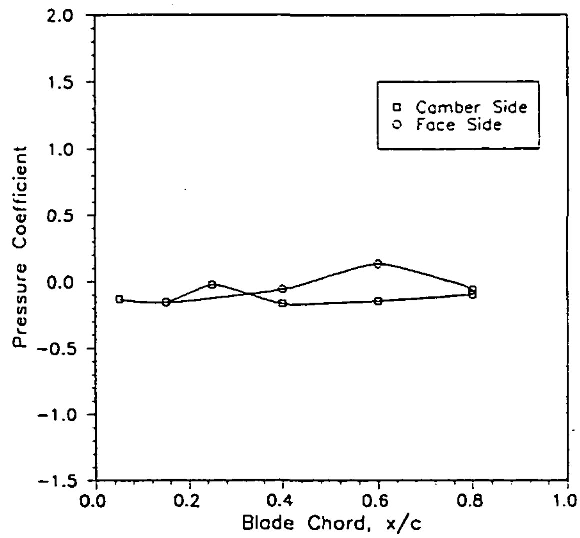

LAP/SR-7L Flight Test
Blade Surface Pressure Distribution

Record : 142
Condition : 2C
Nacelle Tilt : 2
Radial Sta : .860

Altitude (ft) : 31547.
Mach No. : 0.701
True Airspeed (fps) : 720.
Tip Speed (fps) : 712.
Power Coeff. : 1.533
Blade Angle (deg): 56.63

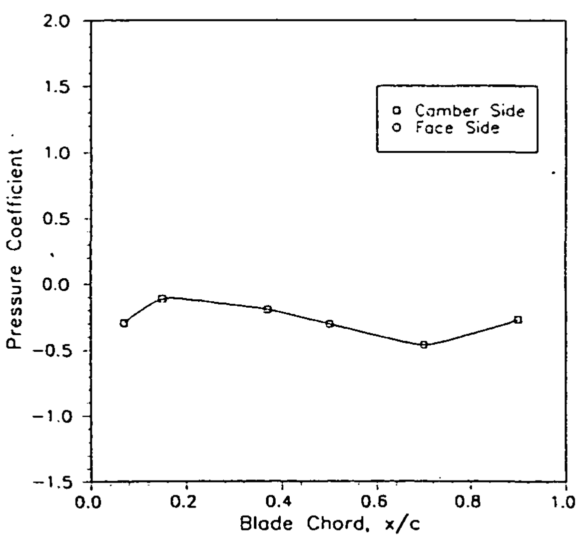

LAP/SR-7L Flight Test
Blade Surface Pressure Distribution

Record : 142
Condition : 2C
Nacelle Tilt : 2
Radial Sta : .964

Altitude (ft) : 31547.
Mach No. : 0.701
True Airspeed (fps) : 720.
Tip Speed (fps) : 712.
Power Coeff. : 1.533
Blade Angle (deg): 56.63

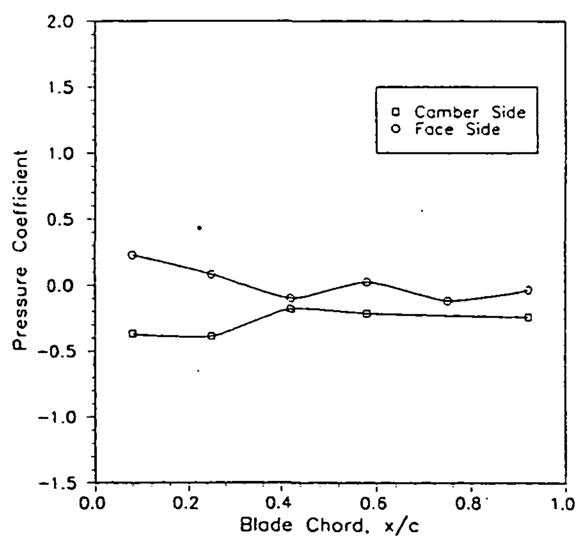

LAP/SR-7L Flight Test
Blade Surface Pressure Distribution

Record : 140
Condition : 3C
Nacelle Tilt : 2
Radial Sta : .680

Altitude (ft) : 37994.
Mach No. : 0.803
True Airspeed (fps) : 794.
Tip Speed (fps) : 797.
Power Coeff. : 1.493
Blade Angle (deg) : 56.66

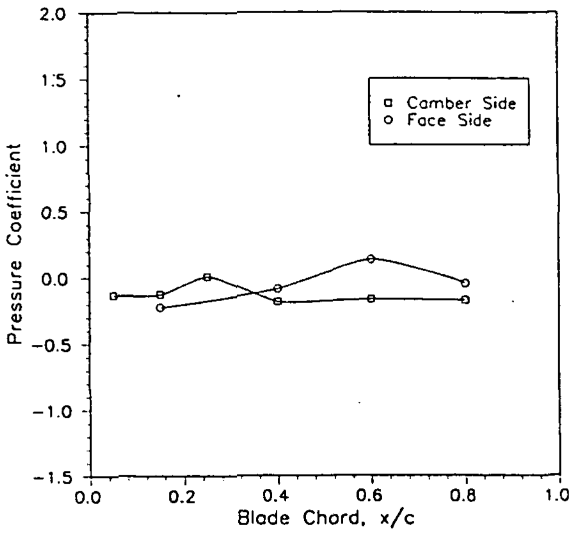

LAP/SR-7L Flight Test
Blade Surface Pressure Distribution

Record : 140
Condition : 3C
Nacelle Tilt : 2
Radial Sta : .860

Altitude (ft) : 37994.
Mach No. : 0.803
True Airspeed (fps) : 794.
Tip Speed (fps) : 797.
Power Coeff. : 1.493
Blade Angle (deg) : 56.66

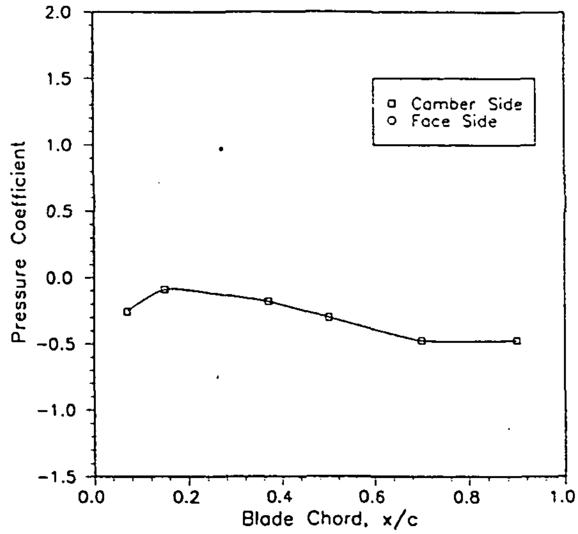

LAP/SR-7L Flight Test
Blade Surface Pressure Distribution

Record : 140
Condition : 3C
Nacelle Tilt : 2
Radial Sta : .964

Altitude (ft) : 37994.
Mach No. : 0.803
True Airspeed (fps) : 794.
Tip Speed (fps) : 797.
Power Coeff. : 1.493
Blade Angle (deg) : 56.66

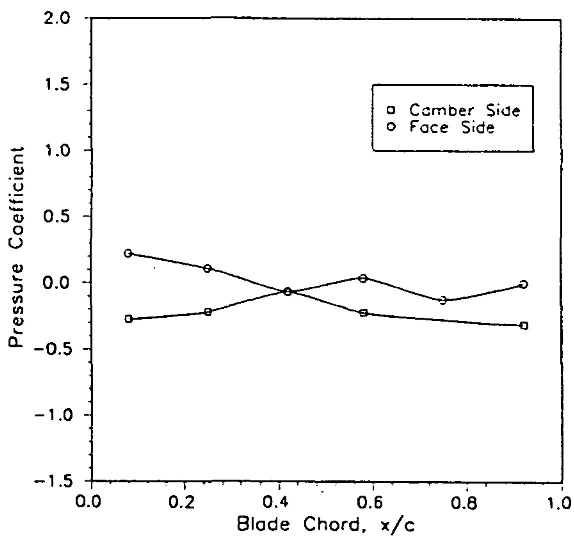

APPENDIX D3

-3 DEGREE STEADY PRESSURE DISTRIBUTION PLOTS

LAP/SR-7L Flight Test
Blade Surface Pressure Distribution

Record : 183
Condition : 1A
Nacelle Tilt : -3
Radial Sta : .680

Altitude (ft) : 2145.
Mach No. : 0.315
True Airspeed (fps) : 361.
Tip Speed (fps) : 623.
Power Coeff. : 1.498
Blade Angle (deg): 43.34

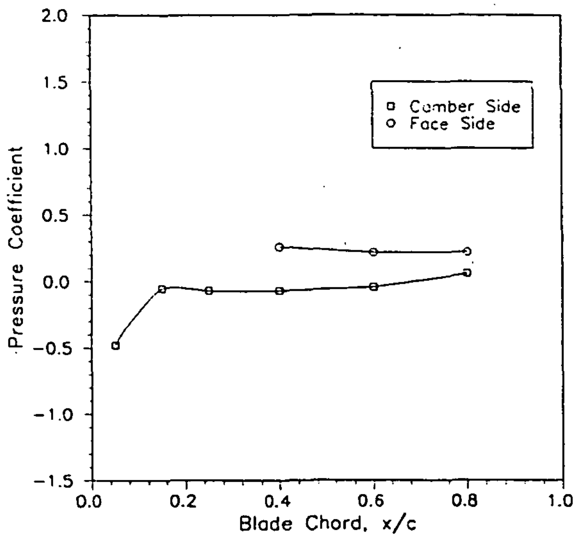

LAP/SR-7L Flight Test
Blade Surface Pressure Distribution

Record : 183
Condition : 1A
Nacelle Tilt : -3
Radial Sta : .860

Altitude (ft) : 2145.
Mach No. : 0.315
True Airspeed (fps) : 361.
Tip Speed (fps) : 623.
Power Coeff. : 1.498
Blade Angle (deg): 43.34

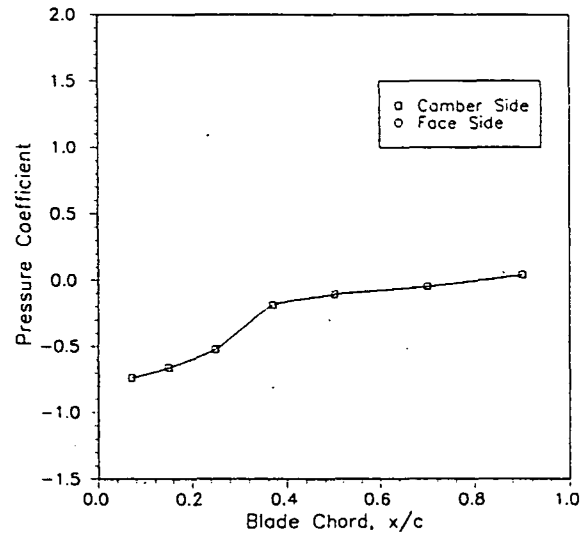

LAP/SR-7L Flight Test
Blade Surface Pressure Distribution

Record : 183
Condition : 1A
Nacelle Tilt : -3
Radial Sta : .964

Altitude (ft) : 2145.
Mach No. : 0.315
True Airspeed (fps) : 361.
Tip Speed (fps) : 623.
Power Coeff. : 1.498
Blade Angle (deg): 43.34

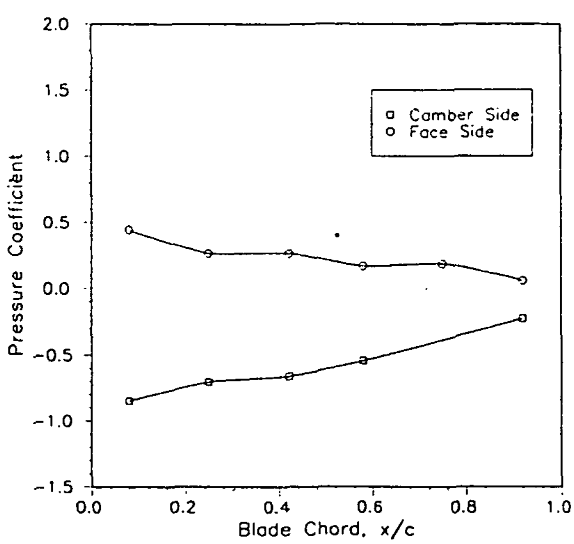

LAP/SR-7L Flight Test
Blade Surface Pressure Distribution

Record : 185
Condition : 2A
Nacelle Tilt : -3
Radial Sta : .680

Altitude (ft) : 1975.
Mach No. : 0.311
True Airspeed (fps) : 357.
Tip Speed (fps) : 622.
Power Coeff. : 2.206
Blade Angle (deg): 48.45

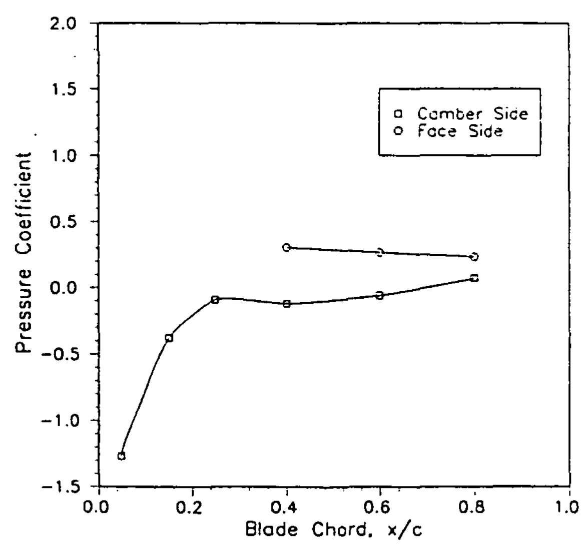

LAP/SR-7L Flight Test
Blade Surface Pressure Distribution

Record	: 185	Altitude (ft)	: 1975.
Condition	: 2A	Mach No.	: 0.311
Nacelle Tilt	: -3	True Airspeed (fps)	: 357.
Radial Sta	: .860	Tip Speed (fps)	: 622.
		Power Coeff.	: 2.206
		Blade Angle (deg)	: 48.45

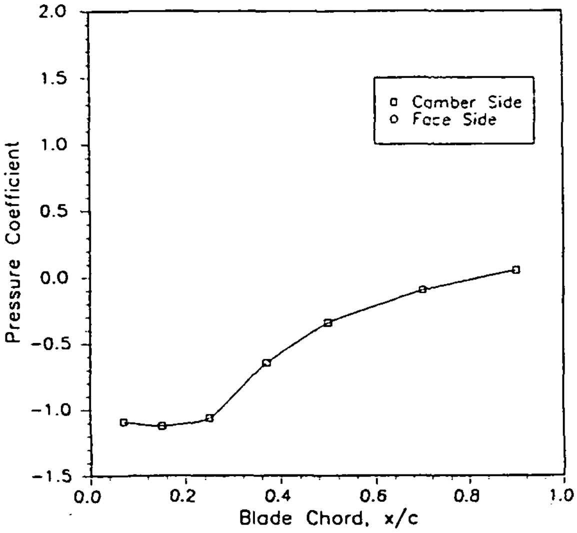

LAP/SR-7L Flight Test
Blade Surface Pressure Distribution

Record	: 185	Altitude (ft)	: 1975.
Condition	: 2A	Mach No.	: 0.311
Nacelle Tilt	: -3	True Airspeed (fps)	: 357.
Radial Sta	: .964	Tip Speed (fps)	: 622.
		Power Coeff.	: 2.206
		Blade Angle (deg)	: 48.45

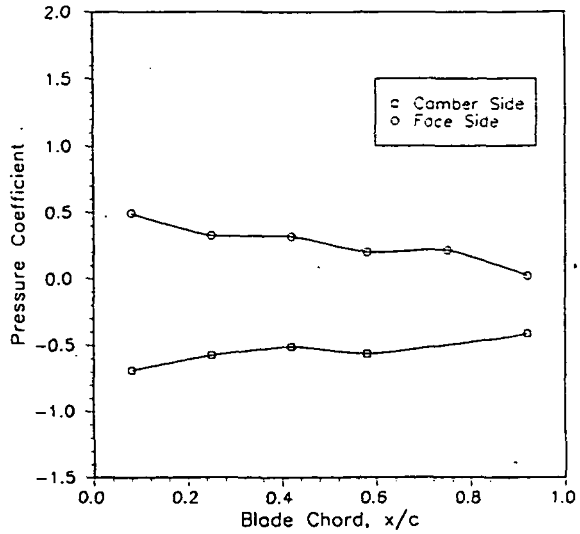

LAP/SR-7L Flight Test
Blade Surface Pressure Distribution

Record	: 187	Altitude (ft)	: 1971.
Condition	: 3A	Mach No.	: 0.310
Nacelle Tilt	: -3	True Airspeed (fps)	: 355.
Radial Sta	: .680	Tip Speed (fps)	: 702.
		Power Coeff.	: 1.016
		Blade Angle (deg)	: 45.90

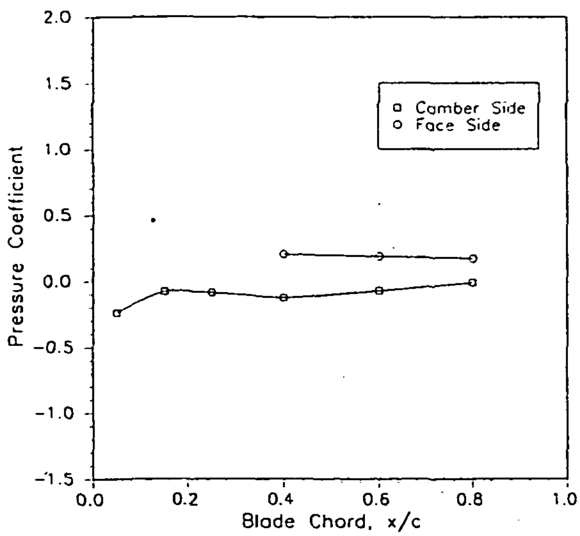

LAP/SR-7L Flight Test
Blade Surface Pressure Distribution

Record	: 187	Altitude (ft)	: 1971.
Condition	: 3A	Mach No.	: 0.310
Nacelle Tilt	: -3	True Airspeed (fps)	: 355.
Radial Sta	: .860	Tip Speed (fps)	: 702.
		Power Coeff.	: 1.016
		Blade Angle (deg)	: 45.90

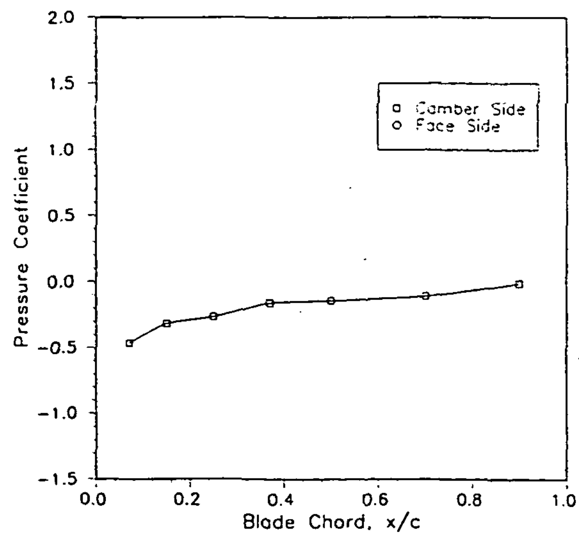

LAP/SR-7L Flight Test
Blade Surface Pressure Distribution

Record	: 187	Altitude (ft)	: 1971.
Condition	: 3A	Mach No.	: 0.310
Nacelle Tilt	: −3	True Airspeed (fps)	: 355.
Radial Sta	: .964	Tip Speed (fps)	: 702.
		Power Coeff.	: 1.016
		Blade Angle (deg)	: 45.90

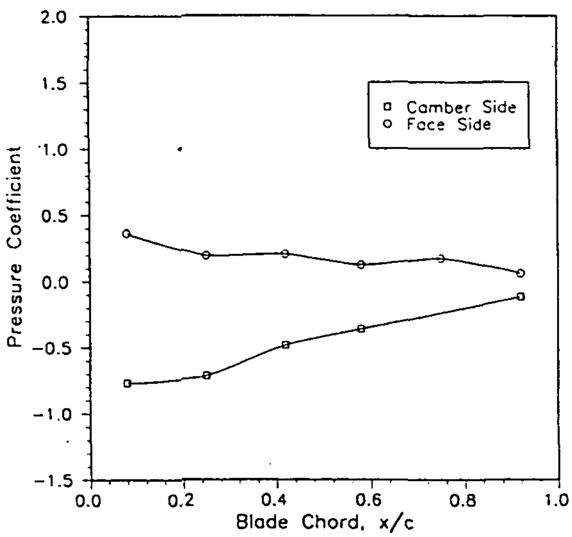

LAP/SR-7L Flight Test
Blade Surface Pressure Distribution

Record	: 188	Altitude (ft)	: 2284.
Condition	: 5A	Mach No.	: 0.312
Nacelle Tilt	: −3	True Airspeed (fps)	: 357.
Radial Sta	: .680	Tip Speed (fps)	: 702.
		Power Coeff.	: 1.662
		Blade Angle (deg)	: 45.90

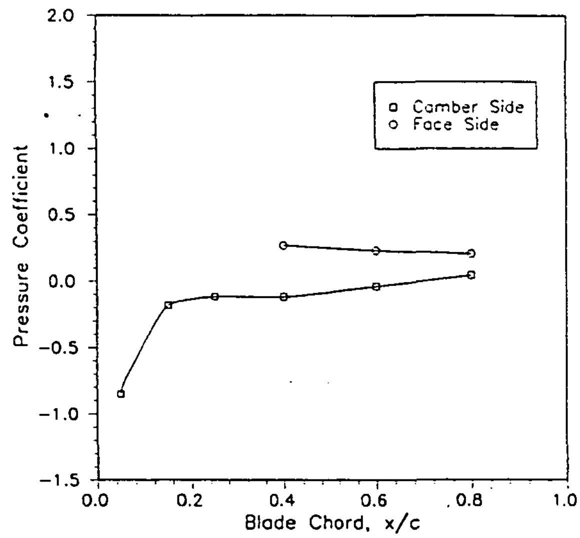

LAP/SR-7L Flight Test
Blade Surface Pressure Distribution

Record	: 188	Altitude (ft)	: 2284.
Condition	: 5A	Mach No.	: 0.312
Nacelle Tilt	: −3	True Airspeed (fps)	: 357.
Radial Sta	: .860	Tip Speed (fps)	: 702.
		Power Coeff.	: 1.662
		Blade Angle (deg)	: 45.90

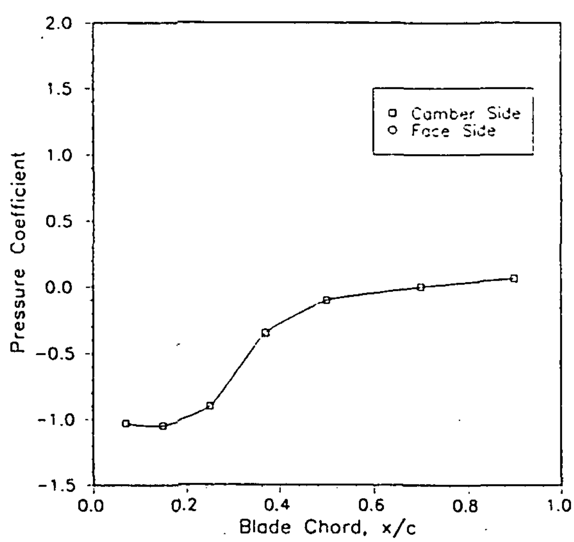

LAP/SR-7L Flight Test
Blade Surface Pressure Distribution

Record	: 188	Altitude (ft)	: 2284.
Condition	: 5A	Mach No.	: 0.312
Nacelle Tilt	: −3	True Airspeed (fps)	: 357.
Radial Sta	: .964	Tip Speed (fps)	: 702.
		Power Coeff.	: 1.662
		Blade Angle (deg)	: 45.90

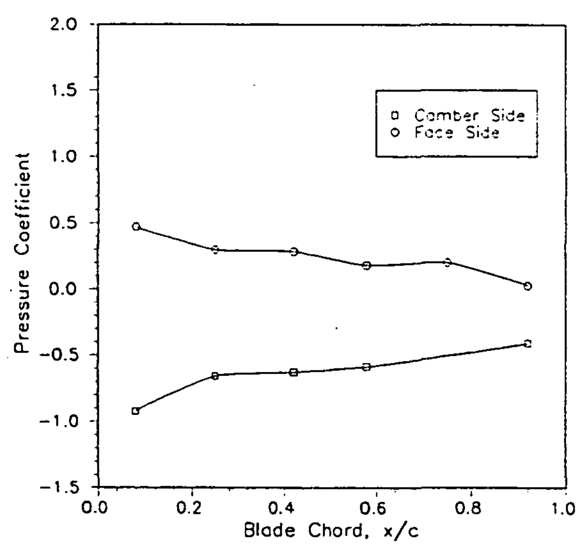

LAP/SR-7L Flight Test
Blade Surface Pressure Distribution

Record : 190
Condition : 6A
Nacelle Tilt : -3
Radial Sta : .680

Altitude (ft) : 2475.
Mach No. : 0.319
True Airspeed (fps) : 366.
Tip Speed (fps) : 797.
Power Coeff. : 1.111
Blade Angle (deg): 46.16

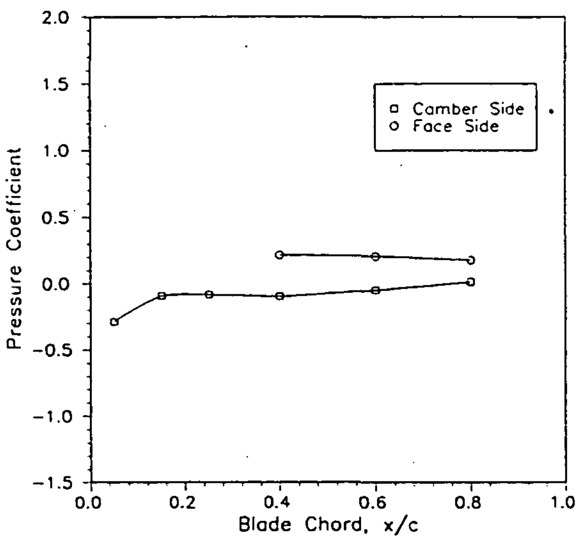

LAP/SR-7L Flight Test
Blade Surface Pressure Distribution

Record : 190
Condition : 6A
Nacelle Tilt : -3
Radial Sta : .860

Altitude (ft) : 2475.
Mach No. : 0.319
True Airspeed (fps) : 366.
Tip Speed (fps) : 797.
Power Coeff. : 1.111
Blade Angle (deg): 46.16

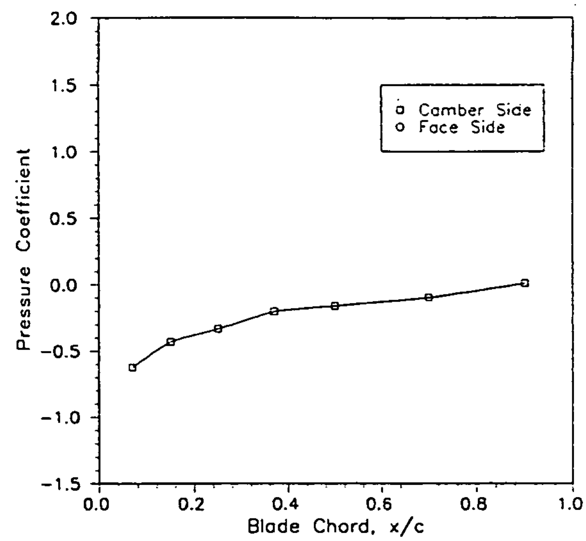

LAP/SR-7L Flight Test
Blade Surface Pressure Distribution

Record : 190
Condition : 6A
Nacelle Tilt : -3
Radial Sta : .964

Altitude (ft) : 2475.
Mach No. : 0.319
True Airspeed (fps) : 366.
Tip Speed (fps) : 797.
Power Coeff. : 1.111
Blade Angle (deg): 46.16

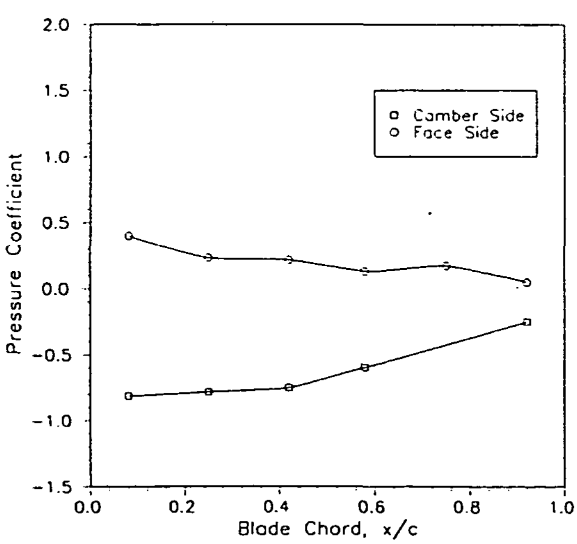

LAP/SR-7L Flight Test
Blade Surface Pressure Distribution

Record : 189
Condition : 7A
Nacelle Tilt : -3
Radial Sta : .680

Altitude (ft) : 1964.
Mach No. : 0.316
True Airspeed (fps) : 362.
Tip Speed (fps) : 797.
Power Coeff. : 0.693
Blade Angle (deg): 46.04

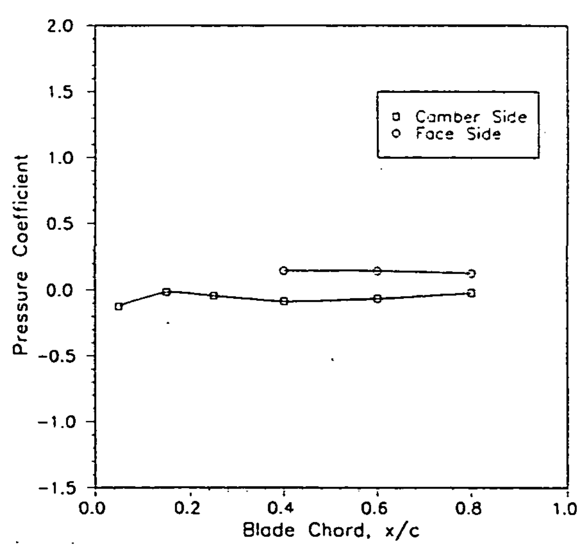

LAP/SR-7L Flight Test
Blade Surface Pressure Distribution

Record : 189
Condition : 7A
Nacelle Tilt : -3
Radial Sta : .860

Altitude (ft) : 1964.
Mach No. : 0.316
True Airspeed (fps) : 362.
Tip Speed (fps) : 797.
Power Coeff. : 0.693
Blade Angle (deg): 46.04

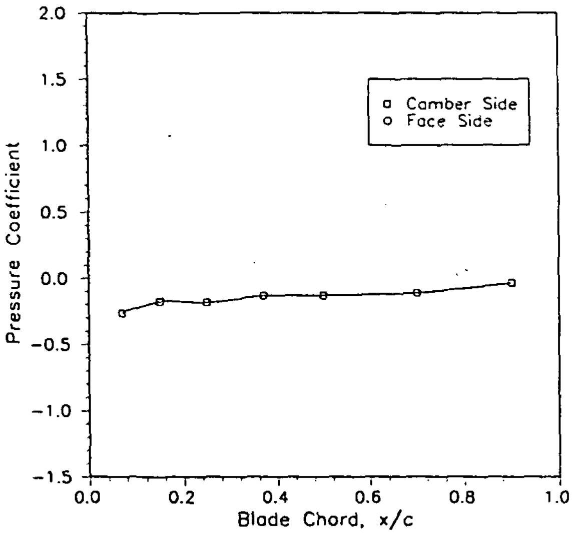

LAP/SR-7L Flight Test
Blade Surface Pressure Distribution

Record : 189
Condition : 7A
Nacelle Tilt : -3
Radial Sta : .964

Altitude (ft) : 1964.
Mach No. : 0.316
True Airspeed (fps) : 362.
Tip Speed (fps) : 797.
Power Coeff. : 0.693
Blade Angle (deg): 46.04

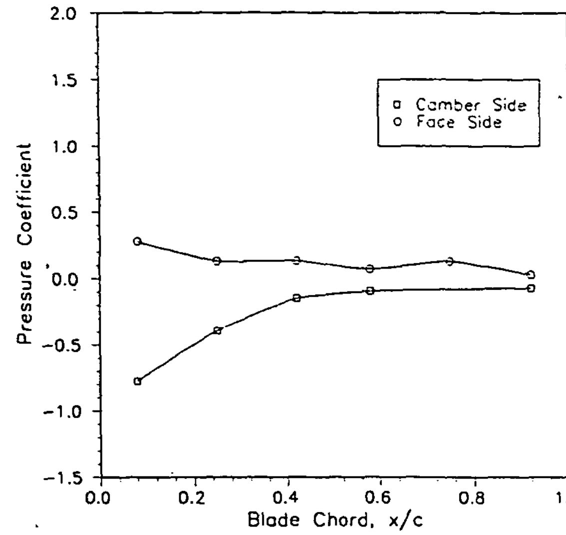

LAP/SR-7L Flight Test
Blade Surface Pressure Distribution

Record : 182
Condition : 10A
Nacelle Tilt : -3
Radial Sta : .680

Altitude (ft) : 2000.
Mach No. : 0.310
True Airspeed (fps) : 356.
Tip Speed (fps) : 624.
Power Coeff. : 0.957
Blade Angle (deg): 38.67

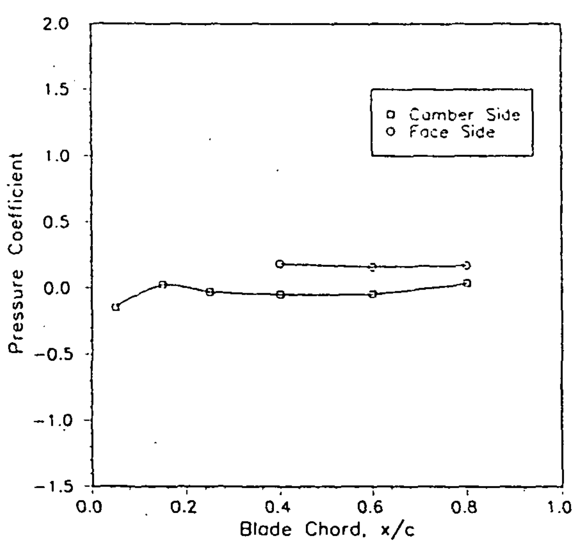

LAP/SR-7L Flight Test
Blade Surface Pressure Distribution

Record : 182
Condition : 10A
Nacelle Tilt : -3
Radial Sta : .860

Altitude (ft) : 2000.
Mach No. : 0.310
True Airspeed (fps) : 356.
Tip Speed (fps) : 624.
Power Coeff. : 0.957
Blade Angle (deg): 38.67

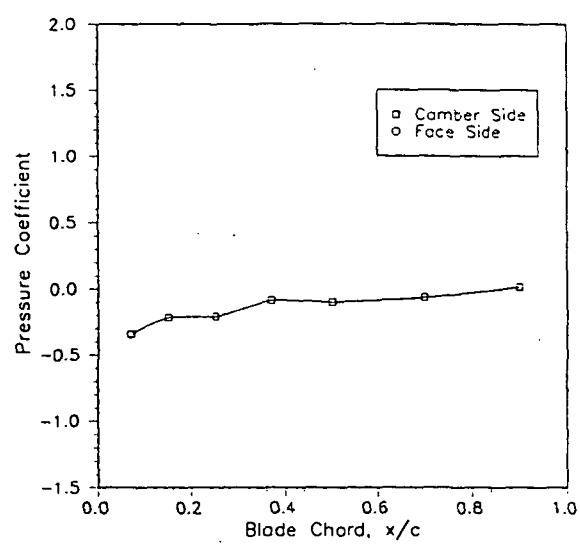

LAP/SR-7L Flight Test
Blade Surface Pressure Distribution

Record : 182
Condition : 10A
Nocelle Tilt : -3
Radial Sta : .964

Altitude (ft) : 2000.
Mach No. : 0.310
True Airspeed (fps) : 356.
Tip Speed (fps) : 624.
Power Coeff. : 0.957
Blade Angle (deg): 38.67

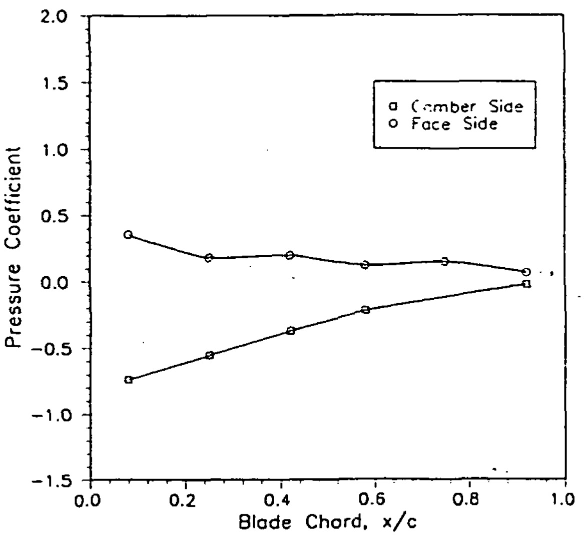

LAP/SR-7L Flight Test
Blade Surface Pressure Distribution

Record : 184
Condition : 11A
Nacelle Tilt : -3
Radial Sta : .680

Altitude (ft) : 2034.
Mach No. : 0.312
True Airspeed (fps) : 357.
Tip Speed (fps) : 622.
Power Coeff. : 1.935
Blade Angle (deg): 46.82

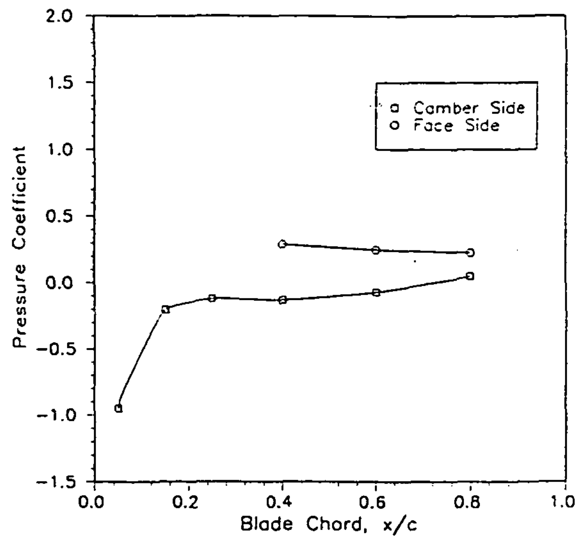

LAP/SR-7L Flight Test
Blade Surface Pressure Distribution

Record : 184
Condition : 11A
Nacelle Tilt : -3
Radial Sta : .860

Altitude (ft) : 2034.
Mach No. : 0.312
True Airspeed (fps) : 357.
Tip Speed (fps) : 622.
Power Coeff. : 1.935
Blade Angle (deg): 46.82

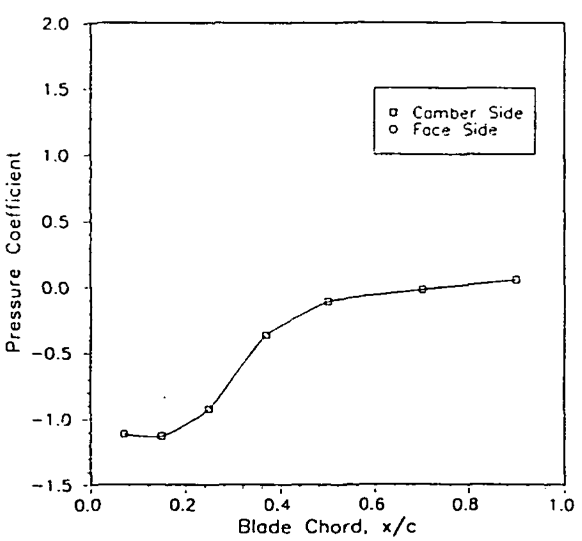

LAP/SR-7L Flight Test
Blade Surface Pressure Distribution

Record : 184
Condition : 11A
Nacelle Tilt : -3
Radial Sta : .964

Altitude (ft) : 2034.
Mach No. : 0.312
True Airspeed (fps) : 357.
Tip Speed (fps) : 622.
Power Coeff. : 1.935
Blade Angle (deg): 46.82

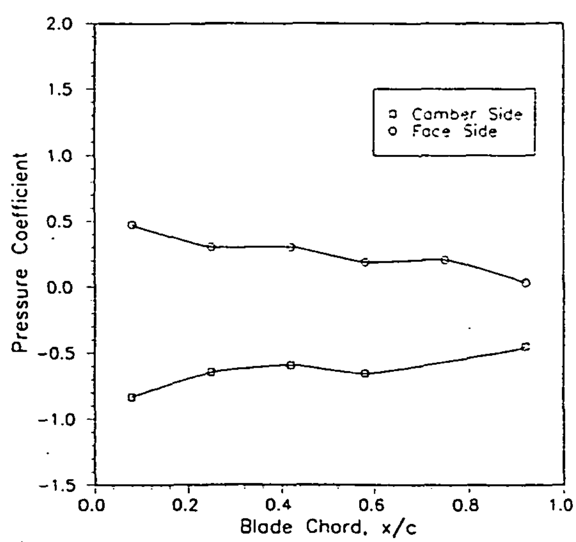

LAP/SR-7L Flight Test
Blade Surface Pressure Distribution

Record : 195
Condition : 18
Nacelle Tilt : -3
Radial Sta : .680

Altitude (ft) : 35445.
Mach No. : 0.815
True Airspeed (fps) : 819.
Tip Speed (fps) : 622.
Power Coeff. : 3.389
Blade Angle (deg): 60.53

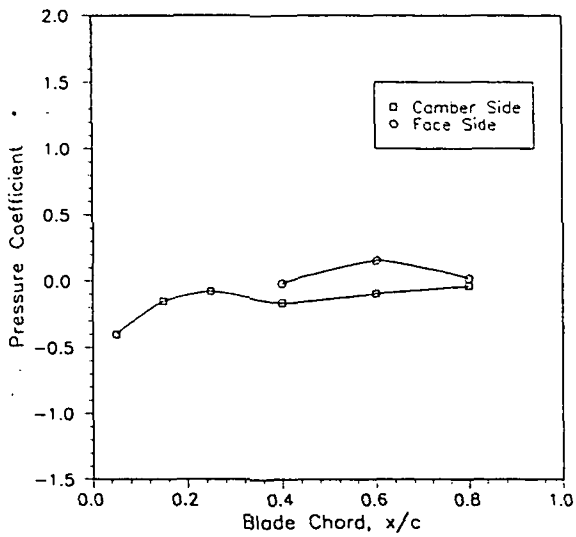

LAP/SR-7L Flight Test
Blade Surface Pressure Distribution

Record : 195
Condition : 18
Nacelle Tilt : -3
Radial Sta : .860

Altitude (ft) : 35445.
Mach No. : 0.815
True Airspeed (fps) : 819.
Tip Speed (fps) : 622.
Power Coeff. : 3.389
Blade Angle (deg): 60.53

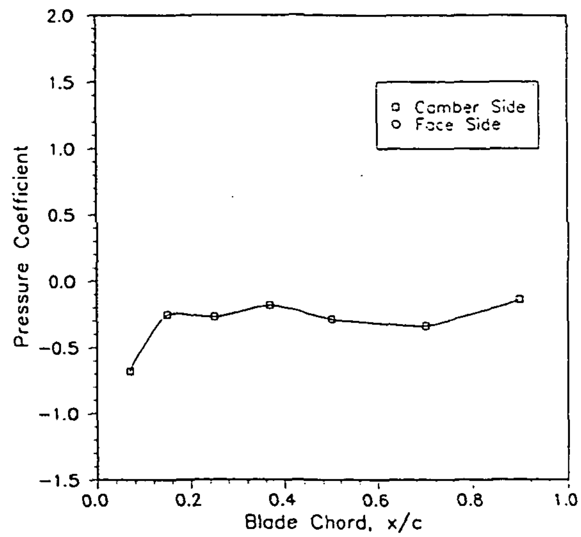

LAP/SR-7L Flight Test
Blade Surface Pressure Distribution

Record : 195
Condition : 18
Nacelle Tilt : -3
Radial Sta : .964

Altitude (ft) : 35445.
Mach No. : 0.815
True Airspeed (fps) : 819.
Tip Speed (fps) : 622.
Power Coeff. : 3.389
Blade Angle (deg): 60.53

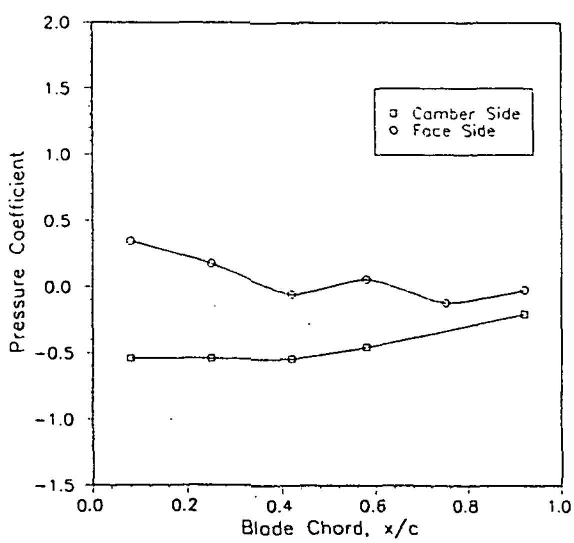

LAP/SR-7L Flight Test
Blade Surface Pressure Distribution

Record : 196
Condition : 38
Nacelle Tilt : -3
Radial Sta : .680

Altitude (ft) : 35444.
Mach No. : 0.803
True Airspeed (fps) : 808.
Tip Speed (fps) : 696.
Power Coeff. : 1.266
Blade Angle (deg): 60.55

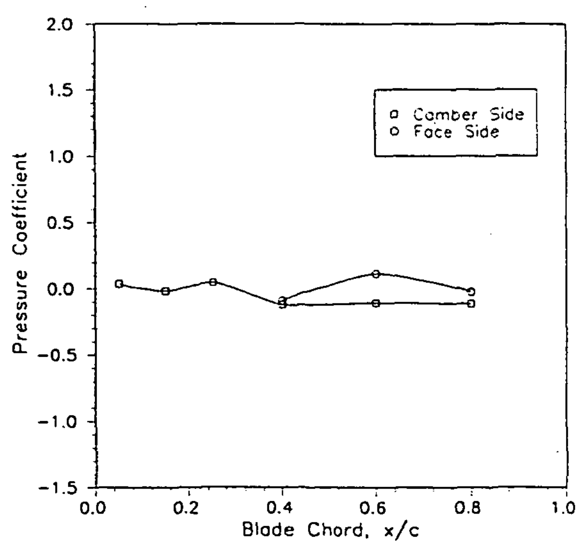

LAP/SR-7L Flight Test
Blade Surface Pressure Distribution

Record	: 196	Altitude (ft)	: 35444.
Condition	: 3B	Mach No.	: 0.803
Nacelle Tilt	: -3	True Airspeed (fps)	: 808.
Radial Sta	: .860	Tip Speed (fps)	: 696.
		Power Coeff.	: 1.266
		Blade Angle (deg)	: 60.55

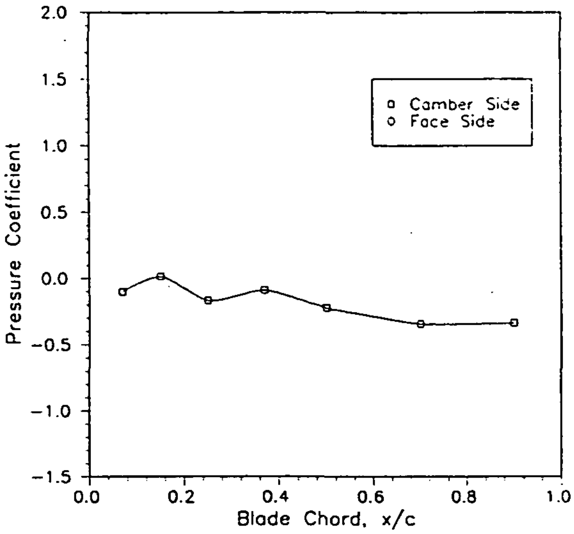

LAP/SR-7L Flight Test
Blade Surface Pressure Distribution

Record	: 196	Altitude (ft)	: 35444.
Condition	: 3B	Mach No.	: 0.803
Nacelle Tilt	: -3	True Airspeed (fps)	: 808.
Radial Sta	: .964	Tip Speed (fps)	: 696.
		Power Coeff.	: 1.266
		Blade Angle (deg)	: 60.55

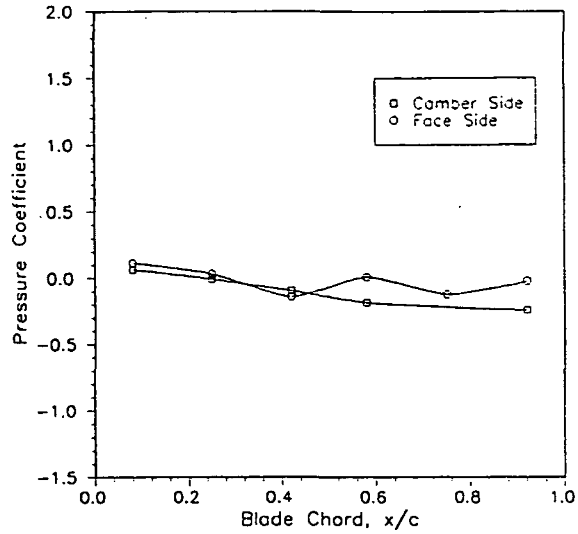

LAP/SR-7L Flight Test
Blade Surface Pressure Distribution

Record	: 197	Altitude (ft)	: 35429.
Condition	: 4B	Mach No.	: 0.809
Nacelle Tilt	: -3	True Airspeed (fps)	: 813.
Radial Sta	: .680	Tip Speed (fps)	: 694.
		Power Coeff.	: 2.082
		Blade Angle (deg)	: 60.55

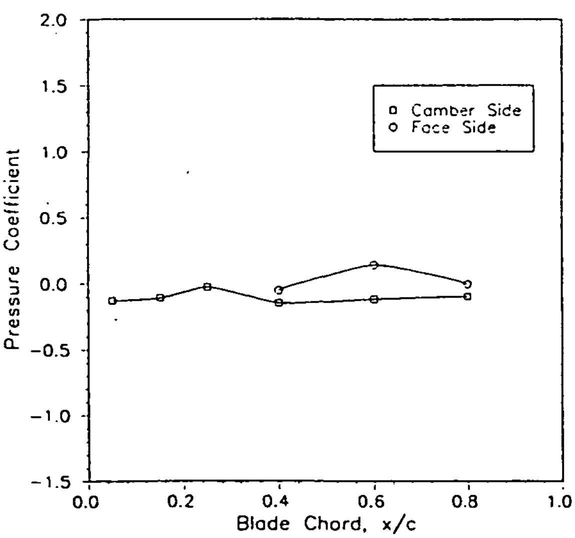

LAP/SR-7L Flight Test
Blade Surface Pressure Distribution

Record	: 197	Altitude (ft)	: 35429.
Condition	: 4B	Mach No.	: 0.809
Nacelle Tilt	: -3	True Airspeed (fps)	: 813.
Radial Sta	: .860	Tip Speed (fps)	: 694.
		Power Coeff.	: 2.082
		Blade Angle (deg)	: 60.55

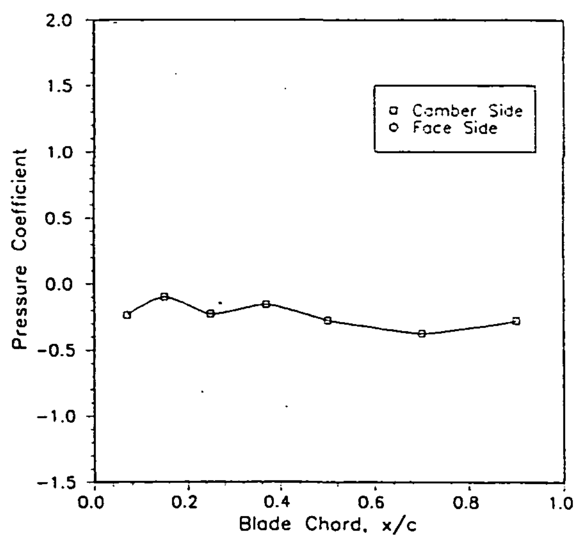

LAP/SR-7L Flight Test
Blade Surface Pressure Distribution

Record	: 197	Altitude (ft)	: 35429.
Condition	: 48	Mach No.	: 0.809
Nacelle Tilt	: -3	True Airspeed (fps)	: 813.
Radial Sta	: .964	Tip Speed (fps)	: 694.
		Power Coeff.	: 2.082
		Blade Angle (deg)	: 60.55

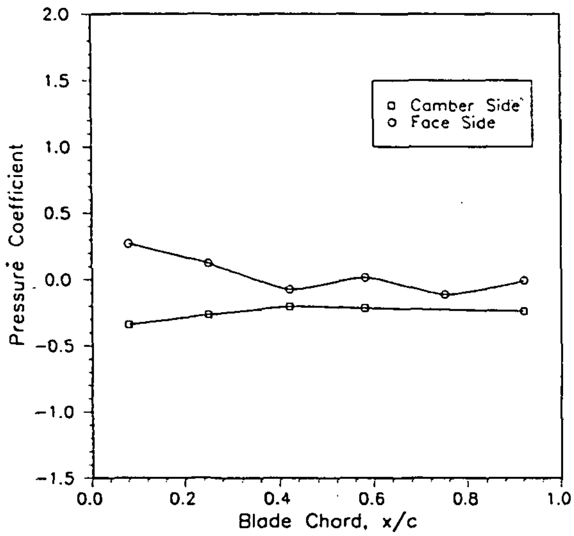

LAP/SR-7L Flight Test
Blade Surface Pressure Distribution

Record	: 198	Altitude (ft)	: 35432.
Condition	: 58	Mach No.	: 0.816
Nacelle Tilt	: -3	True Airspeed (fps)	: 820.
Radial Sta	: .680	Tip Speed (fps)	: 696.
		Power Coeff.	: 2.567
		Blade Angle (deg)	: 60.54

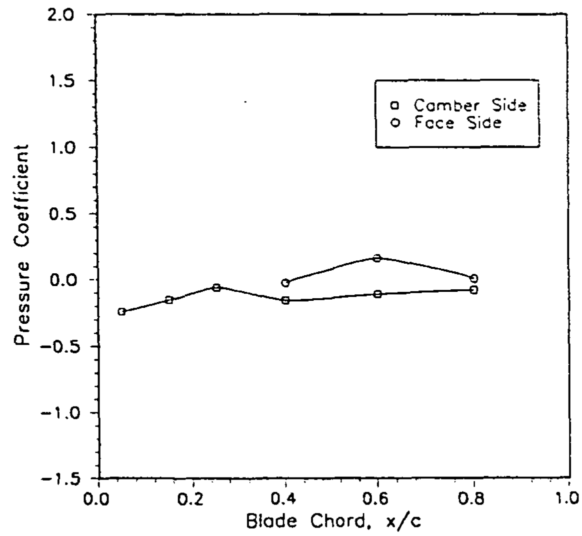

LAP/SR-7L Flight Test
Blade Surface Pressure Distribution

Record	: 198	Altitude (ft)	: 35432.
Condition	: 58	Mach No.	: 0.816
Nacelle Tilt	: -3	True Airspeed (fps)	: 820.
Radial Sta	: .860	Tip Speed (fps)	: 696.
		Power Coeff.	: 2.567
		Blade Angle (deg)	: 60.54

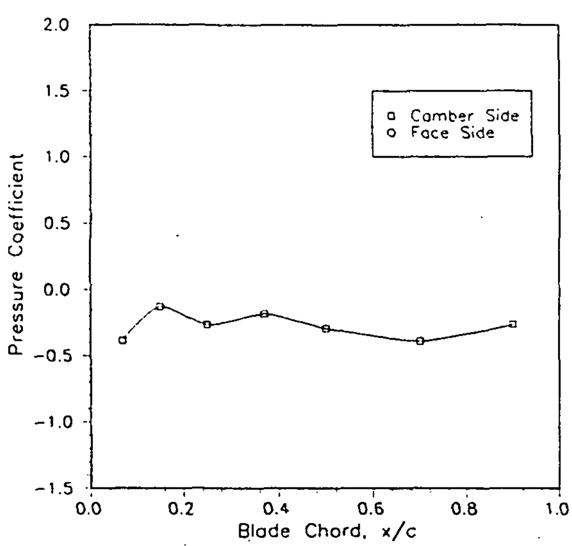

LAP/SR-7L Flight Test
Blade Surface Pressure Distribution

Record	: 198	Altitude (ft)	: 35432.
Condition	: 58	Mach No.	: 0.816
Nacelle Tilt	: -3	True Airspeed (fps)	: 820.
Radial Sta	: .964	Tip Speed (fps)	: 696.
		Power Coeff.	: 2.567
		Blade Angle (deg)	: 60.54

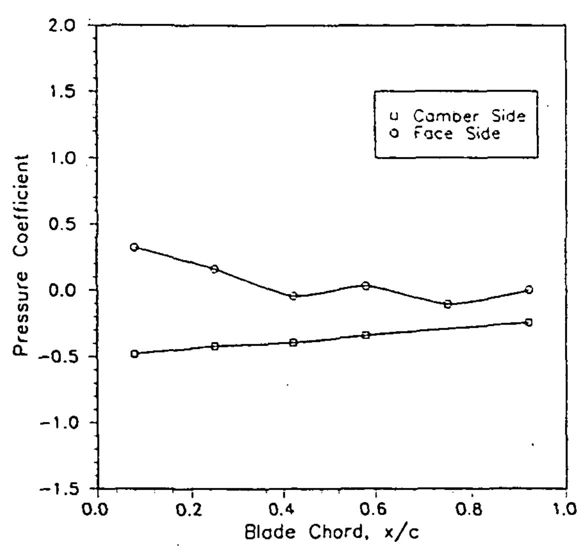

LAP/SR-7L Flight Test
Blade Surface Pressure Distribution

Record : 199
Condition : 7B
Nacelle Tilt : −3
Radial Sta : .680

Altitude (ft) : 35449.
Mach No. : 0.814
True Airspeed (fps) : 818.
Tip Speed (fps) : 800.
Power Coeff. : 0.915
Blade Angle (deg): 60.54

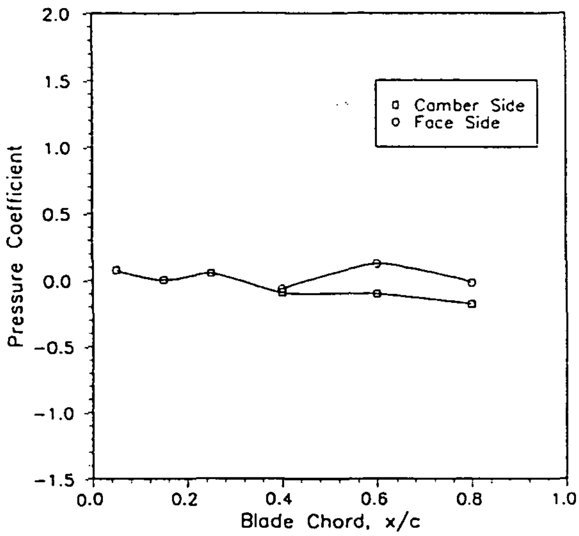

LAP/SR-7L Flight Test
Blade Surface Pressure Distribution

Record : 199
Condition : 7B
Nacelle Tilt : −3
Radial Sta : .860

Altitude (ft) : 35449.
Mach No. : 0.814
True Airspeed (fps) : 818.
Tip Speed (fps) : 800.
Power Coeff. : 0.915
Blade Angle (deg): 60.54

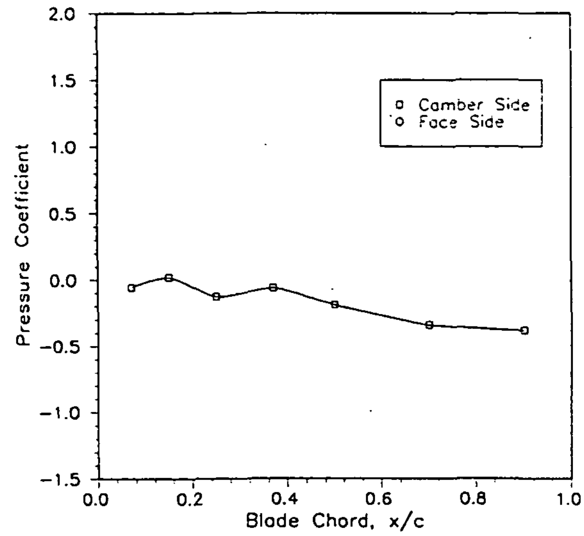

LAP/SR-7L Flight Test
Blade Surface Pressure Distribution

Record : 199
Condition : 7B
Nacelle Tilt : −3
Radial Sta : .964

Altitude (ft) : 35449.
Mach No. : 0.814
True Airspeed (fps) : 818.
Tip Speed (fps) : 800.
Power Coeff. : 0.915
Blade Angle (deg): 60.54

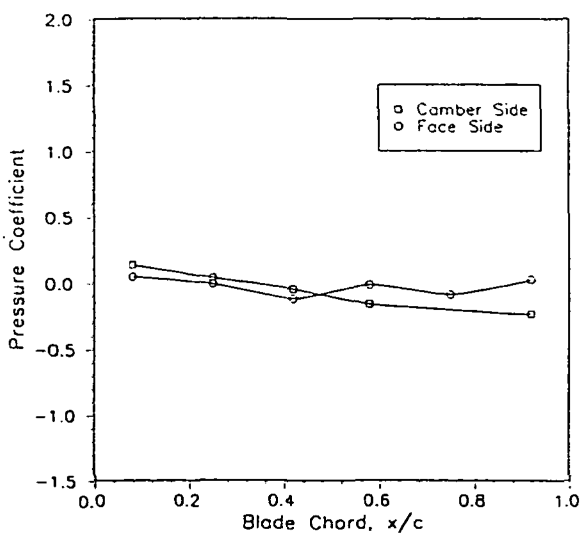

LAP/SR-7L Flight Test
Blade Surface Pressure Distribution

Record : 201
Condition : 8B
Nacelle Tilt : −3
Radial Sta : .680

Altitude (ft) : 35438.
Mach No. : 0.815
True Airspeed (fps) : 819.
Tip Speed (fps) : 797.
Power Coeff. : 1.488
Blade Angle (deg): 60.53

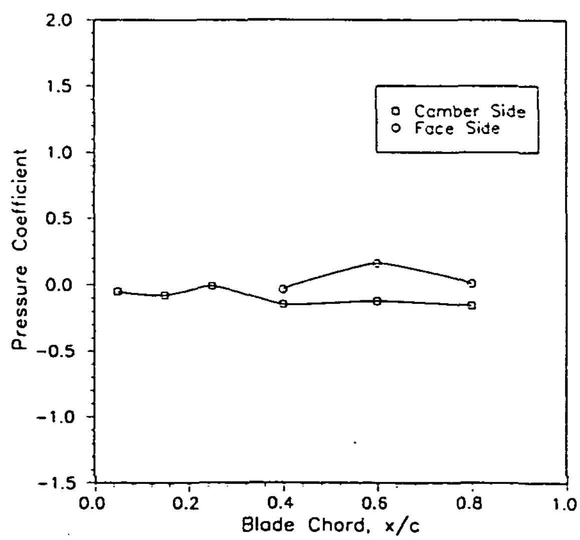

LAP/SR-7L Flight Test
Blade Surface Pressure Distribution

Record	: 201	Altitude (ft)	: 35438.
Condition	: 8B	Mach No.	: 0.815
Nacelle Tilt	: −3	True Airspeed (fps)	: 819.
Radial Sta	: .860	Tip Speed (fps)	: 797.
		Power Coeff.	: 1.488
		Blade Angle (deg)	: 60.53

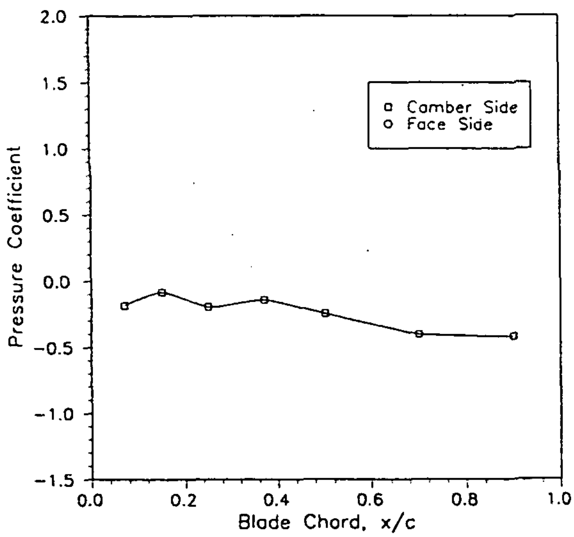

LAP/SR-7L Flight Test
Blade Surface Pressure Distribution

Record	: 201	Altitude (ft)	: 35438.
Condition	: 8B	Mach No.	: 0.815
Nacelle Tilt	: −3	True Airspeed (fps)	: 819.
Radial Sta	: .964	Tip Speed (fps)	: 797.
		Power Coeff.	: 1.488
		Blade Angle (deg)	: 60.53

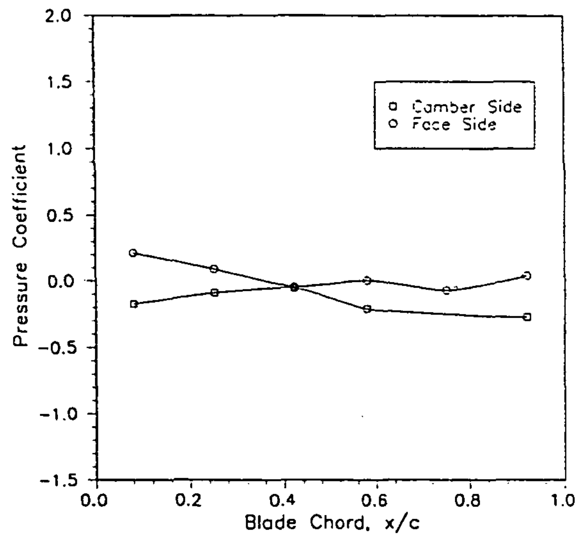

LAP/SR-7L Flight Test
Blade Surface Pressure Distribution

Record	: 202	Altitude (ft)	: 35445.
Condition	: 9B	Mach No.	: 0.817
Nacelle Tilt	: −3	True Airspeed (fps)	: 821.
Radial Sta	: .680	Tip Speed (fps)	: 798.
		Power Coeff.	: 1.824
		Blade Angle (deg)	: 60.53

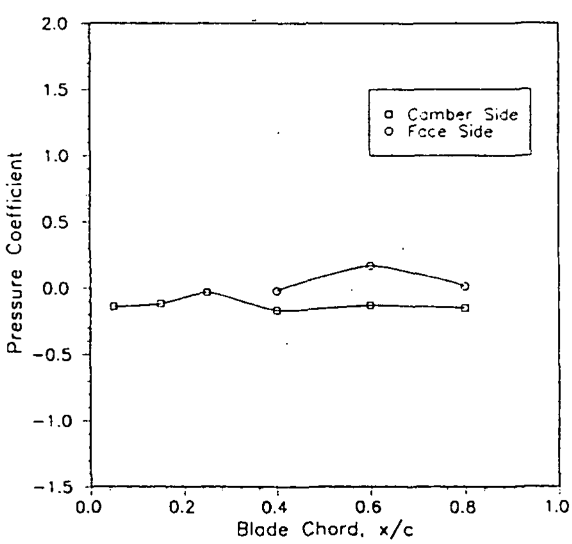

LAP/SR-7L Flight Test
Blade Surface Pressure Distribution

Record	: 202	Altitude (ft)	: 35445.
Condition	: 9B	Mach No.	: 0.817
Nacelle Tilt	: −3	True Airspeed (fps)	: 821.
Radial Sta	: .860	Tip Speed (fps)	: 798.
		Power Coeff.	: 1.824
		Blade Angle (deg)	: 60.53

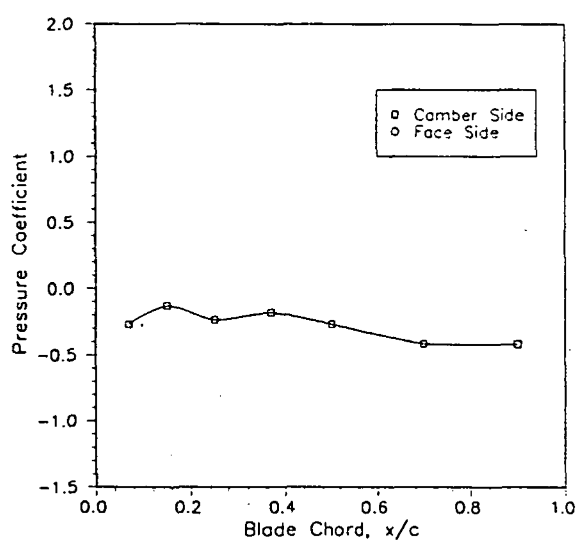

LAP/SR-7L Flight Test
Blade Surface Pressure Distribution

Record	: 202	Altitude (ft)	: 35445.
Condition	: 9B	Mach No.	: 0.817
Nacelle Tilt	: -3	True Airspeed (fps)	: 821.
Radial Sta	: .964	Tip Speed (fps)	: 798.
		Power Coeff.	: 1.824
		Blade Angle (deg)	: 60.53

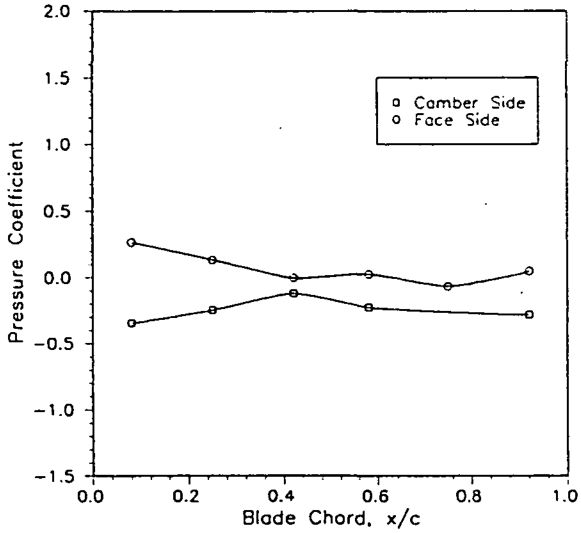

LAP/SR-7L Flight Test
Blade Surface Pressure Distribution

Record	: 193	Altitude (ft)	: 35492.
Condition	: 11B	Mach No.	: 0.821
Nacelle Tilt	: -3	True Airspeed (fps)	: 825.
Radial Sta	: .680	Tip Speed (fps)	: 638.
		Power Coeff.	: 1.640
		Blade Angle (deg)	: 58.04

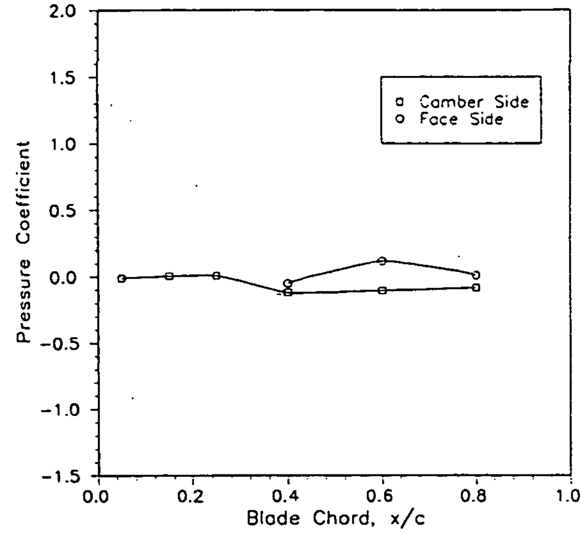

LAP/SR-7L Flight Test
Blade Surface Pressure Distribution

Record	: 193	Altitude (ft)	: 35492.
Condition	: 11B	Mach No.	: 0.821
Nacelle Tilt	: -3	True Airspeed (fps)	: 825.
Radial Sta	: .860	Tip Speed (fps)	: 638.
		Power Coeff.	: 1.640
		Blade Angle (deg)	: 58.04

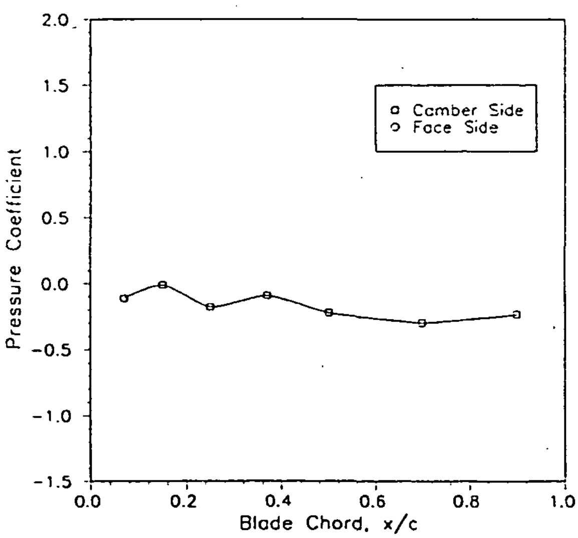

LAP/SR-7L Flight Test
Blade Surface Pressure Distribution

Record	: 193	Altitude (ft)	: 35492.
Condition	: 11B	Mach No.	: 0.821
Nacelle Tilt	: -3	True Airspeed (fps)	: 825.
Radial Sta	: .964	Tip Speed (fps)	: 638.
		Power Coeff.	: 1.640
		Blade Angle (deg)	: 58.04

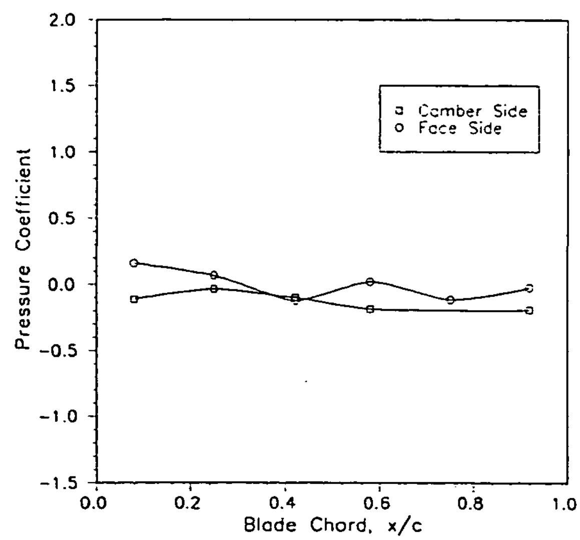

LAP/SR-7L Flight Test
Blade Surface Pressure Distribution

Record	: 194	Altitude (ft)	: 35449.
Condition	: 128	Mach No.	: 0.820
Nacelle Tilt	: -3	True Airspeed (fps)	: 824.
Radial Sta	: .680	Tip Speed (fps)	: 636.
		Power Coeff.	: 2.603
		Blade Angle (deg)	: 58.61

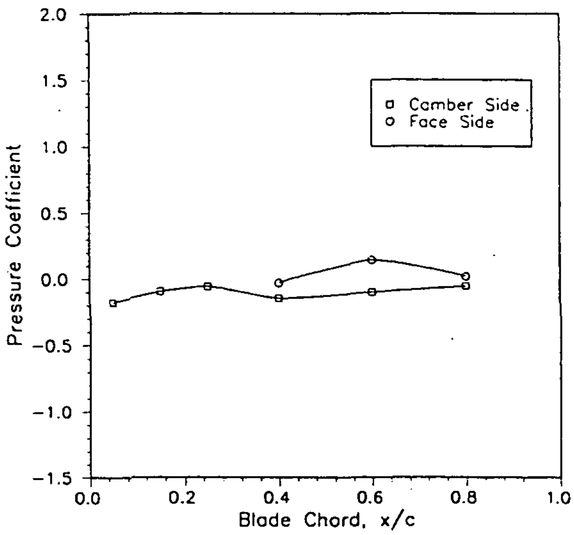

LAP/SR-7L Flight Test
Blade Surface Pressure Distribution

Record	: 194	Altitude (ft)	: 35449.
Condition	: 128	Mach No.	: 0.820
Nacelle Tilt	: -3	True Airspeed (fps)	: 824.
Radial Sta	: .860	Tip Speed (fps)	: 636.
		Power Coeff.	: 2.603
		Blade Angle (deg)	: 58.61

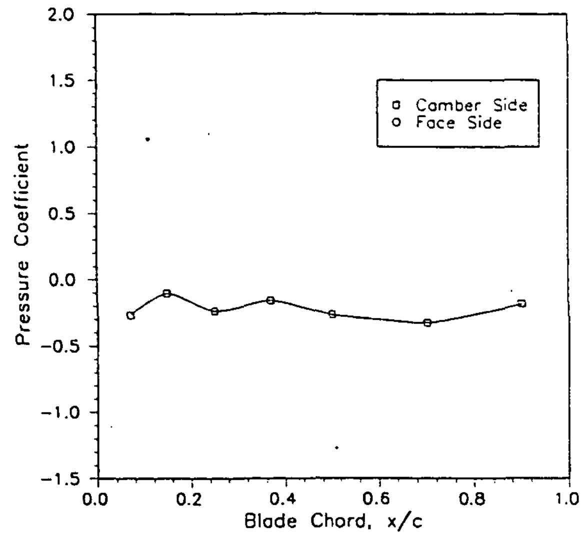

LAP/SR-7L Flight Test
Blade Surface Pressure Distribution

Record	: 194	Altitude (ft)	: 35449.
Condition	: 128	Mach No.	: 0.820
Nacelle Tilt	: -3	True Airspeed (fps)	: 824.
Radial Sta	: .964	Tip Speed (fps)	: 636.
		Power Coeff.	: 2.603
		Blade Angle (deg)	: 58.61

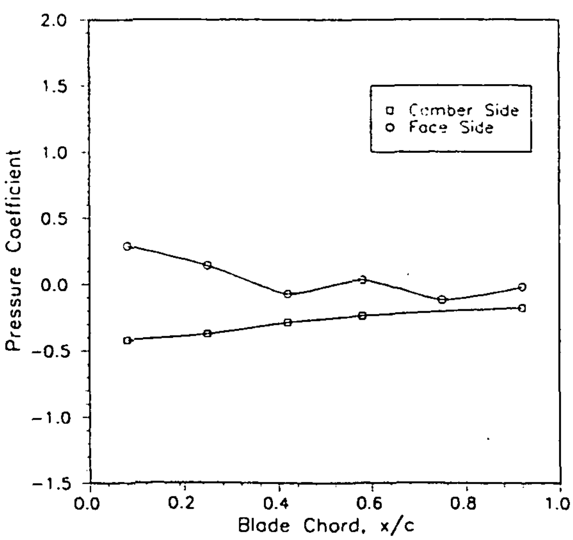

LAP/SR-7L Flight Test
Blade Surface Pressure Distribution

Record	: 207	Altitude (ft)	: 23058.
Condition	: 1C	Mach No.	: 0.605
Nacelle Tilt	: -3	True Airspeed (fps)	: 642.
Radial Sta	: .680	Tip Speed (fps)	: 635.
		Power Coeff.	: 1.529
		Blade Angle (deg)	: 60.46

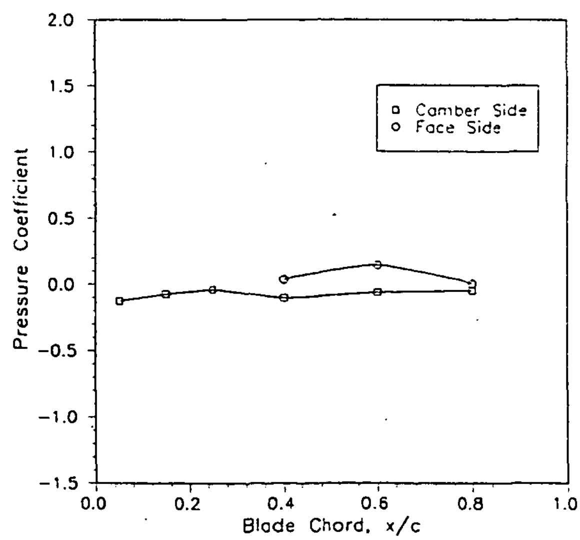

LAP/SR-7L Flight Test
Blade Surface Pressure Distribution

Record : 207
Condition : 1C
Nacelle Tilt : −3
Radial Sta : .860

Altitude (ft) : 23058.
Mach No. : 0.605
True Airspeed (fps) : 642.
Tip Speed (fps) : 635.
Power Coeff. : 1.529
Blade Angle (deg): 60.46

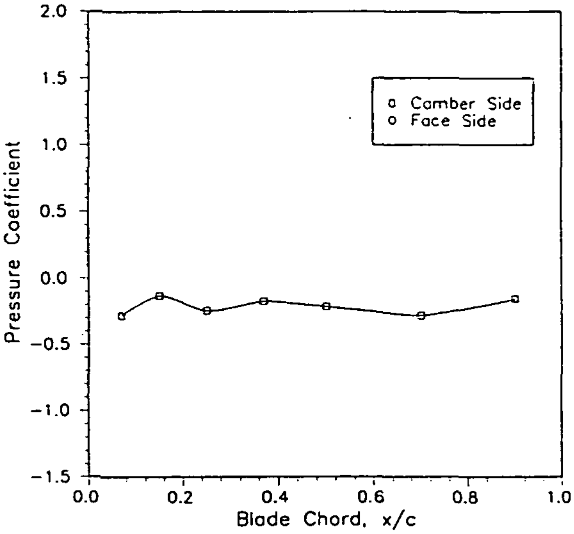

LAP/SR-7L Flight Test
Blade Surface Pressure Distribution

Record : 207
Condition : 1C
Nacelle Tilt : −3
Radial Sta : .964

Altitude (ft) : 23058.
Mach No. : 0.605
True Airspeed (fps) : 642.
Tip Speed (fps) : 635.
Power Coeff. : 1.529
Blade Angle (deg): 60.46

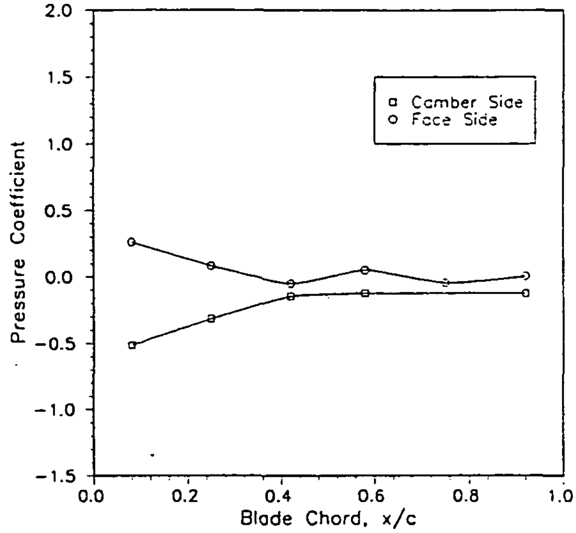

LAP/SR-7L Flight Test
Blade Surface Pressure Distribution

Record : 206
Condition : 2C
Nacelle Tilt : −3
Radial Sta : .680

Altitude (ft) : 31468.
Mach No. : 0.697
True Airspeed (fps) : 715.
Tip Speed (fps) : 715.
Power Coeff. : 1.517
Blade Angle (deg): 60.48

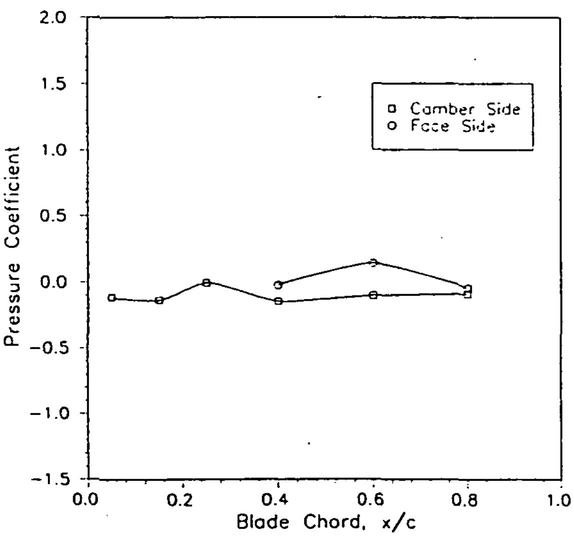

LAP/SR-7L Flight Test
Blade Surface Pressure Distribution

Record : 206
Condition : 2C
Nacelle Tilt : −3
Radial Sta : .860

Altitude (ft) : 31468.
Mach No. : 0.697
True Airspeed (fps) : 715.
Tip Speed (fps) : 715.
Power Coeff. : 1.517
Blade Angle (deg): 60.48

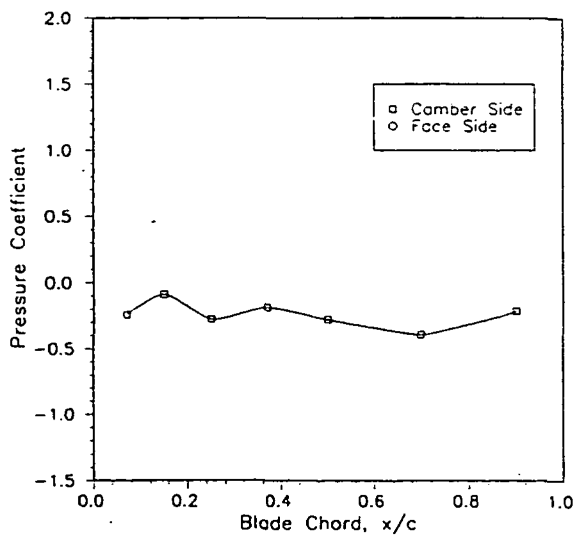

LAP/SR-7L Flight Test
Blade Surface Pressure Distribution

Record : 206
Condition : 2C
Nacelle Tilt : −3
Radial Sta : .964

Altitude (ft) : 31468.
Mach No. : 0.697
True Airspeed (fps) : 715.
Tip Speed (fps) : 715.
Power Coeff. : 1.517
Blade Angle (deg): 60.48

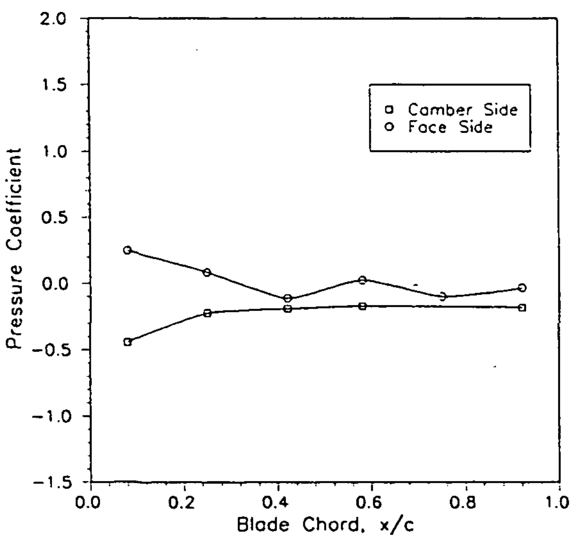

LAP/SR-7L Flight Test
Blade Surface Pressure Distribution

Record : 205
Condition : 3C
Nacelle Tilt : −3
Radial Sta : .680

Altitude (ft) : 37448.
Mach No. : 0.795
True Airspeed (fps) : 793.
Tip Speed (fps) : 798.
Power Coeff. : 1.484
Blade Angle (deg): 60.51

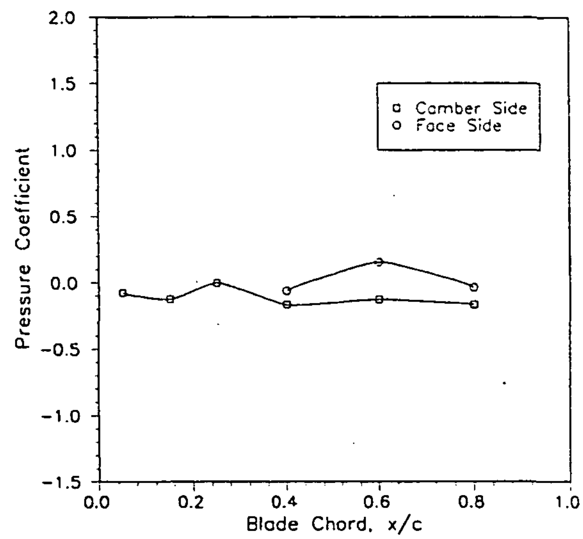

LAP/SR-7L Flight Test
Blade Surface Pressure Distribution

Record : 205
Condition : 3C
Nacelle Tilt : −3
Radial Sta : .860

Altitude (ft) : 37448.
Mach No. : 0.795
True Airspeed (fps) : 793.
Tip Speed (fps) : 798.
Power Coeff. : 1.484
Blade Angle (deg): 60.51

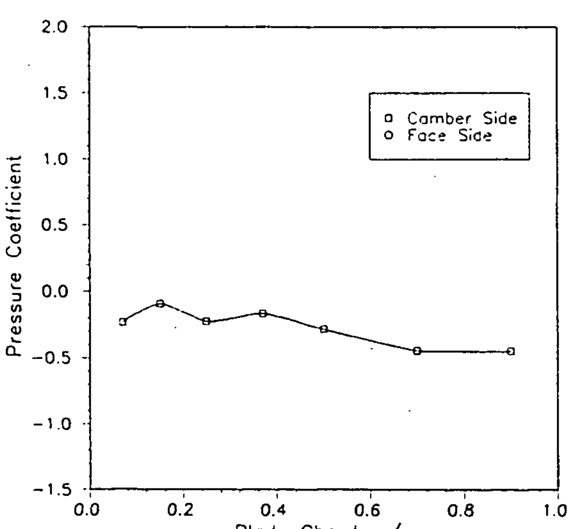

LAP/SR-7L Flight Test
Blade Surface Pressure Distribution

Record : 205
Condition : 3C
Nacelle Tilt : −3
Radial Sta : .964

Altitude (ft) : 37448.
Mach No. : 0.795
True Airspeed (fps) : 793.
Tip Speed (fps) : 798.
Power Coeff. : 1.484
Blade Angle (deg): 60.51

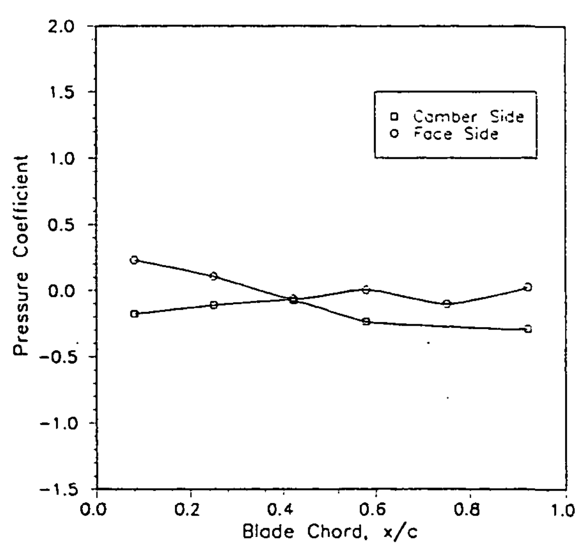

REPORT DOCUMENTATION PAGE

Form Approved
OMB No. 0704-0188

1. AGENCY USE ONLY *(Leave blank)*	2. REPORT DATE	3. REPORT TYPE AND DATES COVERED
		Final Contractor Report

4. TITLE AND SUBTITLE

In Flight Measurement of Steady and Unsteady Blade Surface Pressure of a Single Rotation Large Scale Advanced Prop-Fan Installed on the PTA Aircraft

5. FUNDING NUMBERS

WU-535-03-10
C-NAS3-23051

6. AUTHOR(S)

D. Parzych, L. Boyd, W. Meissner, and A. Wyrostek

7. PERFORMING ORGANIZATION NAME(S) AND ADDRESS(ES)

United Technologies Corporation
Hamilton Standard Division
Windsor Locks, Connecticut 06096

8. PERFORMING ORGANIZATION REPORT NUMBER

9. SPONSORING/MONITORING AGENCY NAMES(S) AND ADDRESS(ES)

National Aeronautics and Space Administration
Lewis Research Center
Cleveland, Ohio 44135-3191

10. SPONSORING/MONITORING AGENCY REPORT NUMBER

NASA CR-187096

11. SUPPLEMENTARY NOTES

Project Manager, Lawrence J. Heidelberg, Propulsion Systems Division, NASA Lewis Research Center, (216) 433-3859.

12a. DISTRIBUTION/AVAILABILITY STATEMENT

LIMITED DISTRIBUTION DOCUMENT

Because of its significant technological potential, this information which has been developed under a U.S. Government program is being given a limited distribution whereby advanced access is provided for use by domestic interests. This legend shall be marked on any reproduction of this information in whole or in part.

Date for general release October 1993. Subject Category 07

12b. DISTRIBUTION CODE

13. ABSTRACT ***(Maximum 200 words)***

An experiment was performed by Hamilton Standard, Division of United Technologies Corporation, under contract by the NASA Lewis Research Center, to measure the blade surface pressure of a large scale, 8 blade, model Prop-Fan in flight. The test bed was the Gulfstream II Prop-Fan Test Assessment (PTA) aircraft. The objective of the test was to measure the steady and periodic blade surface pressure resulting from three different Prop-Fan air inflow angles at various takeoff and cruise conditions. The inflow angles were obtained by varying the nacelle tilt angles, which ranged from -3 to +2 degrees. A range of power loadings, tip speeds and altitudes were tested at each nacelle tilt angle over the flight Mach number range of 0.30 to 0.80. This report presents unsteady blade pressure data tabulated as Fourier coefficients for the first 35 harmonics of shaft rotational frequency and the steady (non-varying) pressure component.

14. SUBJECT TERMS

Unsteady aerodynamics; Propellers; Propeller fans; Propeller blades; Pressure distribution; Flight tests; Thermography

15. NUMBER OF PAGES

228

16. PRICE CODE

A11

17. SECURITY CLASSIFICATION OF REPORT	18. SECURITY CLASSIFICATION OF THIS PAGE	19. SECURITY CLASSIFICATION OF ABSTRACT	20. LIMITATION OF ABSTRACT
Unclassified	Unclassified	Unclassified	[redacted]